Role of insulin receptor substrate 1 in energy homeostasis *in vivo*

Inaugural-Dissertation

zur

Erlangung des Doktorgrades

der Mathematisch-Naturwissenschaftlichen Fakultät

der Universität zu Köln

vorgelegt von

Oliver Stöhr

aus Köln

2011

Berichterstatter:

Prof. Dr. Jens C. Brüning

Prof. Dr. Wilhelm Krone

Tag der letzten mündlichen Prüfung: 18.10.2011

Figure Index

Table Index

List of Abbreviations

AKT	PKB synonym
APS	Ammonium-persulfate
BSA	Bovine serum albumin
°C	degree centrigrade
cDNA	copyDNA
CNS	Central Nervous System
ddH2O	Double-disalled water
DMSO	Dimethyl sulfoxide
DTT	Dithiotreitol
EDTA	Ethylenediaminetetraacetic acid
EGTA	Ethylene glycol acetic acid
ELISA	Enzyme Linked Immunosorbent Assays
ER	Endoplasmic reticulum
ERK	Extracellular signal-regulated kinase
FCS	Fetal calf serum
FFA	Free fatty acid
GDP	Guanosine-diphosphate
GH G	Growth hormone
GRB2	Growth factor receptor binding protein 2
GSK-3α/β	Glycogen synthase kinase 3α/β
GTP	Guanosine-triphosphate
h	hour
HEPES	(4-(-hydroxyethyl)-1-piperazineethanesulfonic acid
HRP	Horseradish peroxidase
IGF	Insulin-like growth factor
IGF-1R	Insulin-like growth factor receptor type I
IR	Insulin Receptor
IRa	Insulin receptor isoform a
IRb	Insulin receptor isoform b
IRS-1	Insulin receptor substrate 1
IRS-2	Insulin receptor substrate 2
IRSs	Insulin receptor substrates

KCl	Potassium chloride
kDA	kilo Dalton
µ	micro (10^{-6})
mA	milli Ampere
MAP-kinase	Mitogen-activated protein kinase
$MgCl_2$	Magnesium chloride
MEK	Mitogen-activated protein kinase kinase
NaCl	Sodium chloride
NaF	Sodium fluoride
Na_3VO_4	Sodium ortho vanadate
P/S	Penicillin-Streptomycin; Pen Strep
PAGE	Polyacrylamide gel electrophoresis
PBS	Phosphate buffered saline
PDK1	Phosphoinositide-dependent protein kinase 1
PMSF	Phenylmethylesulfonyl fluoride
PVDF	Polyvinylidene difluoride
PI3K	Phosphatidylinositol-tri-phosphat kinase
PIP2	Phosphatidylinositol -di-phosphat
PIP3	Phosphatidylinositol -tri-phosphat
PKB	Protein kinase B
PP2A	Protein phosphatase 2A
PTEN	Phosphatase and tensin homolog
rpm	Rotations per minute
SDS	Sodium dodecyl sulfate
SDS-PAGE	Sodium dodecyl sulfate-polyacrylamide gel electrophoresis
SH2	Src-homology 2
SHP2	SH2-Phosphatase 2
TBS	Tris buffered saline
TBS-T	Tris buffered saline 2% TWEEN 20®
TEMED	N,N,N',N'-tetramethylethylenediamine
TWEEN 20®	Polyoxyethylene (20) sorbitan monolaurate (Polysorbate 20)

1 Introduction

1. Introduction

1.1 Insulin signaling

1.1.1 Insulin receptor

The insulin receptor (IR) and the related insulin-like-growth factor-1 receptor (IGF-1R) belong to the receptor tyrosine kinase family (RTKs). The tyrosine kinases are classified in membrane bound tyrosine kinases (e.g. EGF receptor) and non membrane bound kinases (e.g. Janus kinases). The IR and IGF-1R are membrane bound tyrosine kinases with an intrinsic tyrosine kinase activity, meaning that the kinase domain is part of the receptor. RTKs have common structural and functional characteristics. They all consist of an extracellular glycosylated ligand binding domain, a hydrophobic transmembrane domain, linking the ligand binding to the protein kinase domain, and an intracellular domain, subdivided in juxtamembrane region, the tyrosine kinase domain and the C-terminal part (Van Obberghen, 1994; Fantl et al., 1993; Hanks et al., 1988; Robertson et al., 2000; Schlessinger, 1988; Ullrich and Schlessinger 1990; Yarden and Ullrich 1988). RTKs are present in monomeric or dimeric form. After ligand binding the monomeric receptors form a dimeric structure (Massague and Czech, 1982). Src homology (SH) 2 proteins are able to bind and interact directly with the phophorylated RTKs (Pawson and Gish, 1992).

The IR is composed of two alpha (130 kDa) and two beta subunits (90 kDa). The extracellular alpha subunit is crosslinked to the extracellular part of the beta subunit by disulfide bonds, to form a functional transmembrane receptor. The extracellular alpha subunit represents the ligand binding domain; the cytoplasmic beta subunit harbours the receptor tyrosine kinase (AS 947-1343) transducing the ligand signal into the cell (Kasuga et al., 1983, Kahn et al. 1978, White et al. 1986). For dimerization an alpha-beta subunit is linked to another alpha-beta subunit via disulfide bonds, resulting in a $\alpha_2\beta_2$ heterotetramer structure (Van Obberghen, 1994).

Binding of the ligand (insulin) to the extracellular domain of the IR leads to a conformational change in the kinase inhibiting alpha subunit followed by a trans-autophosphorylation of the intracellular β subunit at seven tyrosine residues (Y953, Y960, Y1146, Y1150, Y1151, Y1316 and Y1322), transforming the inactive receptor into an active form (Heldin et al., 1995; Hubbard et al., 1994; DeMeyts et al., 1995; Ottensmeyer et al., 2000; Kahn et al., 1978; White and Kahn, 1994). Strong conformational changes occur in the tyrosine protein kinase after phosphorylation of the tyrosine residues Y1146, Y1150, Y1151, resulting in an open form (regulatory loop), allowing protein substrates to interact with the catalytical domain. Autophosphorylation of all three tyrosines in the regulatory loop leads to a 10-fold more active kinase (White et al., 1988; White and Kahn 1994; Hubbard et al., 1998). Tyrosine phosphorylation at Y960 allows the binding and phosphorylation of intracellular and multifunctional docking proteins (insulin receptor substrates (IRS)) to the activated receptor. These IRS proteins can recruit other intracellular signaling proteins thus transmitting the ligand signal from the cell surface into the cell (White, 1997; White 1998; White 2003).

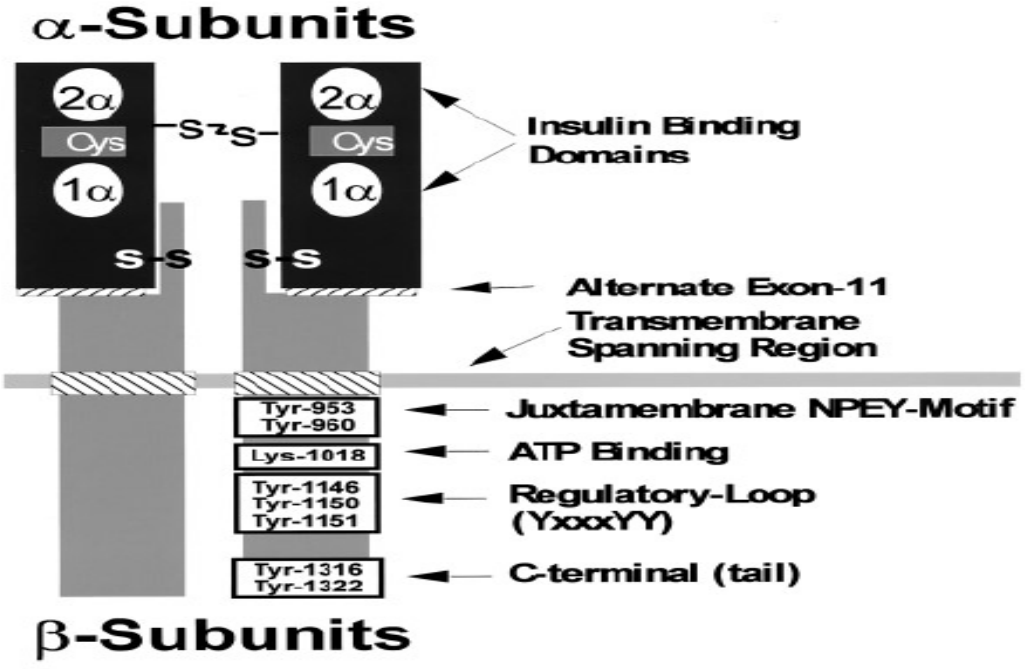

Fig. 1.1 Illustration of the insulin receptor
Insulin binding to the α-subunit of the tetrameric insulin receptor leads to autophosphorylation in the catalytic domain of the IR β-subunit. Four insulin binding domains are present in the α-subunit. The ATP binding site Lys-1018 is essential for the kinase activity of the IR β-subunit (White, 1997).

Besides phosphorylation of tyrosine residues, also serine and threonine residues of the IR are phosphorylated. In contrast to the activating tyrosine phosphorylation, serine or threonine phosphorylation inactivates the IR by inhibiting phosphorylation of receptor tyrosine residues. Serine kinases (e.g. AKT/PKB) and the receptor itself by autophosphorylation are able to phosphorylate IR at Ser 1275 and Ser 1309 (Pang et al., 1994; Mothe et al. 1996; Liu and Roth, 1994; Heidenreich et al., 1994; Al-Hasani et al., 1997; Tennagels et al., 2001).

Insulin is the predominant ligand binding to the IR inducing the dimerization and activation of the receptor. Insulin is a peptide hormone with a molecular weight of 5808 Da. The molecule is composed of 51 amino acids and synthesized in the islets of Langerhans in the pancreas. Insulin is responsible for glucose uptake and storage, food intake and cellular metabolism. Structurally it is a member of the superfamily of related insulin-like hormones. Insulin shares a 50% amino acid homology with IGF-1, another member of this superfamily (Rinderknecht et al., 1978; Le Roith, 1997; Adams et al., 2000; Brüning et al., 2000). Insulin binds to the IR with high affinity whereas no significant binding to IGF-1 is detected although its 50% homology to insulin. Due to the primary structural similarity of the IR and IGF-1R, hybrid receptors consisting of one IR isoform (IRa/IRb) and IGF1R are found. These receptors are dominated by the IGF-1 half thus IGF1 is bound with higher affinity and insulin with various affinities depending on the IR isoform. The physiological role of these hybrid receptors is not clear but they might play a role in switching from insulin to IGF1 signaling (Pandini et al., 2002).

The insulin peptide is derived from the precursor molecule proinsulin, processed by proteolytic enzymes (prohormone convertases 1 and 2, carboxypeptidase E). In this proteolytic process C-peptide is removed from the centre of the molecule, resulting in two polypetides of 21 and 30 amino acids, the A- and B-chain, bound to each other via intermolecular disulfide bonds (Steiner and Oyer, 1967). The bioavailability of insulin is regulated by hormones. Besides glucose itself gastrin, secretin, gastric inhibitory polypeptide (GIP) and glucagons-like-peptide (GLP) are mainly responsible for the secretion of insulin from the pancreas after food intake. Main target tissues for insulin action are liver, muscles and white adipose tissue (Vilsboll and Holst, 2004).

1.1.2 Insulin receptor substrate (IRS) proteins

The four different IRS proteins are functionally and structurally homolog and represent one protein family. IRS-1 was the first identified and cloned member of the IRS family (Sun et al., 1991). Subsequent alternative insulin receptor substrates (IRS-2, IRS-3 and IRS-4) have been identified (Sun et al., 1995; Lavan et al. 1997; Smith-Hall et al., 1997). IRS proteins function as adapter for numerous SH2 proteins, allowing different SH2 proteins attaching to the insulin receptor. The C-terminus of the IRS proteins harbours 8 to 18 potential tyrosine phosphorylation sites enabling IRS proteins the binding of diverse SH2 proteins. Thus phosphorylation of IRS protein tyrosine residues of the insulin receptor allows interaction with specific SH2 proteins, resulting in activation of different signaling pathways, depending on the recruited SH2 proteins (Myers et al., 1993). Differential distribution of IRS proteins on cellular and subcellular level and different affinities of the IRS proteins to a variety of SH2 proteins (due to variations of the sequence surrounding the tyrosine phosphorylation sites) can impact the activation of different signaling pathways. In addition the IR is able to interact with different IRS proteins resulting in an activation of diverse signaling pathways. With the IRS proteins acting as adapter a single receptor is able to amplify its signal via interaction with a large number of SH2 docking proteins (Myers et al., 1996).

IRS-1 and IRS-2 are ubiquitously expressed and mediate insulin and IGF-1 action in most tissues. IRS-3 expression is restricted to rodent adipocytes, expression of IRS-4 was mainly detected in the hypothalamus and pituitary gland, the thymus and kidneys (Schubert et al., 2003; Numan et al., 1999).

IRS proteins consist of defined functional domains. The pleckstrin homology (PH) domain is located at the N-terminus. This PH domain can bind to inositolphosphates of the plasma membrane therefore this region is supposed to play a role in the membrane localisation of the IRS proteins. The phosphotyrosine binding domain (PTB) is located C-terminal of the PH domain and essential for the interaction of IRS proteins with phosphorylated Y960 and the NPEY motive of the juxtamembrane region in the β subunit of the activated IR (White 2003; White 1997; Wang et al., 1993). After the phosphorylation IRS proteins can bind various SH2 effector proteins

e.g. phosphatidylinositol 3-kinase (PI3 kinase), growth-factor-receptor-binding protein (Grb2) or protein-phosphatase 2 (SHP-2) (Myers et al., 1994; Wang et al., 1993).

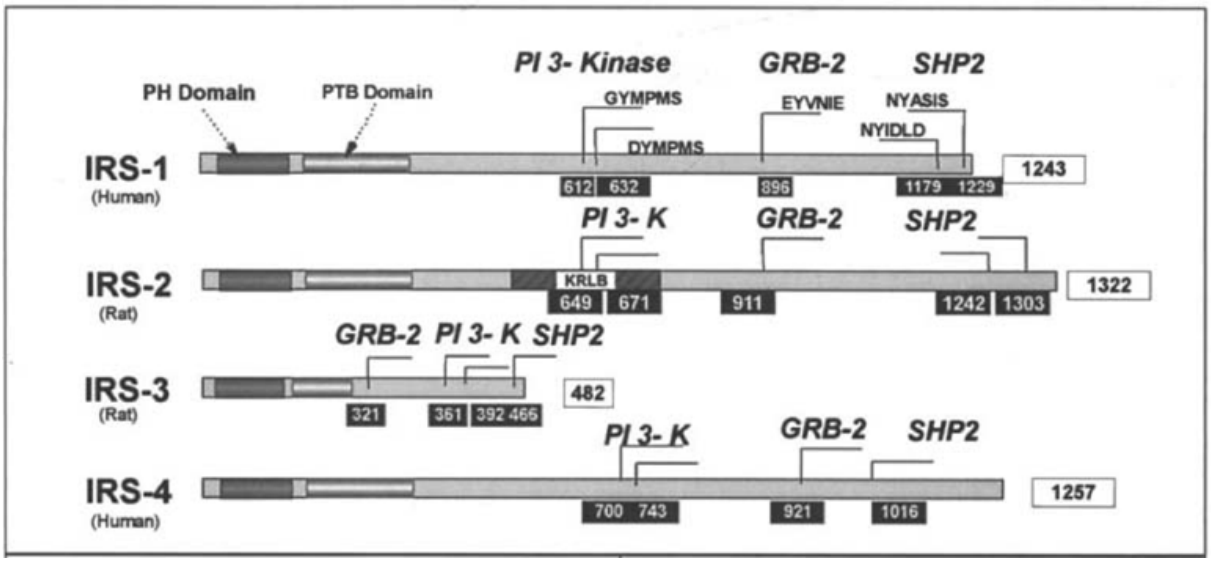

Fig. 1.2 Schematic structure of IRS proteins
Structure of the insulin receptor substrate family IRS-1, -2, -3 and -4 illustrated with their conserved N-terminal potential tyrosine phosphorylation sites PH and PTB. Interaction sites with SH2 proteins are shown in black boxes (Emkey and Kahn, 2001).

Insulin receptor substrate 1 (IRS-1) is widely expressed 185 kDa large protein. IRS-1 contains 22 potential tyrosine phosphorylation sites recruiting different SH2 proteins like PI-3 kinase, Grb2 (an upstream regulator of $p21^{ras}$), Nck, Crk, c-Fyn (Src family tyrosine kinase) and phospholipase Cγ (White et al., 1985, White 1997; Sun et al., 1991). IRS-1 is a key component of the cellular signaling system since it plays an important role in insulin/IGF-1 signaling and might also be phosphorylated indirectly by the Janus kinase, which in turn is phosphorylated by different cytokines, growth hormones, interferones (IFNα, INFβ, INFγ) and interleukins (IL-2, IL-4, IL-9, IL-13) (Burks et al., 2001; Chuang et al., 1994; Johnston et al., 1995; Myers et al., 1996; Uddin et al., 1995; Yenush et al., 1997). In addition inhibiting signals of TNFα and other factors can be transmitted via IRS-1 (Hotamisligil et al., 1994; Velloso et al., 1996). One of the best investigated downstream SH2 protein binding to the tyrosine phosphorylated IRS-1 protein is PI3-kinase. PI3-kinase is a dimeric enzyme composed of a catalytic subunit (p110α, p110β, p110δ) and regulatory subunit (p85α, p85β, $p55^{PIK}$) containing two SH2 domains (Myers et al., 1996). Following insulin stimulation IRS-1 tyrosine residues get phosphorylated, the regulatory subunit of PI3-kinase binds to IRS-1 and its activity increases and diminishes after prolonged insulin exposure due to serine phosphorylation and inhibition/degradation of IRS-1. Hence

insulin effects on gene expression as well as on cell proliferation are mediated and enhanced by IRS-1. These data suggest that IRS-1 plays an important role in cell growth, mitogenesis and proliferation in response to insulin (Myers et al., 1996; Rose et al., 1994; Sun et al., 1991; Sun et al., 1992; Waters et al., 1993; Yamauchi et al. 1994).

Besides the tyrosine phosphorylation sites IRS-1 contains over 30 potential serine/threonine phosphorylation sides (Sun et al., 1991, 1995). In an unstimulated state IRS-1 is mainly serine and weakly threonine phosphorylated. Upon insulin stimulation and IRS-1 tyrosine phosphorylation downstream target proteins like AKT/PKB are activated. AKT/PKB is a serine/threonine kinase, inducing a feed back loop by phosphorylating mTOR/P70-S6 kinase. Subsequently mTOR phosphorylates IRS-1 at Ser 636/639 mediating its proteasomal degradation (Zhande et al., 2002; O´Reilly et al., 2006).

Another effect upon insulin stimulation is the translocation of the GLUT-4 transporter to the plasma membrane. GLUT-1 and GLUT-4 transporters are responsible for removing glucose from the blood stream. GLUT-1 is predominantly expressed on the cell surface and does not respond to insulin; therefore it is supposed to provide basal glucose transport into the cells. GLUT-4 is nearby exclusively present in insulin sensitive tissues (e.g. muscle and adipose tissue). In a non active state GLUT-4 is incorporated in an intracellular vesicular compartment. Binding of PI3-kinase to phosphorylated IRS-1 causes activation of PKB/AKT and translocates GLUT-4 containing vesicles to the plasma membrane. Thus insulin stimulated glucose uptake is mediated by GLUT-4 and its translocation to the plasma membrane (Lienhard et al., 1992; Okada et al., 1994). Since PI3-kinase is a downstream target of IRS proteins, the IRS proteins play an important role in translocation of GLUT-4 to the cell surface upon insulin stimulation and in glucose uptake into insulin sensitive tissues (Backer et al. 1992; Lavan et al., 1997; Sun et al., 1991). Insulin stimulation has also a major impact on protein synthesis of cells by increasing mRNA levels and promoting translation initiation. P70-S6 kinase phosphorylates S6 protein of the 40s ribosomal subunit leading to increased mRNA cap binding and initiation of the mRNA – protein translation (Proud 1994; O´Brien 1994, Hu et al., 1994; Pause et al., 1994). Different experiments show that IRS-1 regulates protein synthesis via PI3-kinase and not as first supposed via the MAP kinases (Lin et al., 1994; Lin et al., 1995; Graves et al., 1995).

Insulin receptor substrate 2 (IRS-2) was the first identified alternative insulin receptor substrate. IRS-2 is about 100 amino acids longer than IRS-1. The C-terminal region of IRS-2 is poorly conserved compared with IRS-1 (35% identity) whereas the PH and PTB domains of both proteins show a 65% and 75% sequence identity, respectively. Overall both proteins show a 43% homology. In the middle of the IRS-2 protein (AS 591-786) a unique region, not existing in the IRS-1 protein, was identified. This so called kinase regulatory loop binding domain interacts with three phosphotyrosines (Tyr 1146, 1150, 1151) of the insulin receptor β subunit and /or accessible regions in this regulatory loop after the autophosphorylation of the tyrosines. Via this domain the receptor is able to differentiate between the two substrates and this heterogeneity contributes to the unique signaling potential of each IRS protein (Giovannone et al., 2000; He et al., 1996; Sawka-Verhelle et al., 1996; Sun et al., 1995; Sun et al., 1997; White, 1997). Like IRS-1, IRS-2 can interact with PI3-kinase, Grb2 and the phospholipase Cγ but unlike IRS-1, IRS-2 is not interacting with Src homology protein tyrosin phosphatase 2 (SH-PTP2, Syp). In adipocytes phosphorylation of IRS-1 increases after insulin stimulation whereas IRS-2 phosphorylation remains almost in basal state. Immunoprecepetation of p85 (regulatory subunit of PI3-kinase) upon insulin stimulation showed a strong interaction of PI3-kinase with phosphorylated IRS-1 and IRS-2. Co-immunoprecipitation with α-PY (phosphotyrosine) antibody revealed the majority of active PI3-kinase bound to IRS-1.

But IRS-2 is able to compensate for IRS-1 deficiency in adipocytes of IRS-1 knockout mice sustaining insulin signaling in these cells. This shows that inhibition of IRS-1 is not sufficient to abrogate insulin signaling because of the presence of IRS-2 in most tissues and a likely compensation (Araki et al., 1994; Sun et al., 1997; Yamauchi et al., 1996).

1.1.3 Insulin signaling cascades

The insulin signal transduction cascade starts with the autophosphorylation of the IR, after ligand binding to the corresponding α subunit of the receptor, and the subsequent binding of the IRS proteins to the IR. Initially a conformational change leading to an activation of the intrinsic receptor tyrosine kinase is followed by intracellular phosphorylation. Full activation of the receptor kinase domain leads to

phosphorylated tyrosine residues in the IR representing docking sites for SH2 domain containing signaling proteins. The consensus sequence of the receptor phosphotyrosines is LxxxxNPxYxSxP (Keegan et al., 1994). IRS and Shc proteins interact with the receptor by recognizing this phophotyrosine motive.

The IRS proteins bind to the receptor via their PTB domain by interacting with phosphorylated Y960 of the activated receptor (White 1997). Deletion of the PH domain of IRS proteins leads to an attenuation of IR-IRS binding, indicating that besides PTB also the PH domain represents an essential domain for IRS receptor binding (Yenush et al., 1996). After being phosphorylated by the tyrosine receptor kinase at specific tyrosine phosphorylation sites, these proteins function as adapter, binding SH2 domains of downstream effector proteins linking the receptor to signaling molecules, like PI3K regulatory subunit (p85) or the MAP kinase pathway (White et al., 1998; Sun et al., 1993, Myers et al., 1994). As a downstream target PI3-kinase represents a key molecule for various cellular processes like proliferation, survival and glucose uptake (Okada et al., 1994). PI3K also functions as a signaling relay for the insulin receptor transmitting insulin´s signal to AKT (proteinkinase B (PKB)), protein S6 kinase or PKC (Franke et al., 1995, Diaz-Meco et al., 1994, Mendez et al., 1996). Upon insulin stimulation PI3K binds to phosphorylated IRS proteins via its two SH2 domains of the p85 subunit. IRS-1 contains nine potential c-terminal tyrosine phosphorylation sites harbouring phosphorylation motives detected by SH2 domains. Following p85 subunit binding to phosphorylated IRS, conformational changes in the regulatory subunit activate the catalytic subunit of PI3K, p110 (Backer et al., 1992; Myers et al., 1992).

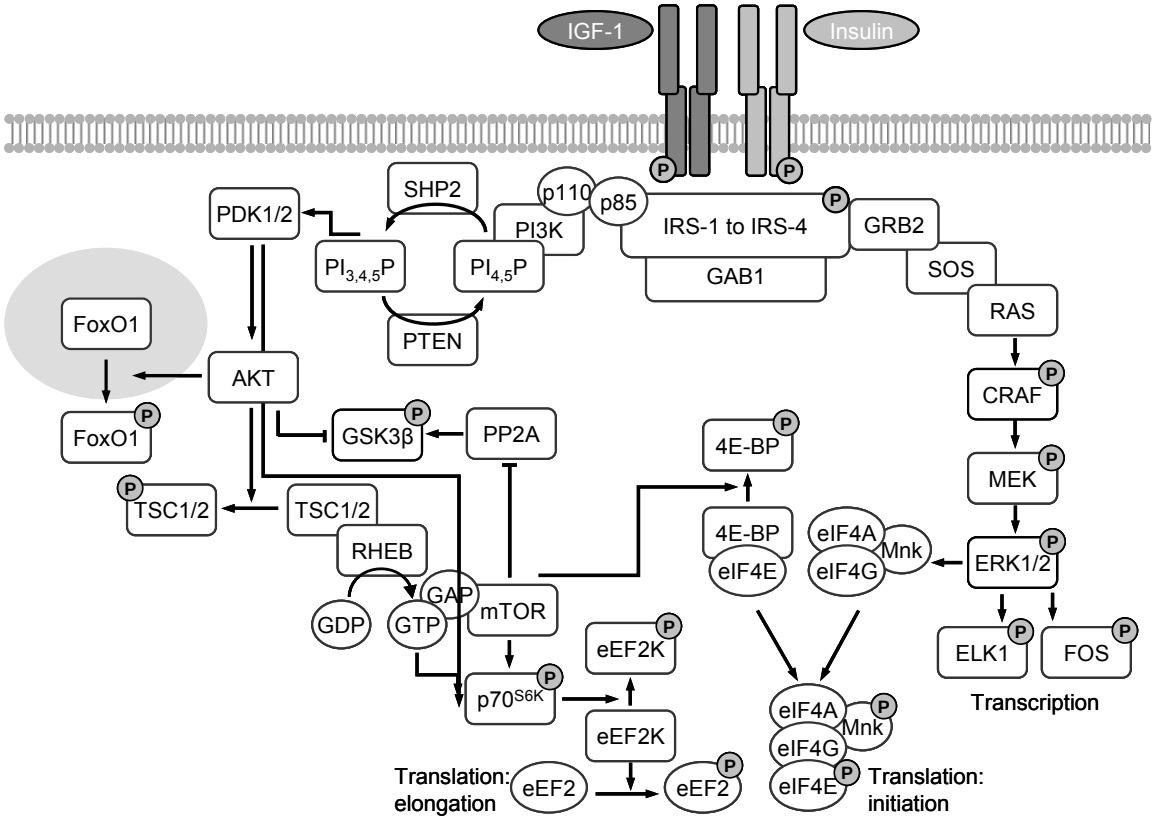

Fig. 1.3 IR/IGF-1R signaling cascade
Binding of Insulin or IGF-1 to the IR/IGF-1R causes autophosphorylation and activation of the receptor. Insulin receptor substrates are recruited to the activated receptor. Phosphorylation of IRS proteins activating signaling cascades via MAP kinase (MAPK, mitogen activated protein kinase) and phosphatidylinositide (PI)3-kinase (PI3K) pathway, transducing insulin signal into the cell (Freude and Schubert, 2010).

The PI3-kinase (PI3K) pathway: PI3K binds via its p85 regulatory subunit to the activated IRS adapter proteins and activates the p110 catalytic subunit of PI3K, to switches on a cascade of several downstream serine and threonine kinases like the serine kinase PDK1 (3-phosphoinositide dependent kinase), PKB (protein kinase B, AKT) and protein kinase C (PKC) (Alessi and Cohen 1998; Myers et al., 1994). Phosphorylation of phospatidylinositol (4, 5)-bisphosphate (PIP2) at the inner plasma membrane results in the production of phospatidylinositol (3, 4, 5)-trisphosphate (PIP3) (Shepherd et al., 1998). In the PI3-kinase-signaling transduction PIP3 recruits PDK to the inner plasma membrane which leads to an activation of PDK which in turn interacts with and phosphorylates AKT at Thr 308 and Ser 473 for full activation. PI3-kinase pathway is negatively regulated by PTEN, a phospholipid phosphatase and tumor suppressor, dephosphorylating PIP3 and shutting down PI3K and downstream activity. Three isoforms of AKT (AKT 1-3) exist in mammals with a high degree of amino acid homology and indistinguishable substrate specifity *in vitro*. AKT-1

represents the dominating isoform in the majority of tissues and AKT-2 might be the dominating isoform in insulin responsive tissues (Maira et al., 2001; Du et al., 2003; Gao et al., 2005; Bhaskar et al., 2007; Sulis and Parsons, 2003; Burgering et al., 1995, Walker et al., 1998). AKT phosphorylates and thereby deactivates GSK3α/β (at $Ser^{21/9}$) and the forkhead-O transcription factor (FoxO1) (Virkamäki et al., 1999; Jiang et al., 2003). Phosphorylated forms of transcription factor FoxO1 are excluded from the nucleus resulting in reduced transcription of FoxO1 target genes leading to various cellular consequences since FoxO1 target genes are involved in different cellular processes like proliferation, metabolic regulation, apopotosis and longevity (Barthel et al., 2005). AKT interacts with another protein called mTOR (mammalian target of rapamycin), a Ser/Thr kinase. mTOR can be found intracellular in two different complexes, mTORC1 and mTORC2. mTORC1 is sensitive to and inhibited by rapamycin whereas TORC2 is not regulated by rapamycin (Loewith et al., 2002). Both complexes have different downstream targets and both complexes have age specific functions and been linked to longevity. Raptor (regulatory associated protein of mTOR) is a unique protein of mTORC1 whereas Rictor (rapamycin insensitive companion of mTOR) is unique for mTORC2. mTORC2 itself can phosphorylate AKT independently of the PI3-kinase pathway (Wullschleger et al., 2006). mTORC1 on the other hand is activated indirectly by AKT. By phosphorylation TSC2 is inhibited a protein dimerized with TSC1. AKT phosphorylation of TSC2 disrupts the TSC1/TSC2 GAP activity thus allowing GTP bound Rheb to activate mTOR. Since TSC1/TSC2 complex is regulating mTORC1 in mammalian cells by integrating intracellular and extracellular signals, AKT regulates mTOR activity and the downstream targets of mTOR eukaryotic initiation factor 4E (eIF-4E) binding protein-1 (4E-BP) and protein S6 kinase 1 (P70-S6K) as upstream kinase. Following mTOR phosphorylation eIF-4E is released from 4E-BP and mRNA translation is initiated leading to synthesis of proteins controlling cell proliferation. Phosphorylation of P70-S6K by mTORC1 causes activation of ribosomal proteins and finally an initiation of protein synthesis. TSC2 is also regulated by other growth factor induced kinases like ERK2 (Bhaskar et al., 2007; Ma et al., 2005). The extracellular regulation of mTORC2 is not clear so far but it has been shown that insulin stimulates mTORC2 activity. Additionally mTORC2 was identified as responsible kinase for AKT Ser 473 phosphorylation and therefore has to act upstream of AKT. But besides mTOR other kinases like ATM can activate AKT by Ser 473 phosphorylation. For full activation of AKT both Ser 473 and

Thr 308 have to be phosphorylated and mentionable in this case is that Thr 308 is phosphorylated independently of Ser 473 (Woodgett 2005; Shiota etal., 2006; Sarbassov et al., 2006; Guertin et al., 2006; Frias et al., 2006; Bhaskar et al., 2007). Lately it has been shown in *C. elegans* and yeast that mutations mTOR pathway are associated with lifespan extension by inhibition of IIS signaling and thus activation of FoxO transcription factors (Kenyon, 2010; Kaeberlein et al., 2005).
Inhibition of GSK3α/β by AKT phosphorylation has a strong impact on glycogen synthesis. Glycogen is the major form of glucose storage in the muscle and is controlled by two pathways the PI3-kinase-pathway and the MAP kinase pathway (Cross et al., 1995; Dent et al., 1990).

MAP-kinase pathway: The MAP-kinase pathway is the second pathway activated after IR activation. Growth factor receptor binding protein 2 (Grb2) links the IR signal to the MAP-kinase pathway by binding to phosphorylated IRS proteins. Grb2 is an adaptor protein for the $p21^{ras}$ guanine exchange factor son of sevenless (SOS) and thus connecting SOS to IRS proteins.
IRS-Grb2-SOS complex interacts with another protein; a membrane bound protein named Ras at which SOS induces the nucleotide exchange of guanosine-diphosphate (GDP) to guanosine-triphosphate (GTP). This exchanges leads to the activation of Ras by converting the protein into its active form. Activated Ras causes the membrane recruitment and activation of Raf-1 (c-Raf; MAPKKK). This enables Raf-1 to phosphorylate Ser and Thr residues of mitogen-activated protein kinase kinase -1/-2 (MEK-1/-2; MAPKK). Phosphorylated MEK-1/-2 in turn transduce insulin signaling further downstream by activation of extracellular signal-regulated kinases (ERK-1/-2; MAPK) by phosphorylation of Tyr and Thr residues (Anderson et al., 1990; Davis 1993; Sasaoka and Kobayashi 2000; Skolnik et al., 1991). The MAP-kinase pathway activates various downstream targets like MAPK-activated protein kinase 1 ($p90^{rsk}$), MYC and ELK. One target of $p90^{rsk}$ is GSK3α/β, inactivating glycogen-synthase-kinase 3 leads to an insulin stimulated elevation of glycogen synthesis since the enzyme for this process glycogen synthase is active and not inhibited by GSK3α/β (Sutherland et al., 1993; Sutherland and Cohen 1994). Besides increasing glycogen synthesis MAP-kinase pathway activates genes important for cell cycle progression and hence affecting cell proliferation and differentiation. In order to enhance gene expression MAP kinases migrate to the nucleus

phosphorylating transcription factors like ELK resulting in increased gene activity (Seth et al., 1992). c-Fos promoter and activation of other transcription factors like c-Jun connecting MAP-kinase pathway to mitogenesis (Pulverer et al., 1991; Shaw et al., 1989).

1.2 Mouse model

The mouse model used in present thesis to investigate the influence of the IRS-1 signaling transduction on energy homeostasis was kindly provided by Professor Takashi Kadowaki. The transgenic mouse model was generated by conventional mutagenesis.

For a conventional gene targeting homologous recombination is used to delete, add or to disrupt a gene. To target a specific gene first a DNA construct with a selectable marker is generated in bacteria. This exogenous DNA construct is then inserted into mouse embryonic stem cells (ES) and exposed to selection. Cells with inserted exogenous DNA construct (or selection marker, respectively) are used for embryonic injection. On the basis of homologous recombination the DNA construct is able to integrate into the host DNA and to displace the natural gene (Sedivy and Joyner, 1992).

To obtain an IRS-1 knockout mouse the first exon of the IRS-1 gene was targeted. The targeting vector was inserted 3´ of the translation initiation site of the IRS-1 gene. The inserted construct contained a *pgk-1* promotor with several stop codons, so that the insertion of the *pgk-1* gene promoter results in a destabilized mRNA of IRS-1 (Tamemoto et al., 1994).

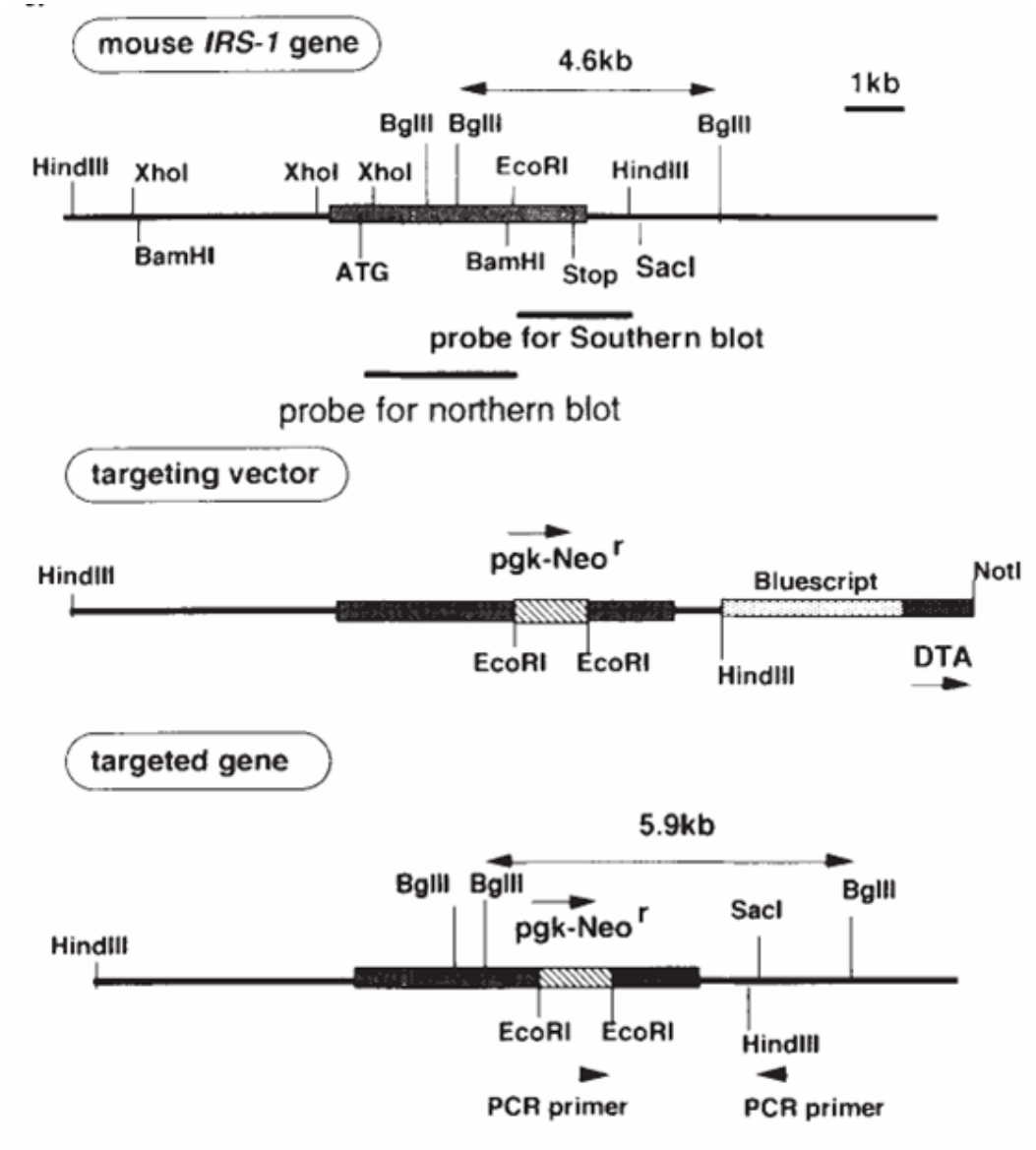

Fig. 1.4 Cloning strategy for conventional IRS-1 knockout in mouse
Schematic representation of mouse IRS-1 gene, targeting vector and targeted allele. Exact principle creating IRS-1 knockout mouse described in the text above (Tamemoto et al., 1994).

The homozygous IRS-1 knockout mouse shows normal development but is retarded in embryonic and postnatal growth, with a weight reduction compared to wild type of about 40-50%. Levels of IGF-1 and growth hormone (GH) were normal and no histological abnormalities have been observed. These mice show a mild to moderate insulin resistance with normal glucose tolerance (Araki et al., 1994; Tamemoto et al., 1994). The IRS-1 deficiency is compensated by elevated production and secretion of insulin from the pancreatic β-cells. The elevated insulin production is achieved by islet hyperplasia meaning that the number of β-cells in these mice is about 2-fold increased compared to wild type mice (Patti et al., 1995). Another aspect of

compensation in these mice leading to a relative unaltered insulin/glucose metabolism is that IRS-1 might be functionally replaced by IRS-2 in some tissues (e.g. liver), whereas in another insulin sensitive target tissue, the muscle insulin response is diminished to 20%. This results in a normal glucose homeostasis by preventing gluconeogenesis via IRS-2 in the liver and a slowed down but not diminished glycogen synthesis in the muscle (Yamauchi et al., 1996). In contrast heterozygous IRS-1/IR knockout mice display a strong diabetic phenotype indicating that these combined gene defects can not be compensated by any other mechanism (Brüning et al., 1997). Overall these data show that IRS-1 deficiency might be compensated in some tissue like liver and pancreatic β-cells more effectively than in skeletal muscle and fibroblasts. Although suffering mild insulin resistance IRS-1 knockout females (not males) demonstrated increased life span, due to resistance to several age related pathologies, age related glucose intolerance and age associated changes of T-cell population (Selman et al., 2008).

IRS-2 knockout mice in contrast to the IRS-1 knockout mouse display a typical diabetic phenotype similar to human type 2 diabetes. They show insulin resistance and glucose intolerance from birth on or a few weeks after birth, respectively. Male IRS-2 knockout mice die due to massive hyperglycaemia and β-cell failure in 10 to 16 weeks after birth (Burks et al., 2000; Withers et al., 1999). Causative for that are peripheral insulin resistance (glucose uptake disruption of the muscle) and failure to inhibit gluconeogenesis in the liver. Accordingly these mice progressively develop a fasting hyperglycemia as a consequence of reduced β-cell mass, leading to β-cell dysfunction (β-cell mass is about 50% declined compared to wild type mice) and peripheral insulin resistance (Withers et al., 1998). In contrast to IRS-1 knockout mice these defects in muscle and liver of IRS-2 mice are not compensated by elevated insulin levels as a result of accelerated insulin production in the β-cells. Since IRS-2 plays an important role in development, neogenesis, proliferation and survival of β-cells IRS-2 knockout mice show the expected diabetic phenotype (Kornmann et al., 1998; Withers et al., 1999). Hepatic insulin resistance and β-cell failure, rather than the lack of IRS-2 are the main mechanisms and causative for diabetic phenotyp in these mice (Higaki et al., 1999).

In summary IRS-1 is supposed to be a major factor for insulin signaling in muscle and adipose tissue whereas IRS-2 is important for insulin signaling in liver. In addition to insulin signaling in peripheral tissues IRS-1 and IRS-2 are involved in

insulin secretion and development of pancreatic β-cells, respectively (Aspinwall et al., 2000; Kido et al., 2000).

1.3 Mitochondria

Mitochondria are organelles of eukaryotic cells of 1 to 5 µm length migrating in the cytoplasm essential for various processes like glucose and fat oxidation and energy production. Mitochondria produce the majority of ATP required for cellular processes. Depending on cell type and energy demand of the tissue the mass of mitochondria differ from about 10 up to 1000 per cell. Mitochondria are maternal inherited. The structure of mitochondria is defined by a phospholipid bilayer membrane consisting of highly specific macromolecular structures, the inner mitochondrial membrane (IMM) and the outer mitochondrial membrane (OMM). Mitochondria are subdivided by this double membrane layer into two different aqueous compartments. In between OMM and IMM the non-plasmic mitochondrial intermembrane space is located (IMS) and the IMM covers the plasmatic mitochondrial matrix. The mitochondrial matrix is further subdivided into mitochondrial inner boarder membrane and the mitochondrial cristae membrane. These cristae represent invagination of the IMM function as surface extension of this membrane, pointing into the mitochondrial matrix. Cristae structure can vary from lamellar to vesicular or tubular morphology depending on cell type and metabolic conditions. Metabolic activity of tissues or cells depend on the characteristic shape of cristae and mitochondrial quantity (Gilkerson et al., 2003; Mannella et al., 2001; Perkins et al., 1998; Prince et al., 2002; Zick et al., 2009; Vogel et al., 2006). The outer mitochondrial membrane is permeable for small metabolic products. In addition to this passive transport active transport of molecules from 5000 to 10000 kDA is achieved via porine channel proteins. In contrast to the outer membrane the inner membrane is impermeable for almost any molecule and ion unless specialized transport systems are used (Bernardi, 1999).

Mitochondria have the ability to fuse and to fission. Hence mitochondria are dynamic organelles. Fusion and fission events influence activity of mitochondria. Fused mitochondria form a mitochondrial network. Fusion is an essential event for mitochondria since besides exchange of proteins dysfunctional mitochondria might

be erased by autophagy during this process (Chan, 2006; Bereiter-Hahn and Voth 1994; Bleazard et al., 1999; Nunnari et al., 1997).

The fact mitochondria are surrounded by a double lipid layer promote the idea of the endosymbiotic theory. Mitochondria originated from a process 1,5 billion years ago in which precursor of α-proteobakteria merged with an eukaryotic precursor cell. This process became essential as a consequence of raising oxygen levels in the atmosphere to avoid toxic effects. Under these conditions the aerobic production of ATP via the mitochondrial respiratory chain was of central interest for survival and evolution. In anaerobic conditions energy is generated by glycolysis and met the energy demand of cells. Symbiotic invading of aerobic into anaerobic cells enabled the cells to cellular respiration and adaptation to an aerobic situation by using an effective system for energy production. The merging of two different cells designed a cell type existing with two different originated sets of DNA. Via different metabolic pathways these two sets of DNA were linked to each other and therefore are not independent of each other. During evolution numerous mitochondrial genes were transferred to the nucleus of the eukaryotic cell causing that mitochondrial DNA is coding for only a few of its essential proteins. The characteristic circular DNA in the mitochondrial matrix (mtDNA) and an own machinery for protein synthesis (mitochondrial ribosomes) support the idea of bacterial background of mitochondria (Lang et al., 1999; Chen and Butow, 2005; Burger et al., 2003; Margulis, 1971; Gray et al., 1999; Reichert and Neupert, 2004; Andersson et al., 1998; Kurland and Andersson, 2000; Lopez et al., 2000).

mtDNA is mainly encoding for subunits of the mitochondrial respiratory chain complexes. Since the major part of mitochondrial proteins is encoded and transcribed in the nucleus, translated and synthesised in the cytoplasm, a coordinated transport of these nuclear encoded mitochondrial proteins into the mitochondria has to be accomplished by the cell. By fusing short signaling peptides to the synthesised protein, these proteins are guided to and into the mitochondria. The conduction of these proteins into the mitochondria is unidirectional and taken over by specialized channel proteins in the mitochondrial membranes, the translocase complexes TIM (translocase of the inner membrane of mitochondria) and TOM (translocase of the outer membrane of mitochondria). TOM complex is located and integrated in the outer mitochondrial membrane directing protein import from cytosol to mitochondria. TIM complex is located and integrated in the inner mitochondrial membrane

mediating protein import over the IMM into the mitochondrial matrix. Only in the case of apoptosis mitochondrial proteins are released into cytoplasm (Danial and Korsmeyer, 2004; Pfanner und Meijer 1997, Neupert, 1997; Ryan et al., 2000; Sirrenberg et al., 1996).

Mitochondria are important for various cell functions e.g. energy supply, fat and glucose oxidation, phospholipid synthesis, amino acid metabolism, apoptosis, calcium homeostasis, synthesis of iron sulfur cluster and heme molecule (Lill and Kispal, 2000; Green and Kroemer, 2004; Bianchi et al., 2004; Szabadkai and Rizzuto, 2004). Proteins and enzymes located in the mitochondrial matrix are largely involved in metabolic processes e.g. β-oxidation (oxidation of FFA), Krebs cycle (oxidation of pyruvate) and oxidative phosphorylation. The IMM contains five integrated multi subunit enzyme complexes. Four of them form the respiratory chain, consisting of NADH-coenzyme Q oxidoreductase (complex I), succinate-coenzyme Q oxidoreductase (complex II), Q-cytochrome c oxidoreductase (complex III), cytochrom c oxidase (complex IV). Complex V represents the ATPase or F_0F_1-synthase, depending of the direction of the catalyzed enzymatic reaction. Electrons of the reductive equivalents NADH and $FADH_2$ generated in enzymatic reactions of the Krebs cycle by oxidation of acetyl-CoA (product of the glycolysis and β-oxidation end product pyruvate) enter the respiratory chain in the case of NADH via complex I and for $FADH_2$ via complex II. Charged electrons are taken over by Coenzyme Q and transported through the hydrophobic surrounding of the IMM to complex III. The transport of the electrons from complex III to complex IV is provided by cytochrome c. In complex IV electrons are passed to molecular oxygen via cytochrome a reducing molecular oxygen to H_2O ($1/2\ H_2O + 2\ H^+ + 2\ e^- \rightarrow H_2O$). Redox reactions of stepwise electron transfer from complex to complex in the respiratory chain are extremely exergonic reactions, the energy of these reactions is used by mitochondria to pump protons (H^+) from the matrix against the present gradient of the IMM into the mitochondrial inter membrane space. This leads to changes in the pH value of the inter membrane space. The gradient harbours energy used by complex V for generating ATP. Protons reflux back to the mitochondrial matrix through a proton channel of the ATP synthase restoring chemical equilibration. Energy released in this process is used by the F_0 subunit of the ATP synthase to phosphorylate ADP, producing ATP with an intrinsic energy of 19,3 kJ/mol conserved in the chemical

bond of ADP and anorganic phosphate (Mitchell, 1961; Bernardi, 1999; Janssen et al., 2006; Sun et al., 2005, Eichler and Schertel 1988; Jockel et al., 1998).

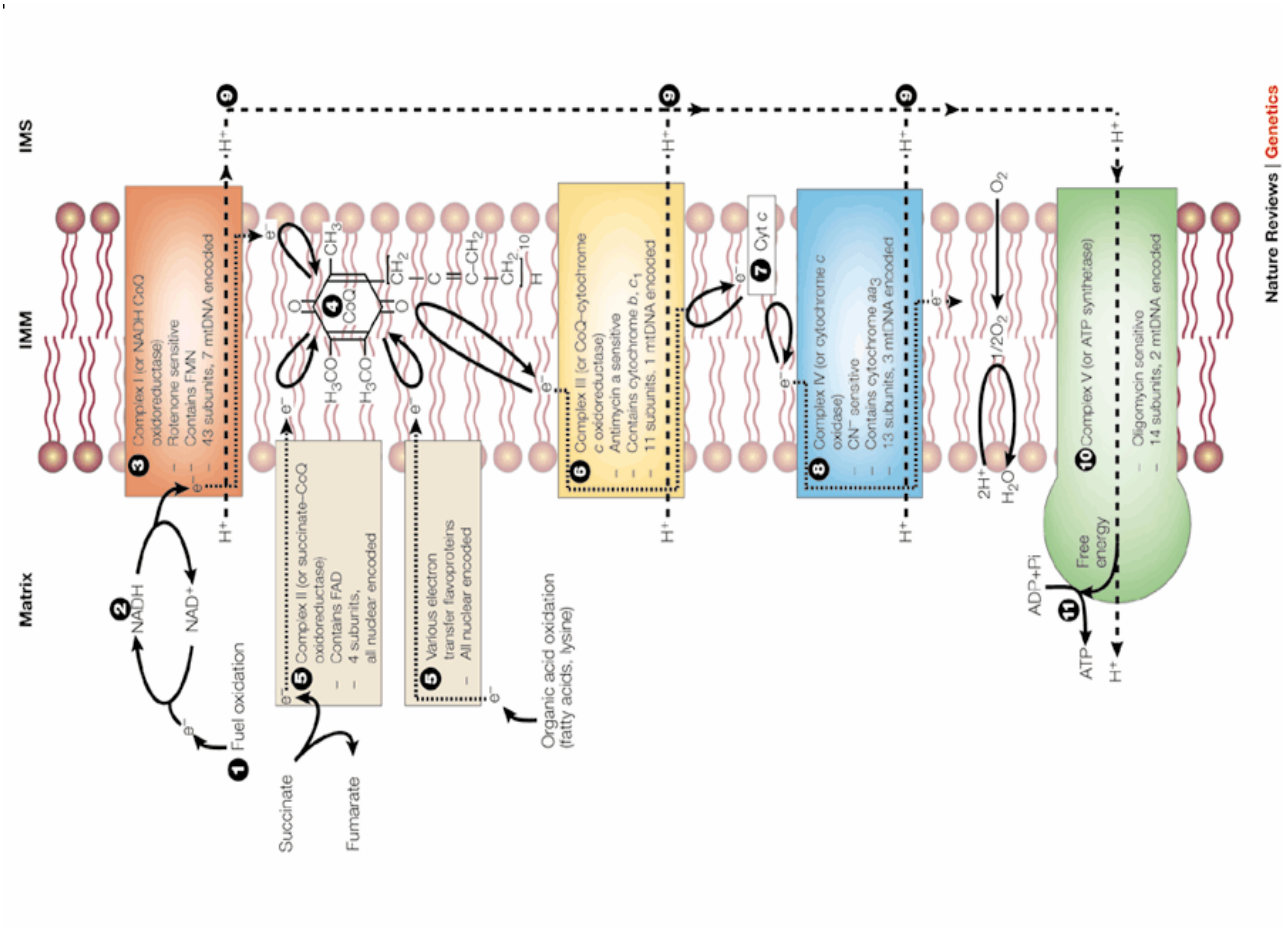

Fig. 1.5 Mitochondrial respiratory chain
Electrons are transferred by the reductive equivalents NADH to complex I and $FADH_2$ to complex II. The electron transport is used by complex I, II and IV to build up a proton gradient. Additionally electrons cause the reduction of oxygen to water at complex IV. The proton gradient is used by complex V to catalyze binding of inorganic phosphate to ADP (Smeitink et al., 2001).

1.4 Mitochondrial dysfunction and insulin resistance

Mitochondrial function is required for normal glucose stimulated β-cell insulin secretion, oxidation of fatty acids, amino acid metabolism as well as ATP production (Luft, 1994). Free fatty acids (FFA) are important energy carrier for muscles and have a striking impact on the pathogenesis of insulin resistance. Decreased mitochondrial activity might be linked to increased intramyocellular fat content (Groop, et al., 1991; Bajaj et al., 2005; Petersen et al., 2003; Petersen et al., 2004). Lipids and intermediates of lipid metabolism accumulate if fatty acid delivery in tissues exceeds

mitochondrial fat (β-)oxidation (Schrauwen-Hinderling et al., 2007). Cytokines secreted by adipose tissue and intracellular fatty acids negatively influence insulin sensitivity of insulin target tissues liver and muscle and hence attenuate their insulin responsiveness. (Lazar, 2005; Boden and Shulman, 2002). Intracellular fatty acids induce insulin resistance by inhibition of glucose uptake. Type 2 diabetes subjects show reduced fat oxidation and a failure of insulin to inhibit lipolysis leading to increased plasma FFA levels and enhanced influx in muscles. Elevated levels of fatty acid metabolites like acetyl coenzyme A (CoA) and diacylglyerol due to impaired mitochondrial fat oxidation, thought to play a critical role in activating pathways leading to suppression of insulin signaling. Diacylglycerol is an activator for protein kinase C (PKC), PKC in turn switches on a serine kinase cascade causing increased serine phosphorylation of IRS-1. Phosphorylation of IRS-1 at Ser 307 inhibits insulin receptor stimulated tyrosine phosphorylation of IRS-1 thus shutting down insulin signaling. Since IRS-1 is important for GLUT-4 translocation to the plasma membrane, hence deactivation of IRS-1 causes suppression of insulin stimulated glucose uptake and inhibits removal of glucose out of the blood stream. Therefore metabolic disturbances like decreased mitochondrial fatty acid oxidation and/or reduced mitochondrial content results in defective fatty acid metabolism and intracellular accumulation of fatty acids and might be responsible for insulin resistance. Obese and type 2 diabetes patients reveal reduced PGC1α/β mRNA levels up to 71% and consequently downregulated protein levels of PGC-1α and PGC-1β as well as their target genes. Reduction in PGC-1 expression is a result of elevated plasma free fatty acids (FFA) demonstrated by high fat feeding causing decrease of PGC-1 mRNA levels (Sparks et al., 2005; Hoeks et al., 2006; Richardson et al., 2005; Heilbronn et al., 2007; Lowell and Shulman, 2005; Dresner et al., 1999; Shulman, 2000, Wu et al., 1999; St-Pierre et al., 2003; Mootha et al., 2003). PGC-1 is a regulator of mitochondrial biogenesis controlling genes being part of a cluster of oxidative proteins. These genes encode for key enzymes in oxidative metabolism and mitochondrial function, hence reduced expression of this cluster has strong effects on mitochondrial function like OXPHOS and might also explain accumulation of fat in affected tissues (Schrauwen-Hinderling et al., 2007; Mootha et al., 2003; Patti et al., 2003). In addition to GLUT-4 translocation and glucose uptake mitochondrial metabolism is required for insulin secretion upon increasing glucose levels. Obese individuals develop diabetes most likely due to failure of β-cells to

increase insulin secretion in response to the growing demand of insulin to elevated glucose levels. This is caused by inadequate compensation of the existing β-cell mass and/or inappropriate β-cell response to higher glucose levels (Lowell and Shulman, 2005; Rhodes, 2005; Gerich, 2003). Patients suffering type 2 diabetes show decreased β-cell mass caused by increased apoptosis (Butler et al., 2003; Pick et al., 1998). Defective glucose sensitivity of β-cells might particularly be caused by mitochondrial malfunction. Adequate β-cell response to glucose requires oxidative mitochondrial metabolism generating the appropriate amount of ATP. Mitochondria increase ATP levels by oxidative phosphorylation arising from glucose oxidation and consequently alter the ATP/ADP ratio in β-cells. Increased ATP/ADP ratios initiate inhibition of ATP/ADP regulated potassium channel (K_{ATP}). Subsequently opening of voltage gated calcium channel stimulates calcium influx into the cell, resulting in insulin secretion. Uncoupling protein 2 (UCP-2) lowers oxidative mitochondrial ATP synthesis by collapsing the inner membrane potential of mitochondria, decreasing ATP/ADP ratio and finally insulin secretion from β-cells. Since the amount of ATP generated by oxidation of glucose is diminished by UCP-2, glucose stimulated insulin secretion is negatively controlled by this protein. UCP-2 expression is stimulated by hyperglycemia (glucotoxicity) and high lipid levels (lipotoxicity) in animal models with type 2 diabetes and UCP-2 deficiency is associated with improved β-cell function. UCP-2 expression is elevated by superoxide and superoxide levels are increased in β-cells of type 2 diabetic individuals, leading to enhanced β-cell dysfunction (Prentki et al., 2002; Chan et al., 2001; Joseph et al., 2002; Bindokas et al., 2003; Zhang et al., 2001; Krauss et al., 2003; Krauss et al., 2002; Lowell and Shulman, 2005; Maechler and Wollheim, 2001).

In addition to this so called “mitochondrial dysfunction” negative effects on cytoplasmic glycogen synthesis and glucose oxidation were observed. Furthermore dysfunctional mitochondria show reduced ability to switch from fat oxidation in fasting state to glucose oxidation after insulin stimulation due to so called “metabolic inflexibility” (Wititsuwannakul and Kim, 1977; Schrauwen-Hinderling et al., 2007; Kelley and Mandarino, 2000).

Furthermore human aging is correlated with alteration in mitochondrial DNA (mtDNA). Decreased mtDNA and mutated mtDNA lead to reduction in mRNA levels of mitochondrial genes and thereby diminishing oxidative enzyme activities. Whether

mitochondrial dysfunction is a consequence of accumulation of mtDNA alteration is controversially discussed (Kelley et al., 2002; Dufour and Larsson, 2004).
Another unsolved issue in this field is the question if mitochondrial defects in insulin resistance are cause or consequence. Other theories in this field of research postulate that increased intramyocellular fat content lead to increased mitochondrial fat oxidation and subsequent resulting in enhanced generation of reactive oxygen species (ROS). To avoid increased cellular damage by elevated ROS and other toxic molecules mitochondrial oxidative phosphorylation is downregulated by cells as physiological response. In this case this mitochondrial defect would be a secondary effect to insulin resistance (Abdul-Ghani and DeFronzo, 2008; Brehm et al., 2006).

1.5 Energy homeostasis

Hypothalamic neurons play a crucial role in regulation energy homeostasis. Two neuron populations of the hypothalamus, proopiomelanocortin (POMC) expressing neurons and agouti-related protein (AgRP)/ neuropeptide Y (NPY) coexpressing neurons, located in the arcuate neucleus (ARC) close to the blood-brain barrier are mainly responsible for controlling food intake and energy expenditure. Positioning at the blood stream give these neurons access to hormonal signals and enables them to perceive changes in blood hormone levels and to respond to short- long-term alterations in an accurate way by activating their signaling cascades. POMC and AgRP/NPY neurons are part of the central melanocortin system representing the connecting of peripheral organs and CNS to detect energy status of the organism. POMC neurons mediate anorexigenic signals whereas AgRP/NPY mediate orexigenic signals acting as counterpart of POMC neurons. It had been shown that these neurons respond to changes of metabolic hormones and nutrient fluctuation, demonstrating a link of peripheral tissues to the CNS. (Benoit et al., 2000; Cone et al., 2001; Gao and Horvath, 2008; Belgardt et al., 2009). Cleavage of neuropeptide precursor protein POMC induces secretion of the melanocyte-stimulating hormones α and β (α- and β-MSH). Neuronal release of α- and β-MSH leads to activation of melanocortin receptor subtypes 3 and 4 (MC3R and MC4R) resulting in increased energy expenditure and food intake reduction (Cone, 2005; Biebermann et al., 2006; Lee et al., 2006). In contrast AgRP/NPY coexpressing neurons stimulate food intake

and reduce energy expenditure. AgRP is a natural competitive antagonist of α-MSH blocking MSH signaling thus reducing anorectic effects and increasing the eating impulse of individuals. AgRP/NPY coexpressing neurons and POMC neurons are nearby located in the arcuate nucleus. Therefore both neuronal populations interact however as known so far only in an unidirectional way. POMC cells are inhibited by release of the inhibitory neurotransmitter gamma-aminobutyric acid (GABA) from AgRP/NPY neurons. POMC inhibition by AgRP/NPY originated GABA signaling is important controlling body energy expenditure. GABAerigic inhibition of downstream effector neurons has been described for POMC and AgRP neurons (Hentges et al., 2004; Horvath et al., 1997, 2008; Goa and Horvath, 2008; Ollmann et al., 1997; Stanley and Leibowitz 1984; Sanchez-Lasheras et al., 2010; Tong et al., 2008). POMC and AgRP neurons express leptin and insulin receptors and respond to these hormones. Both insulin and leptin are modulator and regulator of food intake. Central insulin signaling leads to activation of PI3K-pathway and phosphorylation of FoxO. FoxO is responsible for neurotransmitter transcription regulation in neurons. AgRP expression is inhibited whereas POMC expression is promoted by FoxO. In addition activation of neuronal insulin receptors promote hyperpolarization and inhibition of neuronal firing. Thereby insulin activated PI3K catalyzing phosphorylation of PIP2 generating PIP3. PIP3 binds and activates K_{ATP} channels increasing potassium outflow. (Kim et al., 2006; Rezek, 1976; Havrankova et al., 1978; Kitamura et al., 2006; Schwartz 1992; Sanchez-Lasheras et al., 2010; Plum et al., 2006).

Glucose uptake leads to depolarization of the neuronal membrane and increased electrical activity of K_{ATP} channels. Glucose is metabolized and converted to pyruvate resulting in ATP production. ATP then binds and closes ATP-dependent potassium channels, reducing neuronal potassium outflow, increasing neuronal firing.

Leptin is secreted by adipocytes and serum leptin levels are a direct indicator for body fat storage. Leptin mediates anorectic signals via its central receptors in the hypothalamus thus regulating energy homeostasis. Leptin receptor signal transduction activates the JAK/STAT pathway. Leptin interacts with the melanocortin system by catalyzing phosphorylation, homodimerization and nuclear translocation of the transcription factor STAT3. Upon leptin binding JAK2 binds to the leptin receptor leading to recruitment and phosphorylation of STAT3. STAT3 modulates POMC and AgRP gene expression, increasing POMC and inhibiting AgRP transcription thereby promoting anorectic effects. In contrast to insulin, hyperpolarizing POMC and AgRP

neurons, leptin hyperpolarizes AgRP neurons whereas POMC neurons are depolarized.

The melanocortin system and its role in the regulation of energy homeostasis is well established but recent findings indicate that other hypothalamic and also extra hypothalamic areas may influence energy expenditure (Bates et al., 2003; Considine et al., 1996; Belgardt et al. 2009; Sanchez-Lasheras et al., 2010; Balthasar et al., 2005).

1.6 Aim of thesis

The IRS-1 knockout mouse shows lifespan extension proportional dwarfism and mild insulin resistance (Tamemoto et al., 1994). In addition weight gain and accumulation of abdominal fat pads during adult life is decreased in these mice; however food intake of IRS-1 knockout mice is increased compared to wildtype animals. Aim of this thesis was to address if the higher energy expenditure is associated with accelerated enzyme activity of respiratory chain complexes by using photospectroscopy and to clarify mechanism responsible for increased food intake and to elucidate the molecular mechanism of increased food intake. Since the described phenotype develops in adults, all animals used for experiments were 12 to 15 months of age.

2 Material and methods

2. Material and Methods

2.1 Chemicals

Acrylamide/ Bis-acrylamid 30%	Rotiphorese® Gel 30 (37.5/1) Carl Roth GmbH + Co. KG, Karlsruhe, Germany
Agarose	Invitrogen Corporation, Carlsbad CA, USA
Aprotinin	Sigma-Aldrich Chemie GmbH, Steinheim, Germany
APS	Ammonium-persulfate, AppliChem GmbH, Darmstadt, Germany
β-mercaptoethanol	Sigma-Aldrich Chemie GmbH, Steinheim, Germany
Bradford	Bio-Rad Laboratories GmbH, Germany
Bromophenol blue	AppliChem GmbH, Darmstadt, Germany
BSA > 96 %	Bovine serum albumin Sigma-Aldrich Chemie GmbH, Steinheim, Germany
Protease inhibitor Cocktail	Roche Diagnostics GmbH, Mannheim, Germany
Desoxy-Ribonucleotid-Triphosphate (dNTPs)	Fermentas GmbH, St. Leon-Rot, Germany
DMSO	Dimethyl sulfoxid, Sigma-Aldrich Chemie GmbH, Steinheim, Germany
DNase	Roche Diagnostics GmbH, Mannheim, Germany
DTT	Dithiothreitol, AppliChem GmbH, Darmstadt, Germany
EDTA	Ethylendiamintetraessigsäure, AppliChem GmbH, Darmstadt, Germany

EGTA	Ethylenglycoltetraessigsäure, AppliChem GmbH, Darmstadt; Germany
Ethanol	AppliChem GmbH, Darmstadt, Germany
Ethidiumbromide	Sigma-Aldrich Chemie GmbH, Steinheim, Germany
Glycerol	Glycerin, AppliChem GmbH, Darmstadt, Germany
Glycine	AppliChem GmbH, Darmstadt, Germany
HEPES	Sigma-Aldrich Chemie GmbH, Steinheim, Germany
Insulin solution, human	Sigma-Aldrich Chemie GmbH, Steinheim, Germany
Isopropanol	AppliChem GmbH, Darmstadt, Germany
KCl	Potassium chloride, Sigma-Aldrich Chemie GmbH, Steinheim, Germany
Methanol 99%	Carl Roth GmbH + Co. KG, Karlsruhe, Germany
Magnesium chloride	Merck, Darmstadt, Germany
NaCl	Sodium chloride AppliChem GmbH, Darmstadt, Germany
NP-40	FLUKA Chemika/Biochemika ChemieAG, Buchs, Switzerland
PMSF	Phenylmethylsulphonylfluorid, Sigma-Aldrich Chemie GmbH, Steinheim, Germany
Proteinase K	Roche Diagnostics GmbH, Mannheim, Germany
SDS	AppliChem GmbH, Darmstadt, Germany
Sodium flouride	NaF, Merck, Darmstadt, Germany
Sodium orthovanadate	Na_3VO_4, Sigma-Aldrich Chemie GmbH, Steinheim, Germany
PMSF	Phenylmethylsulfonyl fluoride, Sigma-Aldrich Chemie GmbH, Steinheim

TEMED	N,N,N',N'-Tetramethylethylenediamine Sigma-Aldrich Chemie GmbH, Steinheim, Germany
Tris	AppliChem GmbH, Darmstadt, Germany
Triton X-100	AppliChem GmbH, Darmstadt, Germany
Trypsin	Roche Diagnostics GmbH, Mannheim, Germany
TWEEN 20®	Caesar and Lorentz GmbH, Bonn, Germany
Western Blocking Reagent	Roche Diagnostics GmbH, Mannheim, Germany

2.1.1 Buffer and solution

Cell lysis buffer	50 mM NaCl 10 mM Tris-HCl (pH 7.4) 10 mM EDTA 50 mM NaCl 50 mM NaF 0,1 µg/ml Aprotinine 1 mM PMSF 2 mM Na_3VO_4 1 % Triton X-100
Organ lysis buffer	50 mM HEPES (pH 7.4) 50 mM NaCl 1 % Triton X-100 10 mM EDTA 0.1 M NaF 17 µg/ml Aprotinine 2 mM Benzanidine 0.1 % SDS 1 mM Phenylmethylsulfonyl fluoride (PMSF) 10 mM Na_3VO_4
SDS-PAGE running buffer	194 mM Glycine 25 mM Tris 0.1 % SDS

4 x SDS sample buffer	250 mM Tris-HCl (pH 6.8) 200 mM DTT 40 % Glycerol 8 % SDS 0.01 % Bromphenol blue
Stripping solution	62.5 mM Tris-HCL pH 6.8 100 mM β-mercaptoethanol 2% SDS
TBS buffer (pH 7.6) 1	37 mM NaCl 20 mM Tris
TBS-T buffer (pH 7.6)	137 mM NaCl 20 mM Tris 0.1 % Tween 20®
Western Blot antibody solution	137 mM NaCl 20 mM Tris 5 % Western Blocking Reagent (Roche)
Western Blot blocking solution	137 mM NaCl 20 mM Tris 10 % Western Blocking Reagent (Roche)
Western Blot transfer buffer	194 mM Glycin 25 mM Tris 20 % Methanol (99%) 0.05 % SDS

– ECL; Amersham ECLTM Western Blotting Detection Reagents, GE Healthcare UK Ltd; England

– Fetal bovine serum (FBS); Invitrogen , Corporation, Carlsbad CA, USA

– Pen/Strep; Penicillin Streptomycin (P/S); 10000 Units/ml Penicillin, 10000 µg/ml Streptomycin; Invitrogen Corporation, Carlsbad CA, USA

– PBS 10 x (pH 7.2); Invitrogen Corporation, Carlsbad CA, USA

– Protein Standard Ladder; Precision Plus Protein Kaleidoscope Standards; Bio-Rad Laboratories GmbH, Germany

2.1.2 Primary antibodies

– Actin Antibody; Monoclonal mouse antibody raised against an epitope conserved in human actin; MP Biomedicals, USA; Item # 69100; Western Blotting Dilution 1:5000

– AKT Antibody; Polyclonal rabbit antibody raised against endogenous levels of total AKT1,AKT2 and AKT3 proteins; Cell Signaling Technology, Inc., USA; Item # 9272; Western Blotting Dilution 1:1000

– ANT (N-19) is an affinity purified goat polyclonal antibody raised against a peptide mapping near the N-terminus of ANT of human origin; Santa Cruz Biotechnology, Inc., USA; Item #sc-9299; Western Blotting Dilution 1:1000

– DNP Antibody; Polyclonal rabbit antibody developed in rabbit using DNP-BSA immunogen; Sigma Aldrich; Saint Louis, Missouri, USA; Item # 9656; Assay Dilution 1:1000

– ERK Antibody; Polyclonal rabbit antibody raised against endogenous levels of total p44/42 MAP kinase (Erk1/Erk2) protein; Cell Signaling Technology, Inc., USA; Item # 9102; Western Blotting Dilution 1:1000

– GSK-3β Antibody; Monoclonal rabbit antibody raised against endogenous levels of totalGSK-3β protein; Cell Signaling Technology, Inc., USA; Item # 9315; Western Blotting Dilution 1:1000

– HSP60 Antibody; Monoclonal human antibody raised against human Hsp60 recombinant protein. Cross reactivity with mouse and rat. BD Bioscience, New Jersey, USA; Item # 611562; Western Blotting Dilution 1:1000

– IGF-1 Receptor β Antibody; Polyclonal rabbit antibody raised against endogenous levels of IGF-IR β. Does not cross-react with insulin receptor; Cell Signaling Technology, Inc., USA; Item # 3027; Western Blotting Dilution 1:1000

– IR-β Antibody; Polyclonal rabbit antibody raised against a peptide mapping at the C-terminus of insulin Rβ (C19) of human origin; Santa Cruz Biotechnology, Inc., USA; Item # sc-711; Western Blotting Dilution 1:1000

– IRS-1 Antibody; Monoclonal rabbit antibody raised against C-terminal 14 amino acid peptide ([C]YASINFQKQPEDRQ) of rat liver IRS-1. Rat, mouse and human crossreactivity; Upstate Cell Signaling Solutions, USA; Catalog # 06-248; Western Blotting Dilution 1:1000

– IRS-2 Antibody; Polyclonal rabbit antibody raised against endogenous levels of total IRS-2 protein; Cell Signaling Technology, Inc., USA; Item # 4502; Western Blotting Dilution 1:1000

- MitoProfile® Total OXPHOS Rodent WB Antibody Cocktail, monoclonal mouse antibody containing 5 mAbs, one each against CI subunit NDUFB8 (MS105) CII-30kDa (MS203), CIII-Core protein 2 (MS304) CIV subunit I (MS404) and CV alpha subunit (MS507) optimized premixed cocktail. for Western Blotting analysis of the 5 OXPHOS complexes in mitochondrial preparations from mouse, rat, human, or bovine sources; Acris Antibodies GmBH, Hiddenhausen, Germany; Item #MS-604; Western Blotting Dilution 1:1000
- MnSOD, purified rabbit polyclonal antibody; Immunogen: recombinant human MnSOD (manganous superoxide dismutase); Upstate (Milipore), Milipore Life Science Research and Biomanufacturing, USA Item # 06-984; Western Blotting Dilution 1:1000

- pan-Acetyl, rabbit polyclonal affinity purified antibody raised against an acetylated peptide; Santa Cruz Biotechnology, Inc., USA; Item #sc-8649-R; Western Blotting Dilution 1:1000

- PGC-1α, PGC-1 (H-300) rabbit polyclonal antibody raised against amino acids 1-300 mapping near the N-terminus of PGC-1 of human origin; Santa Cruz Biotechnology, Inc., USA; Item #sc-13067; Western Blotting Dilution 1:1000

- Phospho-AKT Antibody; Polyclonal rabbit antibody raised against endogenous levels of AKT1 only when phosphorylated at Ser473. Also recognizes AKT2 and AKT3 when phosphorylated at the corresponding residues; Cell Signaling Technology, Inc., USA; Item # 9271; Western Blotting Dilution 1:1000

- Phospho-p44/42 MAP Kinase (Thr202/Tyr204) Antibody; Polyclonal rabbit antibody raised against endogenous levels of p44 and p42 MAP Kinase (Erk1 and Erk2) when phosphorylated either individually or dually at Thr202 and Tyr204 of Erk1 (Thr185 andTyr187 of Erk2); Cell Signaling Technology, Inc., USA; Item # 9101; Western Blotting Dilution 1:1000

- Phospho-GSK-3β (Ser9) Antibody; Polyclonal rabbit antibody raised against endogenous levels of GSK-3β only when phosphorylated at serine 9; Cell Signaling Technology, Inc., USA; Item # 9336; Western Blotting Dilution 1:1000

- PI 3-kinase p85α (Z-8), rabbit polyclonal antibody raised against amino acids 333-430 of PI 3-kinase p85α of human origin; Santa Cruz Biotechnology, Inc., USA; Item #sc-423; Western Blotting Dilution 1:1000

- Protein A-Agarose Immunoprecipitation Reagent, Protein A-Agarose is suitable for immunoprecipitation of mouse IgG2a, IgG2b and IgA, rabbit IgG and human IgG1, IgG2 and IgG4, Santa Cruz Biotechnology, Inc., USA; Item #sc-2001

- PTEN, Polyclonal Rabbit mAb detects endogenous levels of total PTEN protein; Cell Signaling Technology, Inc., USA; Item # 138G6; Western Blotting Dilution 1:1000

– p-Tyr (PY99), mouse monoclonal antibody designed to specifically detect phosphorylated tyrosine residues;.Santa Cruz Biotechnology, Inc., USA; Item #sc-7020; Western Blotting Dilution 1:1000

– SIRT1 (H-300), rabbit polyclonal antibody raised against amino acids 448-747 of SIRT1 of human origin;.Santa Cruz Biotechnology, Inc., USA; Item #sc-15404; Western Blotting Dilution 1:1000

– UCP-1, mouse polyclonal antibody, immunogen 19 aa peptide sequence (designated UCP12; cytoplasmic) at the C-terminus of the mouse/rat UCP1 (Bouillaud et al. 1986; Ridley et al. 1986; Kozak et al. 1988; Cassard et al. 1990; Miroux et al. 1993). The peptide has no significant homology with UCP2 or UCP3. Chemicon, Milipore Life Science Research and Biomanufacturing, USA, catalog number AG382.

– UCP-3 (R308), rabbit polyclonal antibody detects endogenous levels of UCP3 protein, immunogen for this antibody was a synthetic UCP3 (R308) peptide; ABR Antibodies, Novus Biologicals, Novus Biologicals, Ltd, Cambridge, United Kingdom; Item #NBP1-51195

2.1.2 Secondary antibodies

– Anti Goat IgG (whole molecule), peroxidase conjugated; Affinity isolated antigen specific antibody obtained from rabbit anti-goat antiserum by immunospecific purification; Sigma-Aldrich, USA; Item # A5420; Western Blotting Dilution 1:1000

– Anti Mouse IgG (Fab specific), peroxidase conjugated; Developed in goat using purified mouse IgG Fab fragment as immunogen, the antibody is isolated from goat anti-mouse IgG antiserum by immunospecific purification; Sigma-Aldrich, USA; Item # A9917; Western Blotting Dilution 1:10000

– Anti Rabbit IgG, peroxidase conjugated; Developed in goat using purified rabbit IgG as immunogen, the antibody is isolated from goat anti-rabbit IgG antiserum by immunospecific purification; Sigma-Aldrich, USA; Item # A6154; Western Blotting Dilution 1:1000

2.1.3 Kits

– ATP Bioluminescence Assay Kit HS II — Roche Diagnostics GmbH, Mannheim, Germany; Catalog # 11699709001

– Free Triidotyronine (fT3) ELISA Kit	ALPHA DIAGGNOSTIC, San Antonio, USA; Catalog # 1650
– Insulin Mouse Ultrasensitive ELISA	DRG, International, Inc., USA; Catalog # EIA-3440
– Mouse Leptin ELISA Kit	IBL International, GmbH, Hamburg, Germany

2.2 Material

Blotting chamber TransBlot® SemiDry Transfer Cell
BioRad Laboratories, USA

Blotting membrane ImmunBlotTM PVDF Membrane for Protein Blotting
BioRad Laboratories, USA

Blotting paper Whatman® Gel Blotting Paper
Schleicher & Schuell, Germany

iCycler Thermocycler
BioRad Laboratories, USA

Gewebe-Homogenisator
VWR International GmbH, Germany

Microplate reader Mithras LB 940 multimode microplate reader
Berthold Technologies GmbH & Co. KG, Germany

Minigel Twin Gel Electrophoresis Apparatus, Minigel□Twin
Biometra GmbH, Germany

NanoDrop NanoDropTM Spectrophotometer ND 1000
ThermoFisher Scientific, USA

NMR Analyzer minispec mq7.5
Burker Optik, Ettlingen, Germany

Photopaper Amersham HyperfilmTM ECL
GE Healthcare UK Ltd, England

Powerpac Biometra Standard Power Pack P25
Biometra GmbH, Germany
PowerPac300 Bio-Rad Laboratories, Germany

Thermomixer
Eppendorf, Thermomixer 5436, Eppendorf AG, Hamburg, Germany

Western blot transfer device
Trans-Blot SD Semi Dry Transfer Cell, Bio-Rad Laboratories, Germany
Fastblot B 34, Biometra GmbH, Germany

Luminometer
Mithras LB 940, Berthold

Incubator
HeraCell 150, Thermo Scientific

Magnetic stir bar
Heizbarer Magnetrührer Combimag RCT, IKA Werke GmbH & Co. KG, Staufen, Germany
Heizbarer Magnetrührer MONOTHERM, Variomag, Daytona Beach, USA

Microscope
Fluorescence Microscope Eclipse E800, Nikon Instech Co., Ltd. Kanagawa, Japan
Mikroskop CKX41, Olympus

pH meter
Docu-pHmeter, Sartorius

Pipettes
Eppendorf research 0,5-10 µL
Eppendorf research 10-100 µL
Eppendorf research 100-1000 µL

Pipettierhilfe
Pipetus, Hirschmann Laborgeräte

Laminar flow
HERA safe, Thermo Scientific

Water bath
Wasserbad SFB-68-TB14, GFL Gesellschaft für Labortechnik mbH, Burgwedel, Germany

Cell culture dishes
∅ 10cm Schalen, TPP AG, Trasadingen, Schweiz
∅ 6cm Schalen, TPP AG, Trasadingen, Schweiz
6-well-, 24-well- & 96-well-Schalen, TPP AG, Trasadingen, Schweiz

Centrifuge
Megafuge 11R , Thermo Scientific
Biofuge Fresco, Heraeus Instruments GmbH, Osterode, Germany

Step one plus Real-time PCR system
Applied Biosystems, Carlsbad, California, USA

Oroboros Oxygraph 2k
Oroboros instruments GmbH, Innsbruck, Austria

2.3 Methods

Protein analysis

2.3.1 Protein- and cell-lysate preparation

Proteinextraction was carried out at 4°C avoiding degradation of proteins. Organs were lysed in 50 mM HEPES (pH 7,4), 50 mM NaCl, 1 % Triton X-100, 10 mM EDTA, 0,1 M NaF, 17 µg/ml aprotinine, 2 mM benzanidine, 0,1 % SDS, 1 mM phenylmethylsulphonyl fluoride (PMSF) and 10 mM sodium orthovanadate (Na_3VO_4) containing buffer. Homogenates were dissolved in 4 x SDS sample buffer (250 mM Tris-HCl (pH 6,8), 200 mM DTT, 40 % glycerol, 8 % SDS, 0,04 % bromophenol blue) and applied to 8 % to 15 % SDS-PAGE depending on protein size.

Cells were grown in cell culture dishes, media was aspirated and cells were washed with ice-cold 1 x PBS. PBS was removed and cell lysis buffer (0,1 % Triton X-100, 10 mM Tris-HCl, 10 mM EDTA, 50 mM NaCl, 50 mM NaF, 0,1 µg/ml aprotinine, 1 mM PMSF, 2 mM Na_3VO_4) was added to cells. Cells were harvested using a cell-scraper, transferred into 1,5 ml Eppendorf-tubes and incubated on ice for 30 min. Subsequently cells were resuspended with a 20 gauche syringe and centrifuged for 30 min and 13000 rpm at 4°C. Cell pellet was discarded and supernatant was used for further procedures. Cell homogenates were dissolved in 4 x SDS sample buffer (250 mM Tris-HCl (pH 6,8), 200 mM DTT, 40 % glycerol, 8 % SDS, 0,04 %

bromophenol blue) and applied to 8 % to 15 % SDS-PAGE depending on protein size.

Concentrations of protein and cell lysates were determined by Bradford assay. This assay is based on the ability of Coomassie brilliant blue G 250 dye to binding to aromatic amino acids of proteins. Binding of Coomassie brilliant blue G 250 to proteins causes a shift in absorption maximum of the dye of 595 nm to 465 nm in relation to amount of protein. Protein amount of sample solution was calculated using a standard curve.

2.3.2 Preparation of nuclear cell fraction

Cells were washed with ice-cold 1 x PBS, harvested and resuspended in 100 µl cytosolic extraction buffer (20 mM HEPES, 10 mM KCl, 1 mM EDTA, 0,1 mM sodium orthovanadate (Na_3VO_4), 10 % (v/v) glycerol, 0,2 % (v/v) NP 40, adjusted to pH 7,4). MEFs were incubated in lysis buffer for 5 minutes on ice, resuspended with a 20 gauche syringe and centrifuged for 30 seconds at 16000 rpm and 4°C. Supernatant was additionally centrifuged for 5 minutes at 16000 rpm and 4°C and resulting supernatant used as cytsolic extract for further experiments. The precipitate of the first centrifugation step was resolved in 100 µl nuclear extraction buffer (420 mM KCl, 20 mM HEPES, 1 mM EDTA, 0,1 mM Na_3VO_4, 20 % (v/v) glycerol, adjusted to pH 7,6) and incubated for 30 minutes on ice. Nuclear lysate was centrifuged for 5 minutes at 16000 rpm and 4°C, resulting supernatant served as nuclear extract for subsequent experiment.

2.3.3 SDS polyacrylamide gel electrophoresis (Laemmli et al., 1970)

SDS-PAGE (sodium dodecylsulfate polyacrylamide gel electrophoresis) is a gel electrophoresis to separate proteins based on their molecular size under denatured conditions in an electric field. Thus molecules are separated on the basis of distinct molecular weights of each protein in a protein conglomerate. SDS, an anionic detergent binds to proteins negative charge to each protein in proportion to its mass or polypeptide chain length, respectively. Proteins are linearized by SDS and β-

mercaptoethanol. Electric tension causes migration of negative charged (anionic) proteins (due to SDS binding) in a size depending manner. The SDS-protein complex migrates to the anode and proteins are separated.

The electrolyte for this electrophoresis is a discontinuous tri-chloric/tris-glycine buffer (25 mM Tris; 192 mM glycine; 0,1 % (w/v) SDS. The matrix for protein separation is a polyacrylamide gel consisting of acrylamide, bisacrylamide (37,5 : 1 acrylamide N,N`-methylenebisacrylamide) (Laemmli, 1970; Wilson and Goulding, 1991), TEMED (N,N,N,N-tetramethylethylenendiamine) and APS (Ammoniumpersulfate(-$(NH_4)_2S_2O_8$)). A small pore resolving gel (with an acrylamide percentage of 10% up to 15%; 3 M Tris/HCl, pH 8,8; 0,8 % (w/v) SDS) for sample separation is covered by a large pore stacking gel (usually with an acrylamide fraction of 5 %; 1 M Tris/HCl, pH 6,8; 0,8 % (w/v) SDS) used for sample concentration and sample focusing providing a simultaneous start of protein separation. APS and TEMED catalyse linking of two acrylamide molecules and finally polymerization of the polyacrylamide gel by radical reaction. Various polyacrylamide concentrations resulting in different pore sizes cause retention of high molecular weight proteins in the resolving gel whereas proteins of low molecular migrate to the anode causing a distinct separation of proteins due to their molecular weight.

100 µg of analyzed samples were admitted to SDS sample buffer (4x : 250 mMTris/HCL, pH 6,8; 10 % (w/v) SDS; 50 % (v/v) glycerol; 0,01 % bromophenol blue; 500 mM DTT), denatured for 5 min at 95°C destroying secondary and tertiary structures of proteins. Molecular weight standards were run on every SDS-PAGE gel allowing identification of proteins due to their molecular weights. Stacking gel was run at constant tension of 120 V, resolving gel at constant tension of 180V.

2.3.4 Western Blot

Western Blots are used to transfer the separated proteins of the SDS-PAGE gel matrix to a nitrocellulose or polyvinylidenediflouride (PVDF) membrane. An electric field horizontal to the polyacrylamide gel provides the transfer of protein samples. Based on hydrophobic interactions proteins are immobilized and fixed to the surface of the membrane, maintaining the separation pattern of the polyacrylamide gel. For

the electrophoretic transfer a semi-dry blot system was used in which the resolving gel and PVDF membrane are sandwiched between buffer soaked filter paper sheets. This stack is placed between two plate electrodes with anode plate on top and cathode plate on the bottom of the stack providing a horizontal electric field. For one SDS-PAGE gel the transfer was performed for 60 min at 200 mA. For target proteins of 100 kDa or larger proteins transfer time was adjusted up to 90 min.

In a second step proteins are immuno-detected and visualized by incubating the membrane with specific antibodies. Therefore PVDF membrane was immersed in blocking solution for at least 60 minutes at RT to block unspecific binding sites, avoiding nonspecific antigen-antibody interactions. Blocking solution was prepared with tris buffered saline (TBS) and Western Blocking Reagent (Roche, Mannheim, Germany), saturating unspecific binding sites with irrelevant proteins (e.g. bovine serum albumin, BSA) avoiding unspecific interaction with or unspecific detection by the primary antibody, thus reducing background staining. Subsequently the membrane was incubated with an appropriate dilution of primary antibody over night at 4°C. Primary antibodies are raised against the protein of interest and diluted in 5 % Western Blocking Reagent. Next the membrane was washed at least 5 times for 15 minutes at room temperature removing unbound and unspecific bound primary antibody. Washing buffer consisted of TBS containing 0,1 % TWEEN 20 (TBS-T). Following the washing procedure secondary antibodies in appropriate dilution were applied to the PVDF membrane for 60 minutes, followed by another washing procedure with TBS-T. Secondary antibodies are species and domain specific for the primary antibody recognizing primary antibodies of a defined species. The secondary antibodies are linked to horseradish peroxidase (HRP) catalyzing. a chemical conversion of luminol in its oxidized form is catalyzed by HRP.

2.3.5 Enhanced Chemiluminescence Assay

For detection of membrane bound proteins enhanced chemiluminescence (ECL) assay was applied to PVDF membranes. Basic principle of this assay is the reaction of secondary antibody conjugated of horseradish peroxidase (HRP) with the ECL substrate luminol. HRP catalyzes the oxidation of luminol causing light emission. Light is chemical enhanced and recorded on film. Membrane was transferred to the

two component detection solution (Amersham ECL™ Western Blotting Detction Reagent) and exposed to photosensitive film (Amersham™ Hyperfilm ECL), exposing times varied between 10 sec and 30 min.

2.3.6 Membrane stripping

PVDF membranes were stripped for detection of different protein of interest. Membranes were cleared of previously bound antibodies by incubation in stripping solution (62,5 mM Tris-HCl (pH 6,8), 2 % SDS and 100 mM 2-β-mercaptoethanol) for 20 minutes at 55°C. Membrane was washed using TBS and blocked for 1 h and re-incubated with designated primary antibody.

2.3.7 Immunoprecipitation (IP)

Immunoprecipitation was performed by incubating 1 mg protein or cell lysate overnight at 4°C on an overhead shaker using designated antibody with agarose beads (Protein A-Agarose immunoprecipitation reagent, Santa Cruz Biotechnology, Santa Cruz, USA). Samples were washed, resuspended in 4 x SDS sample buffer and analyzed by Western blotting.

2.3.8 Enzym-linked-immunosorbend assy (ELISA)

Sera for ELISA analysis were collected from mice by taking blood from the heart of the dazed/anaesthetized animal. Blood samples were centrifuged at 6000 rpm for 30 min at 4°C separating sera from erythrocytes and other blood cells avoiding hemolytic sera samples for ELISA analysis. Insulin, leptin and triiodothyronine (T3) ELISAs were performed following manufacturer´s protocol. Read out was carried out in a microplate reader (Mithras LB 940 multimode microplate reader, Berthold Technologies GmbH & Co. KG, Germany).

2.3.9 OxyBlot assay

Carbonyl groups that are introduced into the amino acid side chain (lysine, arginine, proline or threonine residues) after oxidative modification of proteins can be identified by OxyBlot analysis. Measurement of protein carbonyls represents an indirect analytic toll of reactive oxygen species. In the OxyBlot assay carbonyl groups on protein side chains were detected derivatizing with 2,4-dinitrophenylhydratone (DNP-hydrazone) by reaction with 2,4-dinitrophenylhydrazine (DNPH). DNHP-derivatized proteins can then be separated, analyzed by Western Blotting and visualized by an anti-DNP antibody and a horseradish peroxidase conjugated secondary antibody (Shacter et al., 2000; Levine et al., 1994).

Mouse handling

2.3.10 Mouse breeding

IRS-1 knock-out mice were generated as described in introduction (Tamemoto et al., 1994). IRS-1 knock-out mice and wildtype littermate controls were obtained from IRS-$1^{+/-}$ breeding pairs. Mice were housed in groups of 4 to 5 in a 12-h light/dark cycle (7:00 am on / 7:00 pm off) at 20 to 23°C. Animals were fed standard rodent diet (Altromin Spezialfutter GmbH & Co. KG, Lage, Germany). Handling and breeding of mice was performed in accordance to the German Laws for Animal Protections and were approved by the local animal care committee and the Bezirksregierung Köln.

2.3.11 Mouse genotyping

3 weeks after birth mice were weaned and mouse tail biopsies were taken. Biopsies were incubated in tail lysis buffer (100 mM Tris-HCl (pH 8,5), 5 mM EDTA, 0,2 % (w/v) SDS, 200 mM NaCl, 500 mg/ml proteinase K) in a thermomixer at 55°C and 800 rpm over night. On the following day DNA was precipitated with isopropanol and centrifuged at 13000 rpm and RT for 10 minutes. Supernatants were removed; pellet

was resuspended in 100 µl 70 % ethanol and centrifuged at 13000 rpm and for 5 minutes. Pellet was resolved in 50 µl double destilled water (ddH_2O).

DNA was applied to polymerase chain reaction (PCR) for genotyping of mice. Primers used for PCR are listed in table 2. PCR reaction were performed in a total reaction volume of 50 µl containing 100 ng template DNA, 25 µM dNTP Mix, 10 x goTaq reaction buffer, 25 pmol of each primer and 1 unit of goTaq DNA polymerase. PCR protocol:

Step 1:	1 x		94°C	5 min
Step 2:		⎫	94°C	1 min
	35 x	⎬	55°C	0,5 min
		⎭	72°C	1 min
Step 3:	1 x		72°C	10 min
Step 4:			4°C	∞

Table 2.1: List of oligonucleotides used for PCR reaction

Primer	Sequence 5´- 3´	Orientation
IRS-1 5´	GCA GCC CCA CCT GCC TCG AAA GGT AGA CAC	sense
IRS-1 3´	CTG CCC AAC TCA ACT CCA CC	antisense
IRS-1 neo	TTC TAT CGC CTT CTT GAC GAG TTC	neosense

2.3.12 Body composition

Body composition of mice was determined by using nuclear magnetic resonance (NMR) (NMR analyzer minispec mq7.5). Radiofrequency pulse sequences are transmitted into animals. In response, RF signals are generated by the hydrogen in tissues and detected by minispec. Amplitude and duration of signals are related to properties of tissues.

2.3.13 Indirect calorimetry and physical activity measurement

Open circuit calorimetry system (CaloSys calorimetry module, TSE System GmbH, Bad Homburg, Germany) was used for metabolic rate determination (energy expenditure, respiratory quotient, Food and water intake, CO_2 production, O_2 consumption). Food and water were provided *ad libitium*. Activity of mice was analyzed with an video tracking system (VideoMot2, TSE Systems GmbH, Bad Homburg, Germany).

2.3.14 Glucose and insulin tolerance test

Animals were starved overnight (16 h) and intraperitoneally injected with 0,75 U/kg bodyweight of human insulin (Novo Nordisk, Copenhagen, Denmark) for insulin tolerance test or with 2 g/kg bodyweight of glucose (DeltaSelect, Munich, Germany) for glucose tolerance test respectively. Blood was collected from tail tips of mice and blood glucose values were measured immediately before and 15, 30, 60 minutes after injection for insulin tolerance test or 15, 30, 60, 120 minutes after injection for glucose tolerance test, respectively. Blood glucose levels were determined using GlucoMen glucose meter (A. Menarini diagnostics, Berlin-Chemie, Neuss, Germany). Results were expressed as percentage of initial blood glucose concentration.

2.3.15 MEF generation and MEF cell culture

Primary mouse embryonic fibroblast were isolated from E13,5 embryos. Embryos were dissected from the uterus of female mice of IRS-$1^{+/-}$ breeding pairs. MEFs were isolated following protocol as previously described (Brüning et al., 1996). Primary MEFs were immortalized by SV 40 transformation (Todaro and Green, 1965) at early passages.

MEFs were cultured using Dulbecco´s Modified Eagle Medium (DMEM) (Invitrogen, Carlsbad, CA, USA) with 4,5 g/L D-glucose, 10 % fetal bovine serum (FBS) (Invitrogen), 1 % penicillin/streptomycin (Invitrogen), 100 µM non essential amino acids (Invitrogen), 2 mM L-glutamine (Invitrogen) and 1 mM sodium pyruvate (Invitrogen). Cells were grown at 37°C in an humid atmosphere with 5 % CO_2 content.

2.3.16 Insulin stimulation of mice

Mice were fasted overnight and treated with insulin 0,75 U/kg body mass by interperitoneal injection (Sabio et al., 2008). Liver, WAT and muscle were removed 10 minutes after insulin injection. Tissues were homogenized in 1 ml proteinextraction buffer and further preceded for Western blot determination.

2.3.17 Isolation of adipocytes

Animals were sacrificed and epididymal fat pads were removed under sterile conditions. Adipocytes were isolated by collagenase (1 mg/ml) digestion for 45 min at 37°C in DMEM/Ham's F-12 1:1 (DMEM/F12) containing 1% BSA. Digested tissues were filtered through sterile 150-µm nylon mesh and centrifuged at 250×g for 5 min. The floating fraction consisting of pure isolated adipocytes was then removed and washed three more times. Adipocytes sizes were measured using a culter counter (collaboration with Professor M Blüher, Leipzig).

Cell biology

2.3.18 Insulin stimulation of MEF

MEFs were starved overnight and stimulated with insulin final concentrations 1, 10 and 100 mM, respectively. Following 4 minutes incubation at 37°C MEFs were harvested, resuspended in cell lysis buffer (10 mM HCl (pH 7,4), 50 mM NaF, 50 mM NaCl, 10 mM EDTA, 1% Triton X-100, 0,1 µg/ml aprotinin, 1 mM PMSF, 2 mM Na_3VO_4) and applied to biochemical analysis.

2.3.19 ATP Bioluminescence Assay

ATP Bioluminescence Assay Kit HS II (Roche, Mannheim, Germany) was used for quantitative determination of ATP. Assay is based on the ATP dependency of light emitting luciferase catalyzed oxidation of luciferin (De Luca and McElroy, 1978). The luciferase catalyzes the adenosine triphosphate dependent oxidative decarboxylation of luciferin by simultaneous emission of light (wavelength 562 nm). Light output is directly proportional to ATP concentrations.

$$ATP + \text{D-luciferin} + O_2 \rightarrow \text{oxyluciferin} + PP_i + AMP + CO_2 + \text{light}$$

1 x 10^6 cells were harvested and pelleted. Pellets were resuspended in equal amounts of dilution and cell lysis buffer provided in the kit. Light emission was detected by luminometer (Mithras LB 940 multimode microplate reader, Berthold Technologies GmbH & Co. KG, Germany). ATP concentrations were calculated from ATP standard, standard was diluted with dilution buffer by serial dilutions. ATP content was measured in triplicate according to manufacturer's guidelines.

2.3.20 Isolation of mitochondria from primary mouse embryonic fibroblasts

Mitochondria of primary mouse embryonic fibroblasts (MEFs) were isolated by differential centrifugation of harvested cell homogenates. Fibroblasts were harvested, washed in ice-cold PBS and subsequently resuspended in 5 ml isotonic homogenization buffer (250 mM sucrose, 5 mM Tris-HCl pH 7,5; 0,1 mm PMSF). Resulting cell suspension was homogenized; nuclei and unbroken cells were removed by centrifugation (10 min, 1200 g, 4°C). Received supernatant was applied to additional centrifugation (20 min, 16000 g, 4°C) for collecting mitochondria. Pellet was washed and resuspended in a suitable volume of suspension buffer (250 mM sucrose, 5 mM Tris-HCl, pH 7,5, 1 mM EDTA, 0,1 mM PMSF). Protein concentration determination was performed by using Bradford assay according to manufactor´s guideline (Bio-Rad).

Biochemistry

2.3.21 Polarography

Polarographic analysis is based on the determination of oxygen consumption of cells or isolated mitochondria, respectively. The polarographic device (Polarograph, Hansatech Instruments limited, King´s Lynn, UK) is based on the principle of a Clark electrode consisting of a platinum cathode and an argentic/argentic-chloride anode submerged by a potassium chloride rich electrolyte solution. For determination of

oxygen consumption reaction tank was sealed, excluding atmospheric oxygen, heated to 37°C and stirred at 850 U/min. Clark electrode was connected to reaction chamber by an oxygen permeable PTFE membrane. A total reaction volume of 250 µl of isolated mitochondria and buffer E (10 mM KH_2PO_4; 300 mM mannitol, 10 mM KCl, 5 mM $MgCl_2$, 1 mg/ml BSA) were applied to chamber.

Applying a polarizing electric tension to this device leads to induction of two electrochemical processes at the anode and cathode within the ionized analytic chamber.

Chemical reaction argentic anode:

$Ag + Cl^- \rightarrow AgCl + e^-$

Chemical reaction platinum cathode:

$O_2 + 2\ H_2O + 4\ e^- \rightarrow H_2O_2 + OH^- + 2\ e^- \rightarrow 3OH^-$

Oxygen is converted at the platinum cathode in a first step reaction to hydrogen peroxide (H_2O_2) and finally in a second step reaction to three hydroxide (OH^-) ions. The chemical reaction at the argentic anode is an oxidation of argent to argentic chloride. These two chemical reactions lead to a constant electric flow proportional to the current oxygen concentration within the electrolyte solution.

Blank value was determined by application of sodium dithionite, reducing total amount of oxygen within the chamber. Oxygen content of mitochondria buffer used for this set up was approximately 216 nmol O_2/ml. Received data were recorded on a Linseis plotter and calculated to oxygen consumption (nmol/mg protein*min).

Oxygen consumption determination was carried out with isolated liver mitochondria. For analysis mitochondria were isolated using the protocol described in (Fernandez-Vizarra et al., 2002). Mitochondrial content of suspensions was determined by Bradford analysis. All analyses were carried out following protocols described by (Rustin et al., 1994). Integrative determination of respiratory function including function of pyruvate dehydrogenase complex and of TCA cycle can be identified and calculated by addition of various substrates. Coupling and interplay of respiratory chain complexes, TCA cycle and pyruvate dehydrogenase are determined by

polarography however no detailed analysis of malfunctions in single enzymes of these metabolic cycles is achieved by this method.

Pyruvate oxidation was determined via MPox protocol, analyzing activity of respiratory chain complex I, pyruvate dehydrogenase and TCA cycle. Addition of ADP to mitochondria suspension lead to an increase in oxygen consumption switching mitochondrial respiration from state 4 (basal state) to state 3 (forced respiration).

Pyruvate kinase functionality was addressed by determination of malate-glutamate oxidation (MGox). Malate and glutamate were applied to mitochondrial suspension. Malate is metabolized by the TCA cycle to oxaloacetate. Oxaloacetate is removed by glutamate thus avoiding endproduct accumulation and attenuation of TCA enzymatic reactions.

Evaluation of succinate oxidation (Sox) after inhibition of complex I by rotenone showed information about activity capacity of complex II. In this scenario electrons for the mitochondrial respiratory chain are provided by succinate and its enzymatic reaction with complex II. Following inhibition of complex V by oligomycin and subsequent uncoupling by CCCP enzymatic activity of complex II could be determined.

Addition of complex II inhibitor malonate in this context allowed enzyme activity determination of complex III and complex IV. Electrons are supplied by glycerol-3-phosphate (G3P) via G3P dehydrogenase (GPox) or directly by quinone (Qox). Measured oxygen consumption is directly linked to complex III and complex IV enzymatic activity.

2.3.22 Spectrophotometry

In difference to polarographic analysis spectrophotometric evaluation of respiratory chain and TCA cycle enzyme performance can activate single respiratory chain complexes independent of each other by defined assays. Absorption spectra consist of interfering wave absorptions generated by energy transitions of molecules. Absorption spectra of molecules in reductive or oxidize states differ and chemical

changes of molecular energy states can be calculated. Thus enzymatic turnover of substrates of single respiratory chain complex can be determined by this method. Musculus soleus and musculus gastrocnemius were freshly isolated from mice, transferred into extraction buffer (20 mM Tris, 250 mM Saccharose, 2 mM EGTA, 40 mM KCl, 1 mg/ml BSA, pH 7,2)and homogenized on ice with finger grinder. Homogenized muscle sample were stored at -80°C overnight and analyzed by photospectroscopy the following day. Same procedure was applied to liver samples. MEFs were harvested 1 x 10^7 cells were resuspended in 1 x PBS. Mitochondria were isolated following protocol described in 2.3.3. Assays were carried out under V_{max} conditions. Activities of complex I, II, I+III, II+III, IV and V were analyzed sequentially by using different electron donors or acceptors, respectively. Additionally activities of TCA cycle enzymes and cytoplasmatic enzymes were determined.

Respiratory chain enzyme activities of muscle, liver, MEFs and MEF isolated mitochondria were measured using a temperature controlled double-wavelength spectrophotometer (Varian Cary 50 Scan photo spectrometer; Varian Inc., Spectroscopy instruments, Mulgrave, Australia). Enzyme activity evaluations were carried out following protocols as described in Rustin et al., 1994. Detected activities were calculated to protein concentration of samples determined by Bradford analysis.

2.3.23 Mitochondrial respiration (skinned fiber technique)

Permeabilized muscle fibers were obtained from muscle biopsy and mitochondrial chain function was analyzed *in situ* following protocols previously described (Kuznetsov et al., 2008). M. soleus was dissected into individual muscle fibers and plasma membrane was permeabilized in saponine skinned muscle medium (49 mM MES, 3 mM KH_2PO_4, 20 mM taurine, 0,5 mM DTT, 20 mM imidazole, 10 mM $MgCl_2$, 5 mM ATP, 15 mM phosphocreatine, 10 mM Ca-EGTA (2,77 mM CaK_2EGTA, 7,23 mM K_2EGTA), 0,1 µM calcium, pH 7,1), rotated and incubated for 30 min at 4°C. Respiratory rates were measured at 30°C by polarographic oxygen sensors in a 2-chamber oxygraph (OROBOROS Instruments, Innsbruck, Austria). Oxygen consumption was recorded using DataLab 4.2® software (OROBOROS Instruments, Innsbruck, Austria). Addition of specific substrates of the respiratory chain complexes allow determination of basal respiration of complexes I-IV (state 2), maximal oxidative

capacity was measured after addition of saturating concentration of ADP (state 3, active respiration). Glutamate and malate were used to address complex I dependent respiration. With these substrates maximal physiological capacity is obtained, reconstituting the operation of tricarboxylic acid cycle, preventing depletion of key metabolites (Brands et al., 2011). Results were expressed as nmol oxygen/min*mg fibers (dry weight of fibers was determined after high resolution respirometry).

2.3.24 Proton leak measurement (proton motive force (PMF))

Mitochondrial respiration was measured in the presence of oligomycin to inhibit ATP synthesis (state 4 respiration). The mitochondrial respiration rate in this setting is proportional to the rate at which protons leak across the inner mitochondrial membrane. Kinetic response of proton conductance to its driving force (proton motive force) was determined as relationship between respiration rate and membrane potential. Membrane potential can be varied by titration with specific electron transport chain inhibitors, in this case membrane potential was varied by adding malonate (Jastroch et al., 2009; Nicholls et al., 1974; Brand et al., 1990). Mitochondria from liver (0,5 mg/ml) were incubated in standard assay medium (120 mM KCl, 5 mM KH_2PO_4, 3 mM HEPES and 1 mM EGTA, pH 7,2) at 37°C with 5 µM rotenone, 80 ng nigericin/ml and 1 µg oligomycin/ml. Respiration rate and membrane potential were measured simultaneously using electrodes (AD Instruments, Spechbach, Germany) sensitive to oxygen and to the potential-dependent probe triphenylmethylphosphonium ($TPMP^+$). 4-hydroxy-2-nonenal (4-HNE), major product of oxidant-induced peroxidation of membrane phospholipids, was used to specifically uncouple mitochondria (Jastroch et al., 2009; Echtay et al., 2002 a,b, Echtay et al., 2003; Cadenas et al. 2002).

2.3.25 Carnitine palmitoyl transferase (CPT-) assay

CPT-I assay was carried out following protocols previously described (Bremer et al., 1985, Kerner et al., 2008; de Vries et al., 1997). CPT-I activity was determined by measuring formation of L-[^{3}H]-labeled palmitoylcarnitine from L-[^{3}H]-carnitine and palmitoyl-CoA. Reaction was started by adding 2,5 mM L-[^{3}H]-carnitine. Samples

were incubated for 6 minutes at 37°C. After stopping the reaction formed L-[^{3}H]-labeled palmitoylcarnitine was extracted and organic layer was used for scintillation counting. CPT-I activity was determined by subtracting CPT-II activity (malonyl-CoA sensitive part of reaction) from total CPT activity.

RNA analysis

2.3.26 RNA Extraction (Chomczynski and Sacchi, 1987)

RNA from tissues was extracted according to the TRIzol (Invitrogen GmbH, Darmstadt, Germany) protocol established by Chomczynski and Sacchi (1987).

2.3.27 cDNA synthesis

RNA was translated to cDNA by reverse transcription polymerase chain reaction. Reverse transcription was carried out using SuperScript^{TM} Kit (Invitrogen GmbH, Darmstadt, Germany). Protocol for first-strand cDNA synthesis was applied according to manufacturer´s guideline.

2.3.28 Real time quantitative PCR (RT-PCR)

RT-PCR is based on the principle of conventional PCR. In contrast to conventional PCR amount of amplified sample cDNA is directly quantified by determination of fluorescence during PCR cycles. Fluorescence intensity increases in proportion with amplified DNA amounts. TaqMan-Assay probes (Applied Biosystems) were used for cDNA quantification in this work. Eukaryotic 18S rRNA served as reference. TaqMan probes consist of two components a quencher and fluorescent dye (FAM, 6-FAM-phosphoramidite). 5´-3´ exonucleolitic activity of the Taq-polymerase detaches the reporter dye during DNA elongation and distant fluorescent dye and quencher hence suppression of fluorescence by quenching is abrogated and fluorescence intensity can be determined at 518 nm. Relative gene expression levels were calculated by

comparative $2^{-\Delta\Delta CT}$. List of gene expression assays used in RT-PCR reactions are listed in table 1

Table 2.2: List of gene expression assays used for RT-PCR

Gene	Assay ID-Nr.	Company
UCP-1	Mm00494069_m1	Applied Biosystems, Carlsbad, California, USA
UCP-2	Mm00627597_m1	Applied Biosystems, Carlsbad, California, USA
UCP-3	Mm00494077_m1	Applied Biosystems, Carlsbad, California, USA
PGC-1α	Mm01208835_m1	Applied Biosystems, Carlsbad, California, USA
NPY	Mm00445771_m1	Applied Biosystems, Carlsbad, California, USA
AgRP	Mm00475829_g1	Applied Biosystems, Carlsbad, California, USA
POMC	Mm01242886_g1	Applied Biosystems, Carlsbad, California, USA
CART	Mm00489086_m1	Applied Biosystems, Carlsbad, California, USA

IRS-4	Mm01340253_m1	Applied Biosystems, Carlsbad, California, USA
Insulin receptor	Mm01211875_m1	Applied Biosystems, Carlsbad, California, USA
Ob-R	Mm00440181_m1	Applied Biosystems, Carlsbad, California, USA
IRS-2	Mm03038438	Applied Biosystems, Carlsbad, California, USA
Eucaryotic 18S rRNA endogenous control	4333760T	Applied Biosystems, Carlsbad, California, USA

2.8 Statistical analysis

Western Blot images were scanned and analyzed densitometrically using AIDA (AIDA 2 D Densitometry Software, Version 4.00.027, Raytest, Straubenhardt, Germany). Background was subtracted and protein load was normalized to corresponding β-actin control. Statistical analysis was performed using Student´s *t*-test. Statistical significance was defined as *p<0,05.

3 Results

3. Results

3.1 Expression of IRS-1 protein in different tissues

Insulin receptor substrate 1 knockout mice display growth retardation resulting in dwarfism, mild insulin resistance, elevated food intake associated with higher energy expenditure and a lack of accumulation of abdominal fat with age. In order to evaluate the underlying mechanism responsible for thess phenotype conventional IRS-1 mouse and black six (BL6) wild-type animals as controls were used in this study. Knockout was obtained by insertion of a stop codon in exon 1 of the IRS-1 gene. IRS-1 knockout animals were generated by crossing heterozygous IRS-1 mice. Offspring animals were weaned 21 days after birth and tailcuts were used for genotyping PCR. To verify functional IRS-1 deletion in knockout animals IRS-1 expression in different organs of knockout and wild-type animals was analyzed by western blotting.

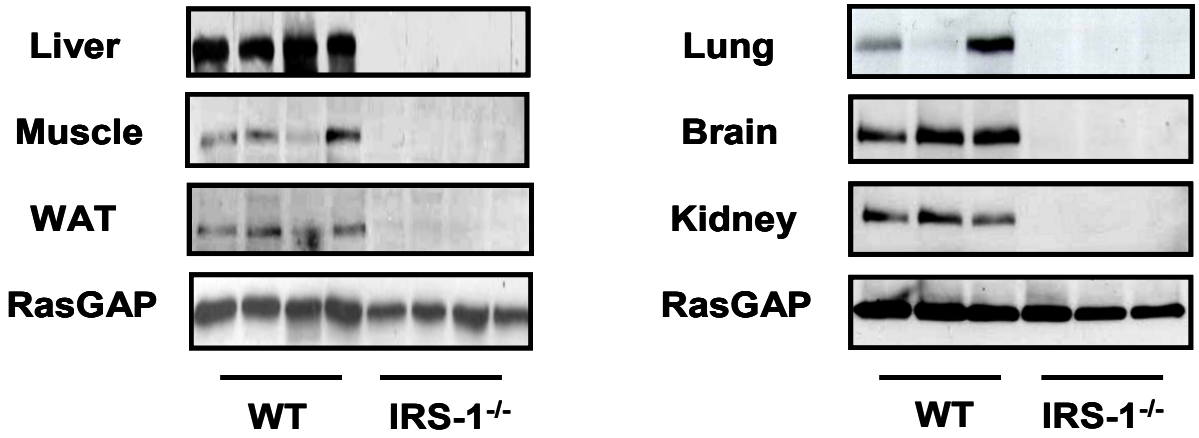

Fig. 3.1 Western blot analysis of IRS-1 protein expression in different tissues
Western blot analysis of IRS-1 expression in lysates of liver muscle, white adipose tissue, lung, brain and kidney. 100 µg of proteinlysate were applied on 8 % SDS-PAGE gel. RasGAP expression was used as loading control. Liver was analyzed by anti-IRS-1 immunoprecipitation of 9 mg organ lysate subjected to western blotting with polyclonal anti IRS-1 antibody.

Analysis of major sites of insulin action (liver, muscle, WAT) and non insulin responsive tissues (lung, brain, kidney) displayed complete IRS-1 deletion only in IRS-1 knockout animals although detection of liver IRS-1 in wild-type controls was only achieved with high amounts of lysate administered to immunoprecipitation and

western blot analysis due to low expression levels of IRS-1 in liver (Araki et al., 1994). Eight independent derived organ lysate samples for liver, muscle and WAT or six independent derived organ lysate samples for lung, brain and kidney, respectively were used for western blotting. In order to investigate influence of IRS-1 deletion on energy homeostasis, liver, muscle and WAT tissues were used for further experiments.

3.2 Expression of IRS-1 protein and basal expression of molecules of the insulin receptor cascade in MEFs

In order to address if systemic effects or signaling effects are the underlying mechanisms for the observed phenotype embryonic fibroblast were isolated from embryos of females of IRS-1$^{+/-}$ breeding pairs at day 13,5 post conception, transferred to cell culture and immortalized serving as an *in vitro* system in this project. To validate IRS-1 deletion in mouse embryonic fibroblasts (MEFs) derived from IRS-1 knockout embryos, cell lysates were administered to Western blotting for analyzing IRS-1 expression as well for analyzing basal expression of IRS-2, IR-β and IGF-1R.

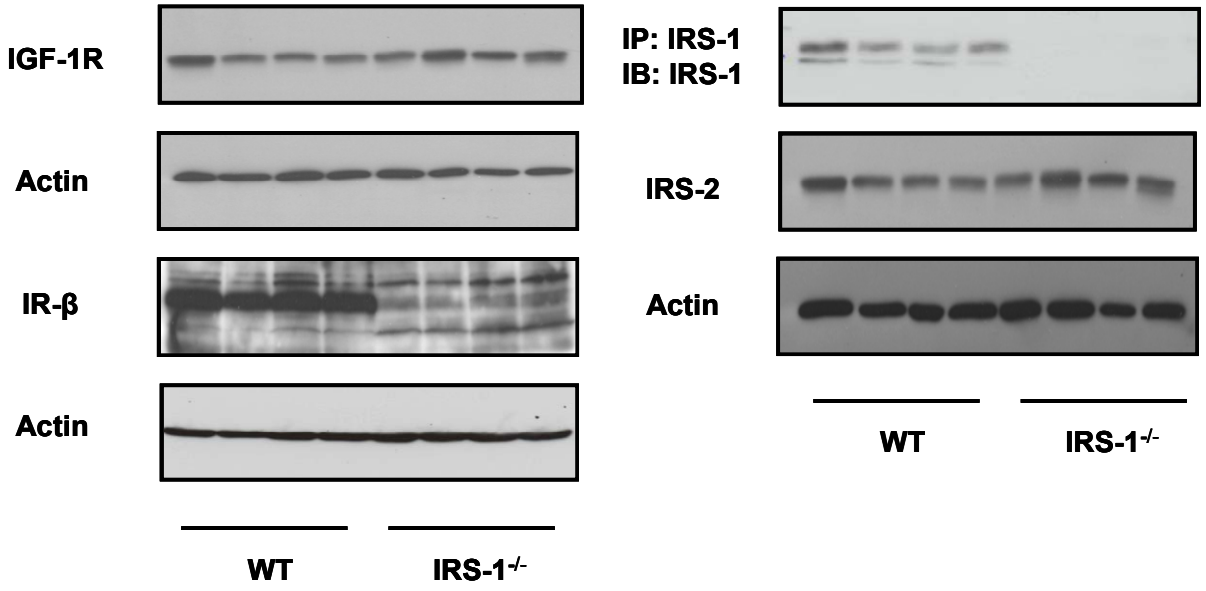

Fig. 3.2 Western blot analysis of IRS-1, IRS-2, IGF-1R and IR-β in MEFs
Western blot showing expression of IRS-1, IRS-2, IGF-1R and IR-β expression in cell lysate of IRS-1 knockout and wild-type derived MEFs as well as the respective corresponding loading control. 100 µg were applied to 8 % SDS-Page. For IRS-1 detection 1 mg cell lysate was used for immunoprecipitation with IRS-1 antibody and subjected to western blot detected by IRS-1 polyclonal antibody.

Western blot analysis revealed a total albescence of IRS-1 expression in transgenic IRS-1 MEFs whereas IRS-1 expression in wild-type control MEFs has been detected by IRS-1 immunoprecipitation of 1 mg cell lysate followed by IRS-1 Western blot detection. Abundance of IRS-2 and IGF-1R is unchanged in IRS-1 deficient MEFs compared with wild-type controls. However reduction of IR-β expression has been observed in IRS-1 knockout MEFs when compared with IR-β expression in wild-type MEFs. For Western blot experiments actin was used as loading control. Analysis was determined three times utilizing discrete PDVF membranes and samples were derived from independent cell lysates.

3.3 Basal expression of IRS-2 and of the insulin receptor signaling cascade key molecules in muscle and liver of IRS-1$^{-/-}$ mice and wild-type controls

Liver and muscle of IRS-1 knockout mice and wild-type were analyzed for basal IRS-2, IR-β and IGF-1 expression. Amount of proteins were determined by Western blotting. Deviations in the amount of protein samples loaded to gels were checked by β-actin staining of each membrane.

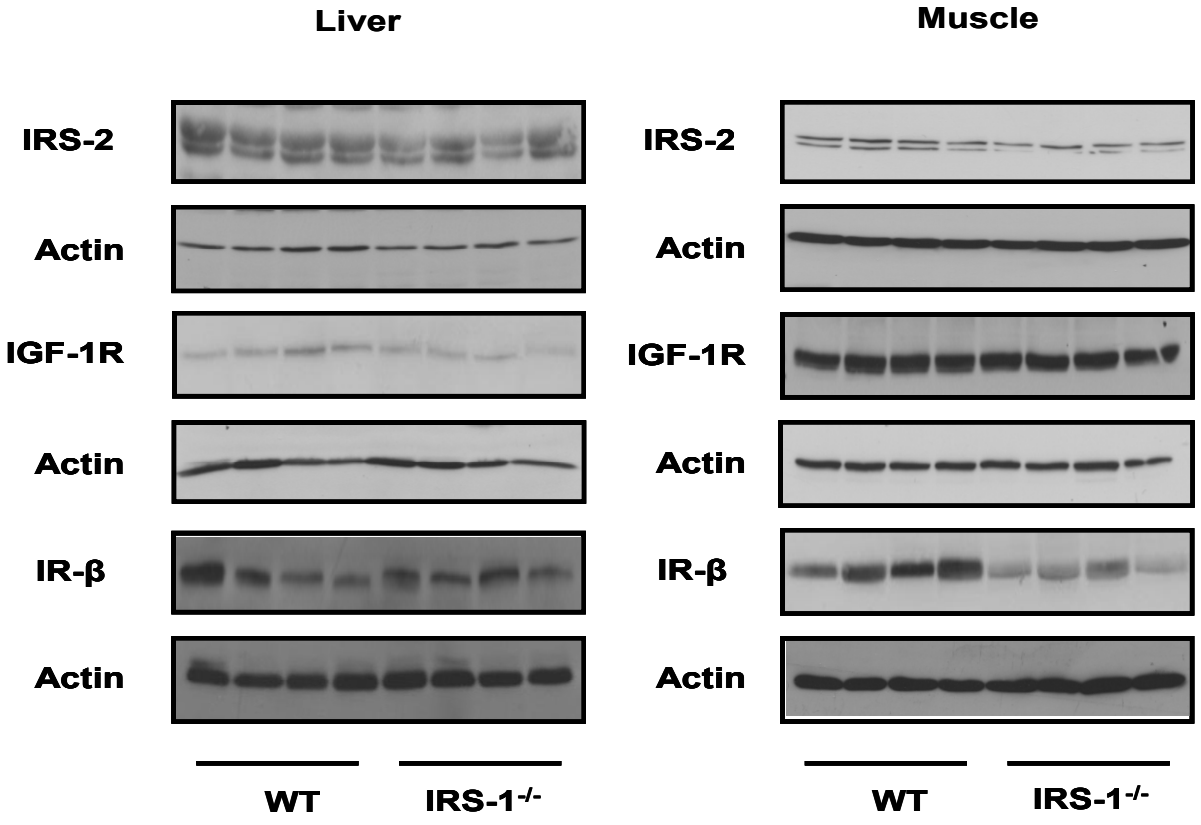

Fig. 3.3 Western blot analysis of basal IRS-2, IGF-1R and IR-β expression in liver and muscle of IRS-1 knockout and wild-type control animals
Basal expression states of IRS-2, IGF-1R, IR-β and actin (loading control) in organ lysates of liver and muscle of wild-type and IRS-1$^{-/-}$ mice. 100 µg of protein were applied to each 8 % SDS-PAGE gel.

Basal expression of IRS-2 protein was unchanged in both liver and muscle of IRS-1 knockout mice as well as wild-type littermates. Same expression pattern of IGF-1R has been detected in muscle and liver samples of wild-type and IRS-$1^{-/-}$ mice. No variations of IR-β expression in liver could be detected among knockout and wild-type animals, whereas evaluation of IR-β expression levels in muscle samples of both groups showed decreased IR-β expression in the knockout animals, resembling IR-β expression pattern seen in MEFs.

3.4 Insulin signaling in MEFs after acute insulin stimulation

For analyzing insulin signal transduction MEFs both genotype were starved over night (16 h) and stimulated with insulin in different concentrations. Unstimulated MEFs represent basal expression of key signaling molecules of the insulin signaling cascade after over night starvation. MEFs of each genotype were titrated with insulin endconcentrations of 1 nM, 10 nM and 100 nM. MEFs were stimulated with insulin for 4 minutes under standard cell cultivation conditions (37°C and 5 % CO_2). Insulin stimulation was stopped by removing insulin supplemented media, washing cells with ice cold PBS, followed by direct cell lysis.

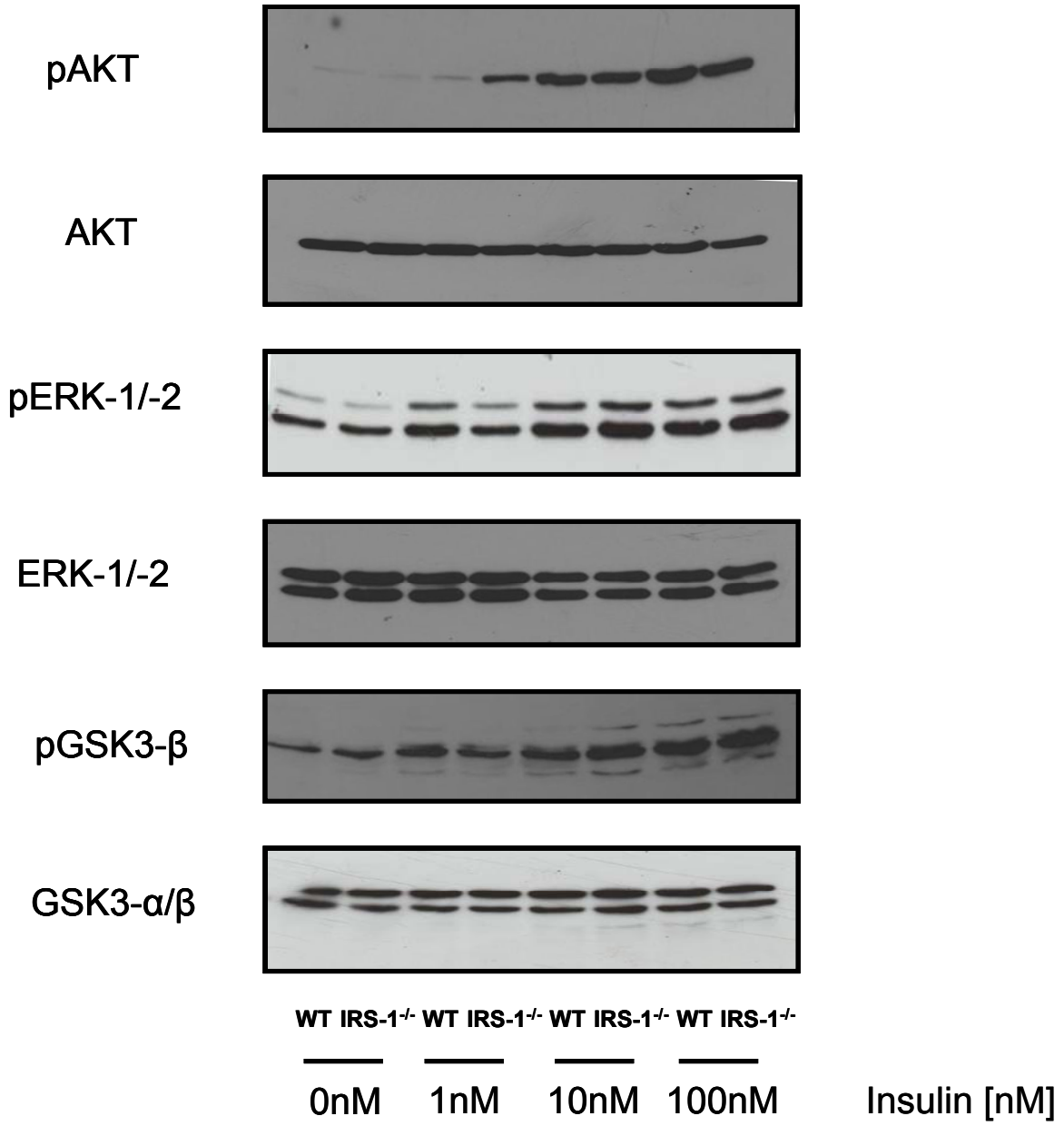

Fig. 3.4 Phosphorylation status of insulin signaling key proteins following insulin stimulation
Expression of phospho-AKT (Ser^{473}), phospho-ERK-1/-2 (Thr^{202}/Tyr^{204}) and phospho-GSK-3β (Ser^{9}) following insulin stimulation. MEFs were incubated in basal medium eagle with various insulin concentrations and without insulin supplementation representing basal protein expression after overnight starvation. Western blot analysis of unphosphorylated AKT, ERK-1/-2 and GSK-3α/β (Ser^{21}/Ser^{9}) expression serves as loading controls. 100 µg of protein samples were applied on 10 % SDS-PAGE gel.

Western blot analysis of protein phosphorylation patterns proved despite leakage of IRS-1 in MEFs derived from knockout animals no signaling deficiencies following insulin stimulation compared with wild-type MEFs. Phosphorylation intensities of the key kinases AKT, ERK and GSK-3β following insulin donation were indistinguishable in knockout and wild-type derived MEFs, suggesting no reduction of downstream effects in $IRS^{-/-}$ MEFs. Phosphorylation of AKT, ERK and GSK-3β rose with raised insulin concentrations. Only slight differences in phosphorylation degree of AKT, ERK

and GSK-3α/β could be observed between 10 nM and 100 nM insulin treatment indicating that stimulation with 10 nM of insulin is sufficient for full activation of the insulin signaling cascade.

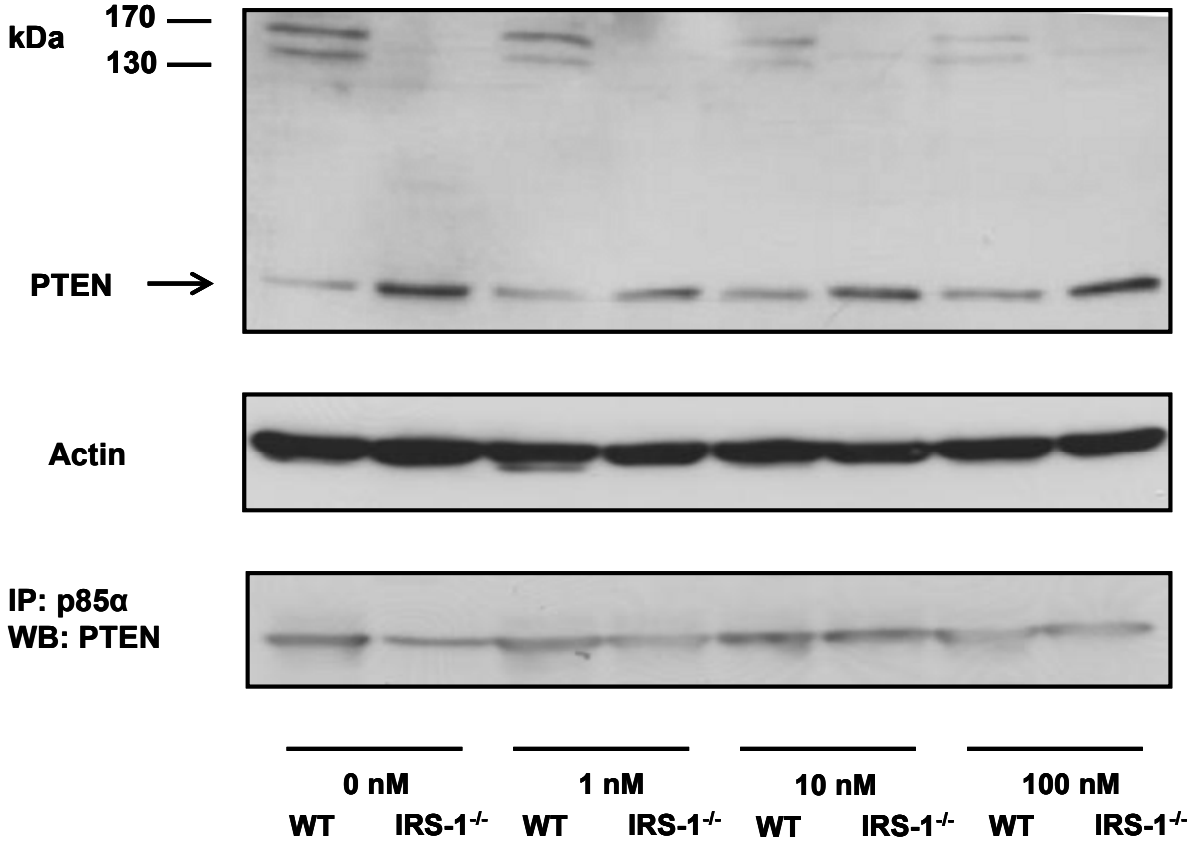

Fig. 3.5 PTEN expression pattern following insulin stimulation
PTEN expression in wild-type and knockout derived MEF upon insulin stimulation. Actin serves as loading control. 100 µg of protein samples were applied on 10 % SDS-PAGE gel for analysis.
Immunoprecipitation of p85α (regulatory subunit of PI3K) and PTEN. 1000 µg of protein sample were subjected to immunoprecipitation with anti p85α and detected with polyclonal anti-PTEN antibody.

PTEN is a constitutively active phosphatidylinositol phosphate phosphatase catalyzing dephosphorylation of $PI(3,4,5)P_3$ to $PI(3,4)P_2$, resulting in disruption of the PI3K-AKT/PKB pathway revealing opposing effects of PTEN and PI3K on cell proliferation and survival. PTEN interacts dynamically with the plasma membrane and function as tumor suppressor since elevated PIP_3 levels confer advantage to cancer cells (Gericke et al., 2006; Vazquez et al., 2006). Western blot analysis of PTEN showed decreased protein expression in wild-type animals compared to knockout mice. Interestingly wild-type PTEN expression increased with insulin stimulation whereas expression in IRS-1 knockouts remained rather unchanged. Parallel to PTEN expression increase in wild-types a decrease of a ~165 kDa protein complex was observed.

p85/PTEN immunoprecipitation showed decreased PTEN signal in knockout compared to wild-type mice under basal conditions and upon stimulation with 1 mM insulin. PTEN signal decrease was not observed upon insulin stimulation with higher doses.

3.5 Insulin signaling in liver and muscle of IRS-1$^{-/-}$ and wild-type mice after intraperitoneal insulin application

In order to evaluate the effect of the IRS-1 knockout on insulin signaling in an *in vivo* system mice were starved overnight (16 h) and intraperitoneal injected with 0,75 U/kg body weight of human insulin (Novo Nordisk, Copenhagen, Denmark) and 0,9 % NaCl (Berlin-Chemie-AG, Berlin, Germany). Western Blot analysis was used to assess phosphorylation status of AKT after insulin or NaCl treatment, respectively. Unphosphorylated AKT was used as loading control.

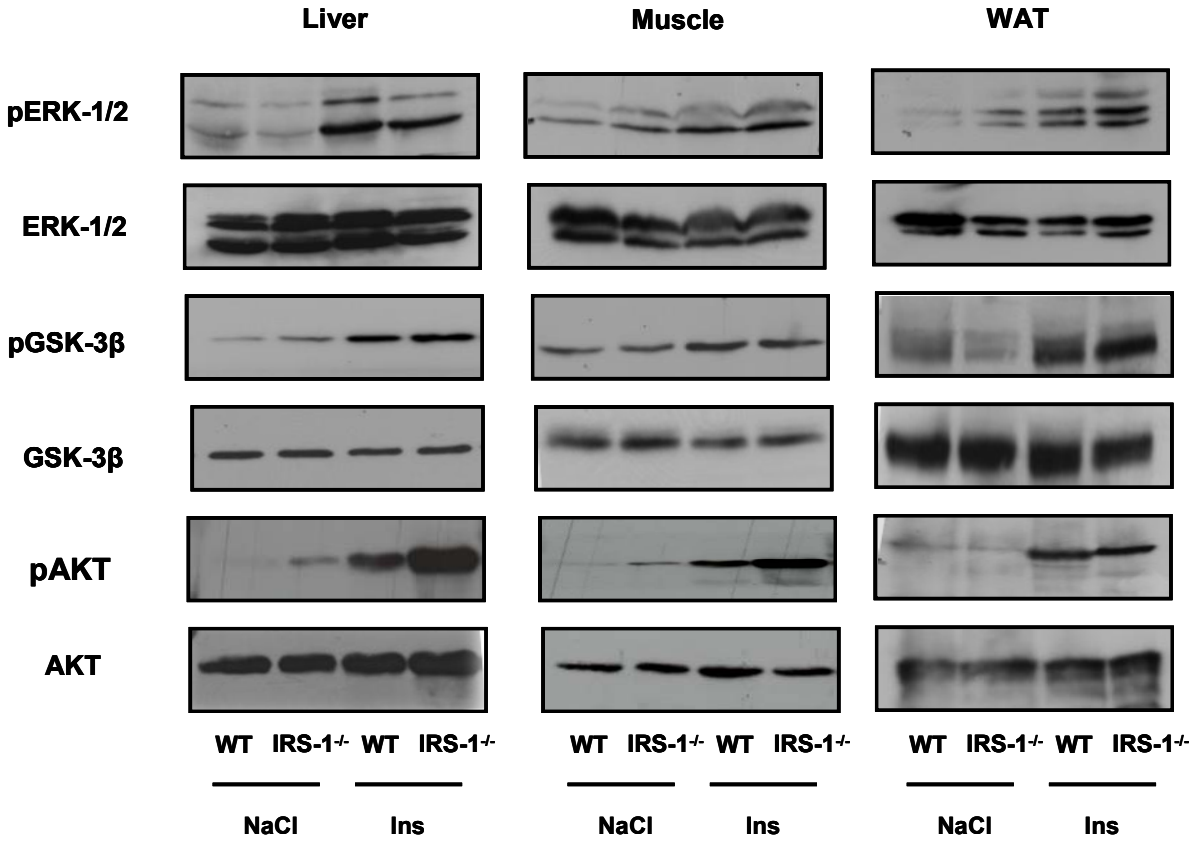

Fig. 3.6 Phosphorylation status of AKT, ERK and GSK-3β following intraperitoneal insulin injection
Phospho-ERK-1/-2 (Thr^{202}/Tyr^{204}), phospho-GSK-3β (Ser^{9}) and phospho-AKT (Ser^{473}) expression in knockout and wild-type mice following insulin treatment. Basal phospho-ERK-1/-2 (Thr^{202}/Tyr^{204}), phospho-GSK-3β (Ser^{9}) and phospho-AKT (Ser^{473}) expression after overnight starvation is represented by NaCl injected wild-type and knockout animals. Western blot analysis of unphosphorylated ERK-1/-2, GSK-3β and AKT expression served as loading control. 10 minutes after insulin injection skeletal muscles and livers were removed, homogenized and applied to Western blot analysis. 100 µg of protein samples were applied on 10 % SDS-PAGE gel. Examples of three independent experiments.

No causal decline in ERK-1/-2, GSK-3β and AKT phosphorylation after intarperitoneal insulin injection has been observed in liver, muscle and WAT of knockout in comparison to the ERK-1/-2, GSK-3β and AKT phosphorylation in wild-type mice. Basal phosphorylation pattern of ERK-1/-2 in WAT, GSK-3β in liver and AKT in liver and muscle determined by Western blot analysis of NaCl injected animals seemed to be increased in IRS-1 deficient mice compared with wild-type controls. ERK-1/-2 phosphorylation in WAT, GSK-3β phosphorylation in liver and AKT phosphorylation in liver and muscle upon insulin stimulation were increased to the same degree in knockout mice compared with wild-type animals.

The group of Kadowaki could show that degree of compensation for IRS-1 deficiency appears to be correlated with the amount of tyrosine-phosphorylated IRS-2 (in IRS-1-

deficient mice) relative to that of IRS-1 (in wild-type mice) (Yamauchi et al., 1996). Therefore IRS-1 deficient and wild-type control mice were starved other night (16 h) and insulin stimulated with 0,75 U/kg body weight. Insulin responsive tissues were removed 10 minutes after injection and homogenized. 3 mg liver lysates of intraperitoneal injected NaCl and insulin wild-type and knockout mice were used for an immunoprecipitation with polyclonal anti-phosphotyrosine antibody, followed by IRS-2 detection by Western blotting.

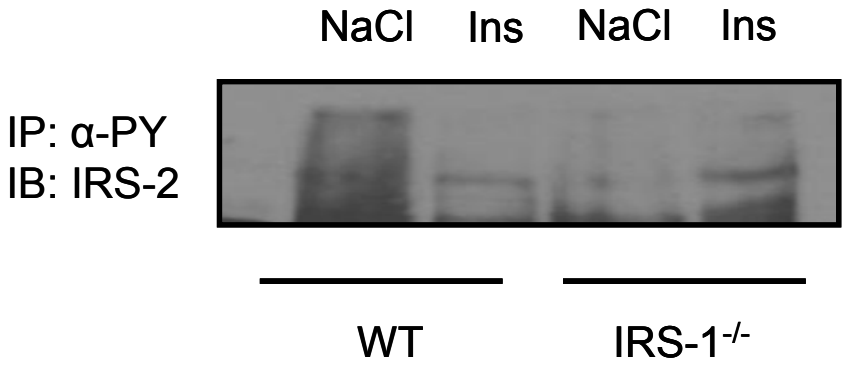

Fig. 3.7 Anti-phophotyrosine immunoprecipitation and IRS-2 detection in livers of intraperitoneal NaCl and insulin injected IRS-1 deficient and control mice
Immunoprecipitation of phosphotyrosine proteins after insulin stimulation and IRS-2 detection by Western blot in livers from wild-type (WT) and IRS-1-deficient (IRS-1$^{-/-}$) mice. Livers were removed 10 min after intraperitoneal insulin injection, homogenized and supernatants were subjected to immunoprecipitation with anti phosphotyrosine (α-PY) and then detected with polyclonal anti-IRS-2 antibody (IRS-2).

Immunoprecipitation with anti-pohosphotyrosine antibody indicated a higher IRS-2 phosphorylation degree upon intraperitoneal insulin injection in liver of IRS-1 deficient mice compared with wild-type controls. No difference was detected in basal IRS-2 expression after NaCl application. No differences of IRS-2 phosphorylation patterns were detected in muscles.

3.6 Phenotypic and metabolic characterization

IRS-1$^{-/-}$ deficient mice show embryonic and postnatal growth retardation compared with wild-type littermates previously described by different groups. Glucose tolerance and insulin tolerance tests revealed mild insulin resistance with normal glucose tolerance (Araki et al., 1994; Tamemoto et al., 1994). Despite mild insulin resistance IRS-1 deficient females showed increased life span (Selman et al., 2008). For further characterization of the IRS-1$^{-/-}$ phenotype; 12 to 24 month old mice were analyzed

regarding energy expenditure, food intake, body composition, activity and glucose metabolism.

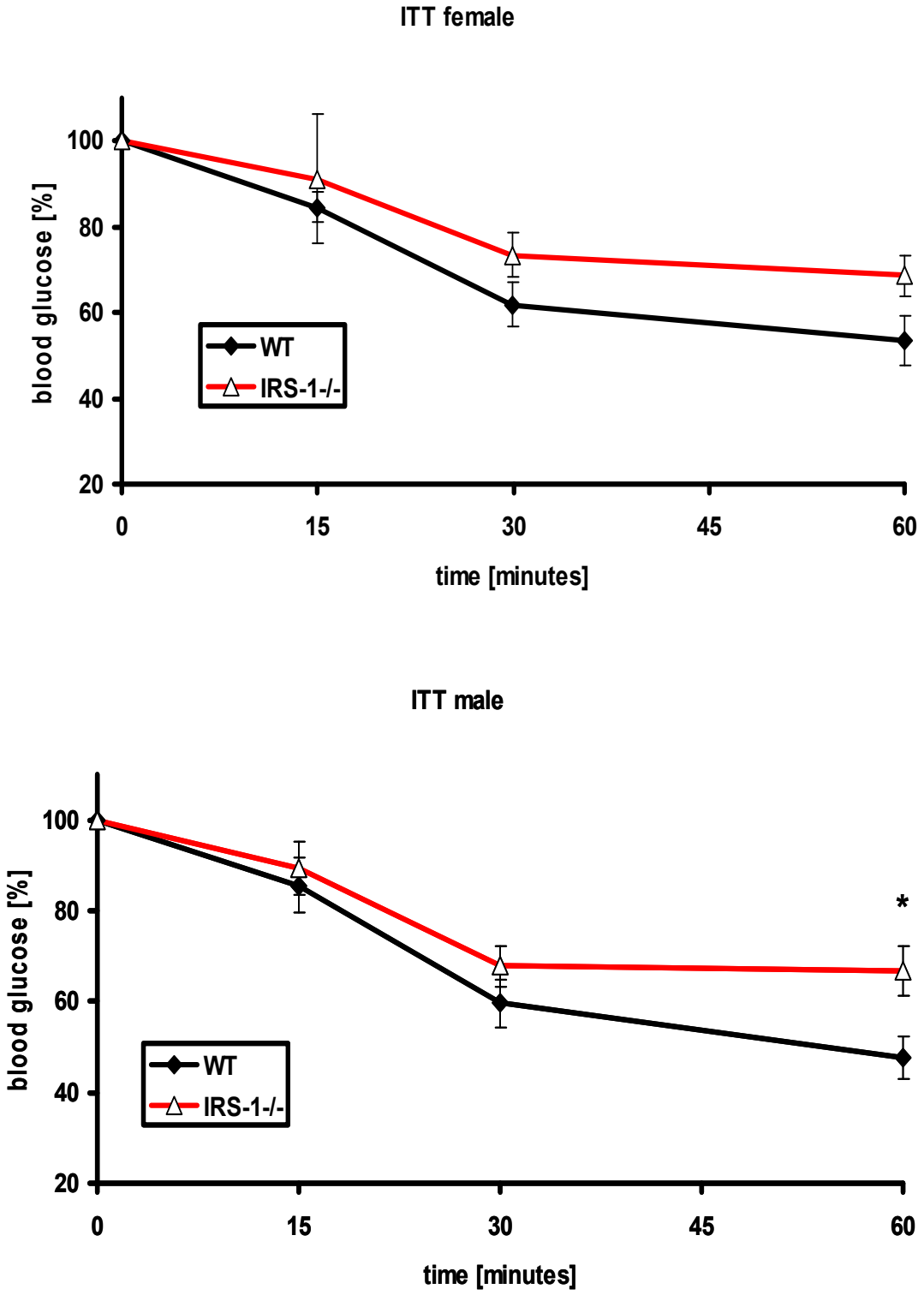

Fig. 3.8 Insulin tolerance test (ITT) of male and female wild-type and IRS-1$^{-/-}$ mice
Average decrease of blood glucose levels in [% of initial] of 12 weeks old wild-type (black line) and knockout (red line) mice. Upper panel ITT of female wild-type (n = 12) and knockout animals (n = 12). Lower panel ITT of male wild-type controls (n = 10) and knockout mice (n = 10). Values are means ± SEM, * unpaired Student´s t-test p-value ≤ 0,05.

Insulin sensitivity was determined by insulin tolerance test, applying 0,75 U/g body weight of human insulin by intraperitoneal injection, blood glucose levels [mg/dl] were determined at indicated time points. Insulin administration decreased blood glucose levels. However glucose decrease was reduced in IRS-1 deficient female and male mice compared to wild-type controls indicating insulin resistance. Blood glucose levels in female IRS-$1^{-/-}$ mice dropped to 69 % of starting glucose levels after 60 minutes whereas glucose levels in wild-type mice dropped to 53 %, however this difference failed to be significant. For all time points decrease in glucose levels of IRS-1 deficient mice was reduced in comparison with the wild-types. ITT in the male group revealed a drop to 67 % of starting glucose levels in the knockout group and to 48 % in the wild-type control group. Like in the female group drop of insulin levels in the knockout group was less at every time point compared with the wild-types, reaching significance at 60 minutes.

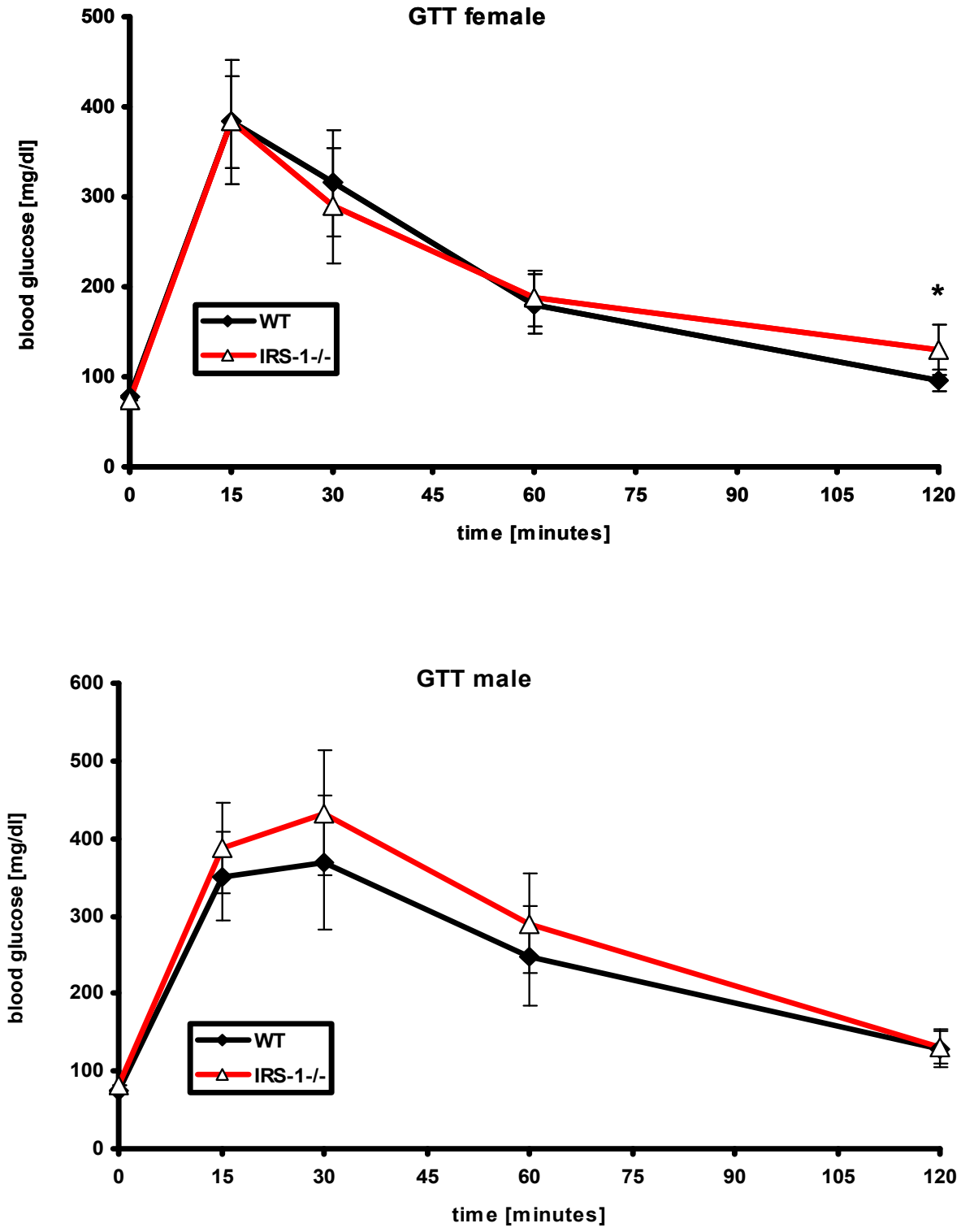

Fig. 3.9 Glucose tolerance test (GTT) of male and female wild-type and IRS-1$^{-/-}$ mice
Average increase of blood glucose levels in 13 weeks old wild-type (black line) and knockout (red line) mice upon glucose administration. Upper panel GTT of female wild-type (n = 12) and knockout animals (n = 12). Lower panel GTT of male wild-type controls (n = 10) and knockout mice (n = 10). Values are means ± SEM, * unpaired Student´s t-test p-value ≤ 0,05.

Glucose homeostasis in animals was evaluated by performing glucose tolerance test, by administration of 2 g glucose/ kg body. Intraperitoneal glucose administration increased blood glucose levels. Glucose levels [mg/dl] or glucose clearance respectively was controlled at indicated time points. In tested males no significant changes were detected, both groups displayed increase in blood glucose levels and glucose clearance following glucose administration. However IRS-1 deficient animals showed elevated blood glucose levels at 15, 30 and 60 minutes compared to wildtype controls. Both groups returned to normal blood glucose levels after 120 minutes. Female animals showed same degree of glucose clearance after glucose administration up to 60 minutes however after 120 minutes blood glucose levels were significantly higher in IRS-1 deficient mice.

ITT and GTT data revealed mild insulin resistance for the IRS-1 knockout animals. For further evaluation of the indicated insulin intolerance ELISA was performed for determination of serum insulin levels in wild-type and IRS-1 deficient mice.

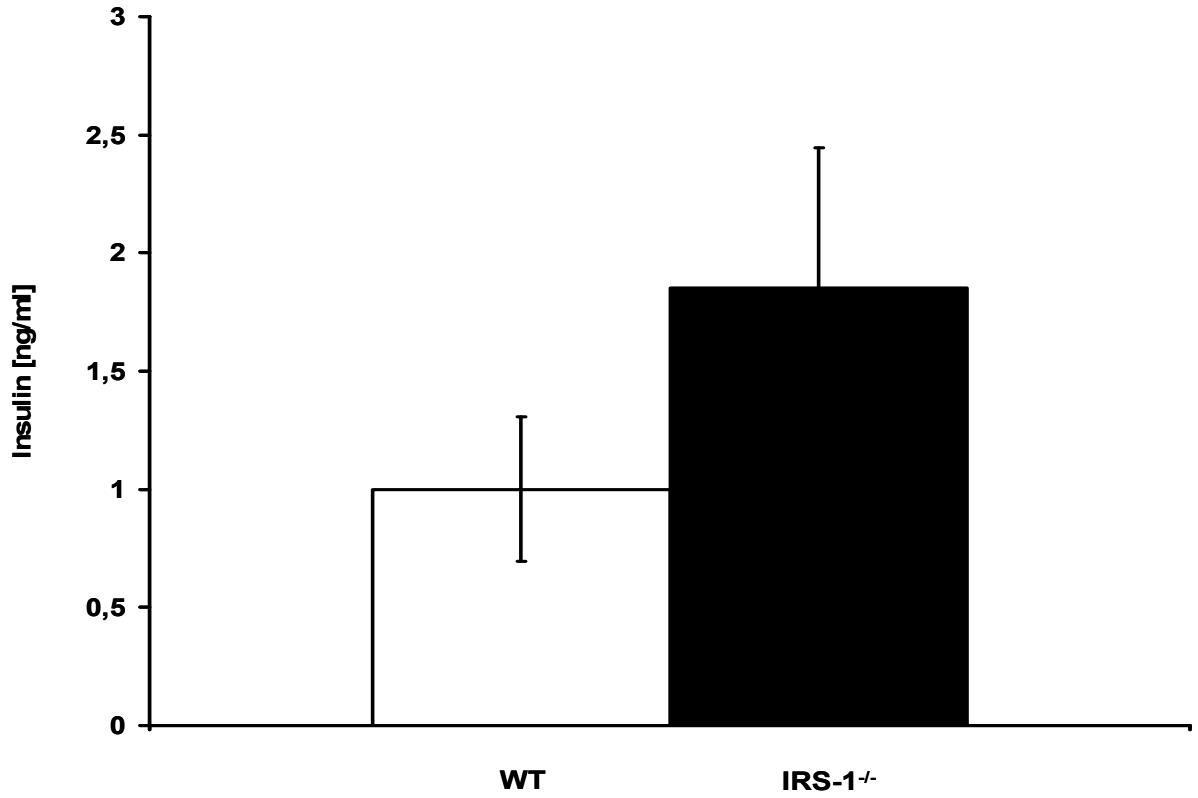

Fig. 3.10 Determination of serum insulin levels of 12 month old mice
Insulin serum levels of both wild-type (n = 7) and IRS-$1^{-/-}$ (n = 7) mice were determined by ELISA. Mice were starved overnight (16 h) and serum was isolated from blood of animals. Values are means ± SEM.

Analysis of insulin serum levels of starved (16 h) wild-type and IRS-1 knockout mice confirmed the observed phenotype of the ITT. ELISA analysis revealed elevated insulin serum levels in IRS-1 deficient mice compared with wild-type controls, due to mild insulin resistance in these animals. Determined mean value of serum insulin levels in the knockout group was 85 % higher in comparison with wild-type group.

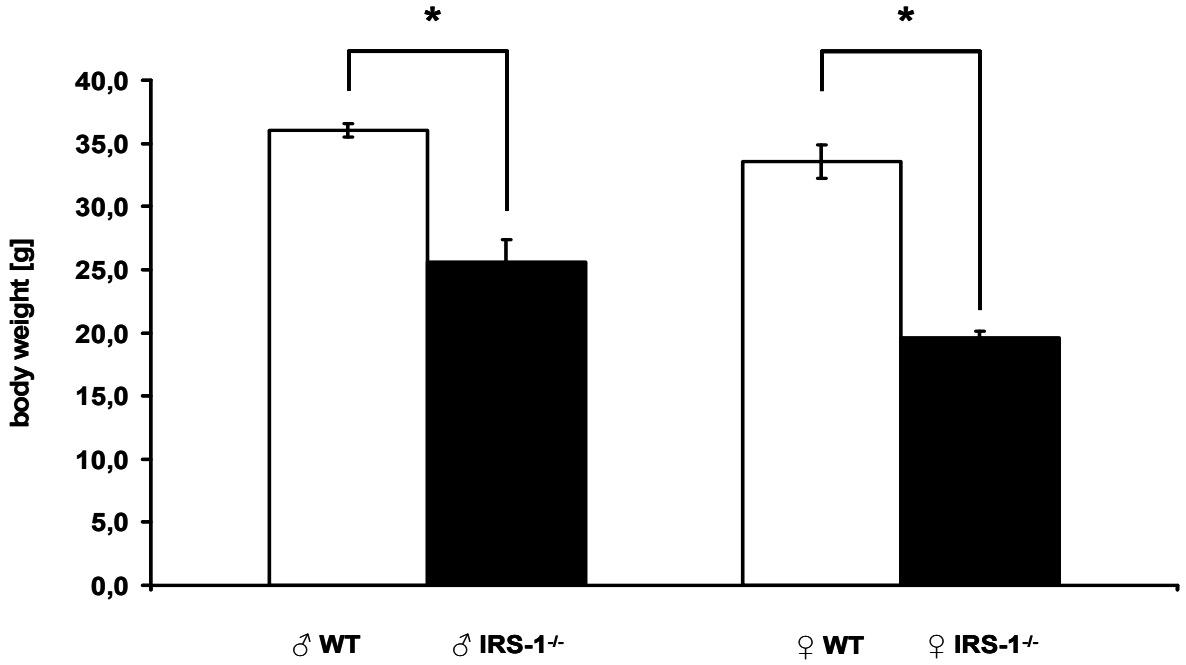

Fig. 3.11 Reduced body weight of IRS-1 deficient mice compared with littermates control in female and male study group
Average weight of 12 month old IRS-$1^{-/-}$ mice (black bars) and wild-type controls (WT; white bars). Left panel representing male groups, IRS-$1^{-/-}$ (n = 12) and WT (n = 15); right panel representing female groups, IRS$^{-/-}$ (n = 15) and WT (n = 17). Values are means ± SEM, * unpaired Student´s t-test p-value ≤ 0,05.

Figure 3.11 shows the average body weight of 12 month old female and male animals of each group. Due to observed embryonic and postnatal growth retardation leading to body size alterations, IRS-1 deficient mice showed significant decreased body weights in comparison with wild-type littermates. Thus body size alterations in IRS-1 knockout mice result in body weight reduction in female and male group. Body weight of female WT mice was about 70 % higher compared with IRS-1 deficient females. For the wild-type male mice 40 % increased body weight compared to IRS-1 knockout males was observed.

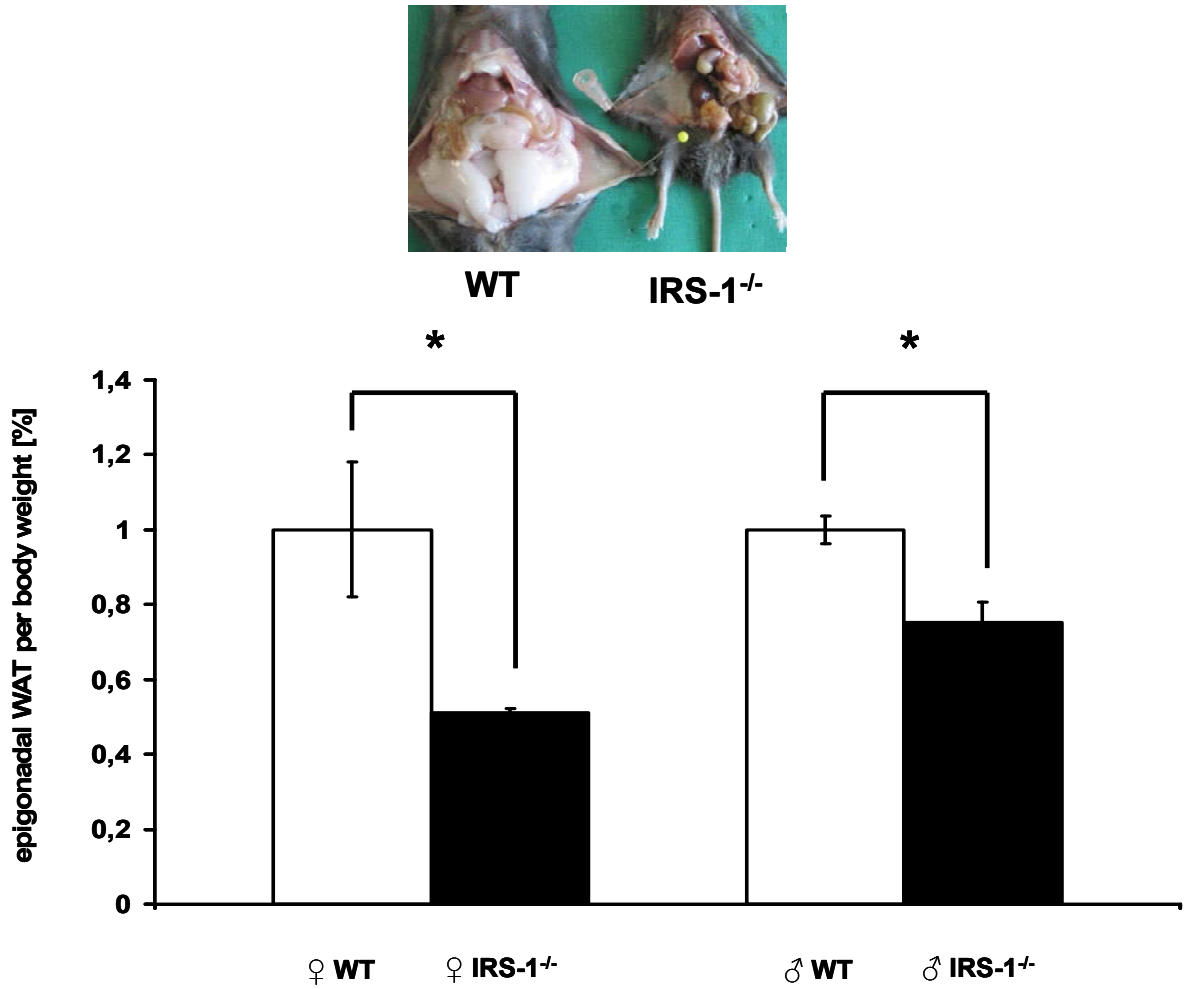

Fig 3.12 Anatomical view of IRS-1$^{-/-}$ and wild-type mice and normalized epigonadal white adipose tissue (WAT) content in female and male mice
Anatomical view of 12 month old female wild-type and IRS-1$^{-/-}$ mice revealed reduced body length, leanness and lack of abdominal fat pads in IRS-1$^{-/-}$ mice. Isolated WAT fat pads of female wild-type (n = 4) and IRS-1 deficient (n = 4) and male wild-type (n = 7) and IRS-1$^{-/-}$ (n = 7) mice were dissected weighed and correlated to body weight.

Additionally to reduced body size 12 month old IRS-1$^{-/-}$ mice showed reduced accumulation of abdominal fat pads compared to wild-type control mice. Dissected abdominal fat pads weighed and normalized to body weight revealed 50 % reduction of abdominal fat mass in IRS-1 deficient females compared to control mice and a 25 % reduction of WAT in IRS-1 knockout males in comparison with wild-type males.
Overall female and male IRS-1$^{-/-}$ mice showed reduced gain of weight and gain of abdominal fat between 12 and 24 month of age. During this period body weight in the wild-type control groups increased about 20 – 25 % whereas in IRS-1 knockout animals body weight increased just about 10 %. Gain of abdominal fat during this period was about 55 % for wild-type animals but just 10 % in the IRS-1 deficient mice (Fig. 3.13).

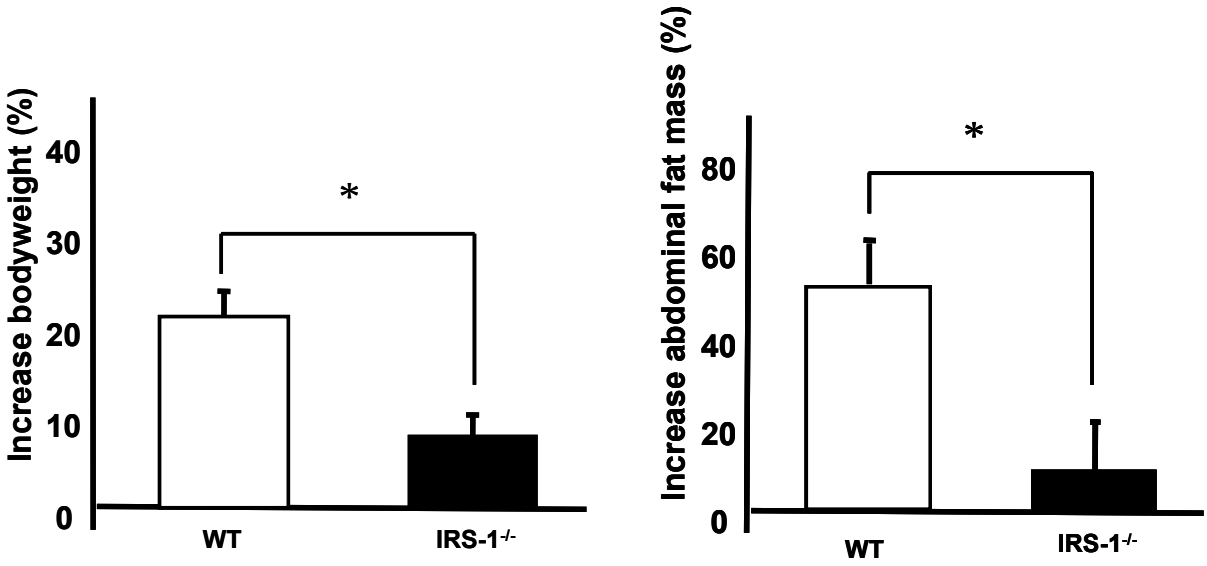

Fig. 3.13 Gain of body weight and increase of abdominal fat mass in wild-type and IRS-1$^{-/-}$ mice during 12 and 24 months of age.
Increase of body weight and increase in abdominal fat mass determined in wild-type (n = 10) and IRS-1$^{-/-}$ (n = 10) mice.

Histological analysis of WAT of IRS-1 knockout and wild-type controls, revealed distinct anatomical differences. Volume of adipocytes of IRS-1$^{-/-}$ mice was decreased compared to control group, indicating decreased lipid storage in adipocytes of IRS-1 knockout mice. Another characteristic of small sized adipocytes is improved insulin sensitivity. Interestingly another cell population was detected between the adipocytes membranes of knockout animals (dark blue formations) whereas in wild-type animals this cell population was absent.

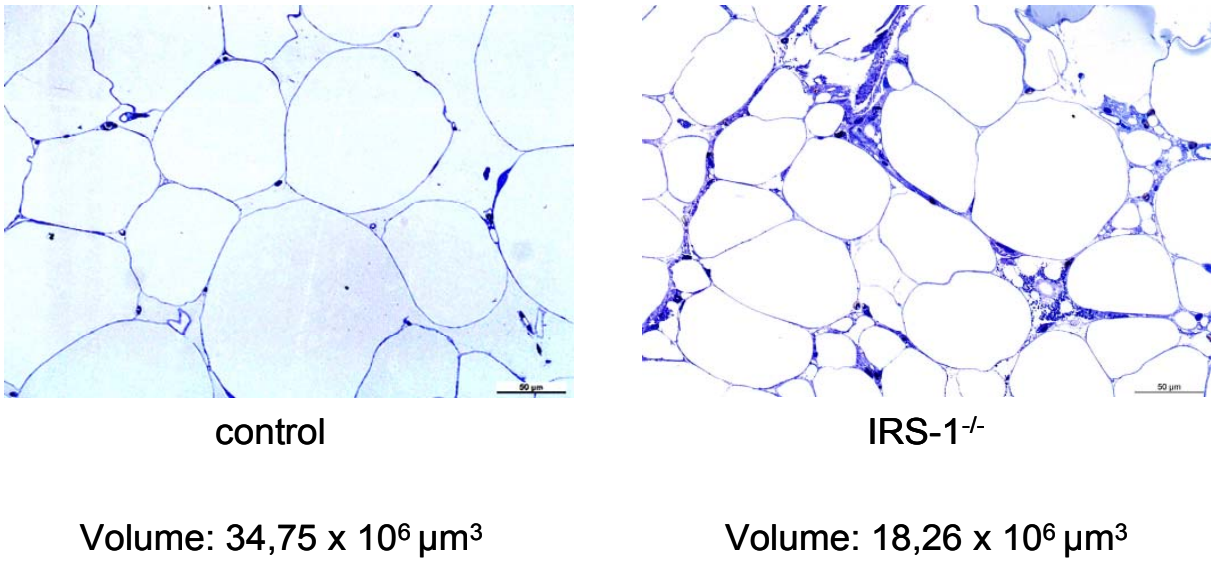

Fig. 3.14 Toluidine blue staining and cell volumetry determination of adipocytes
Adipocytes morphology of IRS-1 deficient mice and wild-type controls were compared by toluidine blue staining. Volume of adipocytes was determinded by volumetry using coulter counter (Beckman, Multisizer COULTER COUNTER) (in collaboration with Prof. M. Blüher, Leipzig).

To address the question if reduced food intake of IRS-1 deficient mice was causative for the observed somatic phenotype in 12 month old animals food intake of wild-type and IRS-1 $^{-/-}$ mice was determined by using food hayrack.

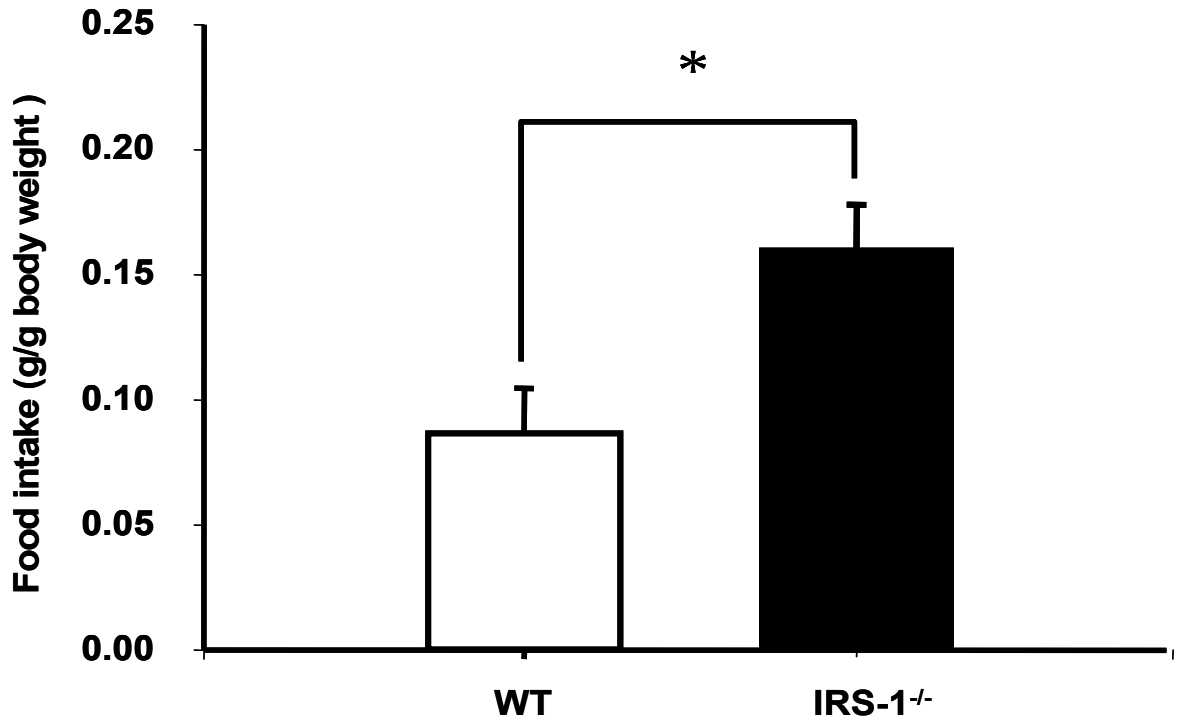

Fig. 3.15 Determination of food intake of IRS-1$^{-/-}$ and wild-type mice
Food intake of wild-type (n = 10) and IRS-1 deficient mice (n = 10) was analyzed using food hayracks. Data represent overall food intake of both genders.

Despite decreased weight gain and non present accumulation of abdominal fat pads IRS-1 deficient mice showed significantly enhanced food intake compared to wild-type controls. Reduced weight gain and reduced fat accumulation might be due to improved fitness of IRS-1$^{-/-}$ mice. Therefore activity (spontaneous and activity in the wheel) of wild-type and IRS-1 knockout mice was tested and analyzed by video-tracking analysis software.

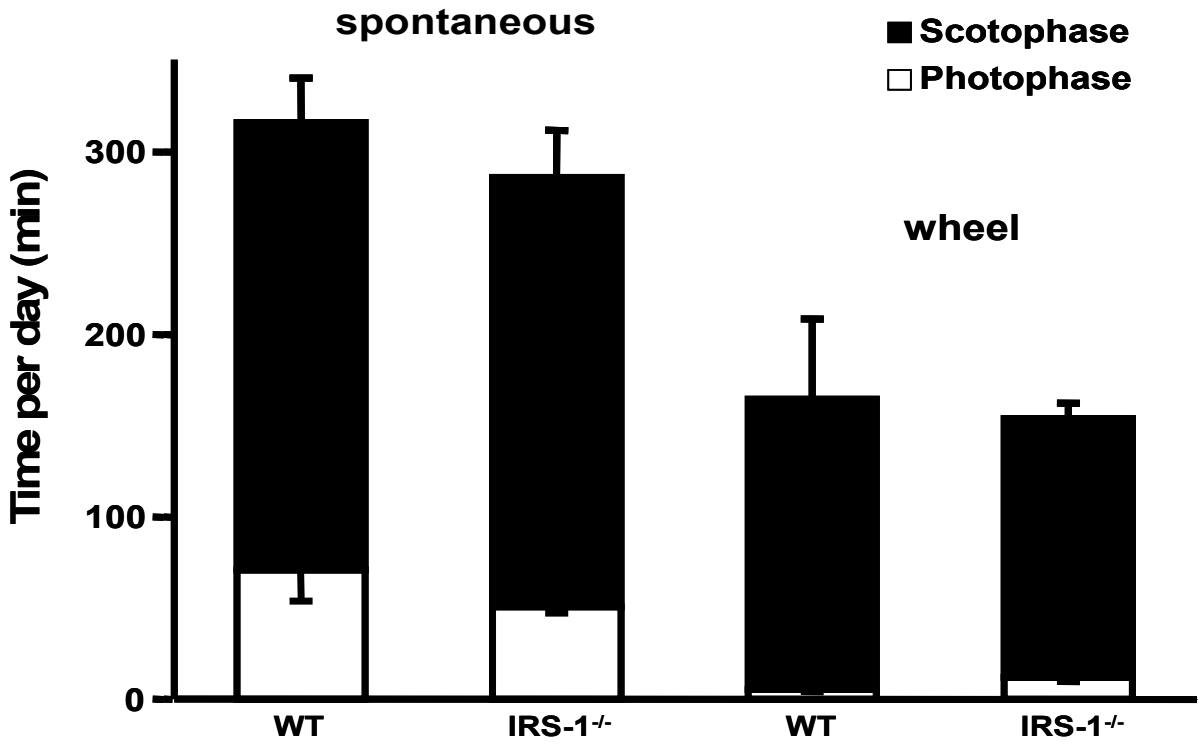

Fig. 3.16 Activity of wild-type and IRS-1 knockout mice per day
Activity of wild-type and knockout mice of both genders were tested in an activity center setup. Data represent mean activity per day. Activity was determined in minutes/day for wild-type (n = 10) and knockout (n = 10) animals (in collaboration with Prof. Schröder , Anatomy, Cologne).

Wild-type as well as knockout mice showed a typical murine nocturnal activity pattern, spontaneous and wheel activity displayed no significant differences between the knockout and wild-type group neither in photophase nor in scotophase.

Indirect calorimetry was used to address alterations in the energy expenditure of wild-type and IRS-1 deficient mice in the photo as well as in the scotophase.

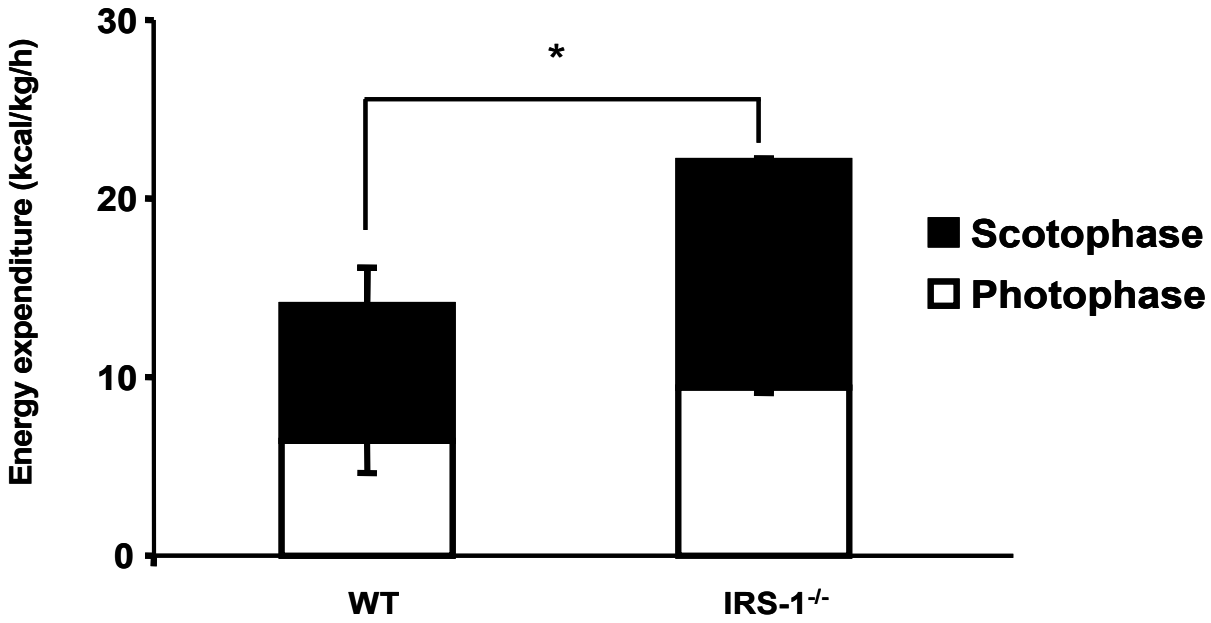

Fig. 3.17 Determination of energy expenditure of wild-type and IRS-1$^{-/-}$ mice via indirect calorimetry
Wild type (n = 5) and knockout (n = 5) animals were analyzed in a CaloSys system determining energy expenditure in photo- and scotophase of each genotype. Both genders were included in tested groups of wild-type and knockout mice (in collaboration with Prof. Schröder, Anatomy, Cologne).

Analyzing wild-type and IRS-1$^{-/-}$ deficient mice via indirect calorimetry revealed significant higher energy expenditure in IRS-1 knockout mice. Knockouts showed 1,4- to 1,6-fold increased energy conversion compared with the wild-type control group. Hyperthyroidism leads to increased food intake and energy expenditure. Thyroid hormones induce marked stimulation of basal metabolic rate associated with loss of body fat, creating a state of negative energy balance leading to increased energy intake (Havel, 2001). Serum levels of free triiodothyronine (T3) the biological active form of triiodothyronine were determined in wild-type and knockout mice by ELISA.

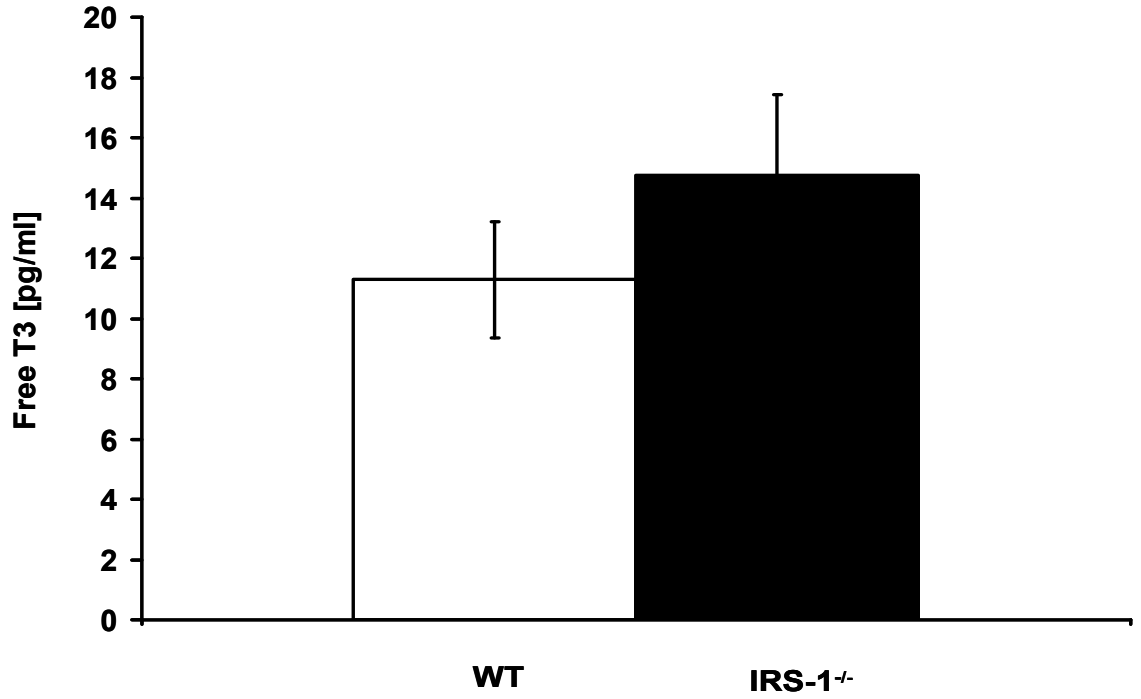

Fig 3.18 Determination of free triiodotyronine (T3) serum levels
Free T3 serum levels in wild-type controls and IRS-1 knockout mice were analyzed by ELISA. Serum samples of eight wild-type (white bars) and seven knockout mice (black bars) were collected and used for ELISA. Values are means ± SEM.

Analysis of free triiodothyronine (T3) revealed no alteration in T3 serum levels towards hyperthyroidism in IRS-1 deficient mice compared with wild-type control mice, indicating normal thyroid function in the knockout mice.
Mitochondria have a key role in energy conversion and metabolic rate of animals. Concerning the molecular mechanisms of higher energy expenditure in IRS-1 deficient animals mitochondrial function, mitochondrial enzyme activity and expression of mitochondrial proteins in IRS-$1^{-/-}$ mice were compared with wild-type controls.

3.7 Mitochondrial activity and function in IRS-1 deficient mice

In order to verify if hyperactivity of mitochondrial respiratory chain enzymes could be the underlying mechanism of elevated energy expenditure in IRS-1 knockout mice, respiratory chain enzymes were analyzed in respect to differences in expression pattern by Western blot and towards their activity and turnover capacities by photo-spectroscopy under V_{max} conditions.

3.7.1 Expression of mitochondrial respiratory chain complexes

Mitochondrial respiratory chain enzyme expression levels were determined in muscle and liver of IRS-1$^{-/-}$ mice and wild-type controls by Western blotting using MitoProfile Total OXPHOS Rodent WB Antibody Cocktail (MitoScience, Acris Antibodies, Hiddenhausen, Germany) and monoclonal complex specific antibodies (Molecular Probes, Mo Bi Tec, Göttingen, Germany). For detection with Total OXPHOS Rodent WB Antibody Cocktail lysate samples were not heated to 95°C, avoiding destruction of epitopes detected by antibody.

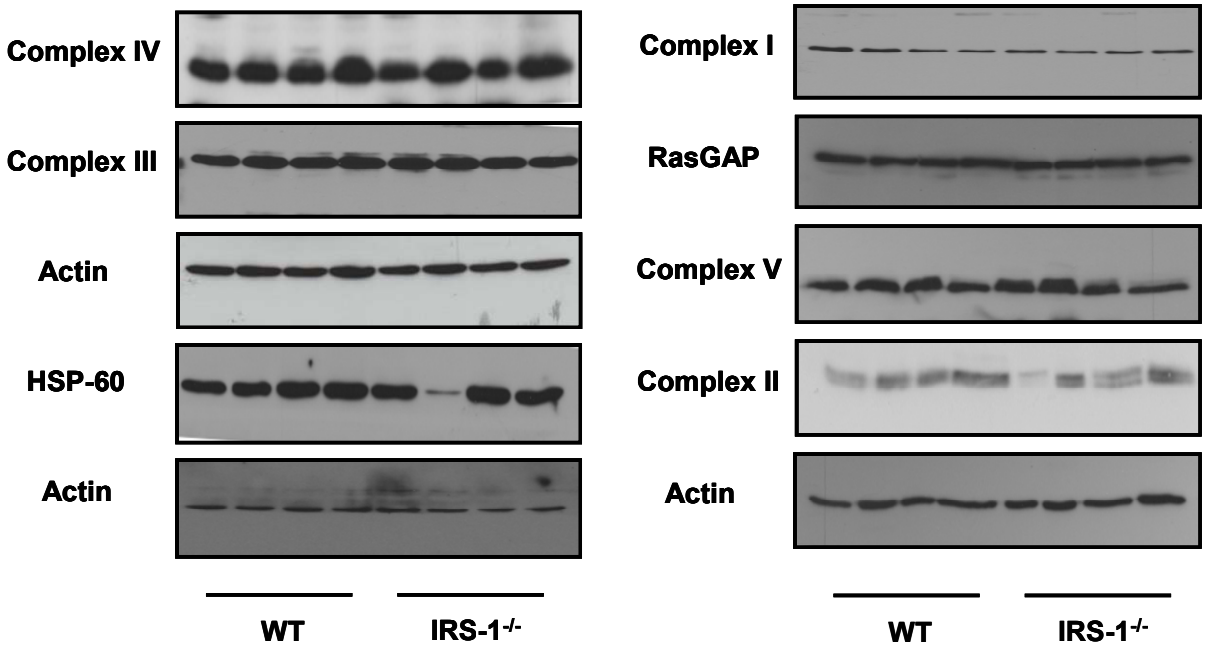

Fig. 3.19 Western blot analysis of respiratory chain complexes I, II, III, IV and V in muscles of IRS-1$^{-/-}$ and wild-type mice
Protein expression of respiratory chain complexes I-V, HSP 60 and corresponding loading controls, β-actin or RasGAP, respectively. Two female wild-type and two male wild-type animals were compared with two female knockout and two male knockout animals on one gel. 100 µg of each protein lysate were applied on 10 % SDS-PAGE gel. Sample lysates were consisting of M.soleus and M. gastrocenemius. Examples of 2 independent experiments.

Determination of protein levels or representative subunits of the five mitochondrial respiratory chain complexes, respectively, revealed no obvious decrease in the expression pattern of respiratory chain enzymes of complex I, III, IV and IV in the muscle of IRS-1 deficient mice compared to wild-type controls. However a tendency of a slight decrease in the expression of complex II in the IRS-1$^{-/-}$ mice has been detected. Western blot against HSP-60 served as reference for mitochondrial mass. HSP-60 is a chaperone located in the mitochondrial matrix (D´Souza et al., 1998;

Rospert and Hallberg, 1995). Protein levels of HSP-60 were unchanged, indicating no effect of the IRS-1 knockout on mitochondrial content.

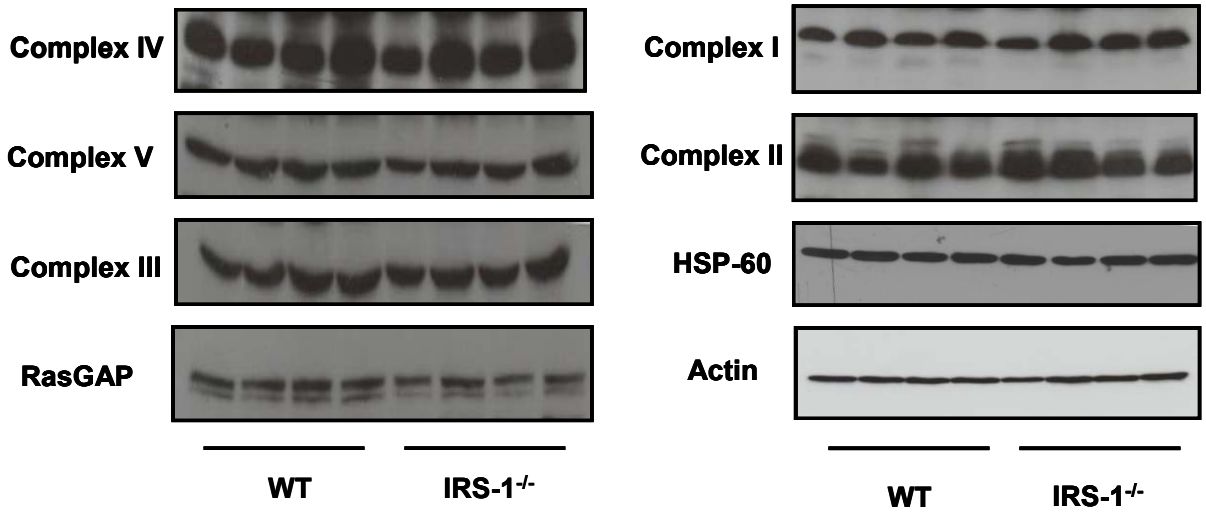

Fig. 3.20 Western blot analysis of respiratory chain complexes I, II, III, IV and V in livers of IRS-1$^{-/-}$ and wild-type mice
Levels of respiratory chain complexes I-V, HSP 60 and corresponding loading controls, β-actin or RasGAP, respectively, determined by Western blotting. Two female wild-type and two male wild-type animals were compared with two female knockout and two male knockout animals on one gel. 100 µg of each protein lysate were applied on 10 % SDS-PAGE gel. Examples of 2 independent experiments.

Steady-state levels of respiratory chain complexes subunits representing fully assembled complexes in liver of wild-type controls and IRS-1$^{-/-}$ mice analyzed by Western blots. No increased or decreased expression of one of the complexes in one of the two compared groups was detected. Like in muscle unaltered levels of HSP-60 protein in the liver of all analyzed animals, indicating normal mitochondrial content in livers of all mice.

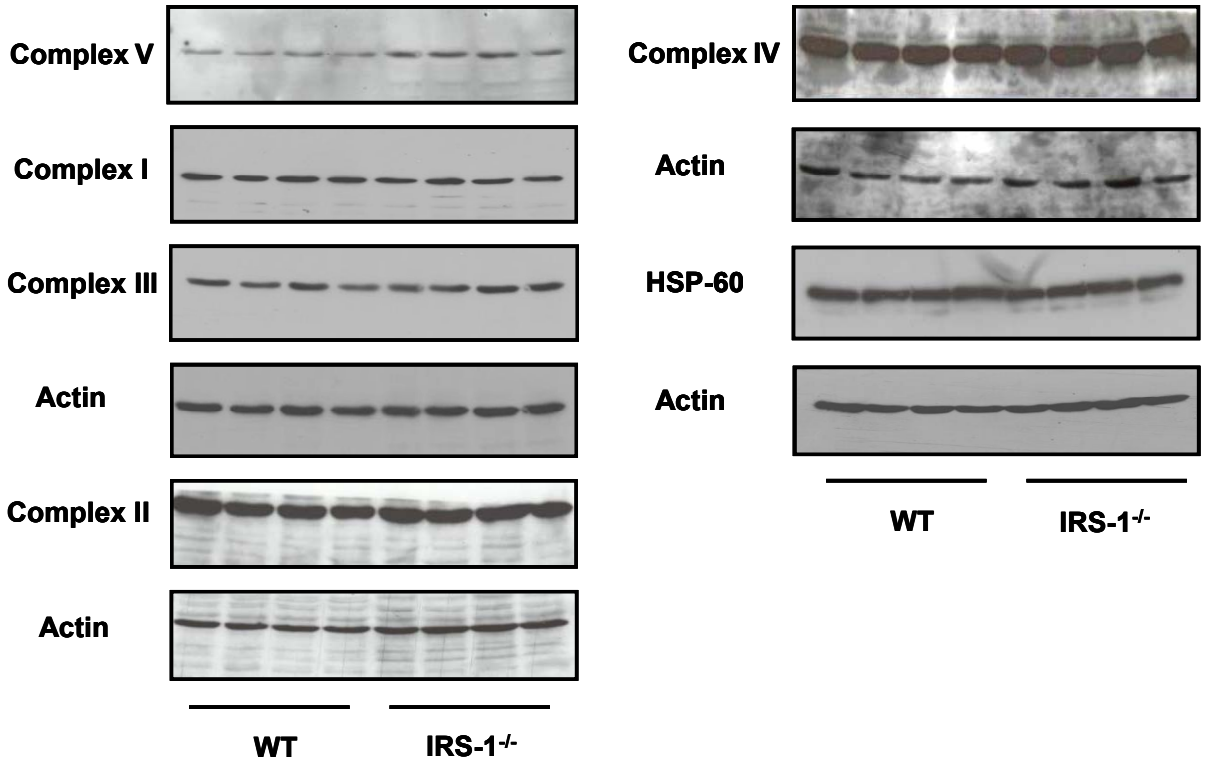

Fig. 3.21 Western blot analysis of respiratory chain complexes I, II, III, IV and V in MEFs of IRS-1$^{-/-}$ and wild-type mice
Expression levels of respiratory chain complexes I-V, HSP 60 and β-actin as corresponding loading control, determined by Western blot. Four wild-type cell lystes were compared with four knockout cell lysates on one gel. 100 µg of each cell lysate were applied on 10 % SDS-PAGE gel. Examples of 2 independent experiments.

Figure 3.21 presents expression of respiratory chain complexes I-V and HSP-60 in wild-type and IRS-1 deficient MEFs. No detectable difference in mitochondrial mass of wild-type and IRS-1 knockout MEFs represented by HSP-60 were observed. Same expression of respiratory chain complexes I, II, III and IV in wild-type and IRS-1$^{-/-}$ MEFs. However respiratory chain complex V (ATP synthetase or ATPase, respectively) was elevated in IRS-1 deficient MEFs compared to wild-type MEFs.

To confirm unchanged expression of mitochondrial respiratory complex in liver muscle and MEFs of IRS-1$^{-/-}$ mice and wild-type controls protein expression levels of peroxisome proliferator-activated receptor gamma coactivator 1-alpha (PGC-1 alpha; PGC-1α), key regulator of mitochondrial biogenesis were determined by Western blot analysis. PGC-1α stimulates mitochondrial biogenesis by binding to and coactivating PPAR family members, transcription factors involved in extra and intramitochondrial fatty acid transport and oxidation. In addition PGC-1α interacts with and co-activates the NRF transcription factors which in turn activate nuclear genes required for

respiration, mitochondrial DNA transcription and replication (Wu et al., 1999; Liang and Ward, 2006; Ventura-Clapier et al., 2008).

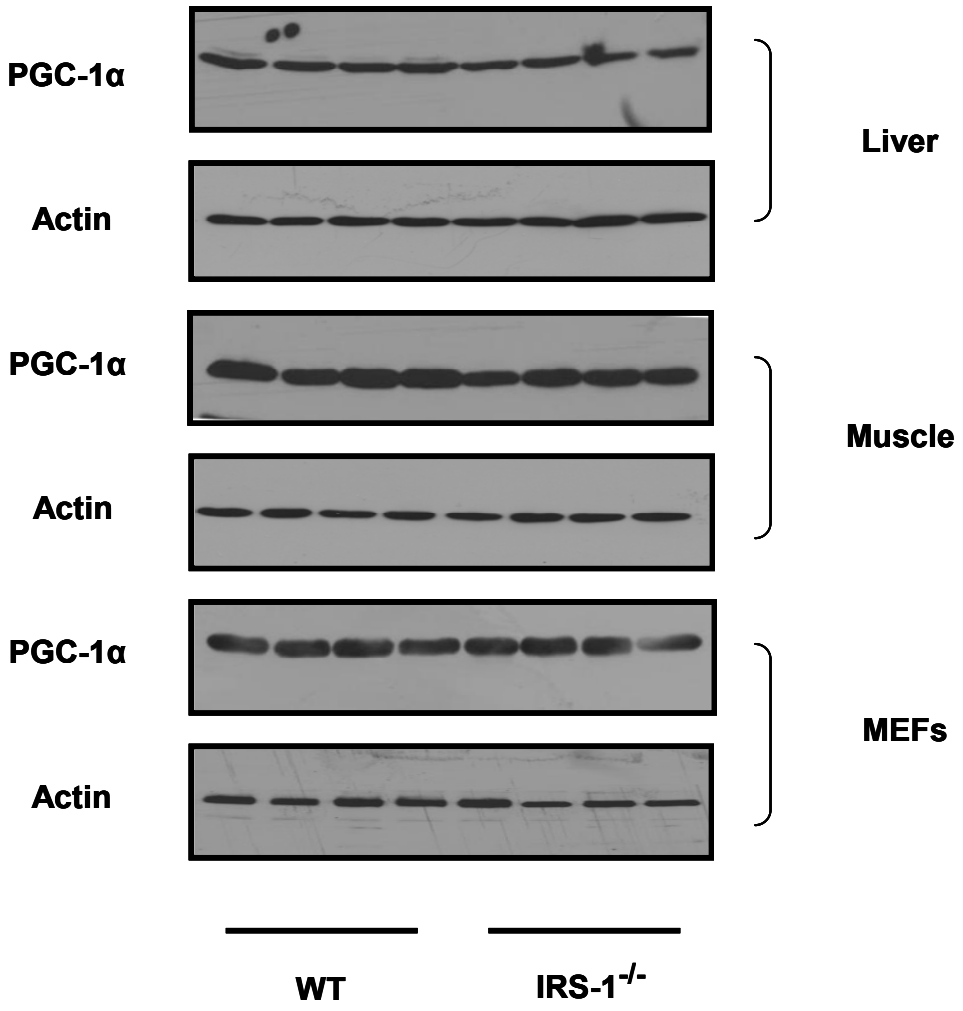

Fig. 3.22 Western blot analysis of PGC-1α in liver, muscle and MEFs of IRS-1$^{-/-}$ mice and wild-type controls
Western blot images showing expression levels of PGC-1α in liver, muscle and MEFs in control and knockout group and actin as the corresponding loading control. Four wild-type cell or organ lystes, respectively were compared with four knockout lysates on one gel. 100 µg of each sample were applied on 10 % SDS-PAGE gel. Examples of 2 independent experiments.

The results of Western blot analysis of PGC-1α expression in muscle, liver and MEFs of IRS-1$^{-/-}$ and wild-type mice indicated no differences in the expression of PGC-1α protein in the knockouts compared with the wild-type controls. PGC-1α expression pattern confirm Western blot results for mitochondrial respiratory chain complexes and HSP-60 in liver, muscle and MEFs for both genotypes, showing no significant impact of the IRS-1 knockout on mitochondrial mass, mitochondrial biogenesis and mitochondrial chain complexes in muscle and liver.

PGC-1α is a relatively unstable protein interacting with various transcription factors. PGC-1α localizes predominately in the nucleus and its activity is decreased by

acetylation. To further investigate the biological active form of PGC-1α nuclear fractions of muscle tissue were prepared and subjected to immunoprecipitation addressing acetylation status of PGC-1α in wild-type and knockout derived samples (Feige et al., 2007; Lerin et al., 2006, Rodgers et al., 2005).

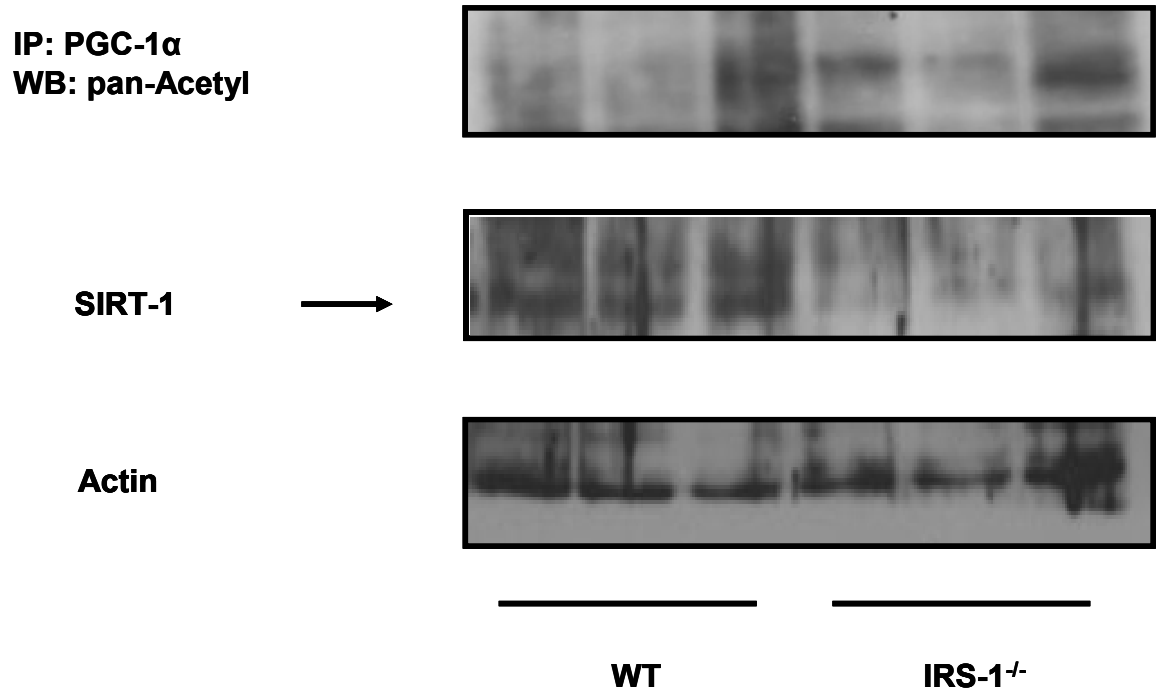

Fig. 3.23 PGC-1α acetylation status in nuclear extracts prepared from muscle
Immunoprecipitation of PGC-1α in muscle derived nuclear extracts. Samples were immunoprecipitated with anti PGC-1α antibody, applied to Western blot analysis and detected by anti-pan-acetyl antibody. Western blot determination of SIRT-1 and actin (loading control) expression in nuclear extracts of wild-type and IRS-1 knockout muscle.

Immunoprecipitation displayed increased PGC-1α acetylation status in knockout derived nuclear extracts. PGC-1α acetylation is directly regulated by GCN5, an acetyltransferase and NAD^+-dependent SIRT-1 deacetylase. SIRT-1 expression was determined in muscle nuclear extracts and was found downregulated in nuclear extracts derived from IRS-1 deficient mice compared to wild-type extracts.

3.7.2 Respiratory chain complex activity

3.7.2.1 Respiratory chain activity in MEFs and MEF isolated mitochondria

Mitochondrial cellular respiration is a central physiological function for all cells. To address influence of IRS-1 knockout on mitochondrial activity photospectroscopy was applied for analyzing enzyme activities of the respiratory chain complexes in red (M. soleus) and white (M. gastrocnemius) muscle, liver, MEFs and MEF isolated

mitochondria. Via photospectrometric analysis enzyme activities of single mitochondrial chain complexes can be determined. Measurements were performed under V_{max} conditions. Enzyme activity analysis contained complex I, complex II, complex II + III, complex III, complex IV complex V and glycerol 3-phosphate dehydrogenase. In addition activities of tricarboxylic acid cycle (TCA cycle) enzymes aconitase, fumerase, isocitrate dehdryogenase and citrate synthase were determined for reference.

Mitochondria isolated from MEFs were analyzed towards enzyme activity of respiratory complexes I-V and glycerol 3-phosphate dehydrogenase.

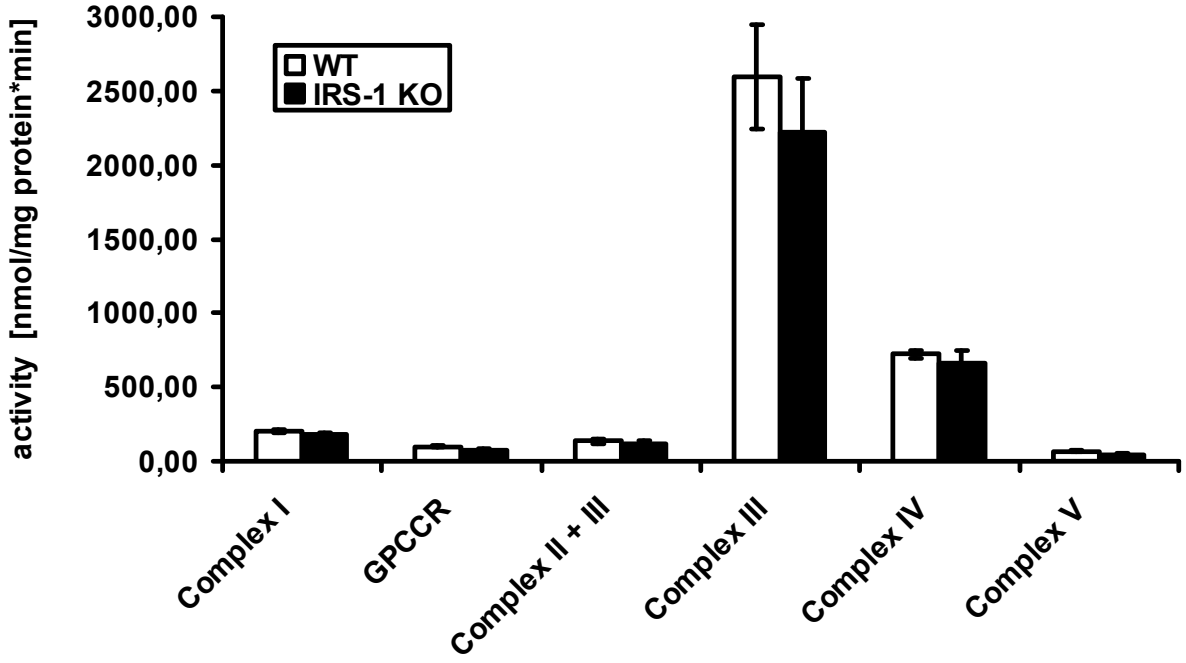

Fig. 3.24 Photospectroscopy of mitochondria isolated from MEFs
Enzyme activities of complexes I, II, II + III, IV, V and glycerol 3-phosphate dehydrogenase (by GPCCR) in mitochondria of wild-type and knockout MEFs. Measured activities were normalized to mitochondrial content determined by Bradford analysis. 5 different samples of isolated mitochondria of each genotype were applied to activity determination. Values are means ± SEM.

No significant differences in activity of respiratory complexes in isolated MEF mitochondria between the knockout and wild-type group have been detected, although knockout mitochondria showed a tendency towards decreased enzyme activity most prominent for complex III.

To further investigate the mitochondrial performance of IRS-1 deficient MEFs, 5 samples of isolated fibroblasts of each genotype were analyzed towards their respiratory chain activity. In this approach activity of enzymes outside the respiratory

were additionally addressed. Furthermore activities of TCA cycle enzymes fumerase and citrate synthase were measured. However activities of complex I and complex V can not be analyzed in this set.

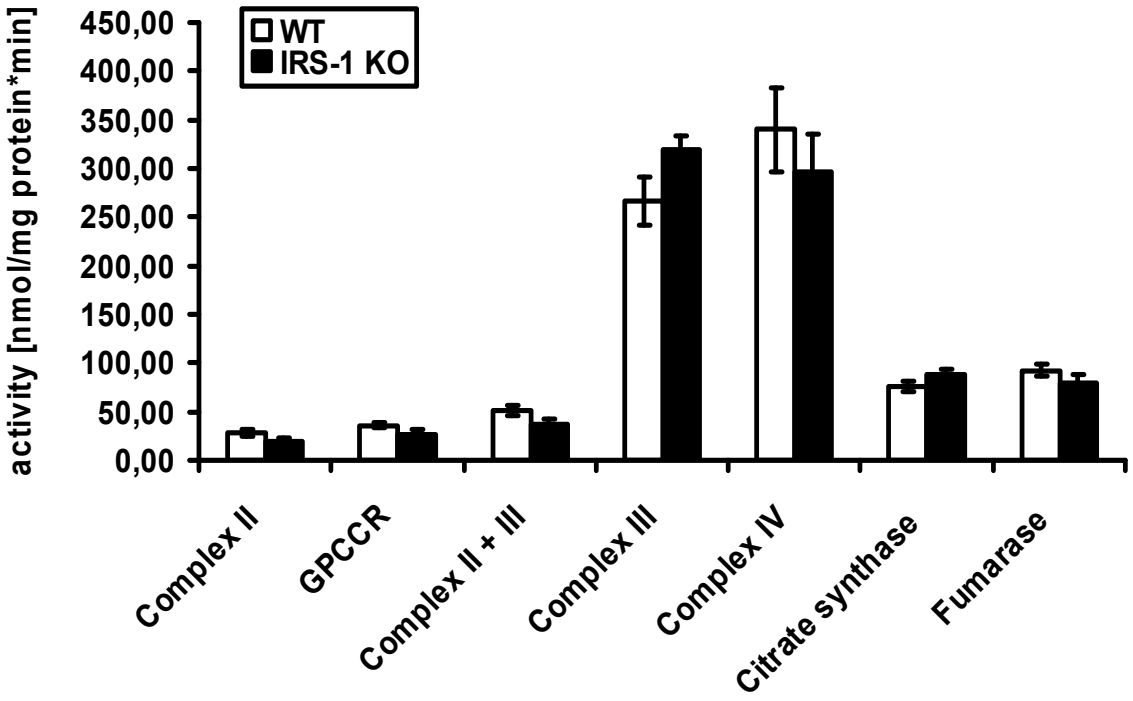

Fig. 3.25 Determination of respiratory chain activity in MEFs
Activities of respiratory chain complexes II, II + III, IV, glycerol 3-phosphate dehydrogenase (GPCCR) and additionally TCA cycle enzymes fumarase and citrate synthase in wild-type and knockout MEFs analyzed by photospectroscopy. 5 different samples of each genotype were applied to activity analysis. Values are means ± SEM.

Analysis of MEFs regarding respiratory chain and TCA cycle enzyme activities showed no significant discrepancy in knockout compared to wild-type MEFs. The trend detected in isolated mitochondria of slight decreased activity in knockout derived mitochondria was also observed in the MEF samples, even though activity of complex III was increased in knockout MEFs in contrast to the obtained results for isolated mitochondria.

Citrate synthase (CS) is a key enzyme of the TCA cycle, catalyzing the conversion of acetyl-CoA and oxalacetate to citrate. Additionally CS activity is used as an indirect indicator for mitochondrial mass (Walenta et al., 1989; Bredel-Geissler et al., 1992; Schwerzmann et al., 1989). Therefore obtained results of enzyme activities in MEFs were normalized to CS activity (Fig. 3.26).

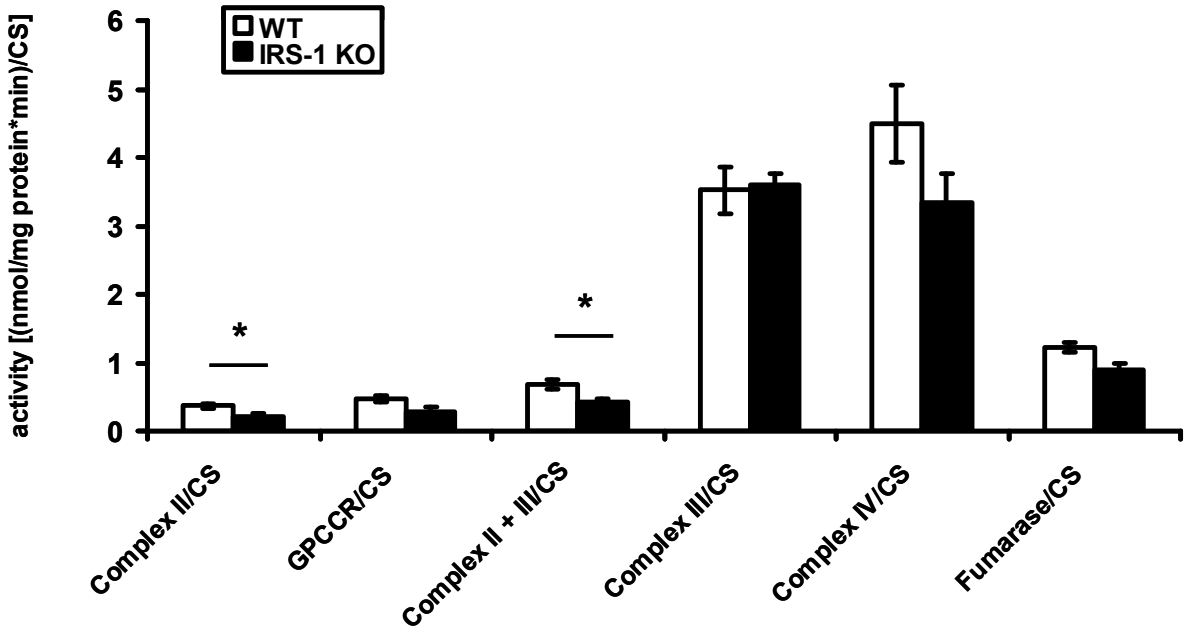

Fig. 3.26 Enzyme activities in knockout and wild-type MEFs normalized to mitochondrial mass Enzyme activities of respiratory chain complexes II, II + III, IV, glycerol 3-phosphate dehydrogenase (GPCCR) and fumarase in wild-type and knockout MEFs normalized to mitochondrial mass by CS ratio. Values are means ± SEM, * unpaired Student´s t-test p-value ≤ 0,05.

Normalized enzyme activities in MEFs support the trend detected by absolute determination of respiratory chain enzymes in MEFs. Normalized IRS-1 deficient MEFs show slightly decreased mitochondrial performance in almost all complexes of the respiratory chain, reaching significance in the activity of complex II and the combined activity of complex II and III.

The mitochondrial electron transport chain is the main source of reactive oxygen species (ROS) generated as a by-product during metabolism. Complex I and complex III of the electron transport chain are the major sites for ROS production in cells (Chen et al., 2003; Lesnefsky et al., 2001; Wallace, 2000; Sugioka et al., 1998; Turrens and Boveris, 1980). Impaired electron transport leads to decreased ATP production and increased formation of free oxygen radicals (Calabrese et al., 2005). Combined activity determination of complex II + III by photospectroscopy revealed a decreased activity in knockout MEFs. This impairment in electron transport might lead to enhanced generation of ROS in these mice. Therefore expression patterns of superoxide dismutase (MnSOD), an enzyme catalyzing dismutation of superoxide free radicals to hydrogen peroxide and oxygen ($2O_2^- + 2H^+ \rightarrow H_2O_2 + O_2$), were determined by western blotting. MnSOD is localized in the mitochondrial matrix therefore an important antioxidant defence mechanism for reactive oxygen species

released towards the mitochondrial matrix by complex I or complex III, respectively (Chen et al., 2003; Raha et al., 2000; Arai et al., 1999; Radi et al., 1991).

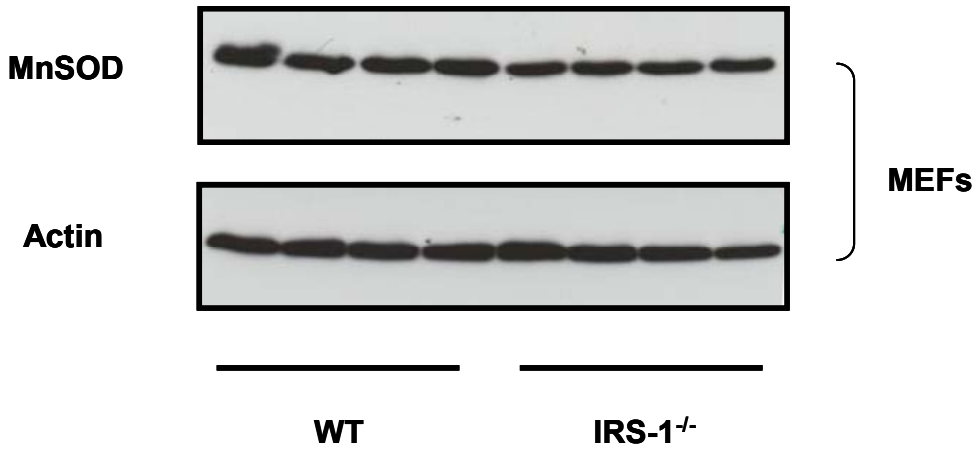

Fig. 3.27 Expression pattern of MnSOD in wild-type and knockout MEFs
Western blot analysis of MnSOD in wild-type and knockout derived MEFs. 100 µg of cell lysate were applied on a 15 % SDS-PAGE gel. Examples of 3 independent experiments.

Determination of the MnSOD expression pattern in wild-type and knockout MEFs revealed no increased MnSOD expression in IRS-1 deficient MEFs, suggesting no elevated ROS production in IRS-$1^{-/-}$ samples.

3.7.2.2 Respiratory chain analysis in IRS-$1^{-/-}$ and wild-type muscle

Muscle of wild-type and knockout mice were dissected. M. solues (representing red muscle) and M. gastrocenmius (representing white muscle) were separated. Separated muscles were homogenized and applied to photospectroscopy analyzing respiratory chain and TCA enzyme activities. All complexes were analyzed by single or combined activity measurements. Activity of TCA enzymes isocitrate dehydrogenase, aconitase, fumerase and citrate synthase were determined functioning as additional indicators for metabolic malfunction, as reference parameter for respiratory chain enzymes and in the case of citrate synthase as an indirect index for mitochondrial mass.

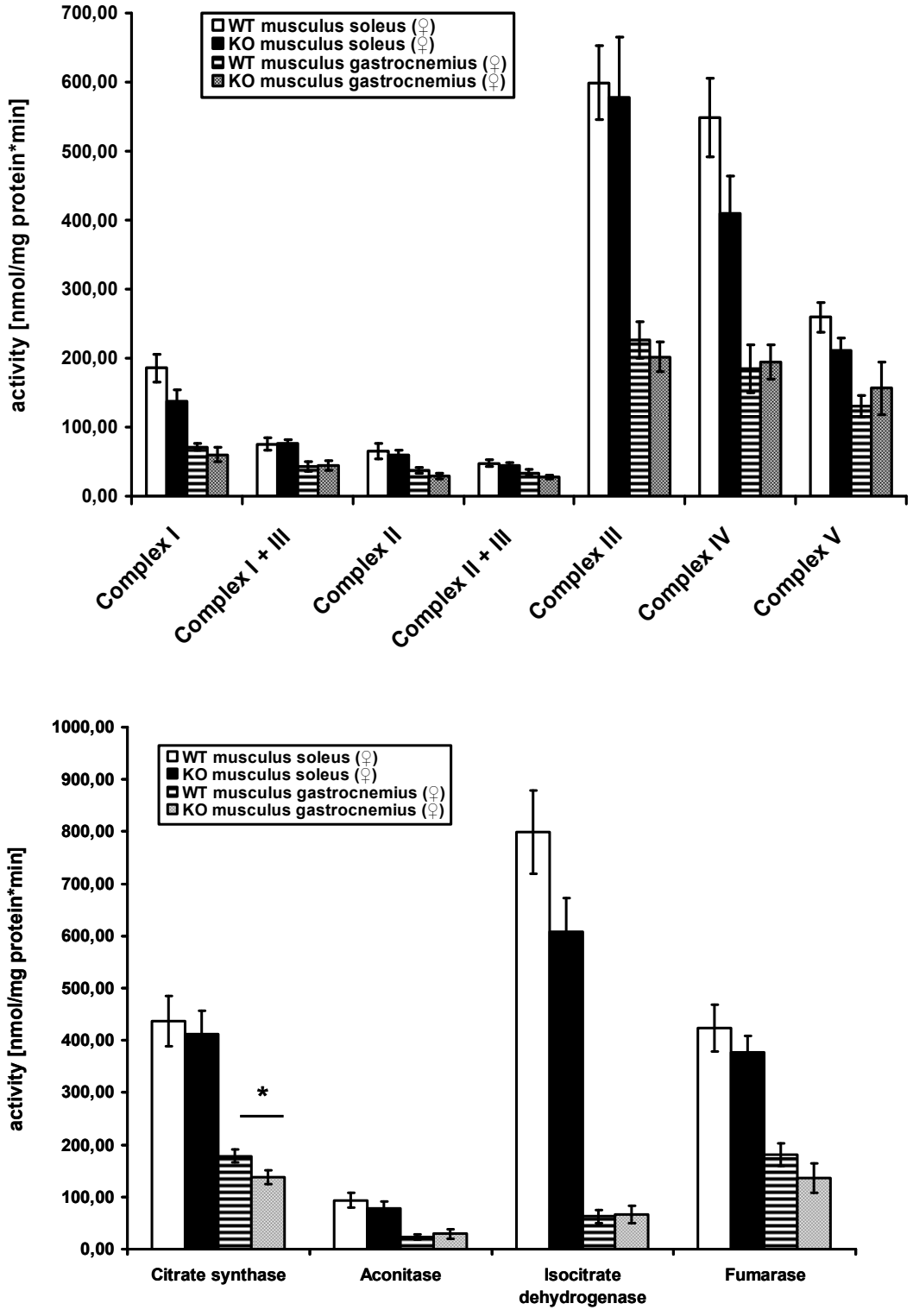

Fig. 3.28 Determination of respiratory chain and TCA enzyme activity in red and white muscles of female wild-type and IRS-1 knockout mice

Upper panel: Activities of respiratory chain complexes I-V in wild-type and knockout mice analyzed by photospectroscopy.

Lower panel: Activities of TCA cycle enzymes isocitrate dehydrogenase (IDH), aconitase, fumarase and citrate synthase in wild-type and knockout mice analyzed by photospectroscopy. 8 different samples of each muscle and genotype were applied to activity assays. Values are means ± SEM, * unpaired Student´s t-test p-value ≤ 0,05.

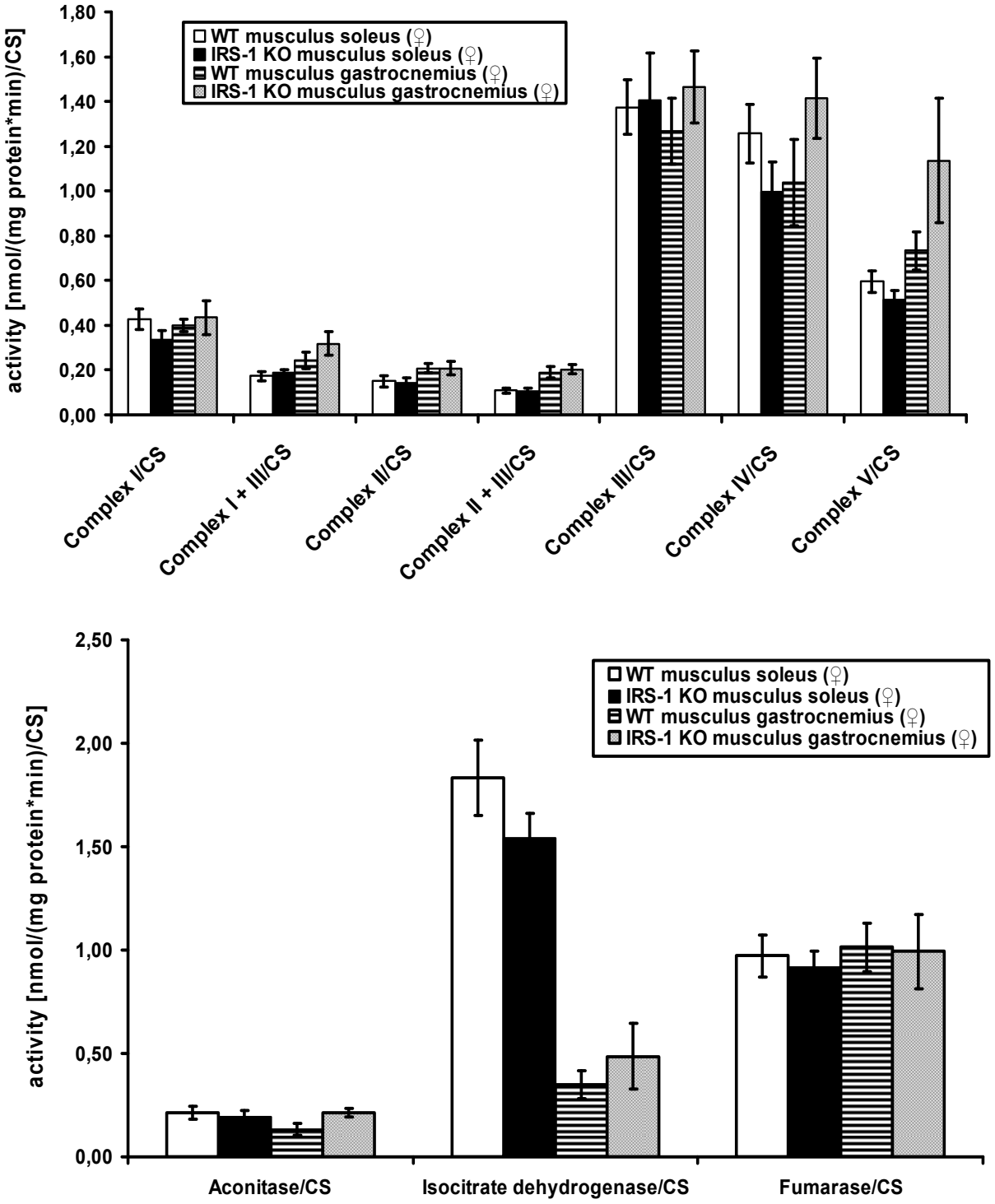

Fig. 3.29 Enzyme activities in red and white muscles of female wild-type and IRS-1 knockout mice normalized to mitochondrial mass
Upper panel: Activities of respiratory chain complexes I-V in wild-type and knockout animals normalized to mitochondrial mass by CS ratio.
Lower panel: Activities of TCA cycle enzymes isocitrate dehydrogenase (IDH), aconitase and fumarase in wild-type and knockout animals normalized to mitochondrial mass by CS ratio. Values are means ± SEM.

Photospectrometric analysis of respiratory chain and TCA enzyme activities showed no significant alterations neither in red muscle nor white muscle samples between

wild-type and IRS-1 deficient females, besides in activity of citrate synthase. The tendency observed in MEFs and isolated MEF mitochondria of slight decreased activities of respiratory chain and TCA enzymes in the IRS-1 knockout group were also obtained for the muscle samples with a significant decrease of citrate synthase (CS) activity in IRS-1 knockout females. However this CS activity drop shifted the calculated results of muscle samples when normalized to mitochondrial mass to a situation of non altered mitochondrial performance in these mice or even slight increased activities for some complexes. Hence no mitochondrial dysfunction could be observed in muscles of female IRS-$1^{-/-}$ mice compared with the wild-type group under maximum stimulation (V_{max}) conditions.

In order to elucidate differences between genders regarding mitochondrial function, muscle of males were prepared according to the protocol applied for muscle dissection of females. Wild-type and knockout samples were analyzed towards enzyme activities by photospectroscopy using the same protocols for activity assays.

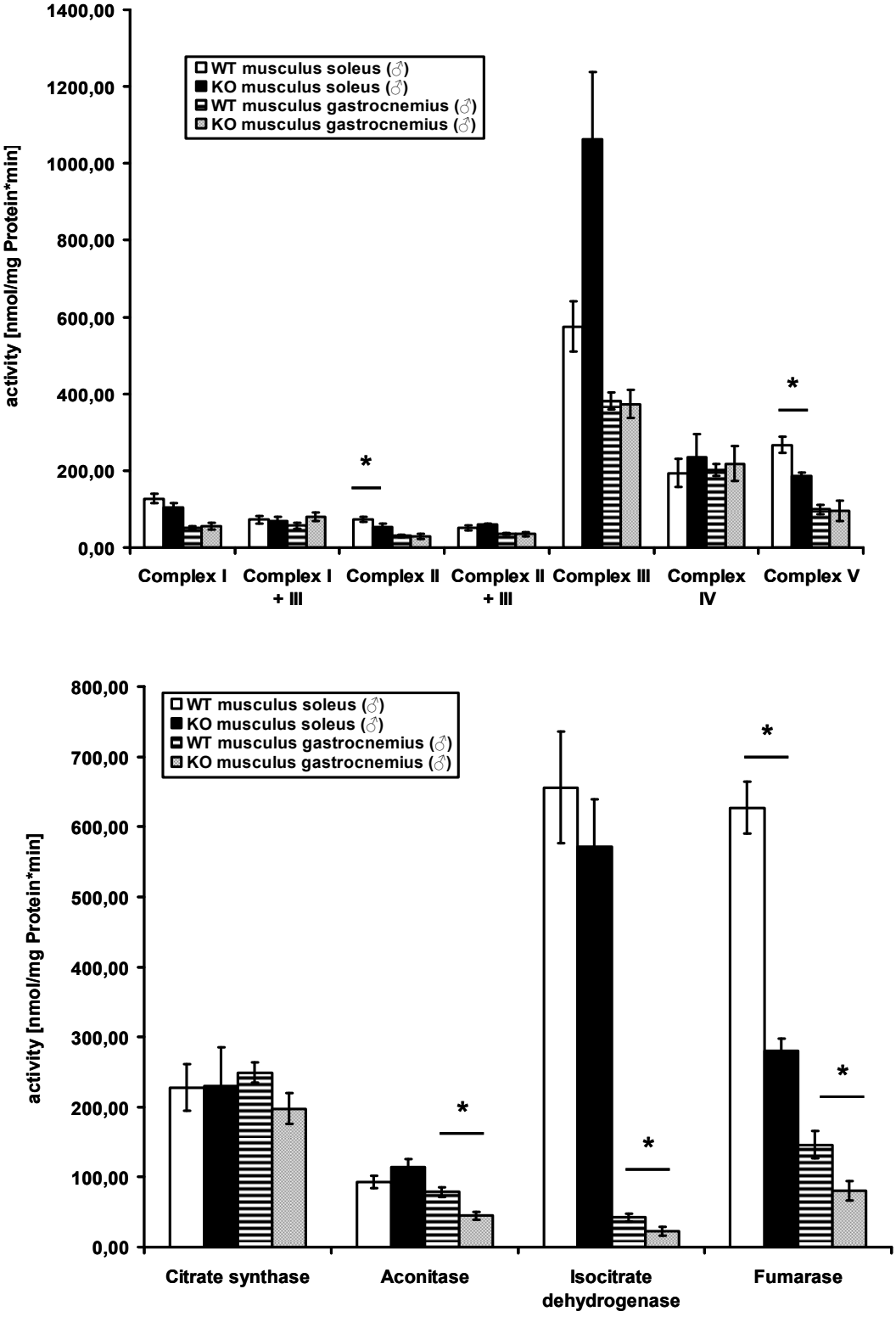

Fig. 3.30 Determination of respiratory chain and TCA enzyme activity in red and white muscles of male wild-type and IRS-1 knockout mice

Upper panel: Activities of respiratory chain complexes I-V in wild-type and knockout mice analyzed by photospectroscopy.

Lower panel: Activities of TCA cycle enzymes isocitrate dehydrogenase (IDH), aconitase, fumarase and citrate synthase (CS) in wild-type and knockout mice analyzed by photospectroscopy. 7 different samples of each muscle- and genotype were applied to activity assays. Values are means ± SEM, * unpaired Student´s t-test p-value ≤ 0,05.

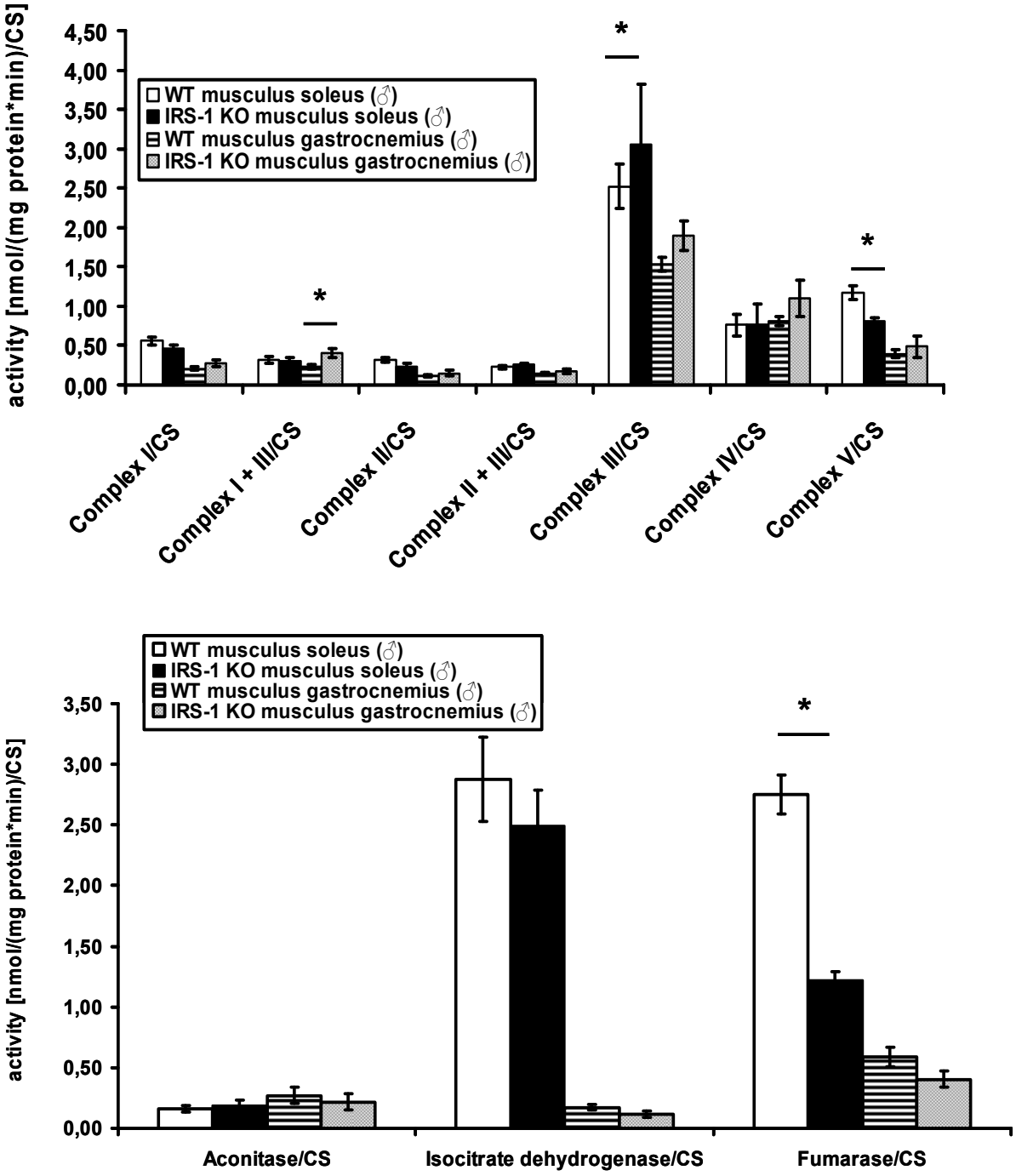

Fig. 3.31 Determination of respiratory chain and TCA enzyme activity in red and white muscles of male wild-type and IRS-1 knockout mice normalized to mitochondrial mass
Upper panel: Activities of respiratory chain complexes I-V in wild-type and knockout mice normalized to mitochondrial mass by CS ratio.
Lower panel: Activities of TCA cycle enzymes isocitrate dehydrogenase (IDH), aconitase and fumarase in wild-type and knockout mice normalized to mitochondrial mass by CS ratio. Values are means ± SEM, * unpaired Student´s t-test p-value ≤ 0,05.

Determination of enzyme activities in muscle of wild-type and IRS-1 knockout males displayed significant alteration between IRS-$1^{-/-}$ animals and the control group. Calculated results showed decreased enzyme activities in IRS-1 deficient mice for

ATPase (complex V) in red muscle, for TCA enzymes IDH, aconitase and fumerase in white muscle as well as for fumerase in red muscle. On the hand complex III activity in red muscle of knockout animals was significantly increased. Normalizing calculations to mitochondrial mass relativized these results however significantly decreased activity of complex V and fumerase in red muscles in IRS-1 deficient animals maintained. Mitochondrial enzyme activity of complex III was increased in both muscle types of the knockout males; even combined activity determination of complex I+III displayed this phenotype for complex III in the IRS-1 knockouts. All other respiratory complexes remained unchanged. The observed decreases in TCA enzyme activity were relativized by normalization although a slight tendency for a decrease maintained, whereas in the case of fumerase a decrease in both muscle types of IRS-1$^{-/-}$ mice was apparent.

Taken together analysis of enzyme activities in red and white muscle of male mice revealed a decreased mitochondrial performance in complex V and fumerase in the red muscle of IRS-1 deficient mice, whereas activity of complex III was increased in both muscle types of IRS-1 knockout mice compared to wild-type controls. No mitochondrial deficiency was detected for complex I and complex III, the main sources for ROS generation. In order to confirm this, expression of MnSOD in the muscles of wild-type and knockout animals of both genders were analyzed by Western blot.

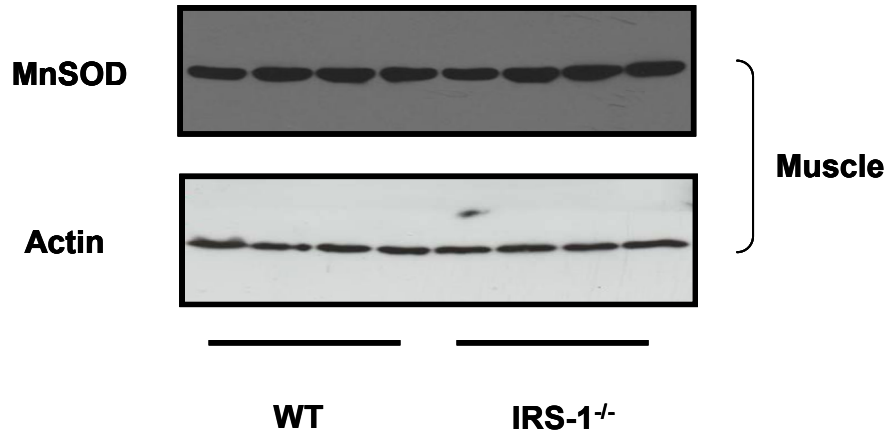

Fig. 3.32 Expression pattern of MnSOD in wild-type and knockout muscle samples
Western blot analysis of MnSOD of muscle samples derived from wild-type and knockout mice. 100 µg of cell lysate were applied on a 15 % SDS-PAGE gel. Wild-type and knockout fraction are represented by two female and two male derived muscles. For Western blot analysis muscle were not separated into M. soleus and M. gastrocnemius, whole muscle lysates were used for experiments. Examples of 3 independent experiments.

Determination of the MnSOD expression patterns in in muscle of wild-type and IRS-1 deficient mice showed no increase or decrease in MnSOD expression in IRS-1 knockouts compared to wild-type controls. In addition to a slightly better performance of complex III and unchanged activity pattern for complex I in the muscles of IRS-1 knockout mice elevated levels of reactive oxygen species is rather unlikely.

Enzyme activity analysis using photospectroscopyis carried out under maximum stimulation conditions. To verify results obtained by photospectroscopy oxygen consumptions of wild-type and IRS-1$^{-/-}$ muscle fibers were analyzed in an oxygraph (OROBOROS, Innsbruck, Austria), representing a more physiological system with intact muscle fibers. Muscle fibers were isolated of 5 male mice each genotype since the male group showed more considerable results in the photospectrometric activity determinations.

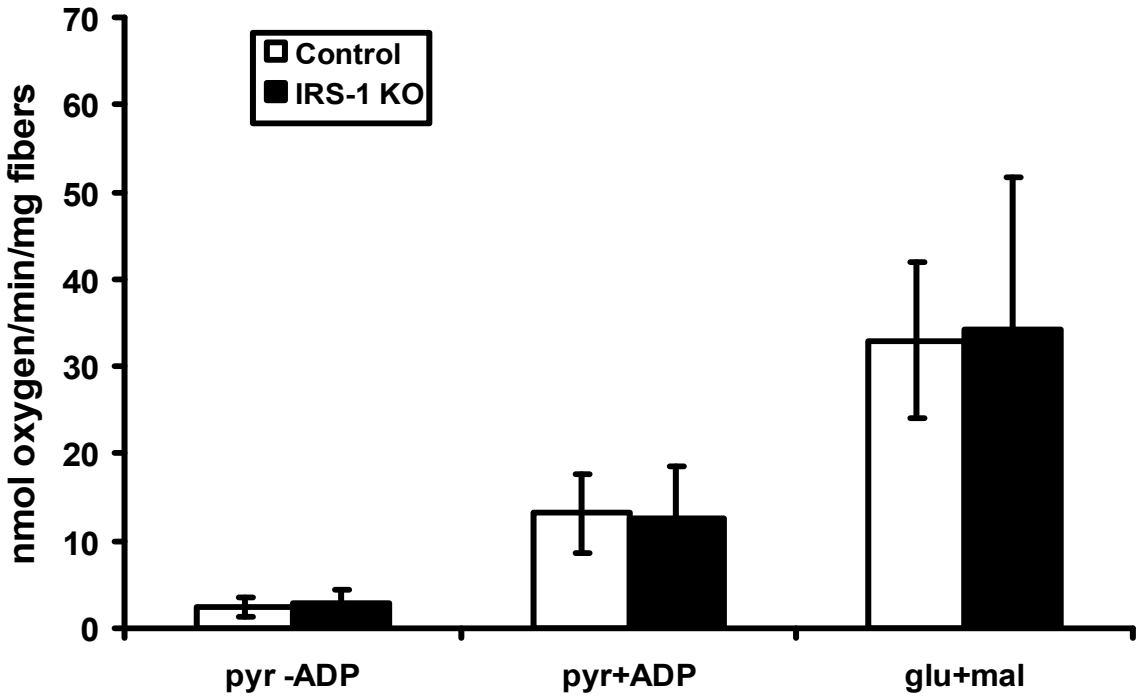

Fig. 3.33 Analysis of oxygen consumption of freshly isolated muscle fibers derived from IRS-1 knockout male (n = 5) mice and wild-type controls (n = 5)
State 2 respiration of mitochondria is represented by determination of oxygen consumption under pyr-ADP conditions. Addition of ADP switched mitochondrial respiration to state 3. Glutamate and malate provide electrons for complex I of the respiratory chain. Determination of oxygen consumption after glutamate and malate addition is an indicator for function or dysfunction of complex I. Values are means ± SD. (in collaboration with Prof. R. Wiesner, Cologne)

Determination of oxygen consumption of muscle fibers derived of IRS-1 knockout and wild-type males via OROBOROS oxygraph showed same oxygen consumption

of IRS-1$^{-/-}$ mice compared with wild-type controls. In contrast to results under maximum stimulation conditions mitochondrial function seemed to be unaltered in IRS-1$^{-/-}$ mice in comparison with wild-type controls. Mitochondrial state 2 respiration (standard state) was determined by addition of respiratory chain substrates and providing oxygen as electron acceptor in the absence of any added ADP. No differences in state 2 respiration was detected indicating functional inner mitochondrial membranes in IRS-1$^{-/-}$ mice. Determination of mitochondrial state 3 respiration (maximal stimulated mitochondrial respiration in the presence of substrate) was achieved by supplementation of state 2 conditions with ADP as phosphate acceptor. This led to raised oxygen consumption however to the same extent in wild-type and the knockout group. Addition of glutamate and malate evaluates the integrity of TCA cycle and the elctrontransport chain (complex I, III and IV). Maximum phosphorylation capacity was determined since sufficient levels of oxygen, ADP, inorganic phosphate, substrates (glutamate/malate) were provided to fibers. No dysfunction in any the complexes has been detected in wild-type or knockout mice, indicating full functional mitochondria in the IRS-1$^{-/-}$ muscle.

3.7.2.3 Determination of respiratory chain activity in liver of IRS-1$^{-/-}$ and wild-type mice

In order to elucidate mitochondrial function in liver of wild-type and knockout animals dissected livers were homogenized and enzyme activities of respiratory chain and TCA enzymes were determined by photo spectroscopy. Citrate synthase was used as indicator for mitochondrial mass. 5 animals of each gender and genotype were analyzed separately.

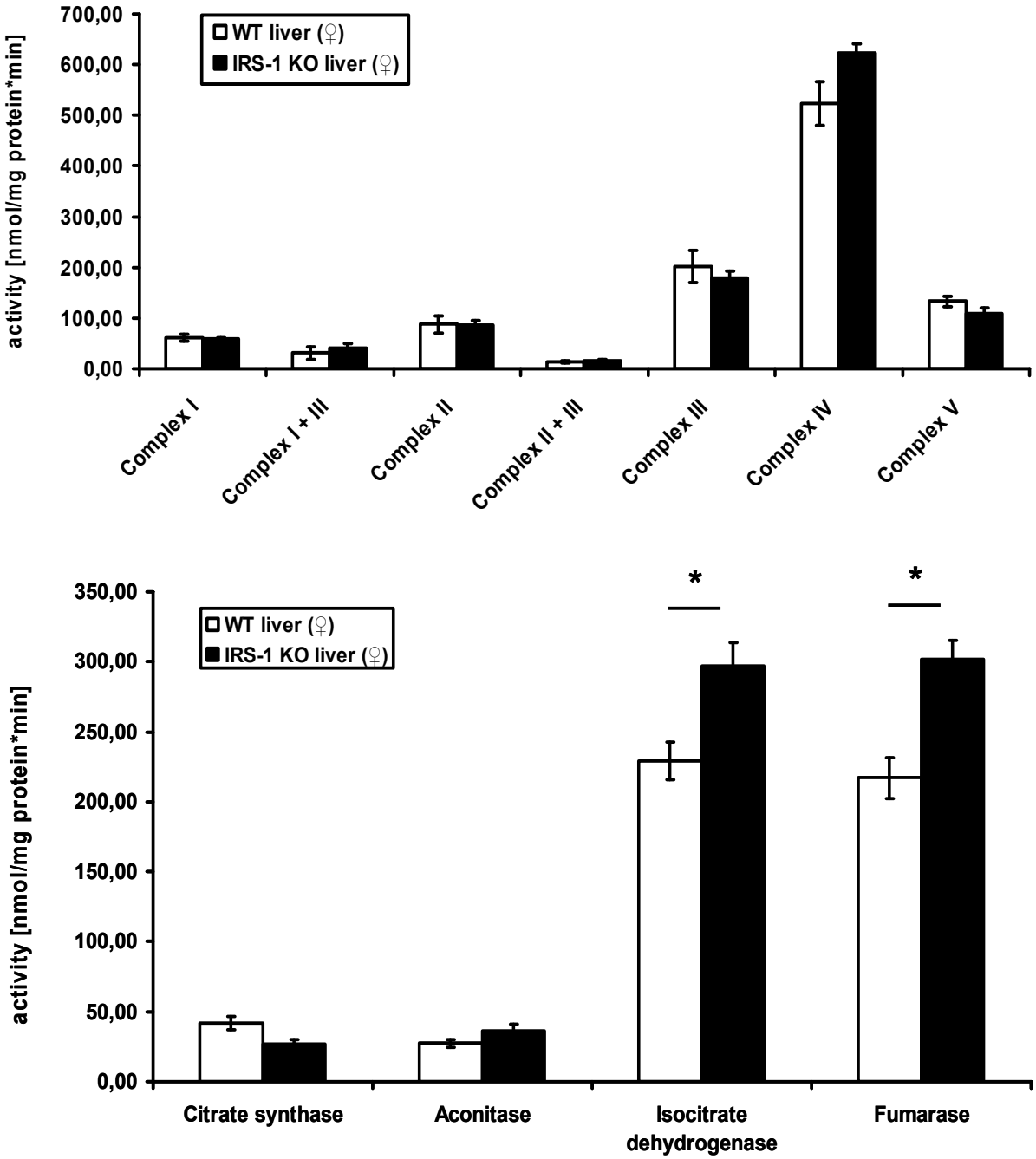

Fig 3.34 Determination of respiratory chain and TCA enzyme activity in livers of female wild-type and IRS-1 knockout mice
Upper panel: Activities of respiratory chain complexes I-V in wild-type and knockout male mice analyzed by photospectroscopy. 5 samples each genotype were applied to activity assays.
Lower panel: Activities of TCA cycle enzymes isocitrate dehydrogenase (IDH), aconitase, fumarase and citrate synthase (CS) in wild-type and knockout animals. Values are means ± SEM, * unpaired Student´s t-test p-value ≤ 0,05.

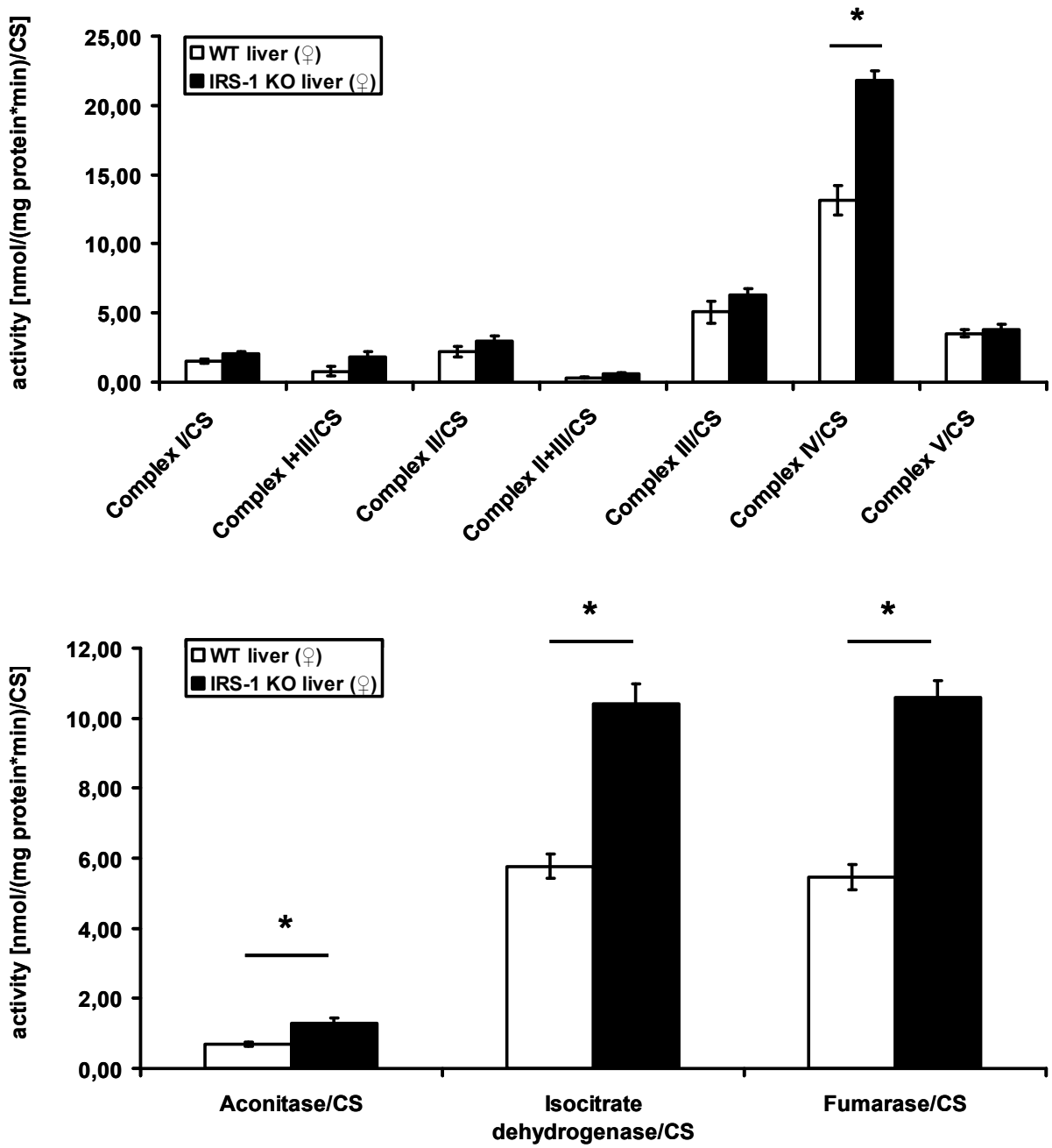

Fig. 3.35 Determination of respiratory chain and TCA enzyme activity in livers of female wild-type and IRS-1 knockout mice normalized to mitochondrial mass
Upper panel: Activities of respiratory chain complexes I-V in wild-type and knockout mice normalized to mitochondrial mass by CS ratio.
Lower panel: Activities of TCA enzymes in wild-type and knockout animals normalized to mitochondrial mass by CS ratio. Values are means ± SEM, * unpaired Student´s t-test p-value ≤ 0,05.

Statistically significant alterations in mitochondrial respiratory chain activity in female mice were detected for isocitrate dehydrogenase (IDH) and fumerase for calculated absolute values. IRS-1$^{-/-}$ females showed an increased activity for these TCA enzymes, additionally an activity elevation of complex IV in the IRS-1 knockout females was detected not reaching significance. All other enzymes were basically unchanged. Normalizing absolute values to mitochondrial mass displayed distinct

activity alterations for complex IV, IDH, aconitase and fumerase in IRS-1$^{-/-}$ females compared to wild-type controls. Overall female IRS-1 deficient mice showed a tendency towards increased mitochondrial enzyme activities for the respiratory chain as well as for the TCA cycle.

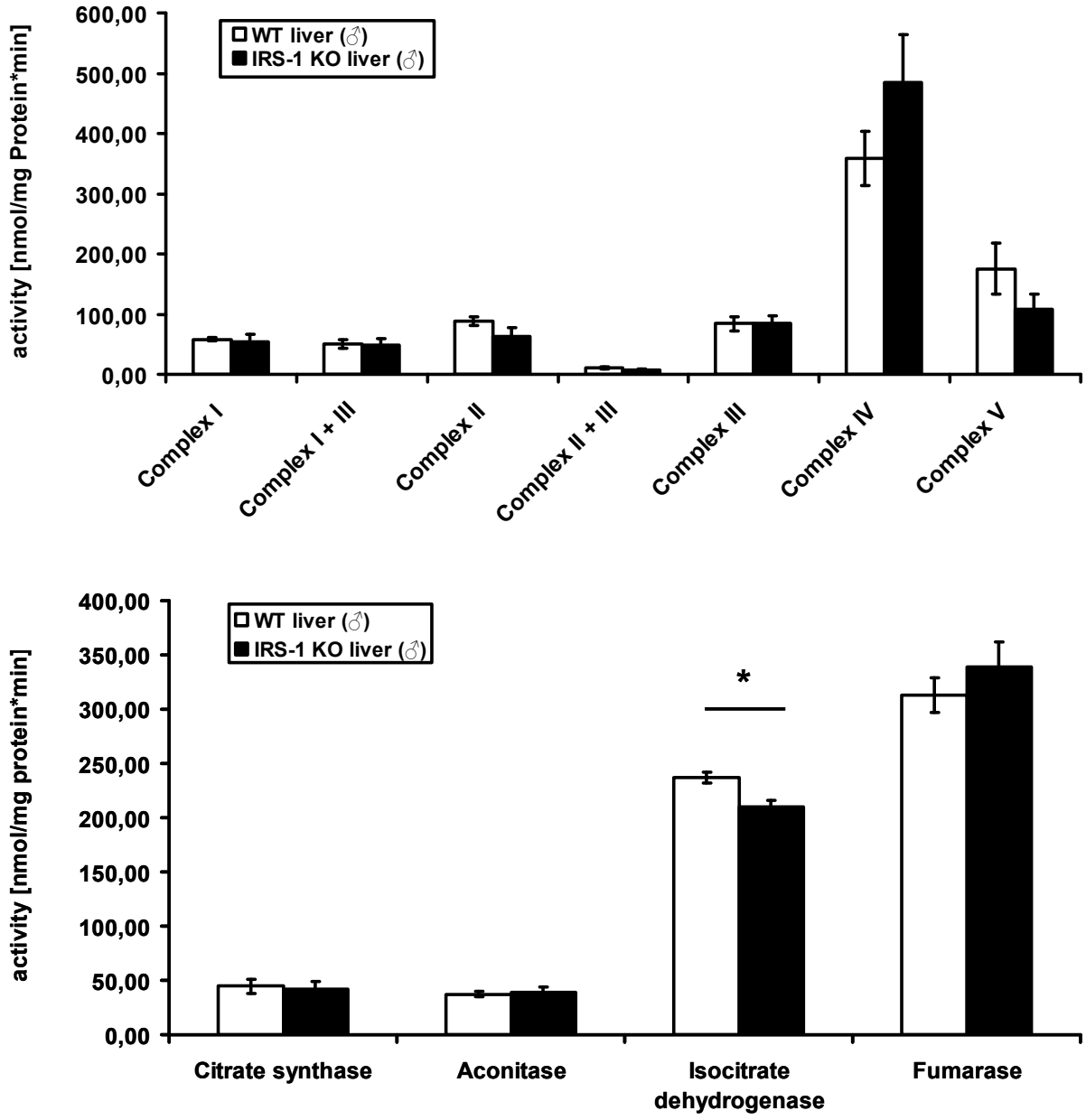

Fig 3.36 Determination of respiratory chain and TCA enzyme activity in livers of male wild-type and IRS-1 knockout mice

Upper panel: Activities of respiratory chain complexes I-V in wild-type and knockout male mice analyzed by photospectroscopy.

Lower panel: Activities of TCA enzymes isocitrate dehydrogenase (IDH), aconitase, fumarase and citrate synthase (CS) in wild-type and knockout animals. 5 samples each genotype were applied to activity assays. Values are means ± SEM, * unpaired Student´s t-test p-value ≤ 0,05.

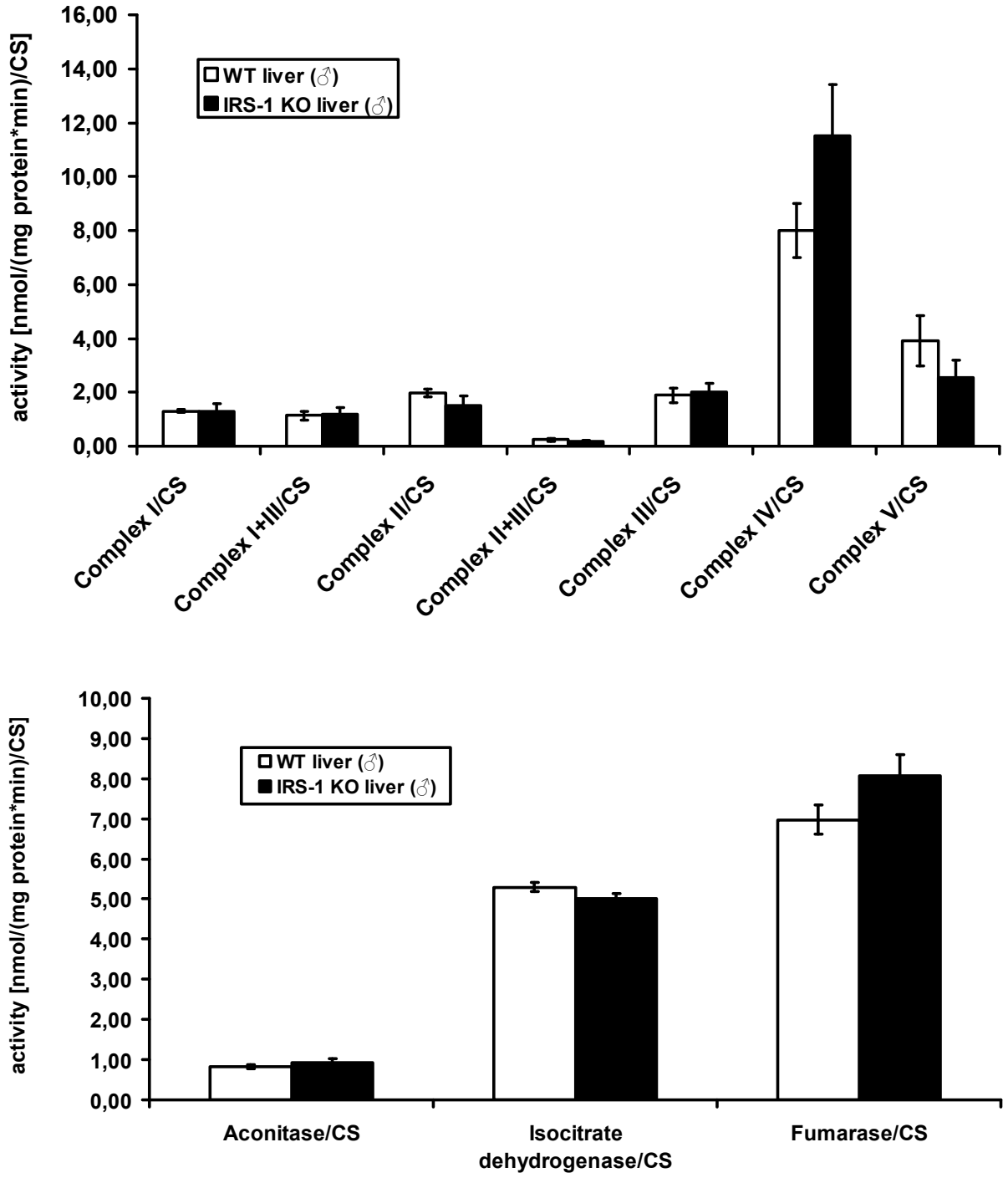

Fig 3.37 Determination of respiratory chain and TCA enzyme activity in livers of male wild-type and IRS-1 knockout mice normalized to mitochondrial mass
Upper panel: Activities of respiratory chain complexes I-V in wild-type and knockout male mice normalized to mitochondrial mass by CS ratio.
Lower panel: Activities TCA enzymes in wild-type and knockout animals normalized to mitochondrial mass by CS ratio. Values are means ± SEM, * unpaired Student´s t-test p-value ≤ 0,05.

Photospectrometric analysis of livers dissected from IRS-1 knockout and wild-type males displayed increased enzyme activities for complex IV and fumerase in IRS-1$^{-/-}$ mice as observed in female mice, however not reaching significance. On the other hand IRS-1 deficient males showed decreased enzyme activity for complex V and

significantly decreased activity for IDH. Normalizing absolute values to mitochondrial mass did not change relation of absolute values; enzyme activities of complex IV and for fumerase were still increased in IRS-1 knockout males compared to wild-type and on the other hand complex V activity was decreased in the animals. Differences in IDH activity were not obvious anymore after normalization. The tendency of slight increased mitochondrial performance of all enzymes as observed in females was not present in livers derived from males with the exceptions for IDH and complex IV. On the other hand activity attenuation for complex V was also observed in soleus muscles of both genotypes with a significant complex V activity reduction in males (Fig. 3.29; 3.31).

In order to analyze the mitochondrial respiratory chain in a functional context polaro graphic determination of oxygen consumption was applied to freshly isolated liver mitochondria. Oxygen consumption was determined after oxidation of substrates added to isolated mitochondria. Complex I, complex II, combined activity of complex II+IV and activity of pyruvate dehydrogenase were determined by oxygen consumption via polarographic analysis.

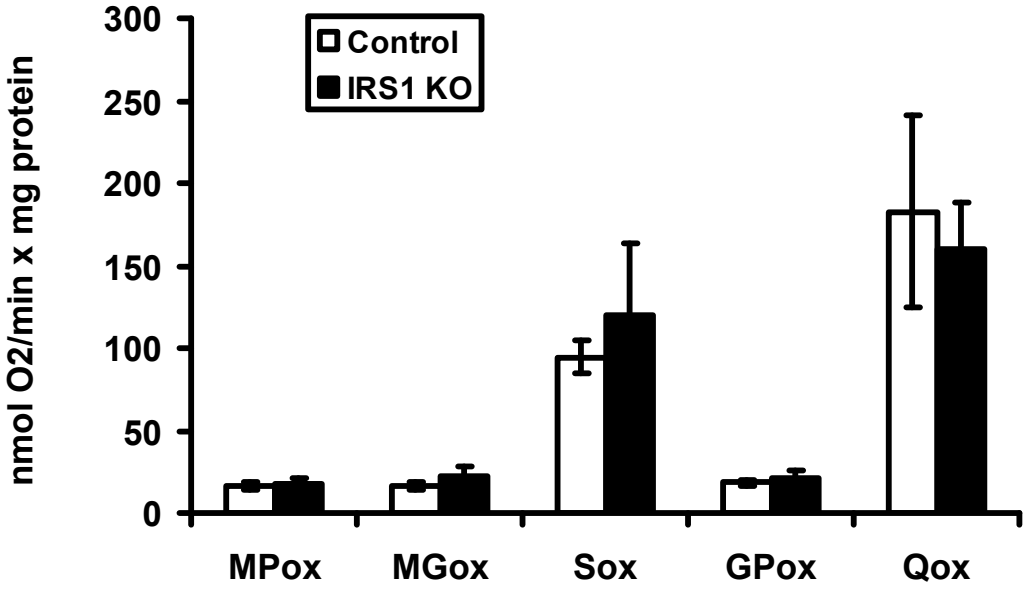

Fig. 3.38 Oxygen consumption of isolated liver mitochondria derived from IRS-1$^{-/-}$ and wild-type males
MPox analysis characterizes complex I, TCA cycle and pyruvate dehydrogenase activity. MGox represents activity of pyruvate dehydrogenase complex. Sox determination displays complex II activity. GPox and Qox detect complex III and IV activities. 5 samples of isolated mitochondria of IRS-1 knockout and wild-type controls were analyzed. Values are means ± SD.

In contrast to photospectrometric analysis not single complex activities are determined by polarography coupling of the different complexes in electron transfer, the TCA cycle and pyruvate dehydrogenase complex are addressed by this method, thus elucidating defects in electron transfer of mitochondria. No differences in oxygen consumption were detected by polarographic analysis of IRS-1 knockout and wild-type derived mitochondria. Enzymatic activities of analyzed complexes were unchanged indicating functional mitochondrial respiratory chain complexes, TCA cycle enzymes and pyruvate dehydrogenase complex in IRS-1 deficient mice.

No activity decrease for complex I and III was detected by the different methods in both genotypes and genders. Dysfunction in either complex I or complex III leads to increased ROS generation and induction of MnSOD as one possible physiological response to that. MnSOD expression was analyzed by Western blot concerning mitochondrial dysfunction of complex I and complex III.

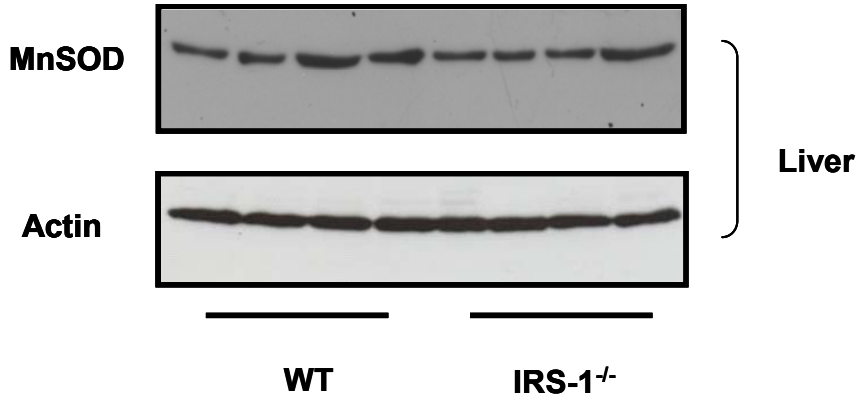

Fig. 3.39 Expression pattern of MnSOD in wild-type and knockout muscle samples
Western blot analysis of MnSOD liver samples derived from wild-type and knockout mice. 100 µg of cell lysate were applied on a 15 % SDS-PAGE gel. Wild-type and knockout fraction are represented by two female and two male derived livers. Examples of 3 independent experiments.

Expression pattern of MnSOD in liver samples of female and male knockout mice and wild-type controls analyzed by Western blot revealed no differences between both groups, thus excluding dysfunction of complex I or complex III.

In order to further exclude mitochondrial dysfunction in IRS-1 deficient animals, liver samples were applied to OxyBlot analysis, detecting carbonylated proteins. Carbonyl groups are introduced into amino acid chain after oxidative modification of proteins (Tezel et al., 2005). Increased production of hydroxyl radicals leads to formation of

lipid hydroperoxides, producing α-,β-unsaturated aldehydes. These are subjected to Michael addition leading to reactive carbonyl functional groups on lysine, histidine and cysteine residues on side chains of proteins. Hyxdroxyl radicals, short lived but the most reactive radicals, are formed via the Harber-Weiss reaction from O_2^- and H_2O_2 (both produced by mitochondria and mitochondria and SOD, respectively). Therefore analyses of protein carbonyls give an insight into oxidative damage at protein level caused by oxidative stress (Grimsrud et al., 20008, Zhang et al., 2006).

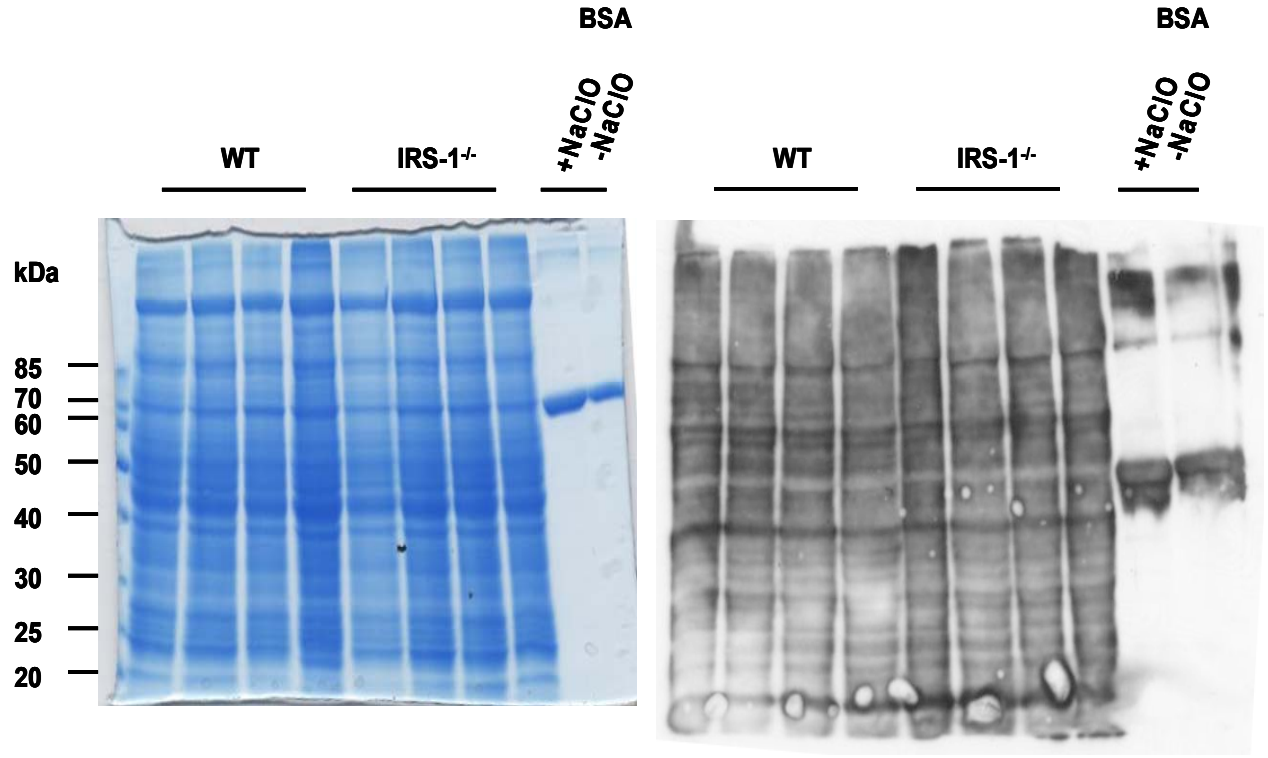

Fig. 3.40 OxyBlot of wild-type and IRS-1 knockout derived liver samples
Proteins modified by reactive species are detected by OxyBlot. OxyBlot provides an indirect evidence of mitochondrial generated ROS indicating defective mitochondrial respiratory chain (complex I and complex III) by detection of protein oxidation. 2,4-dinitrophenylhydrazine (DNPH) was used as derivatizing reagent of protein carbonyls and DNP antibody (Sigma-Aldrich, Cat-Nr. D9656) for detection of DNP-protein-derivatization. BSA plus NaClO was used as control for functional detection of carbonylated proteins. NaClO was used to produce free radicals leading to an increase in protein carbonylation compared to untreated BSA.
Left panel: Coomassie Brilliant Blue gel served as loading control (Oh-Ishi et al., 2002, Kalyanaraman et al., 1985).

No difference in protein carbonylation was observed comparing wild-type with knockout samples, indicating no elevated ROS production or mitochondrial dysfunction, respectively in either wild-type or IRS-1 deficient animals. Functionality of carbonylated protein detection by OxyBlot was proved by NaClO treated and untreated BSA. NaClO treated BSA showed an increase of carbonylated proteins in comparison to untreated BSA sample.

To address functional relevance of decreased complex V activity in the photo spectroscopic analysis in muscle and liver homogenates of male IRS-1 deficient mice, isolated mitochondria of IRS-1 knockout and wild-type mice were analyzed by proton motive force measurement in order to investigate if decreased complex V activity might be due to proton leakage suggesting an uncoupling phenomenon in these mice. Proton leak measurements were carried out in the presence of oligomycin inhibiting ATP synthesis in complex V hence mitochondrial membrane potential is not consumed by ATP synthase. Oxygen consumption of mitochondria in this state is proportional to leakage across the inner mitochondrial membrane. The kinetic response of the proton conductance to its driving force (proton motive force) can therefore be measured as relationship between respiration rate and membrane potential when the potential is varied by titration with electron transport chain inhibitors (Brand, 1990; Nicholls, 1974; Jastroch et al., 2009). Addition of 4-hydroxynonenal (4-HNE), an α,β-unsaturated hydroxyalkenal and major product of oxidant induced peroxidation of membrane phospholipids in cells, uncouples mitochondria and verified functional detection of proton leakage in mitochondria.

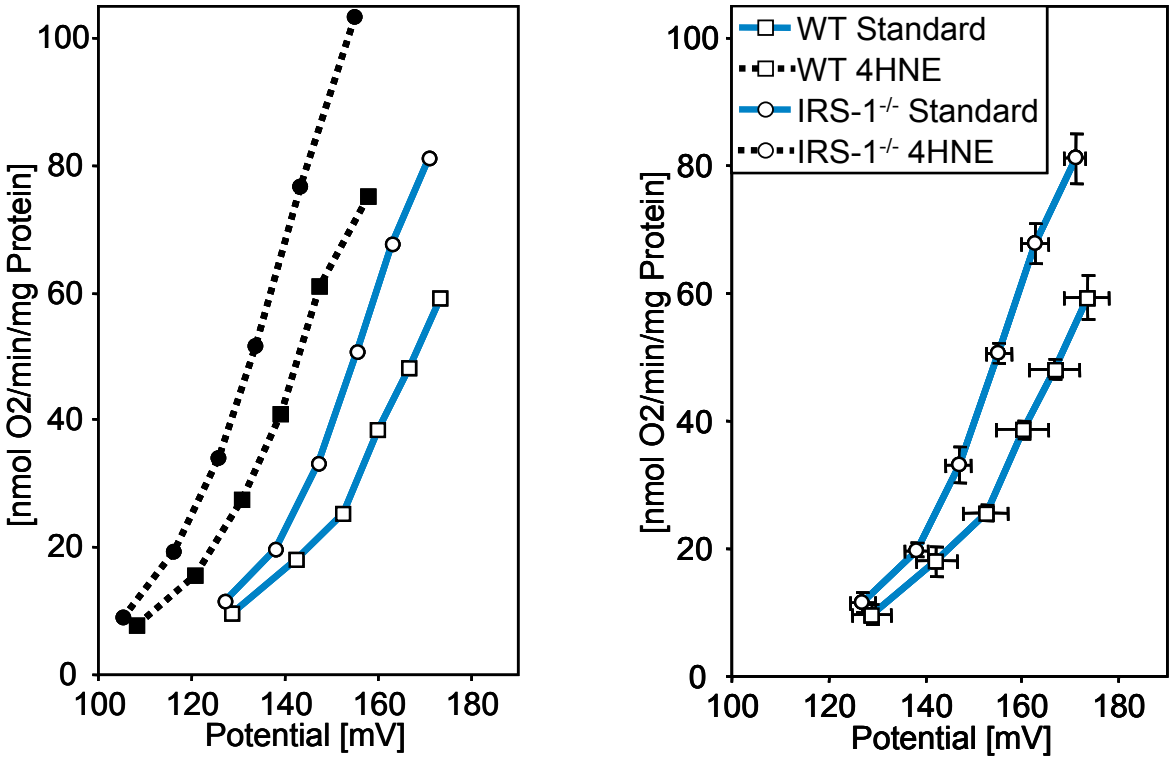

Fig. 3.41 Proton leakage determination of isolated liver mitochondria of knockout and wild-type male mice
Measurement of proton conductance in freshly isolated mitochondria derived from wild-type (n = 5) and IRS-1 knockout (n = 5) males. Right panel displays proton leak of liver mitochondria. Left panel inducible proton conductance in liver mitochondria after addition with 4-HNE in comparison with proton leak of liver mitochondria without addition of 4-HNE. Data are means ± SD. Independent experiments, each performed in duplicates. (in collaboration with Prof. R. Wiesner, Cologne)

Proton leakage analysis showed higher oxygen consumption in IRS-1$^{-/-}$ mice compared with wild-type controls. The IRS-1 deficient males required a higher substrate turnover for building up their membrane potential. Mitochondria of IRS-1 knockout mice consumed about 50 nmol oxygen for creating a membrane potential of 160 mV, whereas wild-type mitochondria used about 40 nmol of oxygen creating this membrane potential. Addition of 4-HNE shifted the graphs to higher oxygen consumption creating distinct membrane potential due to the induced uncoupling effect by 4-HNE. However potential difference for defined oxygen quantities between the two genotypes remained. Shifting of graphs after 4-HNE addition showed that proton leakage is well detected by this assay. Overall, proton leakage determination indicates that IRS-1 knockout animals lowered membrane potential by enhanced leakage of protons across the inner mitochondrial membrane, indicating an uncoupling phenotype in knockout mice.

3.7.3 Identification of mitochondrial respiratory chain uncoupling in IRS-1 deficient mice

To further investigate an uncoupling phenomenon in IRS-1 deficient animals liver, muscle and WAT samples of knockout and wild-type mice were analyzed by Real-time PCR and protein lysate were exposed to Western blot analysis. RNA of tissues was extracted using TRIzol (Invitrogen, Darmstadt, Germany), proteins were extracted using standard protein lysate protocol as described in materials and methods.

Uncoupling protein 3 (UCP-3) is mainly expressed in muscle. Photospectrometric data suggested uncoupling in IRS-1$^{-/-}$ mice. Thus UCP-3 expression in muscle of IRS-1 knockout and wild-type mice were analyzed using Real-Time PCR (RT-PCR) and Western blot analysis.

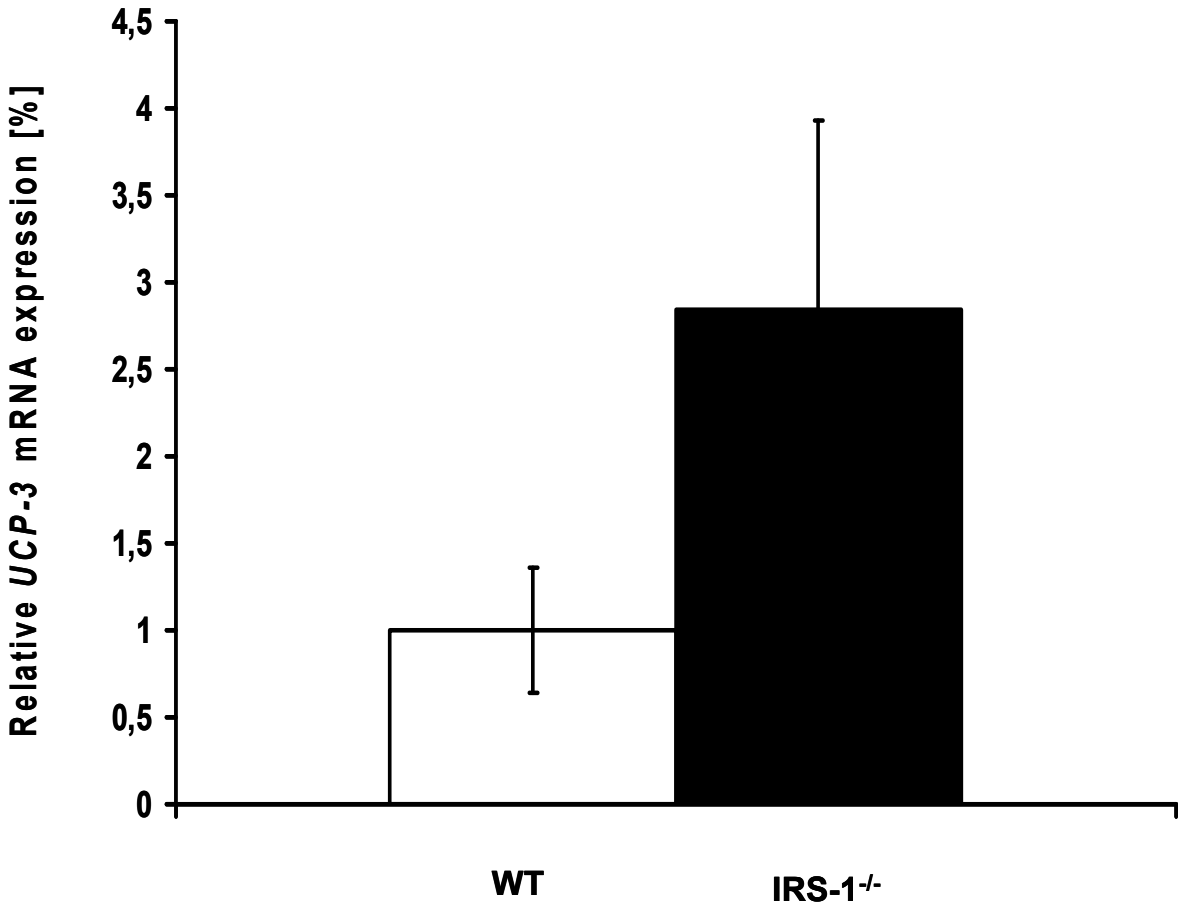

Fig. 3.42 mRNA expression of *UCP-3* in muscles of IRS-1 knockout mice and wild-type controls
mRNA expression of *UCP-3* (uncoupling protein 3) in muscles of IRS-1 deficient (n = 8) and wild-type mice (n = 8). mRNA levels were determined by using UCP-3 and 18s (internal control) TaqMan probes (Applied Biosystems, Darmstadt, Germany). Data represent ΔΔCT calculation. Data are means ± SEM.

mRNA levels determined by RT-PCR showed increased *UCP-3* levels in IRS-1 deficient mice compared with the wild-type group. Results are expressed as fold increase relative to control group. RT-PCR analysis revealed a 184 % (2,84-fold) increase for *UCP-3* expression in IRS-$1^{-/-}$ mice. mRNA does not directly represent protein expression since mRNA can be degraded before been translated, therefore UCP-3 expression was checked by Western blot analysis, trying to link elevated mRNA levels to increased UCP-3 protein expression.

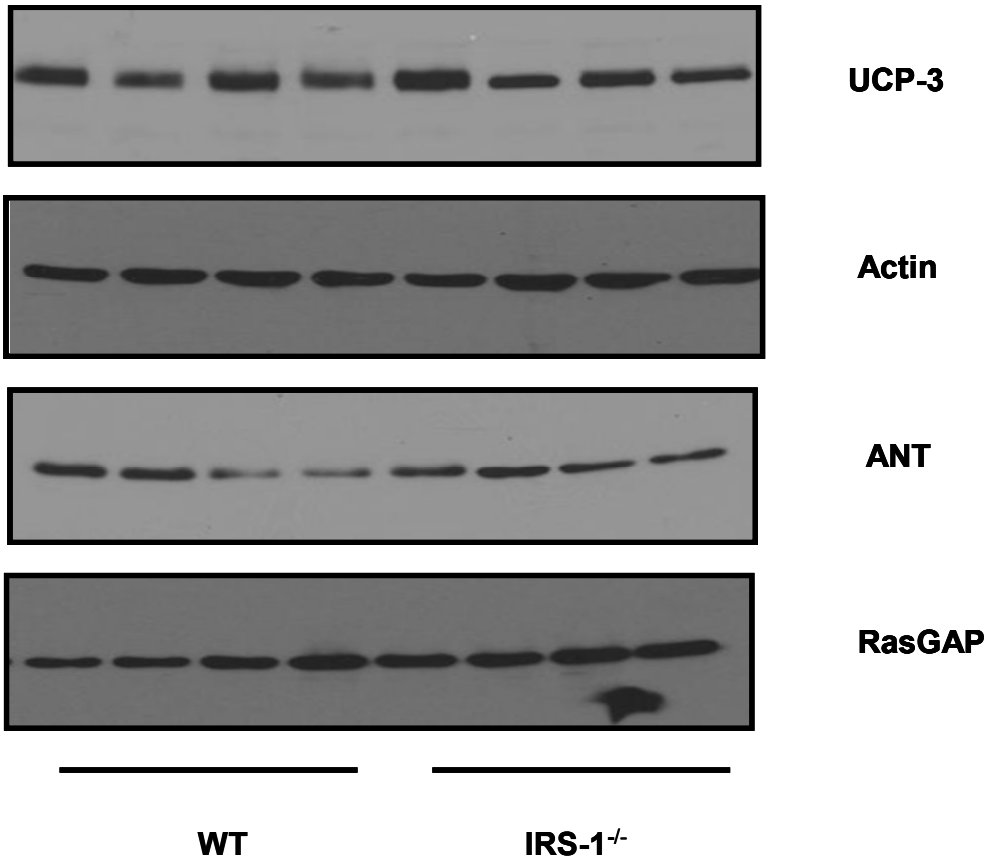

Fig 3.43 Western blot analysis of UCP-3 protein expression in muscle of wild-type controls and IRS-1$^{-/-}$ mice
UCP-3 and ANT (Adenine nucleotide translocase) protein expression in wild-type (n = 4) and knockout (n = 4) mice. Actin and RasGAP were used as loading control. 300 µg of protein lysate were applied on 10 % SDS-PAGE gel.

Western blot analysis showed slightly increased expression of UCP-3 in IRS-1$^{-/-}$ mice. Quantification of Western blot results determined a 15 % increased UCP-3 expression in muscle of IRS-1 knockout mice. Highly elevated levels of *UCP-3* detected by RT-PCR were partially confirmed by the Western blot. Expression levels of ANT another protein involved in proton conductance were additionally checked by Western blot analysis. Protein expression levels of ANT remained unchanged indicating no effect of this protein on elevated oxygen consumption detected by proton leakage measurements.

To address uncoupling in livers of IRS-1$^{-/-}$ animals *UCP-2* mRNA expression was determined by RT-PCR. Kupffer cells are the dominant site of uncoupling protein 2 expression in liver (Larrouy et al., 1997).

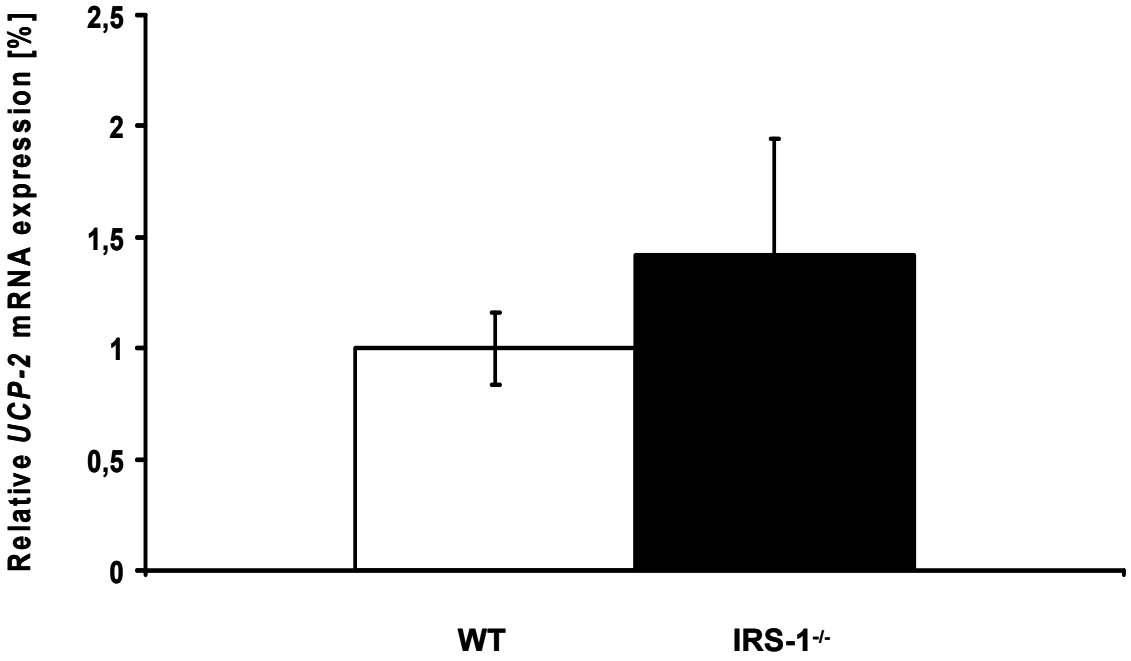

Fig. 3.44 mRNA expression of *UCP-2* in livers of IRS-1 knockout mice and wild-type controls
mRNA expression levels of *UCP-2* (uncoupling protein 2) in livers of IRS-1 deficient (n = 7) and wild-type mice (n = 7). mRNA levels were determined by using UCP-2 and 18s (internal control) TaqMan probes (Applied Biosystems, Darmstadt, Germany). Data represent ΔΔCT calculation. Data are means ± SEM.

An increased *UCP-2* mRNA expression of 41 % was detected in IRS-1 knockout mice compared to the wild-type control group. If 41 % increase of *UCP-2* mRNA levels is sufficient explaining increased oxygen consumption detected by proton leakage measurements or decreased complex V activity determined by photospectroscopy remained questionable. However this phenomenon might contribute to the uncoupling phenotype.

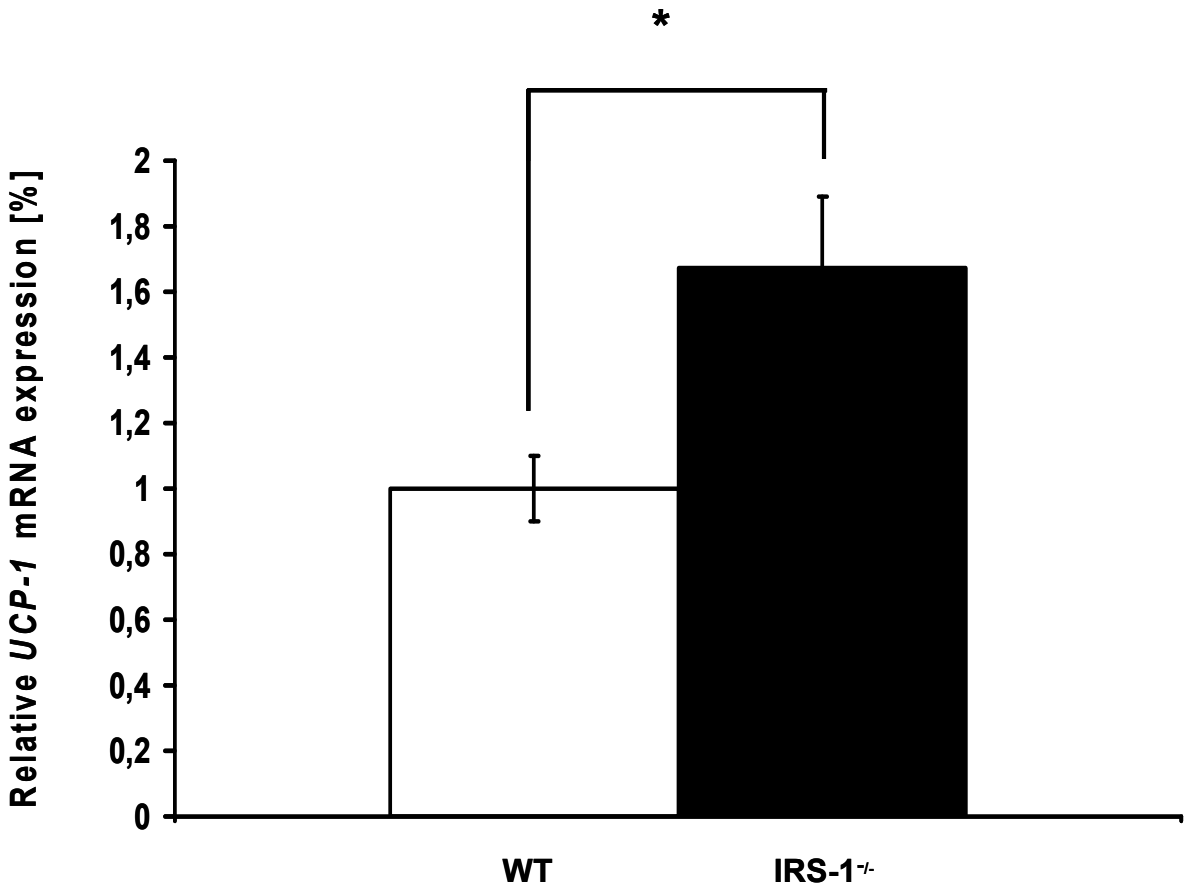

Fig. 3.45 mRNA expression of *UCP-1* in white adipose tissue (WAT) of IRS-1 knockout mice and wild-type controls
mRNA expression of UCP-1 (uncoupling protein 1) in WAT of IRS-1 deficient (n = 6) and wild-type mice (n = 8). Values are means ± SEM, * unpaired Student´s t-test p-value ≤ 0,05.

UCP-1 is a common marker for brown adipose tissue (BAT) (Klaus et al., 2004). Brown fat has a central function in thermogenesis of creatures. Lately UCP-1 was linked to body weight regulation and discussed as therapeutic tool for obesity treatment (Nedergaard et al., 2010). Figure 3.45 shows *UCP-1* mRNA expression in WAT of IRS-1 knockout compared with wild-type mice. *UCP-1* mRNA levels were significantly elevated in the IRS-1 deficient group, indicating development of discrete brown adipocyte characteristics in abdominal white fat depots.

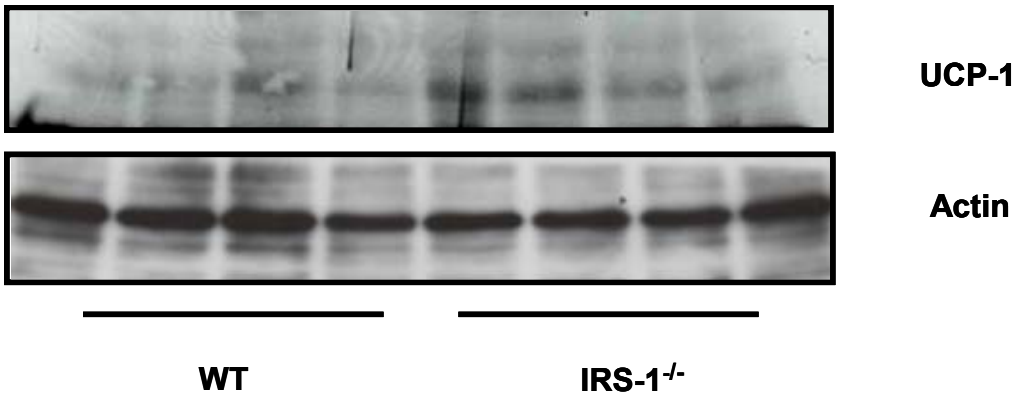

Fig 3.46 Western blot analysis of UCP-1 protein expression in WAT in wild-type controls and IRS-1$^{-/-}$ mice
UCP-1 protein expression in wild-type (n = 4) and knockout (n = 4) mice. Left panel. Actin was used as loading control. 300 µg of protein lysate were applied on 10 % SDS-PAGE gel.

Determination of protein expression by Western blot displayed slight upregulated UCP-1 levels in the knockout group. Quantification of protein expression levels revealed 33 % increased UCP-1 protein levels in the knockout group. Real-time PCR results are supported by the Western blot determination, however in contrast to results obtained by RT-PCR Western blot results do not reach significance.

UCP-1 expression in WAT is an indicator for BAT sections inside WAT. BAT is characterized by high density of mitochondria. Since PGC-1α is essential for mitochondrial biogenesis, *PGC-1α* mRNA expression in WAT was determined by RT-PCR. Elevated *PGC-1α* mRNA levels might provide mitochondrial biogenesis thus providing an indirect proof for BAT sections inside the white adipose tissue.

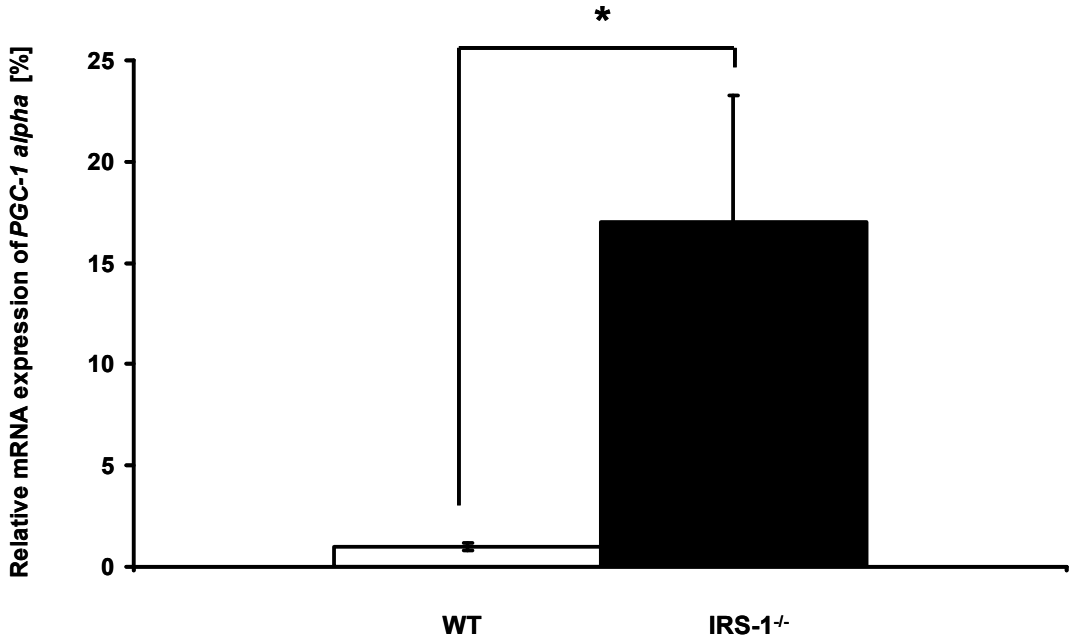

Fig. 3.47 mRNA expression of *PGC-1α* in white adipose tissue (WAT) of IRS-1 knockout mice and wild-type controls
mRNA expression of *PGC-1α* in WAT of IRS-1 deficient (n = 6) and wild-type mice (n = 8). mRNA levels were determined by using PGC-1α and 18s (internal control) TaqMan probes (Applied Biosystems, Darmstadt, Germany). Data represent ΔΔCT calculation. Data are means ± SEM. * unpaired Student´s t-test p-value ≤ 0,05.

Figure 3.47 shows the result of RT-PCR analysis of *PGC-1α* mRNA expression in WAT. Results are expressed as fold increase relative to the control group. IRS-1 deficient mice showed a 1600 % increased mRNA expression of *PGC-1α*. This might represent an indirect effect of BAT sections in WAT, reflecting elevated mitochondrial density in IRS-1$^{-/-}$ mice.

Brown adipose tissue is the key component in regulation of thermogenesis. BAT uncouples mitochondrial respiratory chain and ATP synthesis by UCP-1 using the energy of the inner mitochondrial membrane potential for releasing heat. Therefore increased energy expenditure observed in IRS-1 knockout mice might be induced by elevated uncoupling of BAT. In order to address this question BAT was analyzed towards mRNA expression of uncoupling proteins and enhanced mitochondrial biogenesis by PGC-1 alpha.

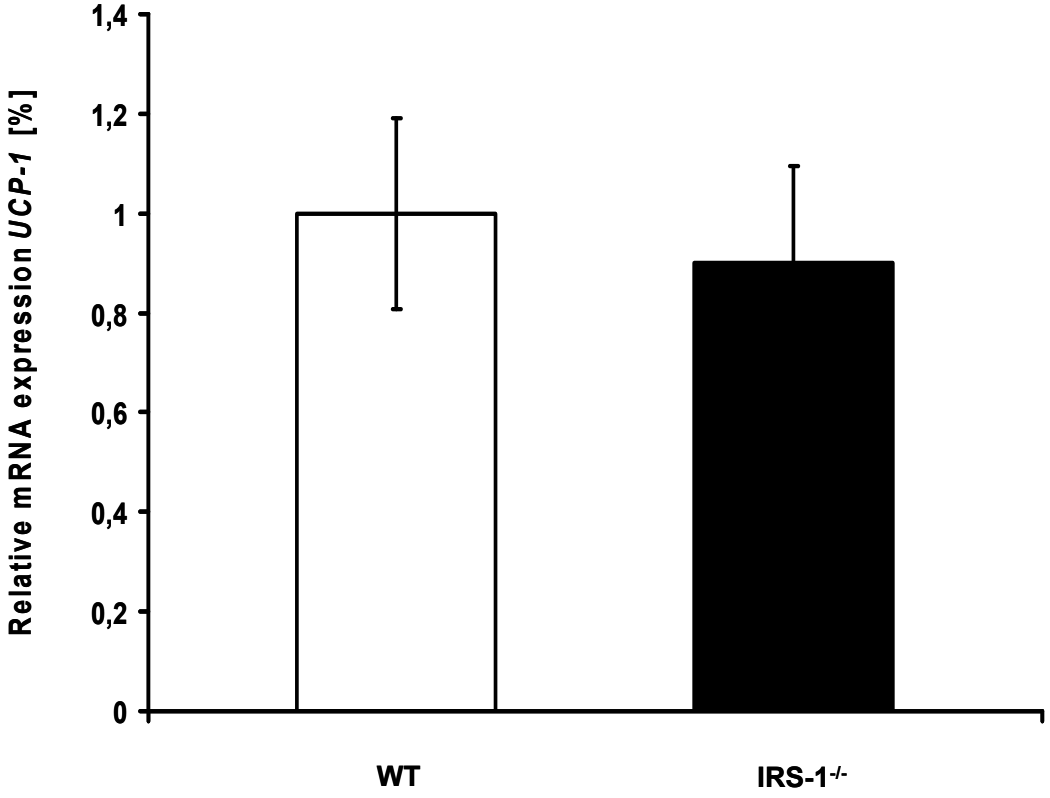

Fig. 3.48 mRNA expression of *UCP-1* in brown adipose tissue (BAT) of IRS-1 knockout mice and wild-type controls
mRNA expression of *UCP-1* in BAT of IRS-1 deficient (n = 5) and wild-type mice (n = 5). mRNA levels were determined by using UCP-1 and 18s (internal control) TaqMan probes (Applied Biosystems, Darmstadt, Germany). Data represent ΔΔCT calculation. Data are means ± SEM.

mRNA expression of *UCP-1* in BAT determined by RT-PCR revealed no alteration in mRNA expression levels of knockout animals compared with wild-type controls. Increased numbers of mitochondria in BAT could also contribute to higher energy expenditure in IRS-1 deficient mice. Hence mRNA expression of *PGC-1 alpha* in BAT was checked by RT-PCR.

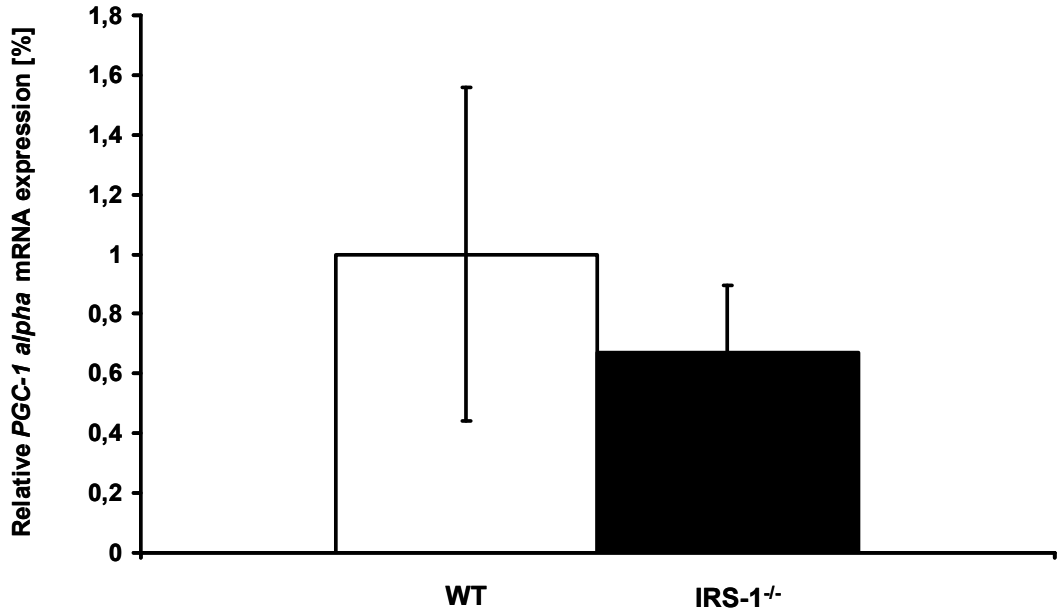

Fig. 3.49 mRNA expression of *PGC-1α* in brown adipose tissue (BAT) of IRS-1 knockout mice and wild-type controls
mRNA expression of *PGC-1α* in BAT of IRS-1 deficient (n = 5) and wild-type mice (n = 5). mRNA levels were determined by using PGC-1α and 18s (internal control) TaqMan probes (Applied Biosystems, Darmstadt, Germany). Data represent ΔΔCT calculation. Data are means ± SEM.

No significant alteration in mRNA expression levels of *PGC-1 alpha* were detected by RT-PCR in IRS-1 knockout animals excluding elevated mitochondrial mass in BAT as underlying mechanism for increased energy expenditure in these mice. No differences in BAT composition of IRS-1 deficient mice compared to wild-type controls could be detected rather decreased levels of *UCP-1* or *PGC-1*α were observed. Therefore neither increased mitochondrial biogenesis nor increased uncoupling in BAT is the basis of increased energy expenditure in knockout animals. Taken together muscle, liver and WAT data indicate uncoupling in these tissues supporting obtained results of respiratory chain activity and proton motive force determinations.

3.8 Generation of ATP in IRS-1 deficient animals

The mitochondrial respiratory chain is the main source for ATP in cells. Dysfunctional mitochondrial respiratory chain complexes can lead to disturbance in ATP content and consequently energy supply of cells. Inner mitochondrial membrane potential is used by ATP synthase, complex V of the respiratory chain, generating ATP. Thus lowering of membrane potential by uncoupling proteins in IRS-1 deficient mice is

supposed to reduce cellular ATP content in these animals. Therefore an ATP bioluminescence assay kit was used for determination of mitochondrial content in MEFs of wild-type and knockout mice.

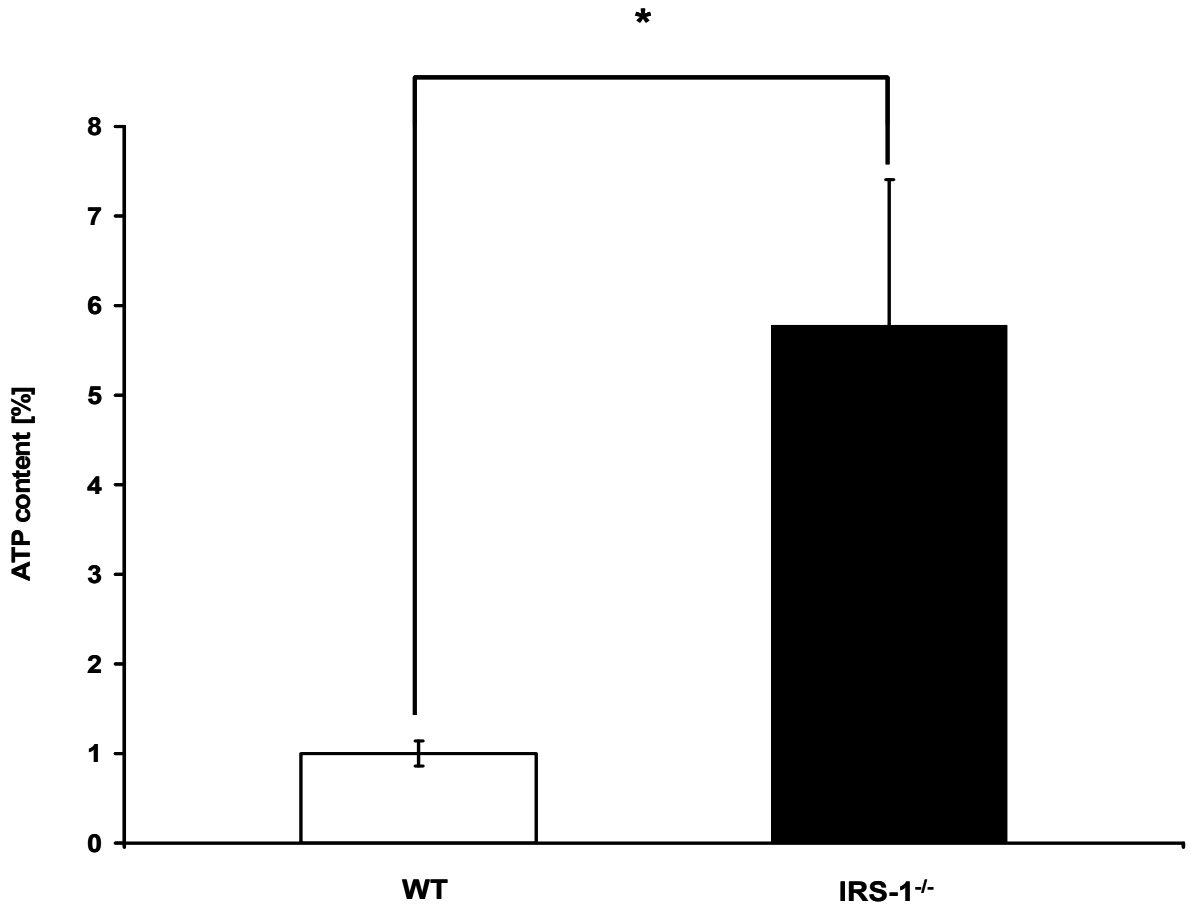

Fig. 3.50 Determination of ATP content in wild-type and knockout MEFs
ATP content of wild-type (n = 5) and knockout (n = 5) derived MEFs. ATP concentrations were determined by ATP bioluminescence assay (Roche, Mannheim, Germany). ATP was measured in triplicates and calculated from standard curve data. Results are expressed as fold increase in relation to the wild-type control group. Values are means ± SEM, * unpaired Student´s t-test p-value ≤ 0,05.

MEF derived from IRS-1 deficient mice showed elevated ATP levels. Since no increased complex V activity was detected by photospectroscopy in IRS-1 knockout MEFs, ATP seemed to be generated by an alternative pathway to OXPHOS. One example of an alternative source for ATP generation is represented by metabolism of glucose via glycolysis to lactate. Therefore enzyme activity of lactate dehydrogenase (LDH) was determined by photospectrometric analysis.

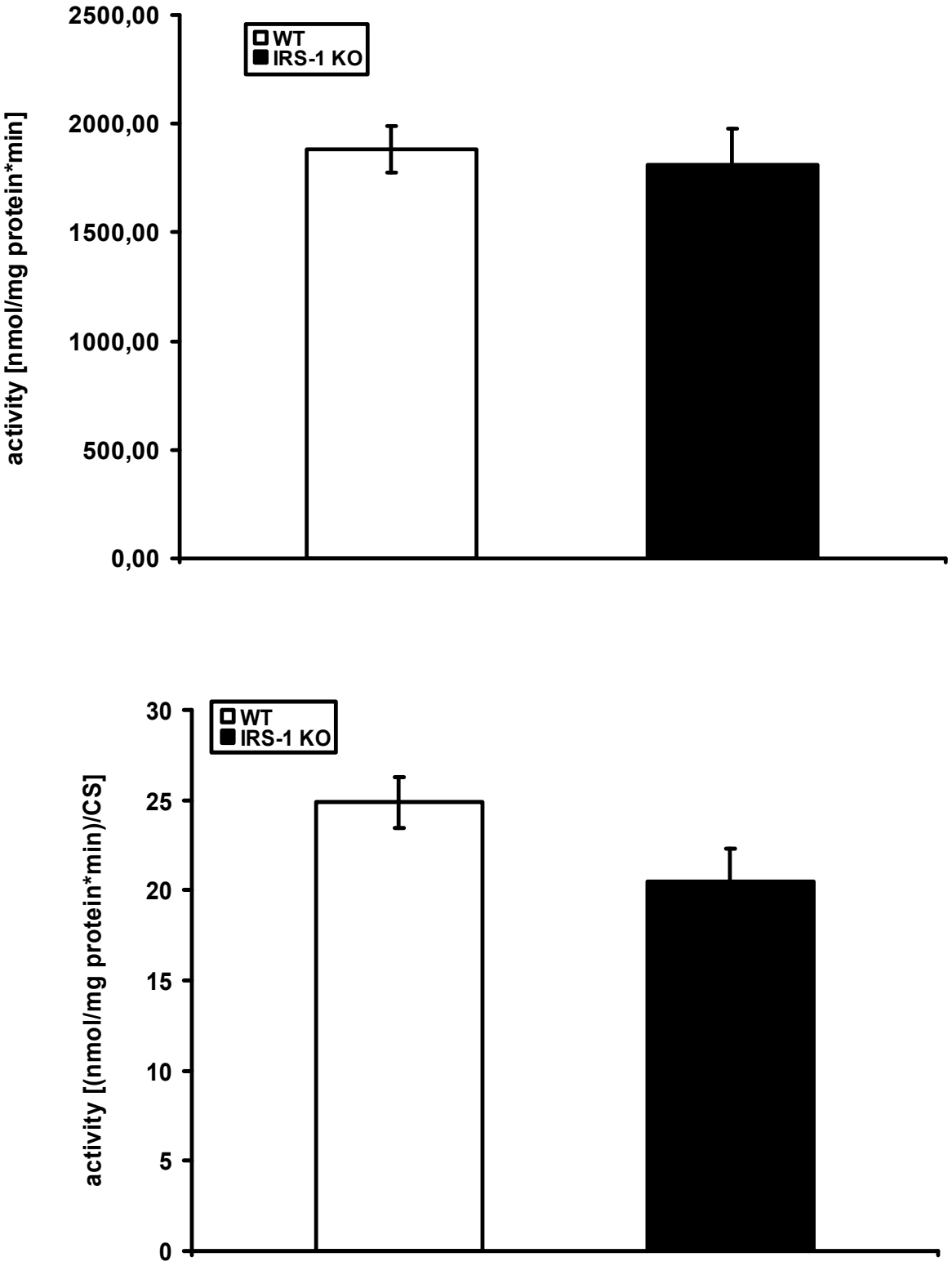

Fig. 3.51 Determination of lactate dehydrogenase activity in MEF derived from wild-type and IRS-1 knockout mice
Upper panel: Activity of LDH in wild-type and knockout MEFs analyzed by photospectroscopy. 5 different samples of each genotype were to applied analysis.
Lower panel: LDH activity in wild-type and knockout animals normalized to mitochondrial mass by CS ratio. Values are means ± SEM.

No alteration in LDH activity has been determined between wild-type and IRS-1$^{-/-}$ mice, IRS-1$^{-/-}$ mice showed rather decreased LDH activity. Apparently enhanced glycolysis and elevated lactic acid fermentation were not the liable source of increased ATP levels in MEFs.

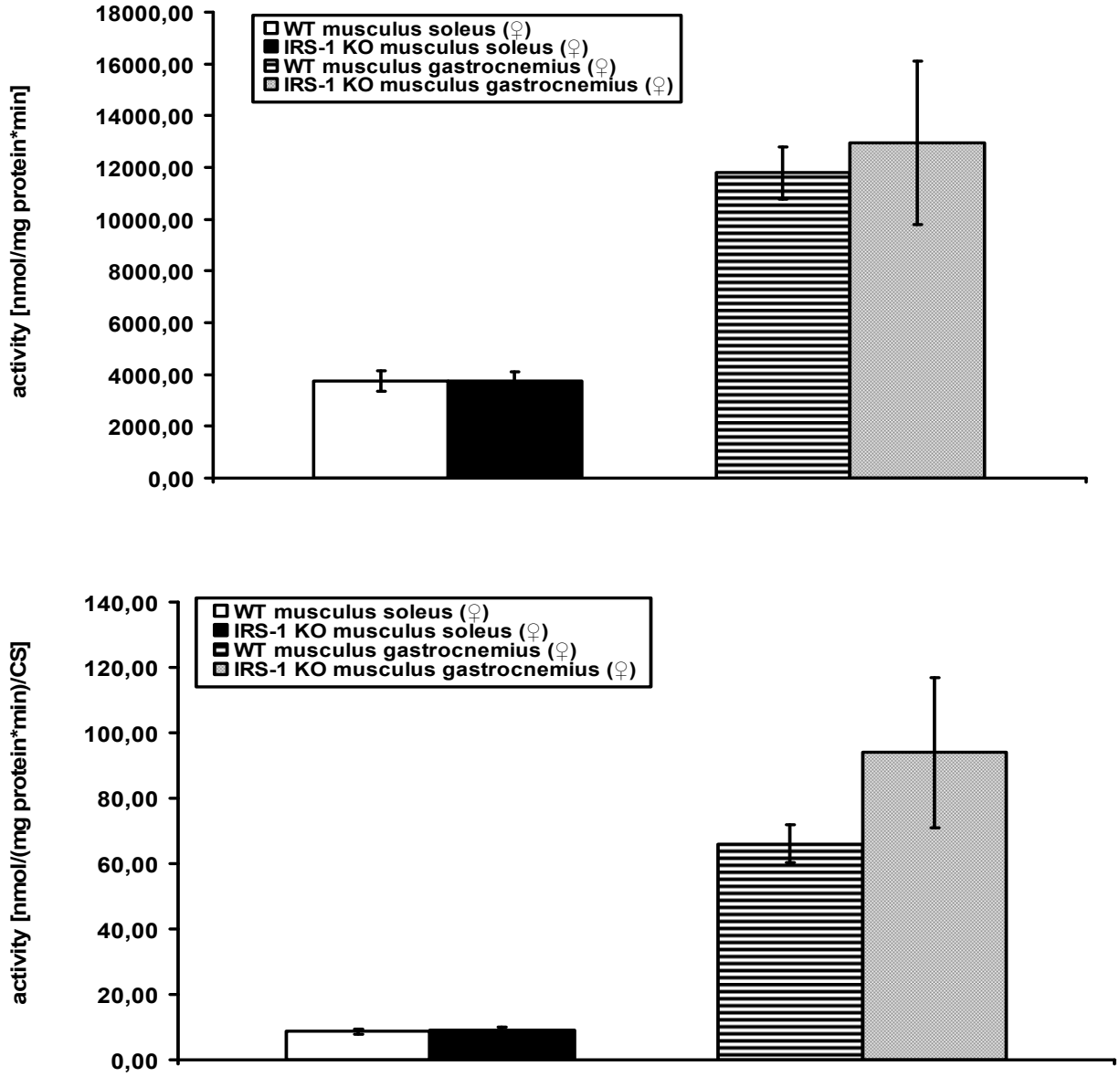

Fig. 3.52 Determination of lactate dehydrogenase activity in red and white muscle of wild-type and IRS-1 knockout female mice
Upper panel: Activity of LDH in wild-type and knockout females analyzed by photo spectroscopy. 8 different samples of each muscle and genotype were applied to analysis.
Lower panel: LDH activity in wild-type and knockout animals normalized to mitochondrial mass by CS ratio. Values are means ± SEM.

Liver and muscle of IRS-1 knockout mice showed decreased activity of ATP synthase indicating decreased ATP levels. Therefore LDH activity was determined in

both tissues in order to check if complex V deficiency is probably compensated by high LDH activity providing an alternative ATP source.

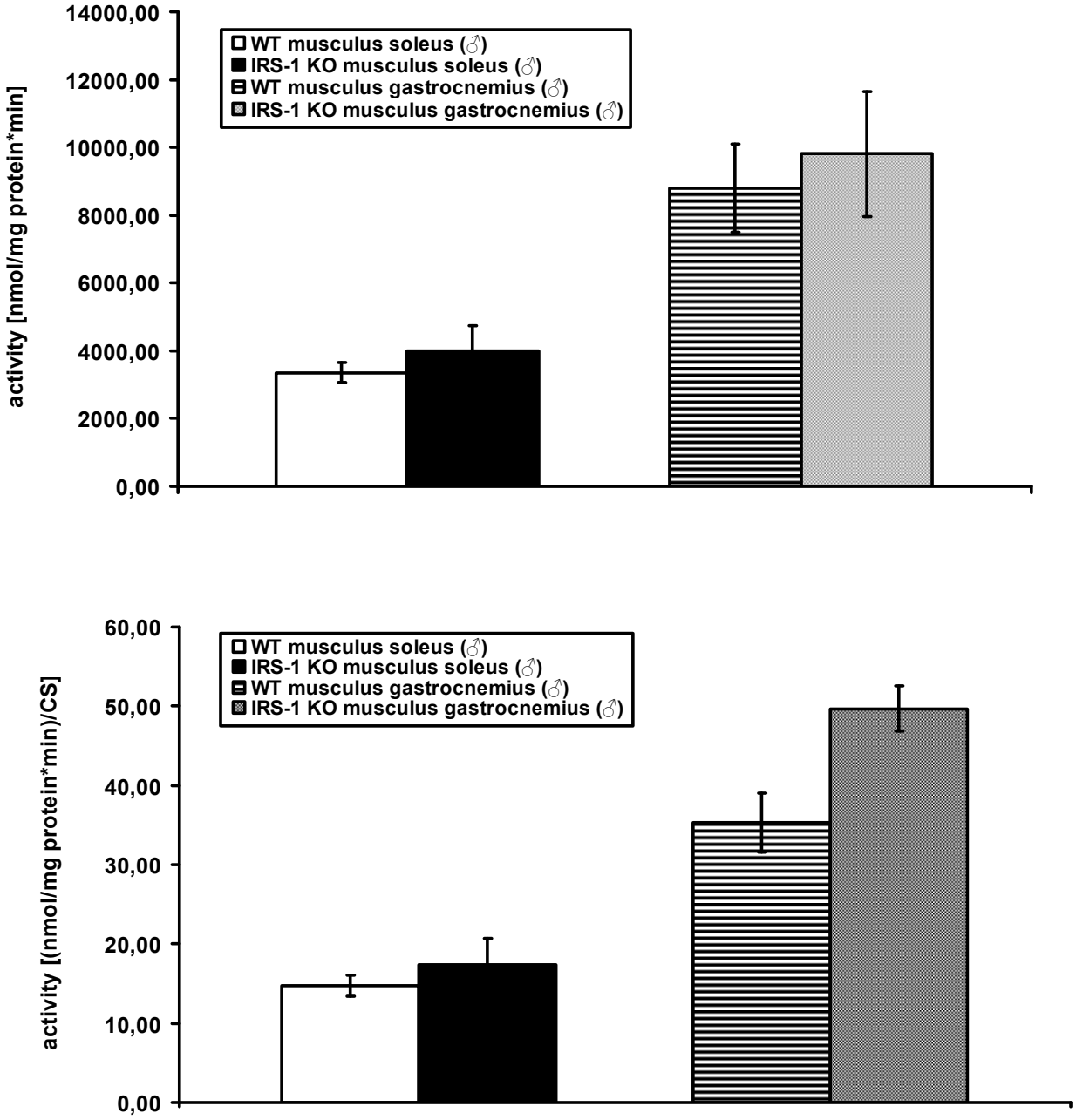

Fig. 3.53 Determination of lactate dehydrogenase activity in red and white muscle of wild-type and IRS-1 knockout male mice
Upper panel: Activity of LDH in wild-type and knockout males analyzed by photo spectroscopy. 7 different samples of each muscle and genotype were applied analysis.
Lower panel: LDH activity in wild-type and knockout animals normalized to mitochondrial mass by CS ratio. Values are means ± SEM.

Photospectrometric analysis of LDH showed increased activity M. gastrocnemius in IRS-1 deficient male and female mice. M. soleus of male IRS-1 knockout mice

displayed slight increased LDH activity, whereas activity in females remained unchanged compared with wild-type controls.

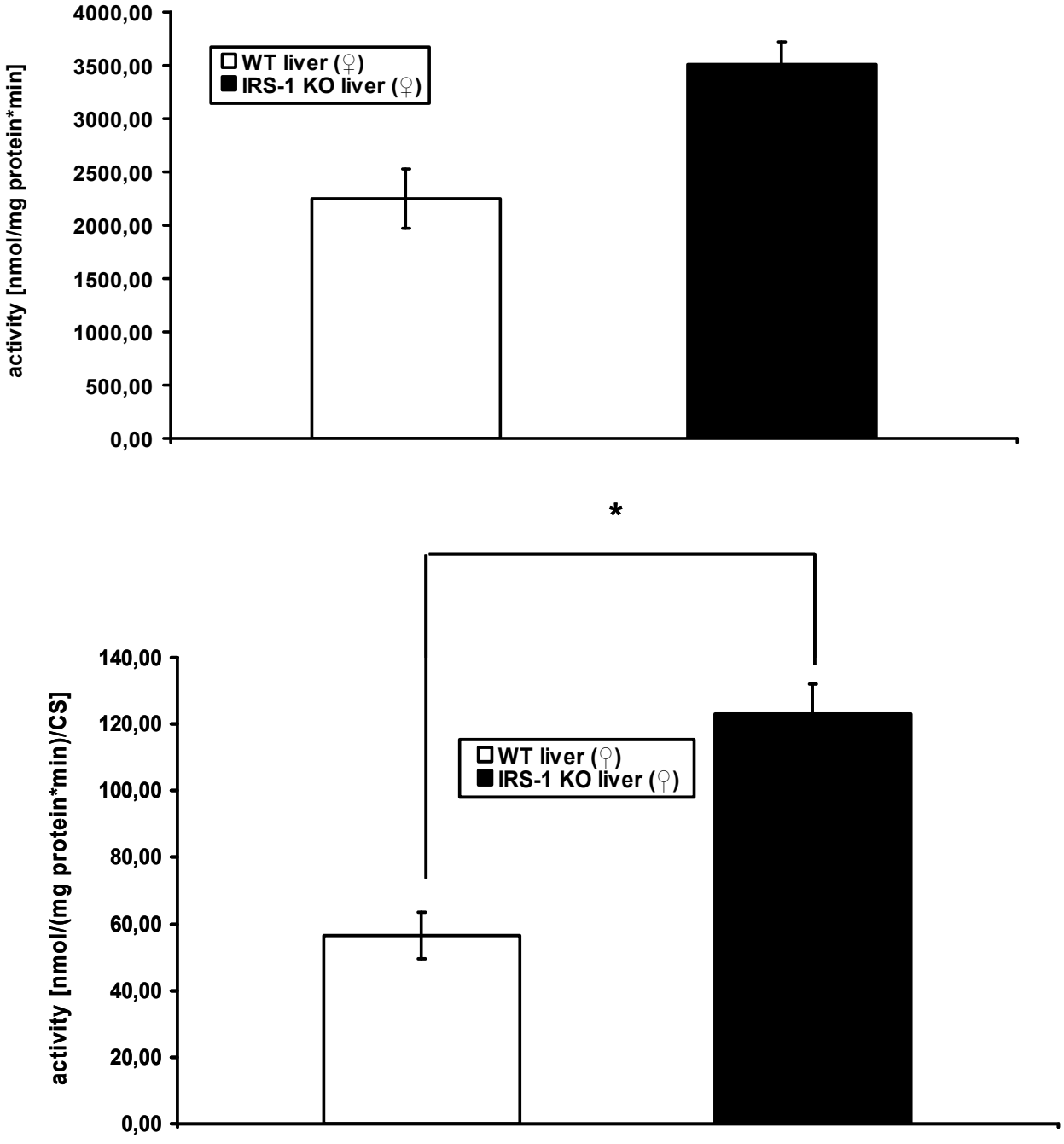

Fig. 3.54 Determination of lactate dehydrogenase activity in livers of wild-type and IRS-1 knockout female mice
Upper panel: Activity of LDH in wild-type and knockout females analyzed by photo spectroscopy. 5 different samples of each muscle and genotype were applied analysis.
Lower panel: LDH activity in wild-type and knockout animals normalized to mitochondrial mass by CS ratio. Values are means ± SEM. * unpaired Student´s t-test p-value ≤ 0,05.

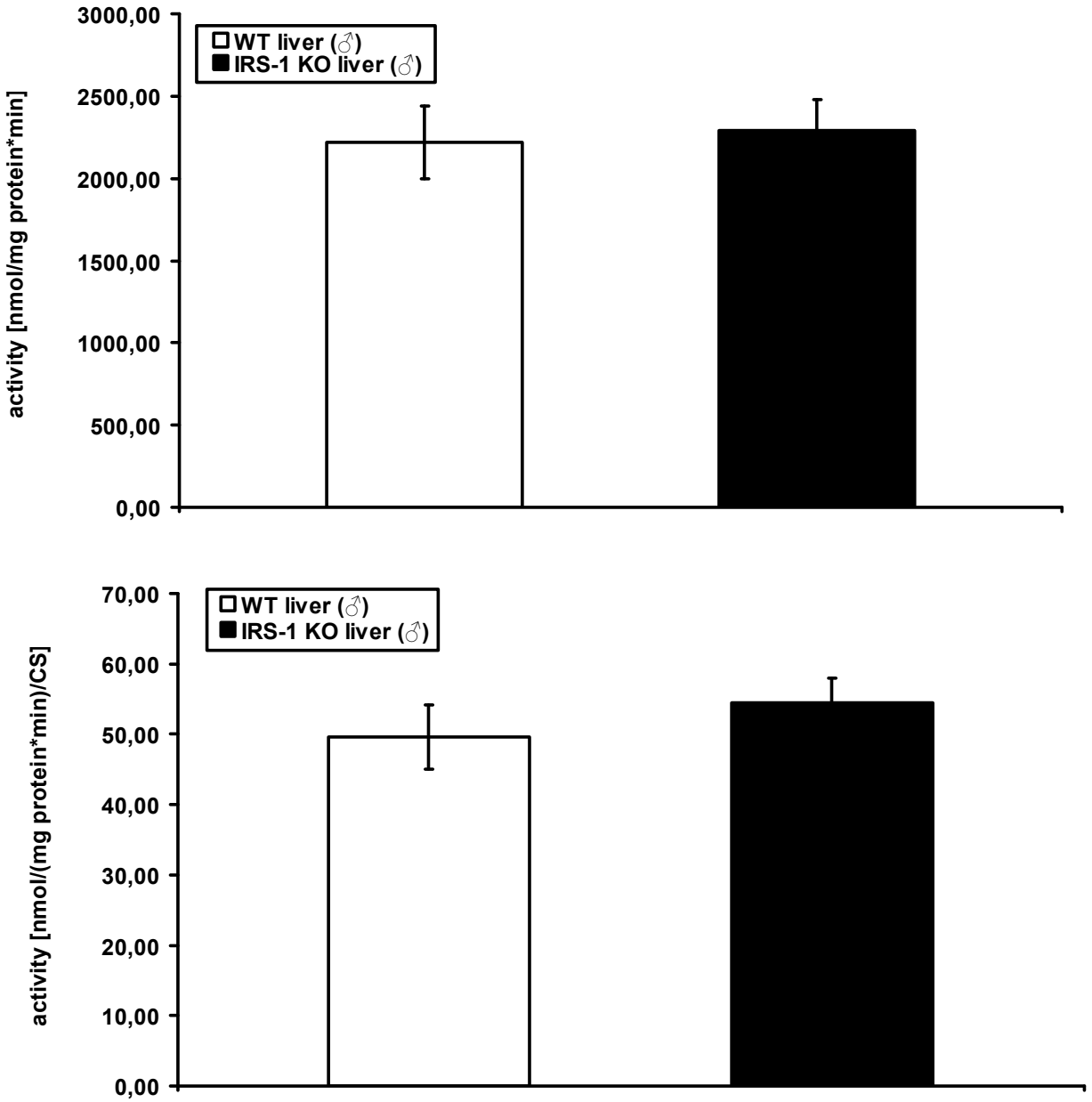

Fig. 3.55 Determination of lactate dehydrogenase activity in livers of wild-type and IRS-1 knockout male mice
Upper panel: Activity of LDH in wild-type and knockout males analyzed by photospectroscopy. 5 different samples of each muscle and genotype were applied analysis.
Lower panel: LDH activity in wild-type and knockout animals normalized to mitochondrial mass by CS ratio. Values are means ± SEM.

LDH activity determination in female (Fig. 3.54) and male (Fig. 3.55) knockout and wild-type mice, displayed unchanged LDH activity in male mice whereas LDH activity in females was elevated compared to wild-type controls, reaching significance when normalized to mitochondrial mass. Taken together obtained results for LDH activity in muscles and livers of IRS-$1^{-/-}$ and wild-type mice showed a tendency of increased LDH activity in the knockout group, may be caused by a physiological compensatory

reaction facing low ATP levels due to decreased ATP synthase activity, observed in these tissues.

3.9 Analysis of fat metabolism in IRS-1$^{-/-}$ mice

To verify the phenotypic characteristic of nearly abrogated abdominal fat accumulation in IRS-1$^{-/-}$ mice body composition was examined by nuclear magnetic resonance analysis (NMR) of female and male knockout and wild-type mice.

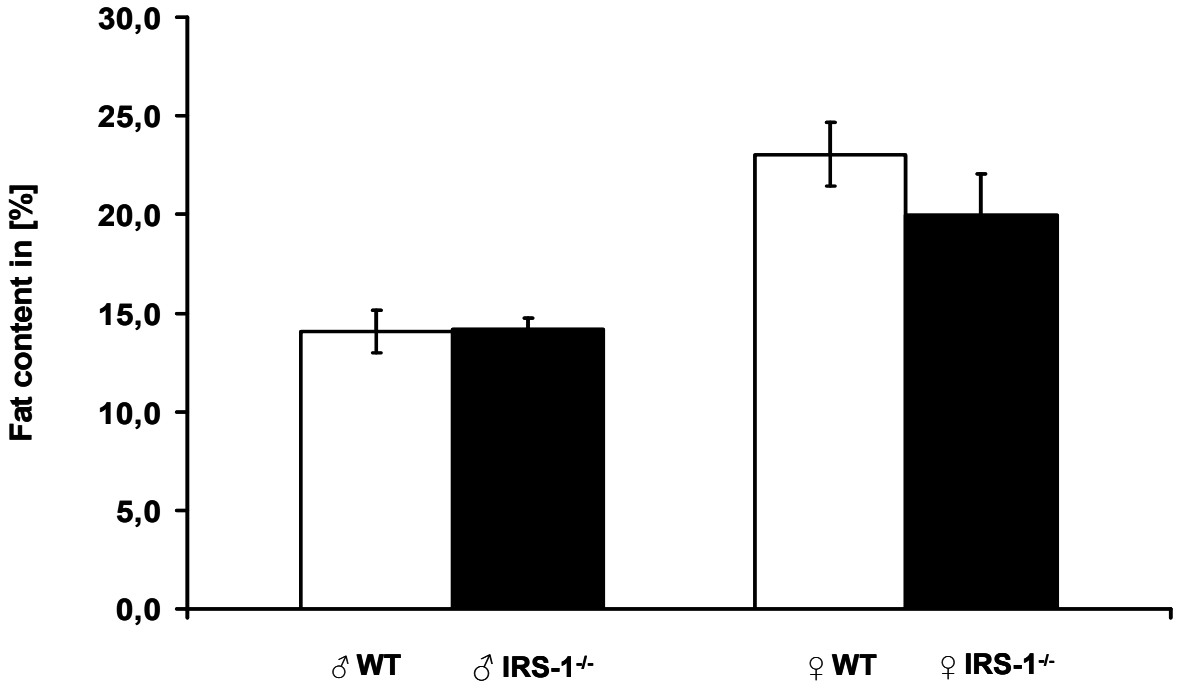

Fig. 3.56 Fat content in IRS-1 deficient and wild-type mice at the age of 12 month
Average fat content of 12 month old wild-type (black bars), females (n = 12) and males (n = 16) and knockout (white bars), females (n = 8) and males (n = 9). Data are means ± SD

Surprisingly no significant differences in fat content of IRS-1 deficient mice compared to wild-type controls could be detected by NMR. Overall fat contents in IRS-1$^{-/-}$ females were slightly decreased (about 5 %) in female knockouts whereas fat content in knockout males were indistinguishable from wild-types. Lean mass analysis (data not shown) underlined the NMR results, no difference in lean tissue mass in male mice and a slight increased lean tissue mass in IRS-1$^{-/-}$ females were detected.

Lack of abdominal fat accumulation was observed in IRS-1 knockout animals whereas total fat content in mice is not altered in comparison with wild-type mice

indicate redistribution of fat in IRS-1$^{-/-}$ mice. It is known that the brain body ratio is increased in IRS-1$^{-/-}$ mice compared with wild-type controls (Schubert et al., 2003). To evaluate whether proportions of other organs besides brain are increased in relation to body weight, livers were dissected and correlated to body weight.

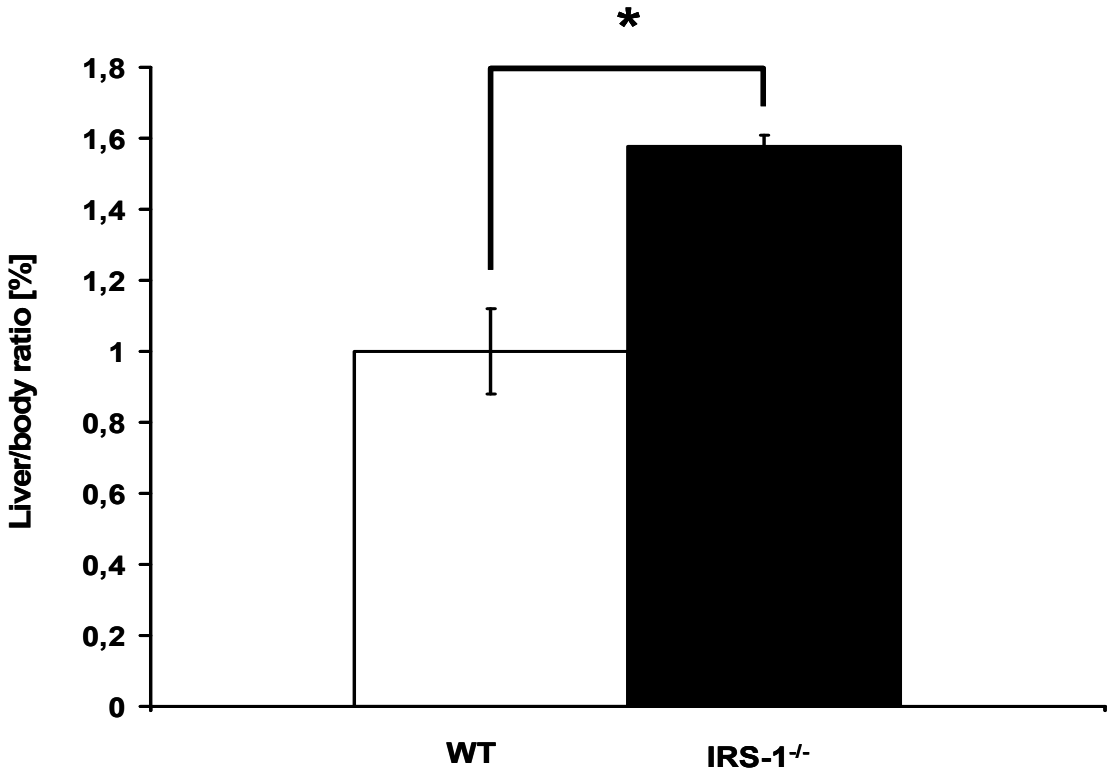

Fig. 3.57 Liver-Body ratio of 12 month old mice
Average liver-body ratio of wild-type (n = 7) and knockout (n = 6) mice 12 month of age. Results were normalized to wild-type controls and expressed as means ± SEM. * unpaired Student´s t-test p-value ≤ 0,05.

Significant differences in liver-body ratio between wild-type and knockout mice were detected. Ratio in IRS-1 deficient animal was elevated indicating enlarged liver sizes in relation to body weight in these mice compared to the wild-type controls. This suggests that abdominal fat may be redistributed to the liver of the animals resulting in unchanged overall fat content.

Besides redistribution of abdominal fat to the livers or other organs of IRS-1 knockout mice, inhibited lipid metabolism might be responsible for unaltered total fat content. Therefore activity of the mitochondrial acid transporter carnitine palmitoyl transferase I (CPT-I) in mitochondria isolated from livers was measured. CPT-I is associated with the outer mitochondrial membrane. CPT-I mediates the transport of free fatty acids

FFA) across the membrane by binding to carnitine, providing FFA from cytosol for β-oxidation in the mitochondrial matrix.

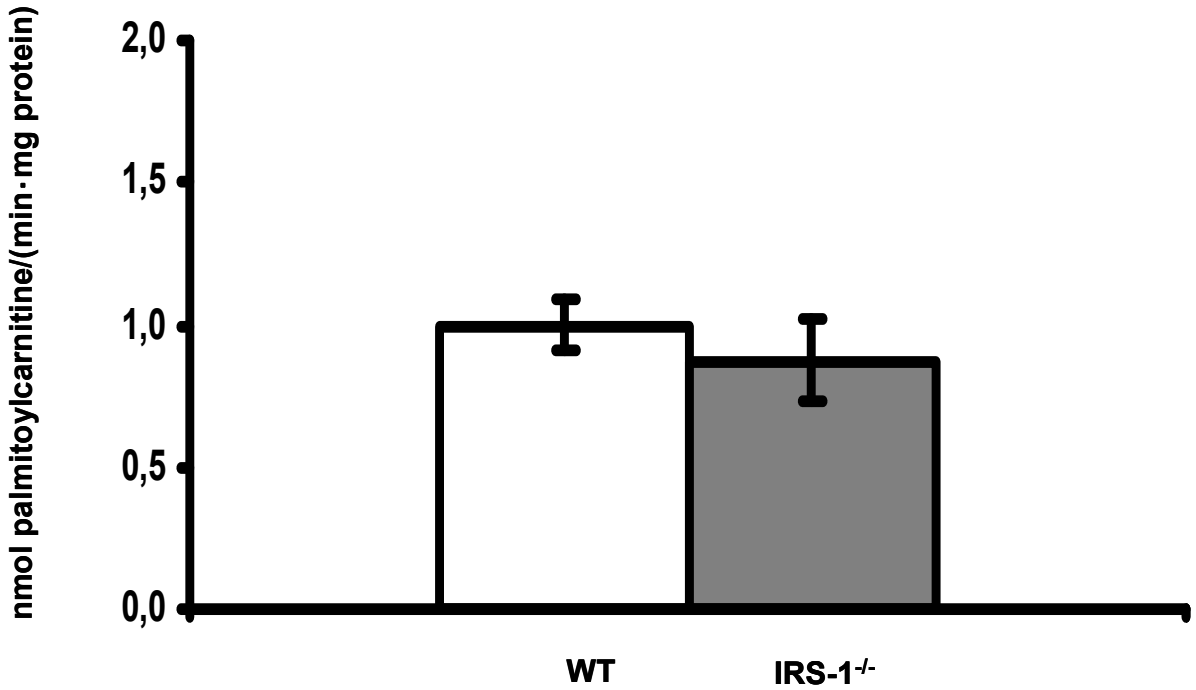

Fig. 3.58 Determination of CPT-I enzyme activity in isolated liver mitochondria
Enzyme activities were determined by ^{14}C-carnitine incorporation into acylcarnitines. Isolated mitochondria from livers of male wild-type (n = 5) and male knockouts (n = 5) were analyzed. Results were normalized to wild-type controls and expressed as means of ± SD.

Considerably decreased CPT-I activities resulting in impaired transfer of FFA from cytosol to mitochondrial matrix were not detected in mitochondria of IRS-1$^{-/-}$ livers. However IRS-1 knockout mice presented slightly decreased CPT-I activity levels compared with wild-type controls not reaching significance.

3.10 Determination of increased food intake

In order to address increased food intake in IRS-1 deficient mice, leptin serum levels were determined. Lowered leptin levels in IRS-1$^{-/-}$ mice could be the underlying mechanism for the observed hyperphagic phenotype in these mice.

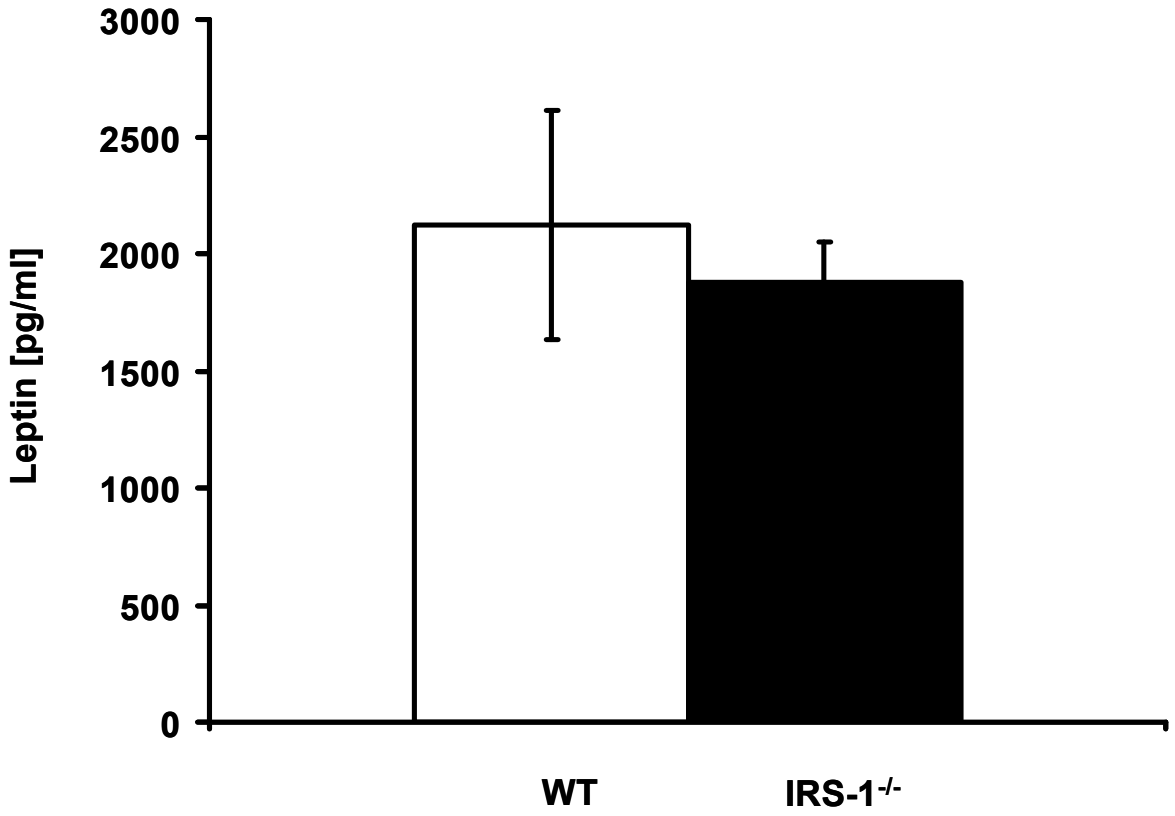

Fig. 3.59 Leptin serum levels of 12 month old mice
Leptin serum levels of both wild-type (n = 7) and IRS-$1^{-/-}$ (n = 7) mice were determined by ELISA. Mice were starved overnight (16 h) and serum was isolated from blood of animals. Data represent serum insulin levels of 12 month old male animals. Values are means ± SEM.

Serum leptin concentrations were decreased in IRS-$1^{-/-}$ mice compared with wild-type controls and consequently accompanied by increased food intake in these mice. Leptin is secreted by adipocytes and serum leptin levels are positively correlated with adipose storage. Additionally serum adiponectin levels (wildtype 5,74±0,37 [µg/ml]; knockout 7,2±1,26 [µg/ml]) were slightly increased in knockout mice. In order to elucidate this effect mRNA expression levels of hypothalamic neuropeptides, POMC, AgRP, CART and NPY were determined by RT-PCR in IRS-1 knockout and wild-type mice.

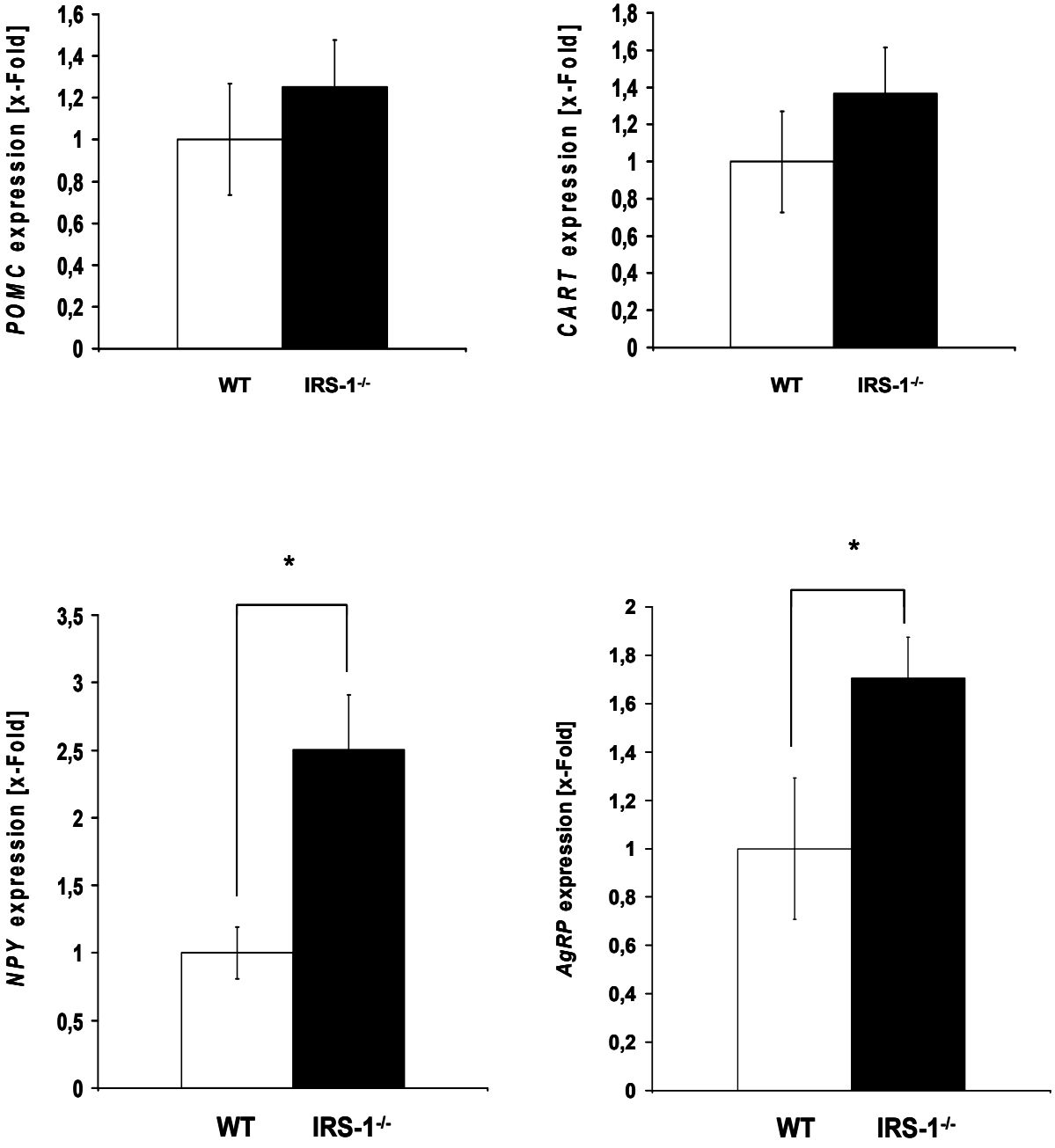

Fig 3.60 Determination of *POMC, CART, NPY* and *AgRP* mRNA levels in wild-type and knockout mice

Relative mRNA expression levels of anorectic hypothalamic neuropeptides *POMC* and *CART* and orectic hypothalamic neuropeptides *NPY* and *AgRP* in random fed wild-type (n = 6) and knockout (n = 6) mice determined by RT-PCR analysis. Results were normalized to wild-type controls and expressed as means ± SEM. * unpaired Student´s t-test p-value ≤ 0,05.

Investigation of mRNA expression levels of hypothalamic neuropeptides essential for energy homeostasis in mammals revealed significant increased mRNA levels for the orectic neuropeptides NPY and AgRP. This observed mRNA expression patterns correlates with the hyperphagic phenotype of IRS-1 deficient mice. On the other hand also the anorectic hypothalamic neuropeptides POMC and CART showed elevated

mRNA levels in IRS-1$^{-/-}$ mice however not reaching significance. POMC mRNA levels were 25 % higher compared with wild-type controls. Additionally CART was 36 % increased in IRS-1$^{-/-}$ hypothalami. Overall data of leptin and hypothalamic neuropetide in IRS-1 deficient mice represent a possible mechanism explaining increased food intake in these mice.

To elucidate if IRS-1 deficiency is compensated in brain mRNA expression of IRS-2 and IRS-4 was determined by RT-PCR. IRS-4 expression is restricted to hypothalamus with high expression in the arcuate nucleus (including NPY/AgRP and PMOC/CART neurons) and therefore could be a strong candidate for partially compensation of IRS-1 deficiency in this part of the hypothalamus (Numan et al., 1999).
Furthermore insulin receptor and leptin receptor expression was addressed by RT-PCR analysis.

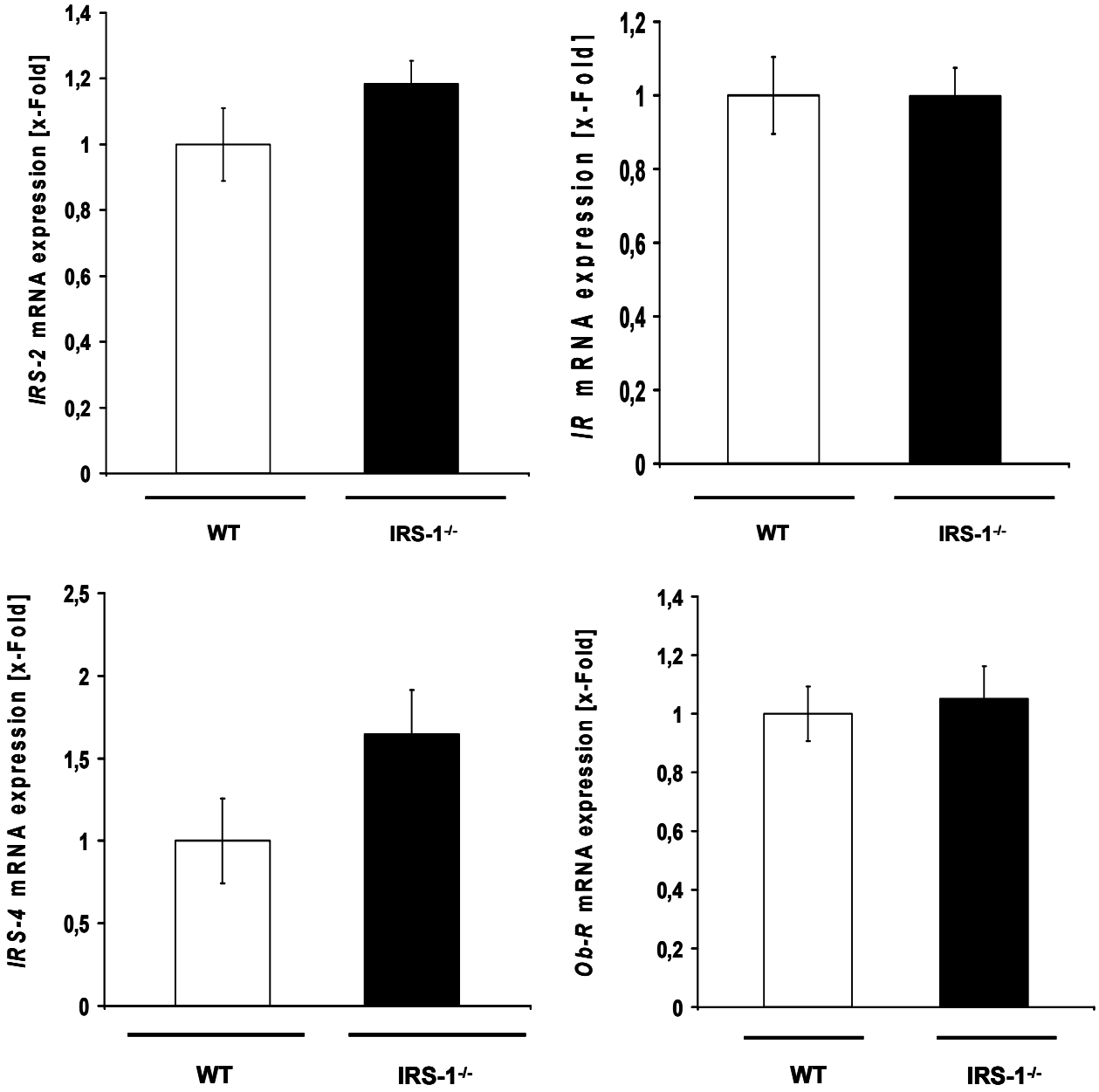

Fig. 3.61 Determination of *IRS-2, IRS-4,* insulin receptor *(IR)* and leptin receptor *(Ob-R)* mRNA levels in arcuate nucleus of wild-type and knockout mice
Relative mRNA expression levels *IRS-2, IRS-4, IR and Ob-R* in random fed wild-type (n = 6) and knockout (n = 6) mice determined by RT-PCR analysis. Results were normalized to wild-type controls and expressed as means ± SEM.

RT-PCR analysis of insulin receptor and leptin receptor displayed unchanged expression levels in knockout mice compared with wild-type animals. *IRS-2* mRNA levels were almost unchanged however *IRS-4* mRNA levels were increased in IRS-1 deficient animals without reaching significance, maybe indicating a compensatory mechanism in hypothalamus of IRS-1 knockout animals.

Summarizing the results of regulation of energy homeostasis in IRS-1 knockout mice revealed possible molecular mechanisms explaining the described phenotype in this mouse model.

i) Increased energy expenditure is based on mitochondrial respiratory chain uncoupling.
ii) Hyperphagic phenotype mediated via changes in expression patterns of orectic hypothalamic neuropeptides

4 Discussion

4. Discussion

Mild insulin resistance, dwarfism as well as increased mean and maximum lifespan have been described as denotative phenotypes of IRS-1 knockout mice (Tamemoto et al., 1994; Selman et al., 2008). Interestingly, during aging gain of body weight and abdominal fat accumulation was reduced in IRS-1 deficient mice compared to wild-types. Surprisingly, this phenotype was accompanied by increased food intake and increased energy expenditure in IRS-$1^{-/-}$ mice.

To elucidate underlying mechanisms for these phenotype, aged IRS-$1^{-/-}$ mice were applied to biochemical, molecular and cellular analysis. Additionally MEFs derived from females of IRS-$1^{-/+}$ breeding pairs were analyzed serving as an *in vitro* system to discriminate between pure cellular or signaling effects caused by IRS-1 deficiency and effects influenced or compensated by a fully functional endocrine environment *in vivo*.

4.1 Basal insulin signaling in IRS-$1^{-/-}$ mice and MEFs

Western blot analyzes from muscle, liver, WAT, lung, brain and kidney revealed IRS-1 expression in these tissues in wild-type mice and confirmed IRS-1 deletion in IRS-$1^{-/-}$ mice (Fig. 3.1). Furthermore, IRS-1 was clearly detectable in MEFs generated from wild-type mice but as expected not in MEFs derived from IRS-$1^{-/-}$ mice (Fig. 3.2).

Basal expression of IRS-2 and IGF-1R in wild-type and IRS-1 knockout MEFs remained unchanged whereas IR expression of IRS-$1^{-/-}$ MEFs was significantly reduced compared to wild-type MEFs. No alteration in protein abundance of IRS-2 and IGF-1R in liver and muscle of IRS-$1^{-/-}$ and wild-type were detected. However as observed in MEFs IR expression was reduced in muscle of IRS-1 deficient mice whereas in liver tissue no changes in IR protein levels were observed suggesting a specific effect of IRS-1 deficiency in skeletal muscle. Hyperinsulinism due to insulin resistance or chronic insulin treatment respectively has been proposed to moderately decrease insulin receptor expression (Yuan et al., 2002, Venkatesan et al., 1995). Since insulin levels are elevated (Fig. 3.10) in IRS-1 $^{-/-}$ mice, downregulation of IR might be induced by hyperinsulinism. Previous studies suggested that increased

insulin signaling affects upstream receptor density in a feed back inhibition leading to decreased insulin signaling (Werner et al., 1995). In IRS-1 knockout mice this effect might be less pronounced due to only mild insulin resistance and hyperinsulinemia (3.8 and 3.9). In liver of IRS-1 knockout mice insulin resistance is compensated via an upregulation of IRS-2 (Fig. 3.7) contributing to nearly unchanged IR signaling. In skeletal muscle IR signaling might be impaired due to IRS-1 deficiency since no compensatory effect was detected and muscle is thought to be responsible for insulin resistance in these mice. Consequences of IRS-1 deficiency for IR signaling are more pronounced in muscle than in liver since IRS-2 seem to be the predominant IRS protein in hepatocytes nearly fully compensating IRS-1 deficiency (Kido et al., 2000; Yamauchi et al., 1996). However, the reduction of IR in skeletal muscle and in MEFs of IRS-$1^{-/-}$ mice but not in liver argues against chronic increased IR signaling stimulation as leading cause for the reduced IR expression and favors a hypothesis where slightly decreased IR signaling in a tissue-specific manner might be responsible.

4.2 Role of IRS-1 in Insulin signaling

To elucidate the role of the IRS-1 for insulin signaling in cells and tissues phosphorylation of downstream signaling proteins were analyzed by Western blots after acute insulin stimulation. Determination of phosphorylation states of key kinases of the insulin signaling cascade in MEFs displayed phosphorylation increment. ERK phosphorylation rose upon insulin titration to the same degree in both wild-type and IRS-$1^{-/-}$ MEFs. Concentrations of 10 nM insulin seemed to be sufficient for full activation of the insulin signaling cascade since no further phosphorylation increment was observed by stimulating MEFs with 100 nM insulin. A slight decreased insulin respond was observed using 1 nM insulin for stimulation suggesting an impact of IRS-1 on mediation of insulin receptor signaltransduction in MEFs. In the line with these data basal phosphorylation after overnight starvation was also lowered in IRS-1 deficient cells (0 nM insulin). Similarly to ERK, GSK-3β showed decreased phosphorylation at Ser9 following treatment with 1nM insulin. However, no further differences between WT and IRS-$1^{-/-}$ MEFs upon insulin stimulation using higher insulin concentration were observed.

PTEN expression in wild-type derived MEFs was decreased compared with PTEN expression in knockout derived MEFs under basal as well as under stimulated conditions (Fig. 3.5). However PTEN expression in wild-type MEFs increased upon insulin stimulation, no alteration of PTEN expression in knockout MEFs was detected indicating disrupted insulin response of PTEN protein in IRS-1 deficient MEFs. Additionally a double band at ~140 kDa and ~165 kDa was exclusively detected in wild-type derived MEFs. In correlation with PTEN expression increment upon insulin stimulation this double band decreased approximately to the same degree as PTEN expression increased. PTEN is described to be incorporated into a high molecular-weight complex (PTEN associated complex [PAC]). p85 is suggested to be part of the PAC. Unphosphorylated PTEN associates with p85 (regulatory subunit of PI3K) promoting its stabilization. Phosphorylation of the PTEN tail regulates its stability and activity. Phosphorylated PTEN protein is more stable but less active compared to unphosphorylated PTEN. PTEN protein is phosphorylated by casein kinases, Src family members and GSK-3β (Vazquez et al., 2000; Rabinovsky et al., 2009; Barber et al., 2006). Co-immunoprecipitation of p85α and PTEN showed enhanced p85/PTEN signal in wild-type derived MEFs in basal state (0 nM) and upon insulin stimulation with 1nM. p85α/PTEN expression upon stimulation with 10 nM or 100 nM insulin, respectively revealed no alteration between wild-type and knockout MEFs. This correlates with the decline of the 140/165 kDa double band and the increase of PTEN expression in the PTEN Western blot, suggesting double bands reflecting p85/PTEN association (p85 (85 kDa) + PTEN (55 kDa), associated 140 kDa) and p110/PTEN (p110 (110 kDa) + PTEN (55 kDa), associated 165 kDa) as described in literature (Rabinovsky et al., 2009). Absence of PTEN aggregates in knockout MEFs could be a compensatory mechanism as a result of mild insulin resistance. PTEN aggregates consist of unphosphorylated but more active PTEN. Lack of these aggregates would indicate a high proportion of phosphorylated less active form of PTEN in knockout MEFs resulting in declined PTEN activity. Reduction of PTEN activity downregulates PIP3/PIP2 conversion resulting in prolonged activation of the PI3K pathway (Barber et al., 2006).

p85 might associate with PTEN in basal and slight stimulation state (1nM). With higher insulin stimulation levels p85 is recruited to tyrosine phosphorylated IRS proteins probably releasing PTEN. This might be an explanation for observed p85/PTEN association discrepancy between wild-type and knockout MEFs in basal

and low stimulated state and diminished discrepancy in higher stimulation states. Due to mild insulin resistance in IRS-1$^{-/-}$ animals or MEFs respectively, GSK-3β is less phosphorylated and hence more active in knockout MEFs. Fig. 3.4 shows slightly decreased GSK-3β phosphorylation in basal state and low stimulated knockout MEFs this effect disappeared with higher insulin concentrations. Since GSK-3β one of the kinases responsible for PTEN phosphorylation is less phosphorylated and therefore more active in basal and slight stimulated knockout MEFs PTEN gets more phosphorylated. The decreased detection of p85α/PTEN complex in knockout MEFs is probably a result of this since unphosphorylated PTEN associates with p85. With increased GSK-3β phosphorylation up to wild-type levels this effect is abolished due to inactivated GSK-3β and decreasing PTEN phosphorylation. However the role of IRS-1 for p85α/PTEN association needs further investigation.

To analyze insulin signaling in a systemic and more physiological context IRS-1 knockout and wild-type animals were stimulated after 16 h starvation via intraperitoneal insulin injection. Phosphorylation states of downstream targets of the IR signaling cascade were determined by Western blotting from muscle, WAT and liver of IRS-1 deficient and wild-type animals (Fig. 3.6). Surprisingly, insulin response of IRS-1 deficient mice was enhanced compared with wild-type mice. Basal phosphorylation levels of AKT in muscle and liver of IRS-1$^{-/-}$ were increased resulting in enhanced increment of phosphorylation upon stimulation in IRS-1$^{-/-}$ animals compared to wild-types. No differences upon AKT phosphorylation were determined in WAT. AKT phosphorylation at Ser473 following insulin treatment showed no signaling malfunction in muscle WAT and livers of IRS-1 deficient mice compared to wild-type supporting the results obtained for *in vitro* stimulation in MEFs. However previous studies (Yamauchi et al., 1996) reported decreased PI3-kinase activity in muscles of IRS-1 knockout mice. Mice used in this previous study were 8 to 12 weeks of age, mice used here were at least 60 weeks of age; therefore a possible adaptation with age due to mild insulin resistance in knockout mice could be responsible for improved PI3-kinase activity in these mice. Additionally no differences in GSK-3β and ERK-1/-2 phosphorylation response upon insulin stimulation were determined in muscle liver or WAT in IRS-1 knockout animals compared to wild-type controls.

In conclusion the presented data indicate that besides deletion of IRS-1 protein and downregulation of IR in muscle acute intracellular signaling upon insulin treatment is only mildly impaired in IRS-1$^{-/-}$ mice. This might be due to compensation by alternative insulin receptor substrates as shown in liver for IRS-2 (Fig. 3.7) or increased insulin signaling via the IGF-1R or hybrid receptors or even alternative pathways. Additionally lack of p85α/PTEN association might be a compensatory mechanism in IRS-1 knockout animals. PTEN is positively regulated by p85, decreased p85/PTEN levels reduce PTEN phosphatase activity, hence sustaining PIP3 levels and PI3 signaling (Chagpar et al., 2010; Fernadez et al., 2001, Higaki et al. 1999; Wojtaszewski et al. 1999).

4.3 Metabolic characterization

Mild insulin resistance in IRS-1 knockout mice has been described in literature (Tamemoto et al., 1994; Araki et al., 1994). Insulin tolerance tests revealed slower decrease of blood glucose levels in IRS-1 deficient mice following insulin treatment compared to wild-type mice for both genders indicating insulin resistance. Even though the effect exerted by IRS-1 deficiency seems to be small compared for example in animals fed a high fat diet, but still visible in ITTs. However, glucose tolerance tests showed only minor alterations of glucose metabolism in female IRS-1 knockout mice suggesting pancreatic β-cell compensation whereas GTTs in males revealed mild glucose intolerance. Accordingly, serum insulin levels in IRS-1 deficient mice were elevated as physiological respond to insulin resistance (Brüning et al., 1997; Haffner et al., 1996). Further explanations for the only mild effects on glucose metabolism despite IRS-1 deficient might be compensation via alternative substrates for the IR combined with other factors improving insulin sensitivity. Particularly, small adipocytes express and secrete adiponectin, which stimulates insulin sensitivity in various cell types (Takahashi et al., 2009). Accordingly, serum adiponectin levels were slightly increased in IRS-1 deficient mice. Thus reduced abdominal fat mass, smaller adipocytes and pancreatic β-cell compensation improve glucose metabolism in IRS-1$^{-/-}$ mice leading to remarkable different phenotypes between the non-diabetic IRS-1 and diabetic IRS-2 knockout mice (Burks et al., 2000; Withers et al., 1999).

4.4 Energy metabolism in IRS-1$^{-/-}$ mice

Growth retardation decreased abdominal fat mass and increased lifespan are known and reproduced phenotypes of IRS-1$^{-/-}$ mice (Tamemoto et al. 1994; Araki et al., 1994, Kadowaki et al., 1996; Tamemoto et al., 1997). To elucidate possible mechanisms contributing to these phenotypes we analyzed energy metabolism and mitochondrial function of IRS-1$^{-/-}$ mice in detail.

As describe previously IRS-1 deficient mice showed significantly reduced body weight in males and females. Anatomical examination revealed reduced epigonadal fat mass normalized to body weight in aged female and male IRS-1$^{-/-}$ mice. Typical mice gain abdominal fat mass during life leading to a age-associated increase of body weight. However, body weight increase during aging and age-associated gain of abdominal fat mass was significant reduced in IRS-1 deficient mice compared to wild-type controls.

First, food intake was measured. Surprisingly, food intake in IRS-1 knockout mice was increased excluding reduced energy intake as possible mechanism for the reduced age-associated fat accumulation. Furthermore, we analyzed locomotor activity. The experiments excluded elevated locomotor activity as underlying mechanism for the lean phenotype in IRS-1 knockout mice. Since elevated energy expenditure would explain the decreased gain of fat mass in aged IRS-1$^{-/-}$ mice we used indirect calorimetry. However it should be considered that smaller animals show elevated energy expenditure levels relative to their body size compared with larger animals due to a disadvantageous surface/volume ratio (Speakman, 1997). Accordingly, we measured increased energy expenditure when normalized to body weight in IRS-1$^{-/-}$ mice compared to WT mice possible contributing to the reduced fat mass during aging. It would be reasonably to normalize data generated by indirect calorimetry to lean body mass

Despite elevated food intake IRS-1$^{-/-}$ females showed increased survival (Selman et al., 2008) contradicting the theory of caloric restriction leading to increased survival in animals in these mice favoring alternative mechanisms inducing longevity (Bartke et al., 2002; Roth et al., 2002; Mattison et al., 2003; Bodkin et al., 1995). On the other hand reduced abdominal fat content due to potentially increased metabolism could be an eventual explanation for increased survival of IRS-1 deficient

mice. Mutant mice with disrupted growth hormone show combined dwarfism with extended lifespan (Carter et al., 2002). Thus, dwarfism combined with higher metabolism might be a possible mechanism for increasing lifespan in IRS-1 deficient mice (Oklejewicz and Daan, 2002; Oklejewicz et al., 1997; Lin et al., 2002).

High metabolic rates and increased food intake are linked to hyperthyroidism (Mitchell et al., 2010; Havel, 2001). Therefore, free T3 serum levels were determined in wild-type and IRS-1$^{-/-}$ mice revealing no significant alterations excluding hyperthyroidism as underlying mechanism for observed phenotype in IRS-1 deficient mice.

IRS-1$^{-/-}$ mice are described with increased maximum lifespan (Selman et al., 2008) possibly due to enhanced mitochondrial performance as underlying molecular mechanism.

4.5 Role of IRS-1 for mitochondrial performance

Recent studies have linked mitochondrial performance to insulin sensitivity and life expectancy. Since increased lifespan, insulin resistance and increased energy expenditure are denoted phenotypes of IRS-1$^{-/-}$ mice alterations in mitochondrial function would at least partially explain the phenotypes of these mice. Therefore mitochondrial performance in IRS-1$^{-/-}$ mice and IRS1 deficient MEFs was analyzed in detail. In the present study protein expression for each complex of the respiratory chain was determined separately. Furthermore, function of the different complexes was investigated using state of the art technologies.

Mitochondrial mass and expression of respiratory chain complexes

Mitochondrial dysfunction or decreased mitochondrial content as possible cause for insulin resistance is postulated and described by several groups (Lowell and Shulman 2005; Szendroedi et al., 2009). Therefore we investigated abundance of HSP-60 as indicator of mitochondrial mass (Fig. 3.19, 3.20, 3.21). HSP-60 protein levels detected by Western blots were unchanged in WT and IRS-1$^{-/-}$ MEFs, muscles and liver, excluding a decrease or compensatory increment of mitochondrial content in IRS-1$^{-/-}$ mice. Additionally PGC-1α expression levels, as marker for mitochondrial biogenesis (Wu et al., 1999; Liang and Ward, 2006; Ventura-Clapier et al., 2008), were analyzed (Fig. 3.22). Western blot revealed no alteration in PGC-1α expression

levels in IRS-1 knockout cells and tissues compared to wild-type mice confirming HSP-60 data. Thus mitochondrial mass is unaltered in IRS-$1^{-/-}$ mice.

In order to exclude changes in concentrations of respiratory chain due to IRS-1 deficiency, abundance of the individual complexes were determined. Interestingly, a slight decrease in muscle complex II and an increased MEF complex V expression was observed. Since PGC-1α is one of the master regulators for mitochondria biogenesis, nuclear extracts derived from knockout and wild-type muscle samples were checked upon PGC-1α acetylation. Enhanced acetylation would indicate an elevated fraction of non-active PGC-1α proteins not functioning as co-activators for transcription factors required for mitochondrial biogenesis. Immunoprecipitation revealed enhanced acetylation of PGC-1α proteins in IRS-$1^{-/-}$ derived samples (Fig. 3.23). Additionally SIRT-1, NAD^+ dependent deacetylase was downregulated in IRS-1 deficient animals probably explaining increased PGC-1α acetylation. Taken together these data indicate less active nuclear PGC-1α in knockout muscle.

Decreased mitochondrial biogenesis caused by PGC-1α acetylation might be counteracted by lowered autophagy in IRS-$1^{-/-}$ animals resulting in decreased mitochondrial regeneration but unchanged mitochondrial content. Lowered autophagy and reduced mitochondrial biogenesis would result in accumulation of defective mitochondria leading to enhanced mitochondrial dysfunction (Takeda et al., 2010; Suzuki et al., 2011). Photopectrometric analysis of mitochondrial respiratory chain complexes (Fig. 3.24; Fig. 3.26; Fig. 3.29; Fig. 3.31; Fig. 3.35; Fig. 3.37), determination of oxygen consumption of respiratory chain complexes by polarography (Fig. 3.38) and OROBORS technique (Fig. 3.33) revealed no obvious and consistent dysfunction in mitochondria in IRS-$1^{-/-}$ mice suggesting that the observed changes in PGC-1α acetylation might be of minor functional relevance.

Mitochondrial performance in vitro

Severe mitochondrial dysfunction would be accompanied by elevated ROS levels leading to induction of scavengers like MnSOD as physiological response (Mitchell et al., 1996). No increased MnSOD expression was found in MEFs, muscle and liver of IRS-1 knockout mice (Fig. 3.27; Fig. 3.32; Fig. 3.39).

Activity determination of respiratory chain and TCA enzymes by photospectrometric analysis of MEFs and MEF derived mitochondria showed a tendency towards decreased respiratory capacities in IRS-1 deficient MEFs and IRS-

$1^{-/-}$ derived mitochondria. However effect were less prominent in isolated MEF mitochondria (Fig. 3.24) but reaching significance in CS normalized activity for complex II and combined determination of complex II and III indicating possibly complex II dysfunction, at least under V_{max} conditions. Impaired coenzyme Q_{10} could be a potential factor limiting complex II and complex III turnover rates. GPCCR activity determination in MEF lysates (Fig. 3.25) might support impaired coenzyme Q_{10} being the underlying mechanism for complex II and complex III activity reductions. GPCCR activity and additionally coenzyme Q_{10} dependent complex I activity in IRS-$1^{-/-}$ MEF mitochondria were unaltered to wild-types, hence contradicting coenzyme Q_{10} impairment. Moreover, the reduced complex II activity could not be confirmed by respiratory chain activity analysis of isolated MEF mitochondria (Fig. 3.24). A trend to reduced complex IV activity (Fig. 3.26) was observed in IRS-$1^{-/-}$ but this trend could not be determined in isolated IRS-$1^{-/-}$ mitochondria.

Overall spectrometric measurements in MEF and isolated mitochondria of MEFs showed a tendency towards a slightly decreased mitochondrial capacity in the IRS-$1^{-/-}$ background; however, not leading to increased ROS or decreased ATP content (Fig. 3.50), excluding severely impaired mitochondrial function due to IRS-1 deficiency.

Mitochondrial performance in vivo

MEFs represent an *in vitro* system not addressing possible compensatory or endocrine/metabolic effects of *in vivo* systems. Therefore respiratory chain enzymes were analyzed in slow–oxidative red muscle (M. soleus), fast-glycolytic white muscle (M. gastrocnemius) (McAllister et al., 2008) as well as in livers of wild-type and IRS-1 knockout mice. Results normalized to mitochondrial mass did not show any significant alteration in female IRS-1 knockout mice compared to wild-type controls for both muscle types (Fig. 3.29). Detected tendency in MEFs towards slight decreased respiratory function in IRS-$1^{-/-}$ background was not confirmed. Rather the opposite was observed in female mice, less prominent in muscle but significant in liver samples of IRS-1 deficient mice compared to wild-type controls (Fig. 3.35). Activities of complex IV and TCA cycle enzymes IDH, aconitase and fumerase were considerably increased in livers of IRS-$1^{-/-}$ mice although insulin resistance is normally accompanied by reduced TCA cycle flux (Befroy et al., 2007; Schrauwen

and Hesselink, 2008) suggesting molecular compensation of IRS-1 deficiency in liver (Fig. 3.7). Elevated TCA cycle enzyme activities provide NADH for complex I in the case of IDH. Consistently, slight increase of mitochondrial activity of complex I, complex III and notably for complex IV was detected in liver.

Normalized respiratory chain enzymes activities displayed unaltered or slightly increased activities for in IRS-1 deficient males reaching significance for complex III in red muscles and for combined determination of complex I and III in white muscles (Fig. 3.31). However, IDH in red and fumerase in red and white muscles were decreased. Complex IV activity in liver of male knockout mice was clearly increased (Fig. 3.37). Turnover rate of complex V was significantly downregulated in red muscles of IRS-$1^{-/-}$ male mice. Complex V activity reduction was also detected in liver of IRS-1 deficient males. Thus, data might indicate an uncoupling of respiratory chain from ATP synthesis in IRS-1 knockout males causing reduced complex V activities.

Oxygen flux determined by high resolution respirometry in saponin skinned fibers of musculus soleus dissected from male mice, revealed no alterations in respiratory chain activities of IRS-1 knockout mice compared to wild-type controls. Hence, slightly increased mitochondrial performances detected by photospectrometric analysis under V_{max} conditions were not supported by OROBORS determination. Overall no mitochondrial respiratory chain dysfunction was detected neither in muscles nor livers of IRS-1 knockout males by different methods. Apparently mild insulin resistance of IRS-1 deficient mice is not linked to impaired mitochondrial function in the *in vivo* situation.

Furthermore, analyzed MnSOD levels (Fig. 3.27; Fig. 3.32; Fig. 3.39) underline functional performance of complex I and complex III, since MnSOD expression patterns of IRS-$1^{-/-}$ were unaltered in comparison to wild-type mice. Elevated MnSOD levels would have indicated enhanced ROS generation by complex I and complex III due to respiratory dysfunction (Chen et al., 2003; Raha et al., 2000; Arai et al., 1999; Radi et al., 1991).

RT-PCR analysis revealed upregulated levels of UCP-3 in muscles of IRS-1 knockout mice (Fig. 3.42) confirmed by Western blot analysis (Fig. 3.43). These data support the idea of enhanced uncoupling being the underlying mechanism of elevated energy expenditure and increased food intake in IRS-$1^{-/-}$ mice. However, high resolution respirometry indicated functional coupling of respiratory chain complexes in muscle mitochondrial. To definitely address increased uncoupling due

to IRS-1 deficiency we investigated proton leakage of isolated liver mitochondria revealing uncoupling in IRS-1 knockout. Elevated oxygen consumption for creating distinct membrane potential was supported by elevated UCP-2 mRNA expression levels in livers of IRS-1 deficient mice (Fig. 3.44)

In addition, UCP-1 protein expression was detected in WAT of IRS-1$^{-/-}$ mice. Western blots supported by UCP-1 mRNA expression levels (Fig. 3.45; Fig. 3.46) indicating contribution of WAT to uncoupling and hence to observed hyperphagic, high energy turnover phenotype in IRS-1 knockout mice. Moreover PGC-1α mRNA expression was significantly elevated in WAT of IRS-1 deficient mice (Fig. 3.47) indicating enhanced mitochondrial biogenesis in WAT compared to wild-type controls. Increased PGC-1α levels causing mitochondrial biogenesis leading to high abundance of mitochondria have been linked to fat loss in adipocytes as observed in IRS-1 knockout mice (Fig. 3.14) (Lee et al., 2007).

High abundance of mitochondria in WAT is often linked to transdifferentiation of white adipocytes into brown adipocytes. Furthermore, brown adipocyte clusters in WAT are believed to regulate energy balance (Kozak et al., 2008). However, other research groups described morphology of mitochondria in WAT and mitochondria detected in BAT distinctly different suggesting white adipocytes with certain characteristics of BAT (Deveaud et al., 2004) but not a real “transdifferentiation”. (Arribas et al., 2003; Fasshauer et al. 2001; Miki et al., 2001, Tseng et al., 2004, Valverde et al., 2003). The functional relevance of increased mitochondrial biogenesis indicated by PGC-1α and enhanced UCP-1 expression on energy homeostasis in IRS-1 deficient mice remains unclear. Abdominal fat mass is significantly reduced in these mice (Fig. 3.12) and elevated mitochondrial density is eventually due to restricted dimension of abdominal fat in knockouts and total mitochondrial number in might be unchanged in comparison with wild-type controls. UCP-1 and PGC-1α mRNA expression in BAT of IRS-1$^{-/-}$ mice were unaltered compared to wild-type controls or slightly decreased excluding elevated thermogenesis in BAT contributing to higher energy expenditure of IRS-1 knockout mice.

Leptin action on mitochondrial is controversially discussed (Gomez-Ambrosi et al., 2001). Induction of PGC-1α expression by leptin is only detected after long-term treatment (Gomez-Ambrosi et al., 2001; Scarpace et al., 1997; Frühbeck et al., 1998). Since leptin levels are slightly lower in IRS-1 deficient mice (Fig. 3.60), leptin

action is unlikely affecting PGC-1α expression and adaptive thermogenesis in these mice.

4.6 Regulation of energy homeostasis in IRS-1 deficient mice

Significant correlation between body fat content and plasma leptin concentration is described in literature (Frederich et al., 1995; Maffei et al., 1995). As a result of decreased abdominal fat mass (Fig. 3.12; Fig. 3.13) leptin serum concentrations were slightly decreased in IRS-1 deficient mice (Fig. 3.60). However serum reduction of leptin was not as striking as expected relative to decreased abdominal fat mass. Fig. 3.56 and Fig. 3.57 indicate a potential fat redistribution in IRS-1 knockout mice resulting in an unaltered overall fat content in wild-type and knockout mice. Leptin resistance as underlying mechanism for orectic phenotyp of IRS-1 knockout mice is unlikely since leptin receptor expression in the hypothalamus was unchanged in IRS-1 deficient mice compared with wild-type controls (Fig. 3.60).

Even slightly reduced leptin serum levels in IRS-$1^{-/-}$ might impact on POMC/CART and AgRP/NPY expressing neurons in the melanocortin system. mRNA expression levels of orectic neuropeptides *AgRP/NPY* were significantly increased (Fig. 3.61) in comparison to wild-type controls indicating diminished anorectic effect of leptin. Unexpectedly mRNA levels of anorectic hypothalamic neuropeptides *POMC/CART* were slightly increased as well (Fig. 3.61), although POMC neurons should be inhibited by GABAergic projections of NPY/AgRP neurons (Cone et al., 2011).

Insulin causes anorectic effects in brain, acting agonistic to leptin (Air et al., 2002; Benoit et al., 2004; Bondareva and Chistyakova, 2007; Schwartz et al., 1991; Spanswick et al., 2000; Niswender et al., 2004). Increased insulin levels (Fig. 3.10) due to insulin resistance in IRS-$1^{-/-}$ mice did not compensate for anorectic insulin function in hypothalamus although insulin receptor expression was not down regulated in IRS-1 deficient mice (Fig. 3.62). However, IRS-1 knockout should have a minor effect on metabolic function regulated via the CNS since IRS-1 is not expressed in the ventral hypothalamus. On the other hand IRS-2 was found in the arcurate nuclei (ARC) of the hypothalamus in high concentrations indicating a central role of IRS-2 in energy homeostasis triggered by insulin. This is supported by IRS-2 knockout in hypothalamic neurons resulting in general hypothalamic dysfunction (Lin et al., 2004; Bondareva and Chistyakova, 2007; Baskin et al., 1993; Kubota et al.,

2004). No alteration in IRS-2 expression in the hypothalamus was observed in IRS-1 knockout in comparison to control mice (Fig. 3.62), hence IRS-2 signaling deficiency is unlikely to negatively influence anorectic insulin effects in brain of IRS-1$^{-/-}$ mice. Additionally IRS-4 expression was elevated (Fig. 3.62) eventually causing improved insulin signaling in hypothalamus of IRS-1 deficient mice.

Therefore increased orectic effects observed in IRS-1$^{-/-}$ mice might be based on reduced intracellular leptin signaling in the presence of unaltered leptin receptor levels. AgRP expressing neurons are not inactivated and *AgRP* expression was not inhibited by leptin. Reduced leptin receptor or insulin receptor levels in the hypothalamus leading to attenuated anorectic effects are not contributing to hyperphagic phenotype of IRS-1 deficient mice since both receptor expression levels remained unchanged compared with wild-type controls. Thus, role of IRS-1 deficiency on neuropeptide regulation and leptin signaling needs further investigation.

4.7 Elevated ATP levels in IRS-1$^{-/-}$ MEFs

Besides respiratory chain other cellular processes can provide ATP and function as alternative ATP sources besides mitochondrial respiration. ATP content of IRS-1 deficient MEF was significantly increased compared to wild-types (Fig. 3.50). However, no enhanced activity of respiratory chain enzymes, even slightly reduced complex V activity was detected in MEFs or MEF isolated mitochondria of knockout mice (Fig. 3.24; Fig 3.26). One possible option explaining elevated ATP levels is increased glucose utilization via alternative pathways as the TCA cycle e.g. lactate production via lactate dehydrogenase. Nevertheless, lactate dehydrogenase (LDH) acitivity determination (Fig. 3.51) revealed no upregulation in IRS-1$^{-/-}$ MEFs. Due to potential uncoupling in muscle (Fig. 3.42; Fig. 3.43) and liver (Fig. 3.41; Fig. 3.44) of IRS-1 knockout males LDH activity increment could compensate for ATP attenuation caused by proton leakage. LDH activity was slightly elevated in M. soleus and elevated in M. gastrocnemius (Fig. 3.53) however unchanged in liver of IRS-1 deficient males (Fig. 3.55). Since only 2 molecules ATP are generated by lactic acid fermentation potential ATP depletion can not be compensated by increased LDH activities detected in soleus and gastrocnemius muscle of IRS-1 deficient males. Female IRS-1 knockout mice showed increased LDH activity in M. gastrocnemius (Fig. 3.52) and significantly enhanced LDH activity in liver (Fig. 3.54). Additionally

activities of TCA cycle enzymes in female knockout were significantly increased in liver (Fig. 3.35). Elevated LDH activity observed in liver of IRS-1 deficient females might suggest processing of lactate in gluconeogenesis (Kaloyianni and Freedland, 1990). Furthermore, insulin resistance of IRS-1 knockout mice might provoke enhanced activation of gluconeogenesis in liver. Gluconeogenesis is an energy consuming process; consequently fatty acid oxidation could provide energy for gluconeogenesis. However CPT-1 activity of isolated liver mitochondria of male IRS-$1^{-/-}$ was rather decreased (Fig. 3.59).

Increased activity of TCA cycle enzymes IDH and fumerase in liver of female knockouts might be indirect indicators for enhanced gluconeogenesis. NADH demand might be provided by IDH. Additionally fumerase reaction product oxaloacetate represents an intermediate of gluconeogenesis. Enhanced gluconeogenesis in IRS-$1^{-/-}$ mice indicated by increased PAS staining suggesting elevated glycogen storage probably explaining increased liver/body weight quotient in knockout mice as shown by previous work (Dong et al., 2006).

5 Summary

5. Summary

Insulin and insulin-like growth factor-1 receptor signaling plays a crucial role in regulation of growth, lifespan and energy homeostasis. Insulin receptor substrates (IRS) mediate intracellular effects of the insulin and insulin-like growth factor-1 receptor. IRS-1 deficient mice (IRS-$1^{-/-}$) display dwarfism, increased food intake, elevated energy expenditure and reduced accumulation of epigonadal fat compared to wild-type littermates. To investigate the molecular basis of increased energy expenditure activity of respiratory chain complexes were determined. Mitochondrial performance was analyzed in liver, musculus soleus, musculus gastrocnemius, embryonic fibroblast (MEF) of wild-type and IRS-1 knockout mice as well as mitochondria isolated from MEFs using different techniques. The molecular mechanism of elevated food intake of IRS-1 deficient mice was addressed by Real-time PCR analysis of hypothalamic neuropeptides. Determination of mitochondrial respiratory chain complex activities revealed no significant and consistent alteration in mitochondrial performance in muscle and liver of IRS-1 knockout mice compared to wild-type controls. Additionally no mitochondrial dysfunction was detected on the cellular level analyzing MEFs and isolated mitochondria. However, complex V activities in liver and musculus soleus IRS-$1^{-/-}$ males were significantly decreased. Additionally female knockout mice showed decreased performance of complex V in musculus soleus. Determination of mitochondrial respiratory chain coupling using proton motive force measurements revealed enhanced uncoupling in the IRS-$1^{-/-}$ mice. This was supported by Real-time PCR analysis of uncoupling protein expression in different tissues. Furthermore elevated food intake in the IRS-1 deficient mice was linked to enhanced expression of orectic neuropeptides in hypothalamus in these mice. Taken together the results of present study indicate enhanced uncoupling in IRS-1 deficient mice as underlying mechanism for increased energy expenditure. Elevated food intake of IRS-1 knockout mice might be a consequence of increased energy expenditure leading to enhanced expression of orectic neuropetides NPY/AgRP providing adequate supply of metabolic fuel (e.g. glucose) in knockout mice in response to higher energy demand.

6 Zusammenfassung

6. Zusammenfassung

Bei der Regulation der Energiehomöostase kommt der Insulin-/Insulin-like growth factor-1 Signaltransduktion eine bedeutende Rolle zu. Die Insulinrezeptor-Substrate (IRS) vermitteln die intrazellulären Effekte des Insulin- und Insulin-like growth factor-1 Rezeptors. IRS-1 defiziente Mäuse (IRS-$1^{-/-}$) zeigen im Vergleich zu Wildtypgeschwistern neben einer milden Insulinresistenz einen Minderwuchs sowie eine vermehrte Futteraufnahme und eine reduzierte abdominale Fettakkumulation bei gesteigertem Energieumsatz. Die molekulare Grundlage dieses gesteigerten Energieumsatzes ist unklar. Eine mögliche Ursache hierfür könnte eine erhöhte Aktivität der mitochondrialen Atmungskette sein. Zur Untersuchung der mitochondrialen Atmungskettenfunktion wurden Leber und Muskel (musculus soleus, musculus gastrocnemius) Homogenate, embryonale Fibroblasten und extrahierte Mitochondrien embryonaler Fibroblasten von IRS-$1^{-/-}$ Mäusen und Wildtypgeschwistern bezüglich der Aktivität der einzelnen Komplexe der Atmungskette analysiert. Mögliche molekulare Mechanismen der erhöhten Futteraufnahme in IRS-1 defizienten Tieren wurden mit Hilfe von Expressionsanalysen der hypothalamischer Neuropeptide untersucht. IRS-$1^{-/-}$ Mäuse zeigten keine einheitlichen signifikanten Veränderungen der mitochondrialen Atmungskettenfunktion in Muskel und Leber verglichen mit Wildtyp-Kontrollen. Auch auf zellulärer Ebene konnten keine Aktivitätsveränderungen der Atmungskette zwischen den verschiedenen Genotypen detektiert werden. Komplex V Aktivität in Leber und musculus soleus in IRS-1 defizienten Männchen war signifikant verringert. Proton motive force Analysen zeigten ein erhöhtes mitochondriales Uncoupling in IRS-1 Knockout Männchen. Real-time PCR Analysen der Expression mitochondrialer Uncoupling Proteinen unterstützten dieses Ergebnis. Die erhöhte Nahrungsaufnahme IRS-1 defizienter Tiere ist mit einer verstärkten Expression orektischer hypothalamischer Neuropeptide in IRS-$1^{-/-}$ Mäusen assoziiert.
Zusammenfassend zeigen die Ergebnisse ein verstärktes mitochondriales Uncoupling in IRS-1 defizienten Mäusen als zugrunde liegenden Mechanismus des erhöhten Energieumsatzes. Die vermehrte Futteraufnahme der IRS-1 Knockout Mäuse könnte eine direkte Konsequenz der erhöhten metabolischen Rate sein, die

zu einer verstärkten Expression der orektischen Neuropetide NPY/AgRP führt, um ausreichend Energie bereitzustellen, den erhöhten energetischen Bedarf in diesen Tieren zu kompensieren.

7 References

7. References

Abdul-Ghani, M. A. and R. A. DeFronzo (2008). "Mitochondrial dysfunction, insulin resistance, and type 2 diabetes mellitus." Curr Diab Rep **8**(3): 173-178.

Adams, T. E., V. C. Epa, et al. (2000). "Structure and function of the type 1 insulin-like growth factor receptor." Cell Mol Life Sci **57**(7): 1050-1093.

Air, E. L., S. C. Benoit, et al. (2002). "Insulin and leptin combine additively to reduce food intake and body weight in rats." Endocrinology **143**(6): 2449-2452.

Alessi, D. R. and P. Cohen (1998). "Mechanism of activation and function of protein kinase B." Curr Opin Genet Dev **8**(1): 55-62.

Al-Hasani, H., B. Eisermann, et al. (1997). "Identification of Ser-1275 and Ser-1309 as autophosphorylation sites of the insulin receptor." FEBS Lett **400**(1): 65-70.

Anderson, D., C. A. Koch, et al. (1990). "Binding of SH2 domains of phospholipase C gamma 1, GAP, and Src to activated growth factor receptors." Science **250**(4983): 979-982.

Anderson, E. J. and P. D. Neufer (2006). "Type II skeletal myofibers possess unique properties that potentiate mitochondrial H(2)O(2) generation." Am J Physiol Cell Physiol **290**(3): C844-851.

Andersson, S. G., A. Zomorodipour, et al. (1998). "The genome sequence of Rickettsia prowazekii and the origin of mitochondria." Nature **396**(6707): 133-140.

Andrews, Z. B., Z. W. Liu, et al. (2008). "UCP2 mediates ghrelin's action on NPY/AgRP neurons by lowering free radicals." Nature **454**(7206): 846-851.

Ankel, E., C. C. Felix, et al. (1986). "The use of spin label oximetry in the study of photodynamic inactivation of Chinese hamster ovary cells." Photochem Photobiol **44**(6): 741-746.

Arai, M., H. Imai, et al. (1999). "Mitochondrial phospholipid hydroperoxide glutathione peroxidase plays a major role in preventing oxidative injury to cells." J Biol Chem **274**(8): 4924-4933.

Araki, E., M. A. Lipes, et al. (1994). "Alternative pathway of insulin signalling in mice with targeted disruption of the IRS-1 gene." Nature **372**(6502): 186-190.

Arribas, M., A. M. Valverde, et al. (2003). "Role of IRS-3 in the insulin signaling of IRS-1-deficient brown adipocytes." J Biol Chem **278**(46): 45189-45199.

Aspinwall, C. A., W. J. Qian, et al. (2000). "Roles of insulin receptor substrate-1, phosphatidylinositol 3-kinase, and release of intracellular Ca2+ stores in insulin-stimulated insulin secretion in beta -cells." J Biol Chem **275**(29): 22331-22338.

Backer, J. M., M. G. Myers, Jr., et al. (1992). "Phosphatidylinositol 3'-kinase is activated by association with IRS-1 during insulin stimulation." EMBO J **11**(9): 3469-3479.

Bajaj, M., S. Suraamornkul, et al. (2005). "Effect of a sustained reduction in plasma free fatty acid concentration on intramuscular long-chain fatty Acyl-CoAs and insulin action in type 2 diabetic patients." Diabetes **54**(11): 3148-3153.

Balthasar, N., L. T. Dalgaard, et al. (2005). "Divergence of melanocortin pathways in the control of food intake and energy expenditure." Cell **123**(3): 493-505.

Barber, D. F., M. Alvarado-Kristensson, et al. (2006). "PTEN regulation, a novel function for the p85 subunit of phosphoinositide 3-kinase." Sci STKE **2006**(362): pe49.

Barthel, A., D. Schmoll, et al. (2005). "FoxO proteins in insulin action and metabolism." Trends Endocrinol Metab **16**(4): 183-189.

Bartke, A., J. C. Wright, et al. (2002). "Dietary restriction and life-span." Science **296**(5576): 2141-2142; author reply 2141-2142.

Baskin, D. G., A. J. Sipols, et al. (1993). "Immunocytochemical detection of insulin receptor substrate-1 (IRS-1) in rat brain: colocalization with phosphotyrosine." Regul Pept **48**(1-2): 257-266.

Bates, S. H., W. H. Stearns, et al. (2003). "STAT3 signalling is required for leptin regulation of energy balance but not reproduction." Nature **421**(6925): 856-859.

Befroy, D. E., K. F. Petersen, et al. (2007). "Impaired mitochondrial substrate oxidation in muscle of insulin-resistant offspring of type 2 diabetic patients." Diabetes **56**(5): 1376-1381.

Belgardt, B. F., T. Okamura, et al. (2009). "Hormone and glucose signalling in POMC and AgRP neurons." J Physiol **587**(Pt 22): 5305-5314.

Benoit, S., M. Schwartz, et al. (2000). "CNS melanocortin system involvement in the regulation of food intake." Horm Behav **37**(4): 299-305.

Benoit, S. C., D. J. Clegg, et al. (2004). "Insulin and leptin as adiposity signals." Recent Prog Horm Res **59**: 267-285.

Bereiter-Hahn, J. and M. Voth (1994). "Dynamics of mitochondria in living cells: shape changes, dislocations, fusion, and fission of mitochondria." Microsc Res Tech **27**(3): 198-219.

Bernardi, P. (1999). "Mitochondrial transport of cations: channels, exchangers, and permeability transition." Physiol Rev **79**(4): 1127-1155.

Bhaskar, P. T. and N. Hay (2007). "The two TORCs and Akt." Dev Cell **12**(4): 487-502.

Bianchi, K., A. Rimessi, et al. (2004). "Calcium and mitochondria: mechanisms and functions of a troubled relationship." Biochim Biophys Acta **1742**(1-3): 119-131.

Biebermann, H., T. R. Castaneda, et al. (2006). "A role for beta-melanocyte-stimulating hormone in human body-weight regulation." Cell Metab **3**(2): 141-146.

Bindokas, V. P., A. Kuznetsov, et al. (2003). "Visualizing superoxide production in normal and diabetic rat islets of Langerhans." J Biol Chem **278**(11): 9796-9801.

Bleazard, W., J. M. McCaffery, et al. (1999). "The dynamin-related GTPase Dnm1 regulates mitochondrial fission in yeast." Nat Cell Biol **1**(5): 298-304.

Boden, G. and G. I. Shulman (2002). "Free fatty acids in obesity and type 2 diabetes: defining their role in the development of insulin resistance and beta-cell dysfunction." Eur J Clin Invest **32 Suppl 3**: 14-23.

Bodkin, N. L., H. K. Ortmeyer, et al. (1995). "Long-term dietary restriction in older-aged rhesus monkeys: effects on insulin resistance." J Gerontol A Biol Sci Med Sci **50**(3): B142-147.

Brand, M. D. (1990). "The proton leak across the mitochondrial inner membrane." Biochim Biophys Acta **1018**(2-3): 128-133.

Brand, M. D., J. L. Pakay, et al. (2005). "The basal proton conductance of mitochondria depends on adenine nucleotide translocase content." Biochem J **392**(Pt 2): 353-362.

Brands, M., J. Hoeks, et al. (2011). "Short-term increase of plasma free fatty acids does not interfere with intrinsic mitochondrial function in healthy young men." Metabolism.

Bredel-Geissler, A., U. Karbach, et al. (1992). "Proliferation-associated oxygen consumption and morphology of tumor cells in monolayer and spheroid culture." J Cell Physiol **153**(1): 44-52.

Brehm, A., M. Krssak, et al. (2006). "Increased lipid availability impairs insulin-stimulated ATP synthesis in human skeletal muscle." Diabetes **55**(1): 136-140.

Bremer, J., G. Woldegiorgis, et al. (1985). "Carnitine palmitoyltransferase. Activation by palmitoyl-CoA and inactivation by malonyl-CoA." Biochim Biophys Acta **833**(1): 9-16.

Bruning, J. C., D. Gautam, et al. (2000). "Role of brain insulin receptor in control of body weight and reproduction." Science **289**(5487): 2122-2125.

Bruning, J. C., M. D. Michael, et al. (1998). "A muscle-specific insulin receptor knockout exhibits features of the metabolic syndrome of NIDDM without altering glucose tolerance." Mol Cell **2**(5): 559-569.

Bruning, J. C., J. Winnay, et al. (1997). "Development of a novel polygenic model of NIDDM in mice heterozygous for IR and IRS-1 null alleles." Cell **88**(4): 561-572.

Bruning, J. C., J. Winnay, et al. (1997). "Differential signaling by insulin receptor substrate 1 (IRS-1) and IRS-2 in IRS-1-deficient cells." Molecular and Cellular Biology **17**(3): 1513-1521.

Burger, G., M. W. Gray, et al. (2003). "Mitochondrial genomes: anything goes." Trends in Genetics **19**(12): 709-716.

Burgering, B. M. and P. J. Coffer (1995). "Protein kinase B (c-Akt) in phosphatidylinositol-3-OH kinase signal transduction." Nature **376**(6541): 599-602.

Burks, D. J., J. Font de Mora, et al. (2000). "IRS-2 pathways integrate female reproduction and energy homeostasis." Nature **407**(6802): 377-382.

Burks, D. J. and M. F. White (2001). "IRS proteins and beta-cell function." Diabetes **50 Suppl 1**: S140-145.

Butler, A. E., J. Janson, et al. (2003). "Beta-cell deficit and increased beta-cell apoptosis in humans with type 2 diabetes." Diabetes **52**(1): 102-110.

Butler, A. E., J. Janson, et al. (2003). "Increased beta-cell apoptosis prevents adaptive increase in beta-cell mass in mouse model of type 2 diabetes: evidence for role of islet amyloid formation rather than direct action of amyloid." Diabetes **52**(9): 2304-2314.

Cadenas, S., K. S. Echtay, et al. (2002). "The basal proton conductance of skeletal muscle mitochondria from transgenic mice overexpressing or lacking uncoupling protein-3." J Biol Chem **277**(4): 2773-2778.

Calabrese, V., R. Lodi, et al. (2005). "Oxidative stress, mitochondrial dysfunction and cellular stress response in Friedreich's ataxia." J Neurol Sci **233**(1-2): 145-162.

Camara, Y., T. Mampel, et al. (2009). "UCP3 expression in liver modulates gene expression and oxidative metabolism in response to fatty acids, and sensitizes mitochondria to permeability transition." Cell Physiol Biochem **24**(3-4): 243-252.

Carter, C. S., M. M. Ramsey, et al. (2002). "Models of growth hormone and IGF-1 deficiency: applications to studies of aging processes and life-span determination." J Gerontol A Biol Sci Med Sci **57**(5): B177-188.

Carter, C. S., M. M. Ramsey, et al. (2002). "A critical analysis of the role of growth hormone and IGF-1 in aging and lifespan." Trends in Genetics **18**(6): 295-301.

Chagpar, R. B., P. H. Links, et al. (2010). "Direct positive regulation of PTEN by the p85 subunit of phosphatidylinositol 3-kinase." Proc Natl Acad Sci U S A **107**(12): 5471-5476.

Chan, C. B., D. De Leo, et al. (2001). "Increased uncoupling protein-2 levels in beta-cells are associated with impaired glucose-stimulated insulin secretion: mechanism of action." Diabetes **50**(6): 1302-1310.

Chan, D. C. (2006). "Mitochondrial fusion and fission in mammals." Annu Rev Cell Dev Biol **22**: 79-99.

Chen, Q., E. J. Vazquez, et al. (2003). "Production of reactive oxygen species by mitochondria: central role of complex III." J Biol Chem **278**(38): 36027-36031.

Chen, X. J. and R. A. Butow (2005). "The organization and inheritance of the mitochondrial genome." Nat Rev Genet **6**(11): 815-825.

Chomczynski, P. and N. Sacchi (1987). "Single-step method of RNA isolation by acid guanidinium thiocyanate-phenol-chloroform extraction." Anal Biochem **162**(1): 156-159.

Chretien, D., P. Rustin, et al. (1994). "Reference charts for respiratory chain activities in human tissues." Clin Chim Acta **228**(1): 53-70.

Chuang, L. M., S. F. Hausdorff, et al. (1994). "Interactive roles of Ras, insulin receptor substrate-1, and proteins with Src homology-2 domains in insulin signaling in Xenopus oocytes." J Biol Chem **269**(44): 27645-27649.

Cone, R. D. (2005). "Anatomy and regulation of the central melanocortin system." Nat Neurosci **8**(5): 571-578.

Cone, R. D., M. A. Cowley, et al. (2001). "The arcuate nucleus as a conduit for diverse signals relevant to energy homeostasis." Int J Obes Relat Metab Disord **25 Suppl 5**: S63-67.

Cone, R. D. and R. B. Simerly (2011). "Leptin grows up and gets a neural network." Neuron **71**(1): 4-6.

Considine, R. V., M. K. Sinha, et al. (1996). "Serum immunoreactive-leptin concentrations in normal-weight and obese humans." N Engl J Med **334**(5): 292-295.

Cross, D. A., D. R. Alessi, et al. (1995). "Inhibition of glycogen synthase kinase-3 by insulin mediated by protein kinase B." Nature **378**(6559): 785-789.

Danial, N. N. and S. J. Korsmeyer (2004). "Cell death: critical control points." Cell **116**(2): 205-219.

Davis, R. J. (1993). "The mitogen-activated protein kinase signal transduction pathway." J Biol Chem **268**(20): 14553-14556.

De Meyts, P., B. Urso, et al. (1995). "Mechanism of insulin and IGF-I receptor activation and signal transduction specificity. Receptor dimer cross-linking, bell-shaped curves, and sustained versus transient signaling." Ann N Y Acad Sci **766**: 388-401.

de Vries, Y., D. N. Arvidson, et al. (1997). "Functional characterization of mitochondrial carnitine palmitoyltransferases I and II expressed in the yeast Pichia pastoris." Biochemistry **36**(17): 5285-5292.

Dent, P., A. Lavoinne, et al. (1990). "The molecular mechanism by which insulin stimulates glycogen synthesis in mammalian skeletal muscle." Nature **348**(6299): 302-308.

Deveaud, C., B. Beauvoit, et al. (2004). "Regional differences in oxidative capacity of rat white adipose tissue are linked to the mitochondrial content of mature adipocytes." Mol Cell Biochem **267**(1-2): 157-166.

Diaz-Meco, M. T., J. Lozano, et al. (1994). "Evidence for the in vitro and in vivo interaction of Ras with protein kinase C zeta." J Biol Chem **269**(50): 31706-31710.

Dong, X., S. Park, et al. (2006). "Irs1 and Irs2 signaling is essential for hepatic glucose homeostasis and systemic growth." J Clin Invest **116**(1): 101-114.

Dresner, A., D. Laurent, et al. (1999). "Effects of free fatty acids on glucose transport and IRS-1-associated phosphatidylinositol 3-kinase activity." J Clin Invest **103**(2): 253-259.

D'Souza, S. M. and I. R. Brown (1998). "Constitutive expression of heat shock proteins Hsp90, Hsc70, Hsp70 and Hsp60 in neural and non-neural tissues of the rat during postnatal development." Cell Stress Chaperones **3**(3): 188-199.

Du, K., S. Herzig, et al. (2003). "TRB3: a tribbles homolog that inhibits Akt/PKB activation by insulin in liver." Science **300**(5625): 1574-1577.

Dufour, E. and N. G. Larsson (2004). "Understanding aging: revealing order out of chaos." Biochim Biophys Acta **1658**(1-2): 122-132.

Dugani, C. B. and A. Klip (2005). "Glucose transporter 4: cycling, compartments and controversies." EMBO Rep **6**(12): 1137-1142.

Echtay, K. S., T. C. Esteves, et al. (2003). "A signalling role for 4-hydroxy-2-nonenal in regulation of mitochondrial uncoupling." EMBO J **22**(16): 4103-4110.

Echtay, K. S., M. P. Murphy, et al. (2002). "Superoxide activates mitochondrial uncoupling protein 2 from the matrix side. Studies using targeted antioxidants." J Biol Chem **277**(49): 47129-47135.

Echtay, K. S., D. Roussel, et al. (2002). "Superoxide activates mitochondrial uncoupling proteins." Nature **415**(6867): 96-99.

Eichler, W. and B. Schertel (1988). "Dihydroorotate induces Ca2+ release from rat liver mitochondria: a contribution to the mechanism of alloxan-induced Ca2+ release." Biol Chem Hoppe Seyler **369**(12): 1287-1293.

Emkey, R. (2001). "Molecular aspects of insulin signaling " Handbook of Physiology.

Eto, K., N. Takahashi, et al. (1999). "Ca(2+)/Calmodulin-dependent protein kinase cascade in Caenorhabditis elegans. Implication in transcriptional activation." J Biol Chem **274**(32): 22556-22562.

Fantl, W. J., D. E. Johnson, et al. (1993). "Signalling by receptor tyrosine kinases." Annu Rev Biochem **62**: 453-481.

Fasshauer, M., J. Klein, et al. (2001). "Essential role of insulin receptor substrate 1 in differentiation of brown adipocytes." Molecular and Cellular Biology **21**(1): 319-329.

Feige, J. N. and J. Auwerx (2007). "Transcriptional coregulators in the control of energy homeostasis." Trends Cell Biol **17**(6): 292-301.

Fernandez, A. M., J. K. Kim, et al. (2001). "Functional inactivation of the IGF-I and insulin receptors in skeletal muscle causes type 2 diabetes." Genes Dev **15**(15): 1926-1934.

Fernandez-Vizarra, E., M. J. Lopez-Perez, et al. (2002). "Isolation of biogenetically competent mitochondria from mammalian tissues and cultured cells." Methods **26**(4): 292-297.

Fox, P. T., M. E. Raichle, et al. (1988). "Nonoxidative glucose consumption during focal physiologic neural activity." Science **241**(4864): 462-464.

Franke, T. F., S. I. Yang, et al. (1995). "The protein kinase encoded by the Akt proto-oncogene is a target of the PDGF-activated phosphatidylinositol 3-kinase." Cell **81**(5): 727-736.

Frederich, R. C., A. Hamann, et al. (1995). "Leptin levels reflect body lipid content in mice: evidence for diet-induced resistance to leptin action." Nat Med **1**(12): 1311-1314.

Freude, S. (2010). "Insulin receptor substrate signaling in the central nervous system." Protein Science and Engineering Series.

Frias, M. A., C. C. Thoreen, et al. (2006). "mSin1 is necessary for Akt/PKB phosphorylation, and its isoforms define three distinct mTORC2s." Curr Biol **16**(18): 1865-1870.

Fruhbeck, G., M. Aguado, et al. (1998). "Lipolytic effect of in vivo leptin administration on adipocytes of lean and ob/ob mice, but not db/db mice." Biochem Biophys Res Commun **250**(1): 99-102.

Gao, Q. and T. L. Horvath (2008). "Neuronal control of energy homeostasis." FEBS Lett **582**(1): 132-141.

Gao, T., F. Furnari, et al. (2005). "PHLPP: a phosphatase that directly dephosphorylates Akt, promotes apoptosis, and suppresses tumor growth." Mol Cell **18**(1): 13-24.

Gates, A. C., C. Bernal-Mizrachi, et al. (2007). "Respiratory uncoupling in skeletal muscle delays death and diminishes age-related disease." Cell Metab **6**(6): 497-505.

Gerich, J. E. (2003). "Contributions of insulin-resistance and insulin-secretory defects to the pathogenesis of type 2 diabetes mellitus." Mayo Clin Proc **78**(4): 447-456.

Gericke, A., M. Munson, et al. (2006). "Regulation of the PTEN phosphatase." Gene **374**: 1-9.

Gilkerson, R. W., J. M. Selker, et al. (2003). "The cristal membrane of mitochondria is the principal site of oxidative phosphorylation." FEBS Lett **546**(2-3): 355-358.

Giovannone, B., M. L. Scaldaferri, et al. (2000). "Insulin receptor substrate (IRS) transduction system: distinct and overlapping signaling potential." Diabetes Metab Res Rev **16**(6): 434-441.

Gomez-Ambrosi, J., G. Fruhbeck, et al. (2001). "Rapid in vivo PGC-1 mRNA upregulation in brown adipose tissue of Wistar rats by a beta(3)-adrenergic agonist and lack of effect of leptin." Mol Cell Endocrinol **176**(1-2): 85-90.

Graves, L. M., K. E. Bornfeldt, et al. (1995). "cAMP- and rapamycin-sensitive regulation of the association of eukaryotic initiation factor 4E and the translational regulator PHAS-I in aortic smooth muscle cells." Proc Natl Acad Sci U S A **92**(16): 7222-7226.

Gray, M. W., G. Burger, et al. (1999). "Mitochondrial evolution." Science **283**(5407): 1476-1481.

Green, D. R. and G. Kroemer (2004). "The pathophysiology of mitochondrial cell death." Science **305**(5684): 626-629.

Grimsrud, P. A., H. Xie, et al. (2008). "Oxidative stress and covalent modification of protein with bioactive aldehydes." J Biol Chem **283**(32): 21837-21841.

Groop, L. C., C. Saloranta, et al. (1991). "The role of free fatty acid metabolism in the pathogenesis of insulin resistance in obesity and noninsulin-dependent diabetes mellitus." J Clin Endocrinol Metab **72**(1): 96-107.

Guertin, D. A., D. M. Stevens, et al. (2006). "Ablation in mice of the mTORC components raptor, rictor, or mLST8 reveals that mTORC2 is required for signaling to Akt-FOXO and PKCalpha, but not S6K1." Dev Cell **11**(6): 859-871.

Haffner, S. M., R. D'Agostino, et al. (1996). "Increased insulin resistance and insulin secretion in nondiabetic African-Americans and Hispanics compared with non-Hispanic whites. The Insulin Resistance Atherosclerosis Study." Diabetes **45**(6): 742-748.

Hammel, K. E., B. Kalyanaraman, et al. (1986). "Oxidation of polycyclic aromatic hydrocarbons and dibenzo[p]-dioxins by Phanerochaete chrysosporium ligninase." J Biol Chem **261**(36): 16948-16952.

Hammel, K. E., B. Kalyanaraman, et al. (1986). "Substrate free radicals are intermediates in ligninase catalysis." Proc Natl Acad Sci U S A **83**(11): 3708-3712.

Hanks, S. K., A. M. Quinn, et al. (1988). "The protein kinase family: conserved features and deduced phylogeny of the catalytic domains." Science **241**(4861): 42-52.

Havel, P. J. (2001). "Peripheral signals conveying metabolic information to the brain: short-term and long-term regulation of food intake and energy homeostasis." Exp Biol Med (Maywood) **226**(11): 963-977.

Havrankova, J., J. Roth, et al. (1978). "Insulin receptors are widely distributed in the central nervous system of the rat." Nature **272**(5656): 827-829.

He, W., A. Craparo, et al. (1996). "Interaction of insulin receptor substrate-2 (IRS-2) with the insulin and insulin-like growth factor I receptors. Evidence for two distinct phosphotyrosine-dependent interaction domains within IRS-2." J Biol Chem **271**(20): 11641-11645.

Heidenreich, K., M. Paduschek, et al. (1994). "The insulin receptor: a protein kinase with dual specificity?" Biol Chem Hoppe Seyler **375**(2): 99-104.

Heilbronn, L. K., S. K. Gan, et al. (2007). "Markers of mitochondrial biogenesis and metabolism are lower in overweight and obese insulin-resistant subjects." J Clin Endocrinol Metab **92**(4): 1467-1473.

Heldin, C. H. (1995). "Dimerization of cell surface receptors in signal transduction." Cell **80**(2): 213-223.

Hentges, S. T., M. Nishiyama, et al. (2004). "GABA release from proopiomelanocortin neurons." J Neurosci **24**(7): 1578-1583.

Hermann, G. J. and J. M. Shaw (1998). "Mitochondrial dynamics in yeast." Annu Rev Cell Dev Biol **14**: 265-303.

Higaki, Y., J. F. Wojtaszewski, et al. (1999). "Insulin receptor substrate-2 is not necessary for insulin- and exercise-stimulated glucose transport in skeletal muscle." J Biol Chem **274**(30): 20791-20795.

Hintz, P. and B. Kalyanaraman (1986). "Metal ion-induced activation of molecular oxygen in pigmented polymers." Biochim Biophys Acta **883**(1): 41-45.

Hoeks, J., M. K. Hesselink, et al. (2006). "Peroxisome proliferator-activated receptor-gamma coactivator-1 and insulin resistance: acute effect of fatty acids." Diabetologia **49**(10): 2419-2426.

Hood, D. A. (2001). "Invited Review: contractile activity-induced mitochondrial biogenesis in skeletal muscle." J Appl Physiol **90**(3): 1137-1157.

Horvath, T. L., I. Bechmann, et al. (1997). "Heterogeneity in the neuropeptide Y-containing neurons of the rat arcuate nucleus: GABAergic and non-GABAergic subpopulations." Brain Research **756**(1-2): 283-286.

Hotamisligil, G. S., A. Budavari, et al. (1994). "Reduced tyrosine kinase activity of the insulin receptor in obesity-diabetes. Central role of tumor necrosis factor-alpha." J Clin Invest **94**(4): 1543-1549.

Hu, C., S. Pang, et al. (1994). "Molecular cloning and tissue distribution of PHAS-I, an intracellular target for insulin and growth factors." Proc Natl Acad Sci U S A **91**(9): 3730-3734.

Hubbard, S. R., M. Mohammadi, et al. (1998). "Autoregulatory mechanisms in protein-tyrosine kinases." J Biol Chem **273**(20): 11987-11990.

Hubbard, S. R., L. Wei, et al. (1994). "Crystal structure of the tyrosine kinase domain of the human insulin receptor." Nature **372**(6508): 746-754.

Janssen, R. J., L. G. Nijtmans, et al. (2006). "Mitochondrial complex I: structure, function and pathology." J Inherit Metab Dis **29**(4): 499-515.

Jastroch, M., K. W. Withers, et al. (2009). "Mitochondrial proton conductance in skeletal muscle of a cold-exposed marsupial, Antechinus flavipes, is unlikely to be involved in adaptive nonshivering thermogenesis but displays increased sensitivity toward carbon-centered radicals." Physiol Biochem Zool **82**(5): 447-454.

Jia, K., D. Chen, et al. (2004). "The TOR pathway interacts with the insulin signaling pathway to regulate C. elegans larval development, metabolism and life span." Development **131**(16): 3897-3906.

Jiang, Z. Y., Q. L. Zhou, et al. (2003). "Insulin signaling through Akt/protein kinase B analyzed by small interfering RNA-mediated gene silencing." Proc Natl Acad Sci U S A **100**(13): 7569-7574.

Jockel, J., B. Wendt, et al. (1998). "Structural and functional comparison of agents interfering with dihydroorotate, succinate and NADH oxidation of rat liver mitochondria." Biochem Pharmacol **56**(8): 1053-1060.

Johnston, J. A., L. M. Wang, et al. (1995). "Interleukins 2, 4, 7, and 15 stimulate tyrosine phosphorylation of insulin receptor substrates 1 and 2 in T cells. Potential role of JAK kinases." J Biol Chem **270**(48): 28527-28530.

Jordan, S. D., A. C. Konner, et al. (2010). "Sensing the fuels: glucose and lipid signaling in the CNS controlling energy homeostasis." Cell Mol Life Sci **67**(19): 3255-3273.

Joseph, J. W., V. Koshkin, et al. (2002). "Uncoupling protein 2 knockout mice have enhanced insulin secretory capacity after a high-fat diet." Diabetes **51**(11): 3211-3219.

Joyner, A. L., A. Auerbach, et al. (1992). "The gene trap approach in embryonic stem cells: the potential for genetic screens in mice." Ciba Found Symp **165**: 277-288; discussion 288-297.

Kadowaki, T., H. Tamemoto, et al. (1996). "Insulin resistance and growth retardation in mice lacking insulin receptor substrate-1 and identification of insulin receptor substrate-2." Diabet Med **13**(9 Suppl 6): S103-108.

Kaeberlein, M., R. W. Powers, 3rd, et al. (2005). "Regulation of yeast replicative life span by TOR and Sch9 in response to nutrients." Science **310**(5751): 1193-1196.

Kahn, C. R., K. L. Baird, et al. (1978). "Direct demonstration that receptor crosslinking or aggregation is important in insulin action." Proc Natl Acad Sci U S A **75**(9): 4209-4213.

Kaloyianni, M. and R. A. Freedland (1990). "Contribution of several amino acids and lactate to gluconeogenesis in hepatocytes isolated from rats fed various diets." J Nutr **120**(1): 116-122.

Kalyanaraman, B., P. Hintz, et al. (1986). "An electron spin resonance study of free radicals from catechol estrogens." Fed Proc **45**(10): 2477-2484.

Kalyanaraman, B. and P. G. Sohnle (1985). "Generation of free radical intermediates from foreign compounds by neutrophil-derived oxidants." J Clin Invest **75**(5): 1618-1622.

Kasuga, M., Y. Fujita-Yamaguchi, et al. (1983). "Tyrosine-specific protein kinase activity is associated with the purified insulin receptor." Proc Natl Acad Sci U S A **80**(8): 2137-2141.

Keegan, A. D., K. Nelms, et al. (1994). "An IL-4 receptor region containing an insulin receptor motif is important for IL-4-mediated IRS-1 phosphorylation and cell growth." Cell **76**(5): 811-820.

Kelley, D. E., J. He, et al. (2002). "Dysfunction of mitochondria in human skeletal muscle in type 2 diabetes." Diabetes **51**(10): 2944-2950.

Kelley, D. E. and L. J. Mandarino (2000). "Fuel selection in human skeletal muscle in insulin resistance: a reexamination." Diabetes **49**(5): 677-683.

Kenyon, C. J. (2010). "The genetics of ageing." Nature **464**(7288): 504-512.

Kerner, J., W. K. Parland, et al. (2008). "Rat liver mitochondrial carnitine palmitoyltransferase-I, hepatic carnitine, and malonyl-CoA: effect of starvation." Arch Physiol Biochem **114**(3): 161-170.

Kido, Y., D. J. Burks, et al. (2000). "Tissue-specific insulin resistance in mice with mutations in the insulin receptor, IRS-1, and IRS-2." J Clin Invest **105**(2): 199-205.

Kim, M. S., Y. K. Pak, et al. (2006). "Role of hypothalamic Foxo1 in the regulation of food intake and energy homeostasis." Nat Neurosci **9**(7): 901-906.

Kirk, T. K., M. Tien, et al. (1986). "Ligninase of Phanerochaete chrysosporium. Mechanism of its degradation of the non-phenolic arylglycerol beta-aryl ether substructure of lignin." Biochem J **236**(1): 279-287.

Kitamura, T., Y. Feng, et al. (2006). "Forkhead protein FoxO1 mediates Agrp-dependent effects of leptin on food intake." Nat Med **12**(5): 534-540.

Klaus, S. (2004). "Adipose tissue as a regulator of energy balance." Curr Drug Targets **5**(3): 241-250.

Kornmann, M., H. Maruyama, et al. (1998). "Enhanced expression of the insulin receptor substrate-2 docking protein in human pancreatic cancer." Cancer Res **58**(19): 4250-4254.

Korytowski, W., B. Kalyanaraman, et al. (1986). "Reaction of superoxide anions with melanins: electron spin resonance and spin trapping studies." Biochim Biophys Acta **882**(2): 145-153.

Kozak, L. P. and R. Anunciado-Koza (2008). "UCP1: its involvement and utility in obesity." Int J Obes (Lond) **32 Suppl 7**: S32-38.

Krauss, S., C. Y. Zhang, et al. (2002). "A significant portion of mitochondrial proton leak in intact thymocytes depends on expression of UCP2." Proc Natl Acad Sci U S A **99**(1): 118-122.

Krauss, S., C. Y. Zhang, et al. (2003). "Superoxide-mediated activation of uncoupling protein 2 causes pancreatic beta cell dysfunction." J Clin Invest **112**(12): 1831-1842.

Kubota, N., Y. Terauchi, et al. (2004). "Insulin receptor substrate 2 plays a crucial role in beta cells and the hypothalamus." J Clin Invest **114**(7): 917-927.

Kurland, C. G. and S. G. Andersson (2000). "Origin and evolution of the mitochondrial proteome." Microbiol Mol Biol Rev **64**(4): 786-820.

Kuznetsov, A. V., V. Veksler, et al. (2008). "Analysis of mitochondrial function in situ in permeabilized muscle fibers, tissues and cells." Nat Protoc **3**(6): 965-976.

Laemmli, U. K. (1970). "Cleavage of structural proteins during the assembly of the head of bacteriophage T4." Nature **227**(5259): 680-685.

Laemmli, U. K., F. Beguin, et al. (1970). "A factor preventing the major head protein of bacteriophage T4 from random aggregation." J Mol Biol **47**(1): 69-85.

Laemmli, U. K., E. Molbert, et al. (1970). "Form-determining function of the genes required for the assembly of the head of bacteriophage T4." J Mol Biol **49**(1): 99-113.

Lang, B. F., M. W. Gray, et al. (1999). "Mitochondrial genome evolution and the origin of eukaryotes." Annu Rev Genet **33**: 351-397.

Lanni, A., F. P. Mancini, et al. (2002). "De novo expression of uncoupling protein 3 is associated to enhanced mitochondrial thioesterase-1 expression and fatty acid metabolism in liver of fenofibrate-treated rats." FEBS Lett **525**(1-3): 7-12.

Larrouy, D., P. Laharrague, et al. (1997). "Kupffer cells are a dominant site of uncoupling protein 2 expression in rat liver." Biochem Biophys Res Commun **235**(3): 760-764.

Lavan, B. E., V. R. Fantin, et al. (1997). "A novel 160-kDa phosphotyrosine protein in insulin-treated embryonic kidney cells is a new member of the insulin receptor substrate family." J Biol Chem **272**(34): 21403-21407.

Lavan, B. E., W. S. Lane, et al. (1997). "The 60-kDa phosphotyrosine protein in insulin-treated adipocytes is a new member of the insulin receptor substrate family." J Biol Chem **272**(17): 11439-11443.

Lazar, M. A. (2005). "How obesity causes diabetes: not a tall tale." Science **307**(5708): 373-375.

Le Roith, D. (1997). "Seminars in medicine of the Beth Israel Deaconess Medical Center. Insulin-like growth factors." N Engl J Med **336**(9): 633-640.

Lee, Y., X. Yu, et al. (2002). "PPAR alpha is necessary for the lipopenic action of hyperleptinemia on white adipose and liver tissue." Proc Natl Acad Sci U S A **99**(18): 11848-11853.

Lee, Y. S., B. G. Challis, et al. (2006). "A POMC variant implicates beta-melanocyte-stimulating hormone in the control of human energy balance." Cell Metab **3**(2): 135-140.

Lerin, C., J. T. Rodgers, et al. (2006). "GCN5 acetyltransferase complex controls glucose metabolism through transcriptional repression of PGC-1alpha." Cell Metab **3**(6): 429-438.

Lesnefsky, E. J., S. Moghaddas, et al. (2001). "Mitochondrial dysfunction in cardiac disease: ischemia--reperfusion, aging, and heart failure." J Mol Cell Cardiol **33**(6): 1065-1089.

Levine, R. L., J. A. Williams, et al. (1994). "Carbonyl assays for determination of oxidatively modified proteins." Methods Enzymol **233**: 346-357.

Liang, H. and W. F. Ward (2006). "PGC-1alpha: a key regulator of energy metabolism." Adv Physiol Educ **30**(4): 145-151.

Lienhard, G. E., J. W. Slot, et al. (1992). "How cells absorb glucose." Sci Am **266**(1): 86-91.

Lill, R. and G. Kispal (2000). "Maturation of cellular Fe-S proteins: an essential function of mitochondria." Trends Biochem Sci **25**(8): 352-356.

Lin, S. J., M. Kaeberlein, et al. (2002). "Calorie restriction extends Saccharomyces cerevisiae lifespan by increasing respiration." Nature **418**(6895): 344-348.

Lin, T. A., X. Kong, et al. (1994). "PHAS-I as a link between mitogen-activated protein kinase and translation initiation." Science **266**(5185): 653-656.

Lin, T. A., X. Kong, et al. (1995). "Control of PHAS-I by insulin in 3T3-L1 adipocytes. Synthesis, degradation, and phosphorylation by a rapamycin-sensitive and mitogen-activated protein kinase-independent pathway." J Biol Chem **270**(31): 18531-18538.

Lin, X., A. Taguchi, et al. (2004). "Dysregulation of insulin receptor substrate 2 in beta cells and brain causes obesity and diabetes." J Clin Invest **114**(7): 908-916.

Liu, F. and R. A. Roth (1994). "Identification of serines-1035/1037 in the kinase domain of the insulin receptor as protein kinase C alpha mediated phosphorylation sites." FEBS Lett **352**(3): 389-392.

Liu, Z. C., D. S. Shin, et al. (2007). "Light-directed synthesis of peptide nucleic acids (PNAs) chips." Biosens Bioelectron **22**(12): 2891-2897.

Loewith, R., E. Jacinto, et al. (2002). "Two TOR complexes, only one of which is rapamycin sensitive, have distinct roles in cell growth control." Mol Cell **10**(3): 457-468.

Loffler, M., J. Jockel, et al. (1997). "Dihydroorotat-ubiquinone oxidoreductase links mitochondria in the biosynthesis of pyrimidine nucleotides." Mol Cell Biochem **174**(1-2): 125-129.

Logan, C., M. C. Hanks, et al. (1992). "Cloning and sequence comparison of the mouse, human, and chicken engrailed genes reveal potential functional domains and regulatory regions." Dev Genet **13**(5): 345-358.

Long, Y. C., Z. Cheng, et al. (2011). "Insulin receptor substrates Irs1 and Irs2 coordinate skeletal muscle growth and metabolism via the Akt and AMPK pathways." Molecular and Cellular Biology **31**(3): 430-441.

Lopez, M. F., B. S. Kristal, et al. (2000). "High-throughput profiling of the mitochondrial proteome using affinity fractionation and automation." Electrophoresis **21**(16): 3427-3440.

Lowell, B. B. and G. I. Shulman (2005). "Mitochondrial dysfunction and type 2 diabetes." Science **307**(5708): 384-387.

Luft, R. (1994). "The development of mitochondrial medicine." Proc Natl Acad Sci U S A **91**(19): 8731-8738.

Ma, L., Z. Chen, et al. (2005). "Phosphorylation and functional inactivation of TSC2 by Erk implications for tuberous sclerosis and cancer pathogenesis." Cell **121**(2): 179-193.

Madsen, P. L., R. Linde, et al. (1998). "Activation-induced resetting of cerebral oxygen and glucose uptake in the rat." J Cereb Blood Flow Metab **18**(7): 742-748.

Maechler, P. and C. B. Wollheim (2001). "Mitochondrial function in normal and diabetic beta-cells." Nature **414**(6865): 807-812.

Maffei, M., J. Halaas, et al. (1995). "Leptin levels in human and rodent: measurement of plasma leptin and ob RNA in obese and weight-reduced subjects." Nat Med **1**(11): 1155-1161.

Maira, S. M., I. Galetic, et al. (2001). "Carboxyl-terminal modulator protein (CTMP), a negative regulator of PKB/Akt and v-Akt at the plasma membrane." Science **294**(5541): 374-380.

Manley, N. R., M. O'Connell, et al. (1993). "Two factors that bind to highly conserved sequences in mammalian type C retroviral enhancers." J Virol **67**(4): 1967-1975.

Mannella, C. A., D. R. Pfeiffer, et al. (2001). "Topology of the mitochondrial inner membrane: dynamics and bioenergetic implications." IUBMB Life **52**(3-5): 93-100.

Manya, H., J. Aoki, et al. (1999). "Biochemical characterization of various catalytic complexes of the brain platelet-activating factor acetylhydrolase." J Biol Chem **274**(45): 31827-31832.

Margulis, L. (1971). "Symbiosis and evolution." Sci Am **225**(2): 48-57.

Massague, J. and M. P. Czech (1982). "Role of disulfides in the subunit structure of the insulin receptor. Reduction of class I disulfides does not impair transmembrane signalling." J Biol Chem **257**(12): 6729-6738.

Mattison, J. A., M. A. Lane, et al. (2003). "Calorie restriction in rhesus monkeys." Exp Gerontol **38**(1-2): 35-46.

McAllister, R. M., S. C. Newcomer, et al. (2008). "Vascular nitric oxide: effects of exercise training in animals." Appl Physiol Nutr Metab **33**(1): 173-178.

McMahon, A. P., A. L. Joyner, et al. (1992). "The midbrain-hindbrain phenotype of Wnt-1-/Wnt-1- mice results from stepwise deletion of engrailed-expressing cells by 9.5 days postcoitum." Cell **69**(4): 581-595.

Mendez, R., G. Kollmorgen, et al. (1997). "Requirement of protein kinase C zeta for stimulation of protein synthesis by insulin." Molecular and Cellular Biology **17**(9): 5184-5192.

Mendez, R., M. G. Myers, Jr., et al. (1996). "Stimulation of protein synthesis, eukaryotic translation initiation factor 4E phosphorylation, and PHAS-I phosphorylation by insulin requires insulin receptor substrate 1 and phosphatidylinositol 3-kinase." Molecular and Cellular Biology **16**(6): 2857-2864.

Miki, H., T. Yamauchi, et al. (2001). "Essential role of insulin receptor substrate 1 (IRS-1) and IRS-2 in adipocyte differentiation." Molecular and Cellular Biology **21**(7): 2521-2532.

Mitchell, C. S., D. B. Savage, et al. (2010). "Resistance to thyroid hormone is associated with raised energy expenditure, muscle mitochondrial uncoupling, and hyperphagia." J Clin Invest **120**(4): 1345-1354.

Mitchell, J., H. Jiang, et al. (1996). "Effect of antioxidants on lipopolysaccharide-stimulated induction of mangano superoxide dismutase mRNA in bovine pulmonary artery endothelial cells." J Cell Physiol **169**(2): 333-340.

Mitchell, P. (1961). "Coupling of phosphorylation to electron and hydrogen transfer by a chemi-osmotic type of mechanism." Nature **191**: 144-148.

Moens, C. B., A. B. Auerbach, et al. (1992). "A targeted mutation reveals a role for N-myc in branching morphogenesis in the embryonic mouse lung." Genes Dev **6**(5): 691-704.

Mootha, V. K., C. M. Lindgren, et al. (2003). "PGC-1alpha-responsive genes involved in oxidative phosphorylation are coordinately downregulated in human diabetes." Nat Genet **34**(3): 267-273.

Mothe, I. and E. Van Obberghen (1996). "Phosphorylation of insulin receptor substrate-1 on multiple serine residues, 612, 632, 662, and 731, modulates insulin action." J Biol Chem **271**(19): 11222-11227.

Myers, M. G., Jr., J. M. Backer, et al. (1992). "IRS-1 activates phosphatidylinositol 3'-kinase by associating with src homology 2 domains of p85." Proc Natl Acad Sci U S A **89**(21): 10350-10354.

Myers, M. G., Jr., T. C. Grammer, et al. (1994). "Insulin receptor substrate-1 mediates phosphatidylinositol 3'-kinase and p70S6k signaling during insulin, insulin-like growth factor-1, and interleukin-4 stimulation." J Biol Chem **269**(46): 28783-28789.

Myers, M. G., Jr., X. J. Sun, et al. (1994). "The IRS-1 signaling system." Trends Biochem Sci **19**(7): 289-293.

Myers, M. G., Jr. and M. F. White (1993). "The new elements of insulin signaling. Insulin receptor substrate-1 and proteins with SH2 domains." Diabetes **42**(5): 643-650.

Myers, M. G., Jr. and M. F. White (1996). "Insulin signal transduction and the IRS proteins." Annu Rev Pharmacol Toxicol **36**: 615-658.

Nagai, Y., J. Aoki, et al. (1999). "An alternative splicing form of phosphatidylserine-specific phospholipase A1 that exhibits lysophosphatidylserine-specific lysophospholipase activity in humans." J Biol Chem **274**(16): 11053-11059.

Namatame, I., H. Tomoda, et al. (1999). "Complete inhibition of mouse macrophage-derived foam cell formation by triacsin C." J Biochem **125**(2): 319-327.

Nedergaard, J. and B. Cannon (2010). "The changed metabolic world with human brown adipose tissue: therapeutic visions." Cell Metab **11**(4): 268-272.

Neupert, W. (1997). "Protein import into mitochondria." Annu Rev Biochem **66**: 863-917.

Nicholls, D. G. (1974). "The influence of respiration and ATP hydrolysis on the proton-electrochemical gradient across the inner membrane of rat-liver mitochondria as determined by ion distribution." Eur J Biochem **50**(1): 305-315.

Nisoli, E., E. Clementi, et al. (2007). "Defective mitochondrial biogenesis: a hallmark of the high cardiovascular risk in the metabolic syndrome?" Circ Res **100**(6): 795-806.

Niswender, K. D., D. G. Baskin, et al. (2004). "Insulin and its evolving partnership with leptin in the hypothalamic control of energy homeostasis." Trends Endocrinol Metab **15**(8): 362-369.

Numan, S. and D. S. Russell (1999). "Discrete expression of insulin receptor substrate-4 mRNA in adult rat brain." Brain Res Mol Brain Res **72**(1): 97-102.

Nunnari, J., W. F. Marshall, et al. (1997). "Mitochondrial transmission during mating in Saccharomyces cerevisiae is determined by mitochondrial fusion and fission and the intramitochondrial segregation of mitochondrial DNA." Molecular Biology of the Cell **8**(7): 1233-1242.

O'Brien, C. (1994). "Missing link in insulin's path to protein production." Science **266**(5185): 542-543.

Oh-Ishi, M., T. Ueno, et al. (2003). "Proteomic method detects oxidatively induced protein carbonyls in muscles of a diabetes model Otsuka Long-Evans Tokushima Fatty (OLETF) rat." Free Radic Biol Med **34**(1): 11-22.

Okada, T., Y. Kawano, et al. (1994). "Essential role of phosphatidylinositol 3-kinase in insulin-induced glucose transport and antilipolysis in rat adipocytes. Studies with a selective inhibitor wortmannin." J Biol Chem **269**(5): 3568-3573.

Oklejewicz, M. and S. Daan (2002). "Enhanced longevity in tau mutant Syrian hamsters, Mesocricetus auratus." J Biol Rhythms **17**(3): 210-216.

Oklejewicz, M., R. A. Hut, et al. (1997). "Metabolic rate changes proportionally to circadian frequency in tau mutant Syrian hamsters." J Biol Rhythms **12**(5): 413-422.

Ollmann, M. M., B. D. Wilson, et al. (1997). "Antagonism of central melanocortin receptors in vitro and in vivo by agouti-related protein." Science **278**(5335): 135-138.

O'Reilly, K. E., F. Rojo, et al. (2006). "mTOR inhibition induces upstream receptor tyrosine kinase signaling and activates Akt." Cancer Res **66**(3): 1500-1508.

Ottensmeyer, F. P., D. R. Beniac, et al. (2000). "Mechanism of transmembrane signaling: insulin binding and the insulin receptor." Biochemistry **39**(40): 12103-12112.

Pandini, G., F. Frasca, et al. (2002). "Insulin/insulin-like growth factor I hybrid receptors have different biological characteristics depending on the insulin receptor isoform involved." J Biol Chem **277**(42): 39684-39695.

Pang, L., K. L. Milarski, et al. (1994). "Mutation of the two carboxyl-terminal tyrosines in the insulin receptor results in enhanced activation of mitogen-activated protein kinase." J Biol Chem **269**(14): 10604-10608.

Patti, M. E., A. J. Butte, et al. (2003). "Coordinated reduction of genes of oxidative metabolism in humans with insulin resistance and diabetes: Potential role of PGC1 and NRF1." Proc Natl Acad Sci U S A **100**(14): 8466-8471.

Patti, M. E., X. J. Sun, et al. (1995). "4PS/insulin receptor substrate (IRS)-2 is the alternative substrate of the insulin receptor in IRS-1-deficient mice." J Biol Chem **270**(42): 24670-24673.

Pause, A., G. J. Belsham, et al. (1994). "Insulin-dependent stimulation of protein synthesis by phosphorylation of a regulator of 5'-cap function." Nature **371**(6500): 762-767.

Pawson, T. and G. D. Gish (1992). "SH2 and SH3 domains: from structure to function." Cell **71**(3): 359-362.

Perkins, G. A., J. Y. Song, et al. (1998). "Electron tomography of mitochondria from brown adipocytes reveals crista junctions." J Bioenerg Biomembr **30**(5): 431-442.

Petersen, K. F., D. Befroy, et al. (2003). "Mitochondrial dysfunction in the elderly: possible role in insulin resistance." Science **300**(5622): 1140-1142.

Petersen, K. F., S. Dufour, et al. (2004). "Impaired mitochondrial activity in the insulin-resistant offspring of patients with type 2 diabetes." N Engl J Med **350**(7): 664-671.

Pfanner, N. and M. Meijer (1997). "The Tom and Tim machine." Curr Biol **7**(2): R100-103.

Pick, A., J. Clark, et al. (1998). "Role of apoptosis in failure of beta-cell mass compensation for insulin resistance and beta-cell defects in the male Zucker diabetic fatty rat." Diabetes **47**(3): 358-364.

Pilas, B., C. C. Felix, et al. (1986). "Photolysis of pheomelanin precursors: an ESR-spin trapping study." Photochem Photobiol **44**(6): 689-696.

Plum, L., X. Ma, et al. (2006). "Enhanced PIP3 signaling in POMC neurons causes KATP channel activation and leads to diet-sensitive obesity." J Clin Invest **116**(7): 1886-1901.

Prentki, M., E. Joly, et al. (2002). "Malonyl-CoA signaling, lipid partitioning, and glucolipotoxicity: role in beta-cell adaptation and failure in the etiology of diabetes." Diabetes **51 Suppl 3**: S405-413.

Prince, F. P. (2002). "Lamellar and tubular associations of the mitochondrial cristae: unique forms of the cristae present in steroid-producing cells." Mitochondrion **1**(4): 381-389.

Proud, C. G. (1994). "Translation. Turned on by insulin." Nature **371**(6500): 747-748.

Pulverer, B. J., J. M. Kyriakis, et al. (1991). "Phosphorylation of c-jun mediated by MAP kinases." Nature **353**(6345): 670-674.

Rabinovsky, R., P. Pochanard, et al. (2009). "p85 Associates with unphosphorylated PTEN and the PTEN-associated complex." Molecular and Cellular Biology **29**(19): 5377-5388.

Radi, R., J. F. Turrens, et al. (1991). "Detection of catalase in rat heart mitochondria." J Biol Chem **266**(32): 22028-22034.

Raha, S., G. E. McEachern, et al. (2000). "Superoxides from mitochondrial complex III: the role of manganese superoxide dismutase." Free Radic Biol Med **29**(2): 170-180.

Reichert, A. S. and W. Neupert (2004). "Mitochondriomics or what makes us breathe." Trends in Genetics **20**(11): 555-562.

Rezek, M. (1976). "The role of insulin in the glucostatic control of food intake." Can J Physiol Pharmacol **54**(5): 650-665.

Rhodes, C. J. (2005). "Type 2 diabetes-a matter of beta-cell life and death?" Science **307**(5708): 380-384.

Richardson, D. K., S. Kashyap, et al. (2005). "Lipid infusion decreases the expression of nuclear encoded mitochondrial genes and increases the expression of extracellular matrix genes in human skeletal muscle." J Biol Chem **280**(11): 10290-10297.

Ricort, J. M., J. F. Tanti, et al. (1994). "Parallel changes in Glut 4 and Rab4 movements in two insulin-resistant states." FEBS Lett **347**(1): 42-44.

Rinderknecht, E. and R. E. Humbel (1978). "The amino acid sequence of human insulin-like growth factor I and its structural homology with proinsulin." J Biol Chem **253**(8): 2769-2776.

Robertson, S. C., J. A. Tynan, et al. (2000). "RTK mutations and human syndromeswhen good receptors turn bad." Trends in Genetics **16**(6): 265-271.

Rodgers, J. T., C. Lerin, et al. (2005). "Nutrient control of glucose homeostasis through a complex of PGC-1alpha and SIRT1." Nature **434**(7029): 113-118.

Rose, D. W., A. R. Saltiel, et al. (1994). "Insulin receptor substrate 1 is required for insulin-mediated mitogenic signal transduction." Proc Natl Acad Sci U S A **91**(2): 797-801.

Rospert, S. and R. Hallberg (1995). "Interaction of HSP 60 with proteins imported into the mitochondrial matrix." Methods Enzymol **260**: 287-292.

Roth, G. S., M. A. Lane, et al. (2002). "Biomarkers of caloric restriction may predict longevity in humans." Science **297**(5582): 811.

Russell, L. K., C. M. Mansfield, et al. (2004). "Cardiac-specific induction of the transcriptional coactivator peroxisome proliferator-activated receptor gamma coactivator-1alpha promotes mitochondrial biogenesis and reversible cardiomyopathy in a developmental stage-dependent manner." Circ Res **94**(4): 525-533.

Rustin, P., D. Chretien, et al. (1994). "Biochemical and molecular investigations in respiratory chain deficiencies." Clin Chim Acta **228**(1): 35-51.

Ryan, M. T., R. Wagner, et al. (2000). "The transport machinery for the import of preproteins across the outer mitochondrial membrane." Int J Biochem Cell Biol **32**(1): 13-21.

Sabio, G., M. Das, et al. (2008). "A stress signaling pathway in adipose tissue regulates hepatic insulin resistance." Science **322**(5907): 1539-1543.

Sanchez-Lasheras, C., A. C. Konner, et al. (2010). "Integrative neurobiology of energy homeostasis-neurocircuits, signals and mediators." Front Neuroendocrinol **31**(1): 4-15.

Sanz, L., J. Moscat, et al. (1995). "Molecular characterization of a novel transcription factor that controls stromelysin expression." Molecular and Cellular Biology **15**(6): 3164-3170.

Sarbassov, D. D., S. M. Ali, et al. (2006). "Prolonged rapamycin treatment inhibits mTORC2 assembly and Akt/PKB." Mol Cell **22**(2): 159-168.

Sasaoka, T. and M. Kobayashi (2000). "The functional significance of Shc in insulin signaling as a substrate of the insulin receptor." Endocr J **47**(4): 373-381.

Sawka-Verhelle, D., S. Tartare-Deckert, et al. (1996). "Insulin receptor substrate-2 binds to the insulin receptor through its phosphotyrosine-binding domain and through a newly identified domain comprising amino acids 591-786." J Biol Chem **271**(11): 5980-5983.

Scarpace, P. J., M. Matheny, et al. (1997). "Leptin increases uncoupling protein expression and energy expenditure." Am J Physiol **273**(1 Pt 1): E226-230.

Schlessinger, J. (1988). "Signal transduction by allosteric receptor oligomerization." Trends Biochem Sci **13**(11): 443-447.

Schrauwen, P. and M. K. Hesselink (2008). "Reduced tricarboxylic acid cycle flux in type 2 diabetes mellitus?" Diabetologia **51**(9): 1694-1697.

Schrauwen-Hinderling, V. B., M. Roden, et al. (2007). "Muscular mitochondrial dysfunction and type 2 diabetes mellitus." Curr Opin Clin Nutr Metab Care **10**(6): 698-703.

Schubert, M., D. P. Brazil, et al. (2003). "Insulin receptor substrate-2 deficiency impairs brain growth and promotes tau phosphorylation." J Neurosci **23**(18): 7084-7092.

Schwartz, M. W., J. L. Marks, et al. (1991). "Central insulin administration reduces neuropeptide Y mRNA expression in the arcuate nucleus of food-deprived lean (Fa/Fa) but not obese (fa/fa) Zucker rats." Endocrinology **128**(5): 2645-2647.

Schwartz, M. W., A. J. Sipols, et al. (1992). "Inhibition of hypothalamic neuropeptide Y gene expression by insulin." Endocrinology **130**(6): 3608-3616.

Schwerzmann, K., H. Hoppeler, et al. (1989). "Oxidative capacity of muscle and mitochondria: correlation of physiological, biochemical, and morphometric characteristics." Proc Natl Acad Sci U S A **86**(5): 1583-1587.

Sedivy, J. M. and A. L. Joyner (1992). Gene targeting. New York, W.H. Freeman.

Selman, C., S. Lingard, et al. (2008). "Evidence for lifespan extension and delayed age-related biomarkers in insulin receptor substrate 1 null mice." Faseb Journal **22**(3): 807-818.

Seth, A., F. A. Gonzalez, et al. (1992). "Signal transduction within the nucleus by mitogen-activated protein kinase." J Biol Chem **267**(34): 24796-24804.

Shacter, E. (2000). "Protein oxidative damage." Methods Enzymol **319**: 428-436.

Shaw, P. E., H. Schroter, et al. (1989). "The ability of a ternary complex to form over the serum response element correlates with serum inducibility of the human c-fos promoter." Cell **56**(4): 563-572.

Shepherd, P. R., D. J. Withers, et al. (1998). "Phosphoinositide 3-kinase: the key switch mechanism in insulin signalling." Biochem J **333 (Pt 3)**: 471-490.

Shiota, C., J. T. Woo, et al. (2006). "Multiallelic disruption of the rictor gene in mice reveals that mTOR complex 2 is essential for fetal growth and viability." Dev Cell **11**(4): 583-589.

Shulman, G. I. (2000). "Cellular mechanisms of insulin resistance." J Clin Invest **106**(2): 171-176.

Silvestri, E., P. de Lange, et al. (2006). "Fenofibrate activates the biochemical pathways and the de novo expression of genes related to lipid handling and uncoupling protein-3 functions in liver of normal rats." Biochim Biophys Acta **1757**(5-6): 486-495.

Sirrenberg, C., M. F. Bauer, et al. (1996). "Import of carrier proteins into the mitochondrial inner membrane mediated by Tim22." Nature **384**(6609): 582-585.

Skolnik, E. Y., B. Margolis, et al. (1991). "Cloning of PI3 kinase-associated p85 utilizing a novel method for expression/cloning of target proteins for receptor tyrosine kinases." Cell **65**(1): 83-90.

Smeitink, J., L. van den Heuvel, et al. (2001). "The genetics and pathology of oxidative phosphorylation." Nat Rev Genet **2**(5): 342-352.

Smith-Hall, J., S. Pons, et al. (1997). "The 60 kDa insulin receptor substrate functions like an IRS protein (pp60IRS3) in adipose cells." Biochemistry **36**(27): 8304-8310.

Spanswick, D., M. A. Smith, et al. (2000). "Insulin activates ATP-sensitive K+ channels in hypothalamic neurons of lean, but not obese rats." Nat Neurosci **3**(8): 757-758.

Sparks, L. M., H. Xie, et al. (2005). "A high-fat diet coordinately downregulates genes required for mitochondrial oxidative phosphorylation in skeletal muscle." Diabetes **54**(7): 1926-1933.

Speakman, J. (1997). "Factors influencing the daily energy expenditure of small mammals." Proc Nutr Soc **56**(3): 1119-1136.

Stanley, B. G. and S. F. Leibowitz (1984). "Neuropeptide Y: stimulation of feeding and drinking by injection into the paraventricular nucleus." Life Sci **35**(26): 2635-2642.

Steiner, D. F. and P. E. Oyer (1967). "The biosynthesis of insulin and a probable precursor of insulin by a human islet cell adenoma." Proc Natl Acad Sci U S A **57**(2): 473-480.

St-Pierre, J., J. Lin, et al. (2003). "Bioenergetic analysis of peroxisome proliferator-activated receptor gamma coactivators 1alpha and 1beta (PGC-1alpha and PGC-1beta) in muscle cells." J Biol Chem **278**(29): 26597-26603.

Sugioka, K., M. Nakano, et al. (1988). "Mechanism of O2- generation in reduction and oxidation cycle of ubiquinones in a model of mitochondrial electron transport systems." Biochim Biophys Acta **936**(3): 377-385.

Sulis, M. L. and R. Parsons (2003). "PTEN: from pathology to biology." Trends Cell Biol **13**(9): 478-483.

Sun, F., X. Huo, et al. (2005). "Crystal structure of mitochondrial respiratory membrane protein complex II." Cell **121**(7): 1043-1057.

Sun, X. J., D. L. Crimmins, et al. (1993). "Pleiotropic insulin signals are engaged by multisite phosphorylation of IRS-1." Molecular and Cellular Biology **13**(12): 7418-7428.

Sun, X. J., M. Miralpeix, et al. (1992). "Expression and function of IRS-1 in insulin signal transmission." J Biol Chem **267**(31): 22662-22672.

Sun, X. J., S. Pons, et al. (1997). "The IRS-2 gene on murine chromosome 8 encodes a unique signaling adapter for insulin and cytokine action." Mol Endocrinol **11**(2): 251-262.

Sun, X. J., P. Rothenberg, et al. (1991). "Structure of the insulin receptor substrate IRS-1 defines a unique signal transduction protein." Nature **352**(6330): 73-77.

Sun, X. J., L. M. Wang, et al. (1995). "Role of IRS-2 in insulin and cytokine signalling." Nature **377**(6545): 173-177.

Sutherland, C. and P. Cohen (1994). "The alpha-isoform of glycogen synthase kinase-3 from rabbit skeletal muscle is inactivated by p70 S6 kinase or MAP kinase-activated protein kinase-1 in vitro." FEBS Lett **338**(1): 37-42.

Sutherland, C., I. A. Leighton, et al. (1993). "Inactivation of glycogen synthase kinase-3 beta by phosphorylation: new kinase connections in insulin and growth-factor signalling." Biochem J **296 (Pt 1)**: 15-19.

Suzuki, S. W., J. Onodera, et al. (2011). "Starvation induced cell death in autophagy-defective yeast mutants is caused by mitochondria dysfunction." PLoS One **6**(2): e17412.

Szabadkai, G. and R. Rizzuto (2004). "Participation of endoplasmic reticulum and mitochondrial calcium handling in apoptosis: more than just neighborhood?" FEBS Lett **567**(1): 111-115.

Szendroedi, J., A. I. Schmid, et al. (2009). "Impaired mitochondrial function and insulin resistance of skeletal muscle in mitochondrial diabetes." Diabetes Care **32**(4): 677-679.

Takahashi, N., T. Goto, et al. (2009). "Bixin regulates mRNA expression involved in adipogenesis and enhances insulin sensitivity in 3T3-L1 adipocytes through PPARgamma activation." Biochem Biophys Res Commun **390**(4): 1372-1376.

Takeda, K., T. Yoshida, et al. (2010). "Synergistic roles of the proteasome and autophagy for mitochondrial maintenance and chronological lifespan in fission yeast." Proc Natl Acad Sci U S A **107**(8): 3540-3545.

Tamemoto, H., T. Kadowaki, et al. (1994). "Insulin resistance and growth retardation in mice lacking insulin receptor substrate-1." Nature **372**(6502): 182-186.

Tamemoto, H., K. Tobe, et al. (1997). "Insulin resistance syndrome in mice deficient in insulin receptor substrate-1." Ann N Y Acad Sci **827**: 85-93.

Tanti, J. F., T. Gremeaux, et al. (1994). "Insulin receptor substrate 1 is phosphorylated by the serine kinase activity of phosphatidylinositol 3-kinase." Biochem J **304 (Pt 1)**: 17-21.

Tanti, J. F., T. Gremeaux, et al. (1994). "Serine/threonine phosphorylation of insulin receptor substrate 1 modulates insulin receptor signaling." J Biol Chem **269**(8): 6051-6057.

Tezel, G., X. Yang, et al. (2005). "Proteomic identification of oxidatively modified retinal proteins in a chronic pressure-induced rat model of glaucoma." Invest Ophthalmol Vis Sci **46**(9): 3177-3187.

Todaro, G. J. and H. Green (1965). "Successive Transformations of an Established Cell Line by Polyoma Virus and Sv40." Science **147**: 513-514.

Tong, Q., C. P. Ye, et al. (2008). "Synaptic release of GABA by AgRP neurons is required for normal regulation of energy balance." Nat Neurosci **11**(9): 998-1000.

Tseng, Y. H., K. M. Kriauciunas, et al. (2004). "Differential roles of insulin receptor substrates in brown adipocyte differentiation." Molecular and Cellular Biology **24**(5): 1918-1929.

Turrens, J. F. and A. Boveris (1980). "Generation of superoxide anion by the NADH dehydrogenase of bovine heart mitochondria." Biochem J **191**(2): 421-427.

Uddin, S., L. Yenush, et al. (1995). "Interferon-alpha engages the insulin receptor substrate-1 to associate with the phosphatidylinositol 3'-kinase." J Biol Chem **270**(27): 15938-15941.

Ullrich, A. and J. Schlessinger (1990). "Signal transduction by receptors with tyrosine kinase activity." Cell **61**(2): 203-212.

Valverde, A. M., M. Arribas, et al. (2003). "Insulin-induced up-regulated uncoupling protein-1 expression is mediated by insulin receptor substrate 1 through the phosphatidylinositol 3-kinase/Akt signaling pathway in fetal brown adipocytes." J Biol Chem **278**(12): 10221-10231.

Van Obberghen, E. (1994). "Signalling through the insulin receptor and the insulin-like growth factor-I receptor." Diabetologia **37 Suppl 2**: S125-134.

Vazquez, F. and P. Devreotes (2006). "Regulation of PTEN function as a PIP3 gatekeeper through membrane interaction." Cell Cycle **5**(14): 1523-1527.

Vazquez, F., S. Ramaswamy, et al. (2000). "Phosphorylation of the PTEN tail regulates protein stability and function." Molecular and Cellular Biology **20**(14): 5010-5018.

Velloso, L. A., F. Folli, et al. (1996). "Cross-talk between the insulin and angiotensin signaling systems." Proc Natl Acad Sci U S A **93**(22): 12490-12495.

Venkatesan, N. and M. B. Davidson (1995). "Insulin resistance in rats harboring growth hormone-secreting tumors: decreased receptor number but increased kinase activity in liver." Metabolism **44**(1): 75-84.

Ventura-Clapier, R., A. Garnier, et al. (2008). "Transcriptional control of mitochondrial biogenesis: the central role of PGC-1alpha." Cardiovasc Res **79**(2): 208-217.

Vilsboll, T. and J. J. Holst (2004). "Incretins, insulin secretion and Type 2 diabetes mellitus." Diabetologia **47**(3): 357-366.

Virkamaki, A., K. Ueki, et al. (1999). "Protein-protein interaction in insulin signaling and the molecular mechanisms of insulin resistance." J Clin Invest **103**(7): 931-943.

Vogel, F., C. Bornhovd, et al. (2006). "Dynamic subcompartmentalization of the mitochondrial inner membrane." J Cell Biol **175**(2): 237-247.

Walenta, S., A. Bredel, et al. (1989). "Interrelationship among morphology, metabolism, and proliferation of tumor cells in monolayer and spheroid culture." Adv Exp Med Biol **248**: 847-853.

Walker, K. S., M. Deak, et al. (1998). "Activation of protein kinase B beta and gamma isoforms by insulin in vivo and by 3-phosphoinositide-dependent protein kinase-1 in vitro: comparison with protein kinase B alpha." Biochem J **331 (Pt 1)**: 299-308.

Wallace, D. C. (2000). "Mitochondrial defects in cardiomyopathy and neuromuscular disease." Am Heart J **139**(2 Pt 3): S70-85.

Wallimann, T., M. Wyss, et al. (1992). "Intracellular compartmentation, structure and function of creatine kinase isoenzymes in tissues with high and fluctuating energy demands: the 'phosphocreatine circuit' for cellular energy homeostasis." Biochem J **281 (Pt 1)**: 21-40.

Wang, L. M., A. D. Keegan, et al. (1993). "Common elements in interleukin 4 and insulin signaling pathways in factor-dependent hematopoietic cells." Proc Natl Acad Sci U S A **90**(9): 4032-4036.

Wang, L. M., M. G. Myers, Jr., et al. (1993). "IRS-1: essential for insulin- and IL-4-stimulated mitogenesis in hematopoietic cells." Science **261**(5128): 1591-1594.

Waters, S. B., K. Yamauchi, et al. (1993). "Functional expression of insulin receptor substrate-1 is required for insulin-stimulated mitogenic signaling." J Biol Chem **268**(30): 22231-22234.

Werner, H., C. Hernandez-Sanchez, et al. (1995). "The regulation of IGF-I receptor gene expression." Int J Biochem Cell Biol **27**(10): 987-994.

White, M. F. (1997). "The insulin signalling system and the IRS proteins." Diabetologia **40 Suppl 2**: S2-17.

White, M. F. (1998). "The IRS-signalling system: a network of docking proteins that mediate insulin action." Mol Cell Biochem **182**(1-2): 3-11.

White, M. F. (2003). "Insulin signaling in health and disease." Science **302**(5651): 1710-1711.

White, M. F. and C. R. Kahn (1994). "The insulin signaling system." J Biol Chem **269**(1): 1-4.

White, M. F., R. Maron, et al. (1985). "Insulin rapidly stimulates tyrosine phosphorylation of a Mr-185,000 protein in intact cells." Nature **318**(6042): 183-186.

White, M. F., S. E. Shoelson, et al. (1988). "A cascade of tyrosine autophosphorylation in the beta-subunit activates the phosphotransferase of the insulin receptor." J Biol Chem **263**(6): 2969-2980.

Withers, D. J., D. J. Burks, et al. (1999). "Irs-2 coordinates Igf-1 receptor-mediated beta-cell development and peripheral insulin signalling." Nat Genet **23**(1): 32-40.

Withers, D. J., J. S. Gutierrez, et al. (1998). "Disruption of IRS-2 causes type 2 diabetes in mice." Nature **391**(6670): 900-904.

Wititsuwannakul, D. and K. H. Kim (1977). "Mechanism of palmityl coenzyme A inhibition of liver glycogen synthase." J Biol Chem **252**(21): 7812-7817.

Wojtaszewski, J. F., Y. Higaki, et al. (1999). "Exercise modulates postreceptor insulin signaling and glucose transport in muscle-specific insulin receptor knockout mice." J Clin Invest **104**(9): 1257-1264.

Woodgett, J. R. (2005). "Recent advances in the protein kinase B signaling pathway." Curr Opin Cell Biol **17**(2): 150-157.

Wu, Z., P. Puigserver, et al. (1999). "Mechanisms controlling mitochondrial biogenesis and respiration through the thermogenic coactivator PGC-1." Cell **98**(1): 115-124.

Wullschleger, S., R. Loewith, et al. (2006). "TOR signaling in growth and metabolism." Cell **124**(3): 471-484.

Yamauchi, K. and J. E. Pessin (1994). "Enhancement or inhibition of insulin signaling by insulin receptor substrate 1 is cell context dependent." Molecular and Cellular Biology **14**(7): 4427-4434.

Yamauchi, T., K. Tobe, et al. (1996). "Insulin signalling and insulin actions in the muscles and livers of insulin-resistant, insulin receptor substrate 1-deficient mice." Molecular and Cellular Biology **16**(6): 3074-3084.

Yarden, Y. and A. Ullrich (1988). "Molecular analysis of signal transduction by growth factors." Biochemistry **27**(9): 3113-3119.

Yenush, L., K. J. Makati, et al. (1996). "The pleckstrin homology domain is the principal link between the insulin receptor and IRS-1." J Biol Chem **271**(39): 24300-24306.

Yenush, L. and M. F. White (1997). "The IRS-signalling system during insulin and cytokine action." Bioessays **19**(6): 491-500.

Yuan, L., R. Ziegler, et al. (2002). "Chronic hyperinsulinism induced down-regulation of insulin post-receptor signaling transduction in Hep G2 cells." J Huazhong Univ Sci Technolog Med Sci **22**(4): 313-316.

Zhande, R., J. J. Mitchell, et al. (2002). "Molecular mechanism of insulin-induced degradation of insulin receptor substrate 1." Molecular and Cellular Biology **22**(4): 1016-1026.

Zhang, C. Y., G. Baffy, et al. (2001). "Uncoupling protein-2 negatively regulates insulin secretion and is a major link between obesity, beta cell dysfunction, and type 2 diabetes." Cell **105**(6): 745-755.

Zhang, D. X. and D. D. Gutterman (2007). "Mitochondrial reactive oxygen species-mediated signaling in endothelial cells." Am J Physiol Heart Circ Physiol **292**(5): H2023-2031.

Zick, M., R. Rabl, et al. (2009). "Cristae formation-linking ultrastructure and function of mitochondria." Biochim Biophys Acta **1793**(1): 5-19.

8 Supplements

8. Supplementary

8.1 Acknowledgement

I sincerely thank PD Dr. Markus Schubert for the opportunity to join his lab and to work on this interesting and challenging project. I appreciate your support, motivation and productive discussions. Thank you so much for all that I have learned over the last years.

I would like to thank Prof. Dr. Jens Brüning, Prof. Dr. Wilhelm Krone, Prof. Dr. Peter Kloppenburg and PD Dr. Thomas Wunderlich for agreeing to form my thesis committee.

I would like to thank all former and present members of the lab for help, discussions and instructions. Many thanks to Uschi Leeser, Dr. Moritz Hettich, Dr. Roman Bilkovski, Dr. Michael Udelhoven, Dr. Susanna Freude, Dr. Katharina Schilbach and Frank Oberhäuser.

I specially like to thank PD Dr. Jürgen-Christoph von Kleist for his help with proton motive force and polarographic measurements, Dr. Andras Franko for his help with OROBOROS and Prof. Dr. Rudolf Wiesner for giving me the opportunity to do mitochondrial activity assays in his department.

Finally I would like to thank my family for support and motivation and friends for support, believing and beer.

8.2 Eidesstattliche Erklärung

Ich versichere, dass ich die von mir vorgelegte Dissertation selbstständig angefertigt, die benutzten Quellen und Hilfsmittel vollständig angegeben und die Stellen der Arbeit – einschließlich Tabellen, Karten und Abbildungen -, die andren Werken in Worten oder Sinn nach entnommen sind, in jedem Einzelfall als Entlehnung kenntlich gemacht habe; dass diese Dissertation noch keiner andren Fakultät oder Universität zur Prüfung vorgelegen hat; dass sie noch nicht Veröffentlich worden ist sowie, dass ich eine solche Veröffentlichung vor Abschluss des Promotionsverfahrens nicht vornehmen werde. Die Bestimmungen der Promotionsordnung sind mir bekannt. Die von mir vorgelegte Dissertation ist von Herrn Prof. Dr. Jens Brüning betreut worden.

Köln, im August 2011 Oliver Stöhr